4

General Principles Governing Dissolution of Materials in Solvents

4.1 SIMPLE SOLVENT CHARACTERISTICS

Valery Yu. Senichev, Vasiliy V. Tereshatov
Institute of Technical Chemistry
Ural Branch of Russian Academy of Sciences, Perm, Russia

Polymer dissolution is a necessary step in many of the polymer processing methods, such as blending, separation, coating, casting, etc. The developments in physical chemistry of non-electrolyte solutions relate the capabilities of solvents to dissolve materials with their physical properties. The relationships were developed within the framework of the concept of solubility parameters.

4.1.1 SOLVENT POWER

The usual problem of polymer engineering is a selection of proper solvent(s) for a given polymer. This selection implies that the solvent must form with polymer a thermodynamically stable mixture in the whole range of concentrations and temperatures. Such choice is facilitated by use of numerical criterion of a solvent power. Solvent power might be taken from the thermodynamic treatment (for example, a change of Gibbs' free energy or chemical potentials of mixing of polymer with solvent) but these criteria depend not only on the solvent properties but also on polymer structure and its concentration. For this reason, various approaches were proposed to estimate solvent power.

Kauri-butanol value, KB is used for evaluation of dissolving ability of hydrocarbon solvents. It is obtained by titration of a standard Kauri resin solution (20 wt% in 1-butanol) with the solvent until a cloud point is reached (for example, when it becomes impossible to read a text through the solution). The amount of the solvent used for titration is taken as KB value. The relationship between KB and solubility parameter, δ, fits the following empirical dependence:[1]

$$\delta = 12.9 + 0.06KB \qquad [4.1.1]$$

The KB value is primarily a measure of the aromaticity of solvents. Using KB value, it is possible to arrange solvents in sequence: aliphatic hydrocarbons < naphthenic hydrocarbons < aromatic hydrocarbons.

Dilution ratio, DR, is used to express the tolerance of solvents to diluents, most frequently, toluene. DR is the volume of a solvent added to a given solution that causes precipitation of the dissolved resin. This ratio can characterize the compatibility of a diluent with a resin solution in primary solvent. When compatibility is high, more diluent can be added. Only a multi-parameter approach provides a satisfactory correlation with solubility parameters.[2-3] DR depends on the polymer concentration. With polymer concentration increasing, DR increases as well. Temperature influences DR in a similar manner. Determination of DR must be performed at standard conditions. DR can be related to the solubility parameters but such correlation depends on concentration.

Aniline point, AP, is the temperature of a phase separation of aniline in a given solvent (the volume ratio of aniline : solvent = 1:1) in the temperature decreasing mode. AP is a critical temperature of the aniline - solvent system. AP can be related to KB value using the following equations:

At KB<50

$$KB = 99.6 - 0.806\rho - 0.177AP + 0.0755\left(358 - \frac{5}{9}T_b\right) \qquad [4.1.2]$$

At KB>50

$$KB = 177.7 - 10.6\rho - 0.249AP + 0.10\left(358 - \frac{5}{9}T_b\right) \qquad [4.1.3]$$

where:

T_b a solvent boiling point.

AP depends on the number of carbon atoms in the hydrocarbon molecule. AP is useful for describing complex aromatic solvents.

The solvent power can also be presented as a sum of factors that promote solubility or decrease it:[4]

$$S = H + B - A - C - D \qquad [4.1.4]$$

where:

H a factor characterizing the presence of active sites of opposite nature in solvent and polymer that can lead to formation of hydrogen bond between polymer and solvent

B a factor related to the difference in sizes of solute and solvent molecules

A a factor characterizing solute “melting”

C a factor of the self-association between solvent molecules

D a factor characterizing the change of nonspecific cohesion forces in the course of transfer of the polymer molecule into solution.

The equations for calculation of the above-listed factors are as follows:

$$B = (\alpha + b)\frac{V_m}{V_s}\left(1 - \varphi_p\right) \qquad [4.1.5]$$

$$D = \frac{V_m}{RT}\left(\delta'_p - \delta'_s\right)^2 \left(1-\varphi_p\right)^2 \qquad [4.1.6]$$

$$H = \ln\left[1 + \frac{K\left(1-\varphi_p\right)}{V_s}\right] \qquad [4.1.7]$$

$$C = \ln\frac{1+\left(K_{pp}\,/\,V_m\right)}{1+\left(K_{pp}\varphi_p\,/\,V_m\right)} \qquad [4.1.8]$$

where:

α	constant depending on the choice of the equation for the entropy of mixing. Usually it equals 0.5.
b	constant depending on the structure of solvent. b=1 for unstructured solvents, b=-1 for solvents with single H-bond (e.g. alcohols) and b=-2 for solvents with double H-bonds chains such as water.
V_m	the molar volume of a repeating segment
V_s	the molar volume of solvent
φ_p	the volume fraction of polymer
δ_p, δ_s	modified solubility parameters without regard to H-bonds.
K	the stability constant of the corresponding solvent-polymer hydrogen bond
K_{pp}	the constant of the self-association of polymer segments

Several polymers such as polyethylmethacrylate, polyisobutylmethacrylate and polymethylmethacrylate were studied according to Huyskens-Haulait-Pirson approach. The main advantage of this approach is that it accounts for entropy factors and other essential parameters affecting solubility. The disadvantages are more numerous, such as lack of physical meaning of some parameters, great number of variables, and insufficient coordination between factors influencing solubility that have reduced this approach to an approximate empirical scheme.

4.1.2 ONE-DIMENSIONAL SOLUBILITY PARAMETER APPROACH

The thermodynamic affinity between components of a solution is important for quantitative estimation of mutual solubility. The concept of solubility parameters is based on enthalpy of the interaction between solvent and polymer. Solubility parameter is the square root of the cohesive energy density, CED:

$$\delta = (CED)^{1/2} = \left(\frac{\Delta E_i}{V_i}\right)^{1/2} \qquad [4.1.9]$$

where:

ΔE_i	cohesive energy
V_i	molar volume

Solubility parameters are measured in $(MJ/m^3)^{1/2}$ or $(cal/sm^3)^{1/2}$ (1 $(MJ/m^3)^{1/2}$=2.054 $(cal/sm^3)^{1/2}$). The cohesive energy is equal in magnitude and opposite in sign to the potential energy of a volume unit of a liquid. The molar cohesive energy is the energy associated with all molecular interactions in one mole of the material, i.e., it is the energy of a liquid relative to its ideal vapor at the same temperature (see Chapter 5).

δis a parameter of intermolecular interaction of an individual liquid. The aim of many studies was to find relationship between energy of mixing of liquids and their δ. The first attempt was made by Hildebrand and Scatchard[5,6] who proposed the following equation:

$$\Delta U^m = (x_1V_1 + x_2V_2)\left[\left(\frac{\Delta E_1}{V_1}\right)^{1/2} - \left(\frac{\Delta E_2}{V_2}\right)^{1/2}\right]^2 \varphi_1\varphi_2 =$$

$$= (x_1V_1 + x_2V_2)(\delta_1 - \delta_2)^2 \varphi_1\varphi_2 \qquad [4.1.10]$$

where:

ΔU^m	internal energy of mixing, that is a residual between energies of a solution and components,
x_1, x_2	molar fractions of components
V_1, V_2	molar volumes of components
φ_1, φ_2	volume fractions of components

The Hildebrand-Scatchard equation became the basis of the Hildebrand theory of regular solutions.[5] They interpreted a regular solution as a solution formed due to the ideal entropy of mixing and the change of an internal energy. The assumed lack of the volume change makes an enthalpy or heat of mixing equated with the right members of the equation. The equation permits calculation heat of mixing of two liquids. It is evident from equation that these heats can only be positive. Because of the equality of of components, $\Delta H^m=0$.

The free energy of mixing of solution can be calculated from the equation

$$\Delta G^m = (x_1V_1 + x_2V_2)\left[\left(\frac{\Delta E_1}{V_1}\right)^{1/2} - \left(\frac{\Delta E_2}{V_2}\right)^{1/2}\right]^2 \varphi_1\varphi_2 -$$

$$-T\Delta S_{id} = V(\delta_1 - \delta_2)^2 \varphi_1\varphi_2 - T\Delta S \qquad [4.1.11]$$

The change of entropy, ΔS_{id}, is calculated from the Gibbs equation for mixing of ideal gases. The calculated values are always positive.

$$\Delta S_{id} = -R(x_1 \ln x_1 + x_2 \ln x_2) \qquad [4.1.12]$$

where:

R	gas constant

Considering the signs of the parameters ΔS_{id} and ΔH^m in Eq. [4.1.10], the ideal entropy of mixing promotes a negative value of ΔG^m, i.e., the dissolution and the value of ΔH^m reduces the ΔG^m value. It is pertinent that the most negative ΔG^m value is when $\Delta H^m=0$, i.e., when δ of components are equal. With these general principles in mind, the components with solubility parameters close to each other have the best mutual solubility. The theory of regular solutions has essential assumptions and restrictions.[7] The Eq. [4.1.10] is deduced under assumption of the central role of dispersion forces of interaction between components of solution that is correct only for the dispersion forces. Only in this case it is possible to accept that the energy of contacts between heterogeneous molecules is a geometric mean value of energy of contacts between homogeneous molecules:

$$\varepsilon_{12}^{*} = \sqrt{\varepsilon_{11}^{*}\varepsilon_{22}^{*}} \qquad [4.1.13]$$

where:

ε_{ii}^{*} potential energy of a pair of molecules

This assumption is not justified in the presence of the dipole-dipole interaction and other more specific interactions. Therefore the theory of regular solutions poorly suits description of the behavior of solutions of polar substances. Inherent in this analysis is the assumption of molecular separation related to molecular diameters which neglects polar or specific interactions. The theory also neglects volume changes on dissolution. This leads to a disparity (sometimes very large) between internal energy of mixing used in the theory and the constant pressure enthalpy measured experimentally.

The correlation between these values is given by equation:

$$\left(\Delta H^{m}\right)_{p} = \left(\Delta U^{m}\right)_{V} + T\left(\partial p / \partial T\right)_{V}\left(\Delta V^{m}\right)_{p} \qquad [4.1.14]$$

where:

$(\partial p / \partial T)_V$ thermal factor of pressure which has value of the order 10-14 atm/degree for solutions and liquids.

Therefore, even at small changes of volume, the second term remains very large and brings substantial contribution to the value of $(\Delta H^m)_p$. For example, for a system benzene (0.5 mol) - cyclohexane (0.5 mol):

$$\Delta V^{m} = 0.65\ cm^{3}, \quad \left(\Delta H^{m}\right)_{p} = 182\ cal, \quad \left(\Delta U^{m}\right)_{V} = 131\ cal$$

The theory also assumes that the ideal entropy is possible for systems when $\Delta H^m \neq 0$. But the change of energy of interactions occurs in the course of dissolution that determines the inevitable change of entropy of molecules. It is assumed that the interactive forces are additive and that the interactions between a pair of molecules are not influenced by the presence of other molecules. Certainly, such an assumption is simplistic, but at the same time it has allowed us to estimate solubility parameters using group contributions or molar attractive constants (see Subchapter 5.3).

The solubility parameter δ is relative to the cohesion energy and it is an effective characteristic of intermolecular interactions. It varies from a magnitude of 12 $(MJ/m^3)^{1/2}$ for nonpolar substances up to 23 $(MJ/m^3)^{1/2}$ for water. Knowing δ of solvent and solute, we can estimate solvents in which particular polymer cannot be dissolved. For example, polyisobutylene for which δ is in the range from 14 to 16 $(MJ/m^3)^{1/2}$ will not be dissolved in solvents with δ=20-24 $(MJ/m^3)^{1/2}$. The polar polymer with δ=18 $(MJ/m^3)^{1/2}$ will not dissolve in solvents with δ=14 or δ=26 $(MJ/m^3)^{1/2}$. These are important data because they help to narrow down a group of solvents potentially suitable for a given polymer. However, the opposite evaluation is not always valid because polymers and solvents with the identical solubility parameters are not always compatible. This limitation comes from integral character of the solubility parameter. The solubility depends on the presence of functional groups in molecules of solution components which are capable to interact with each other and this model does not address such interactions. The latter statement has become a premise for the development of the multi-dimensional approaches to solubility that will be the

subject of the following subchapter. The values of solubility parameters are included in Table 4.1.1.

Table 4.1.1 Solubility parameters and their components (according Hansen's approach) for different solvents

Solvent	V_1, Kmol/m^3	δ, (MJ/m^3)$^{1/2}$	δ_d, (MJ/m^3)$^{1/2}$	δ_p, (MJ/m^3)$^{1/2}$	δ_h, (MJ/m^3)$^{1/2}$
Alkanes					
n-Butane	101.4	14.1	14.1	0	0
n-Pentane	116.2	14.3	14.3	0	0
n-Hexane	131.6	14.8	14.8	0	0
n-Heptane	147.4	15.1	15.1	0	0
n-Octane	163.5	14.0	14.0	0	0
n-Nonane	178.3	15.4	15.4	0	0
n-Decane	195.9	15.8	15.8	0	0
n-Dodecane	228.5	16.0	16.0	0	0
Cyclohexane	108.7	16.7	16.7	0	0
Methylcyclohexane	128.3	16.0	16.0	0	0.5
Aromatic hydrocarbons					
Benzene	89.4	18.7	18.4	1.0	2.9
Toluene	106.8	18.2	18.0	1.4	2.0
Naphthalene	111.5	20.3	19.2	2.0	5.9
Styrene	115.6	19.0	17.8	1.0	3.1
o-Xylene	121.2	18.4	17.6	1.0	3.1
Ethylbenzene	123.1	18.0	17.8	0.6	1.4
Mesitylene	139.8	18.0	18.0	0	0.6
Halo hydrocarbons					
Chloromethane	55.4	19.8	15.3	6.1	3.9
Dichloromethane	63.9	20.3	18.2	6.3	7.8
Trichloromethane	80.7	18.8	17.6	3.0	4.2
n-Propyl chloride	88.1	17.4	16.0	7.8	2.0
1,1-Dichloroethene	79.0	18.6	17.0	6.8	4.5
1-Chlorobutane	104.5	17.2	16.2	5.5	2.0
1,2-Dichloroethane	79.4	20.0	19.0	7.4	4.1
Carbon tetrachloride	97.1	17.6	17.6	0	0

Solvent	V_1, Kmol/m^3	δ, $(MJ/m^3)^{1/2}$	δ_d, $(MJ/m^3)^{1/2}$	δ_p, $(MJ/m^3)^{1/2}$	δ_h, $(MJ/m^3)^{1/2}$
Perchloroethylene	101.1	19.0	19.0 18.8	6.5 0	2.9 1.4
1,1,2,2-Tetrachloroethane	105.2	19.8	18.8	5.1	9.4 5.3
Chloro-difluoromethane (Freon 21)	72.9	17.0	12.3	6.3	5.7
1,1,2-Trichloro-trifluoro-ethane (Freon 113)	119.2	14.8	14.5	1.6	0
Dichloro-difluoro-methane (Freon 12)	92.3	12.2	12.2	2.0	0
Chlorobenzene	102.1	19.5	18.9	4.3	2.0
o-Dichlorobenzene	112.8	20.4	19.1	6.3	3.3
Bromoethane	76.9	19.6	15.8	3.1	5.7
Bromobenzene	105.3	20.3	20.5 18.9	5.5 4.5	4.1 5.1
Ethers					
Epichlorohydrin	72.5	18.5	17.8	1.8	5.3
Tetrahydrofuran	79.9	22.5	19.0	10.2	3.7
1,4-Dioxane	81.7	18.5	16.8	5.7	8.0
Diethyl ether	85.7	20.5	19.0	1.8	7.4
Diisopropyl ether	104.8	15.6	14.4	2.9	5.1
Ketones					
Acetone	74.0	19.9	15.5	10.4	6.9
Methyl ethyl ketone	90.1	18.9	15.9	9.0 8.4	5.1
Cyclohexanone	104.0	18.8	16.3	7.1	6.1
Diethyl ketone	106.4	18.1	15.8	7.6	4.7
Mesityl oxide	115.6	16.7	15.9 17.6	3.7	4.1
Acetophenone	117.4	19.8	16.5	8.2	7.3
Methyl isobutyl ketone	125.8	17.5	15.3	6.1	4.1
Methyl isoamyl ketone	142.8	17.4	15.9	5.7	4.1
Isophorone	150.5	18.6	16.6	8.2	7.4
Diisobutyl ketone	177.1	16.0	16.0	3.7	4.1

Solvent	V_1, Kmol/m^3	δ, (MJ/m^3)$^{1/2}$	δ_d, (MJ/m^3)$^{1/2}$	δ_p, (MJ/m^3)$^{1/2}$	δ_h, (MJ/m^3)$^{1/2}$
Aldehydes					
Acetaldehyde	57.1	21.1	14.7	8.0	11.3
Furfural	83.2	22.9	18.6	14.9	5.1
n-Butyraldehyde	88.5	18.4	14.7 18.7	5.3 8.6	7.0
Benzaldehyde	101.5	19.2	19.4	7.4	5.3
Esters					
Ethylene carbonate	66.0	30.1	29.6	19.4	21.7
Methyl acetate	79.7	19.6	15.5	7.2	7.6
Ethyl formate	80.2	19.6	15.5	8.4	8.4
Propylene-1,2-carbonate	85.0	27.2	20.0	18.0	4.1
n-Propyl formate	97.2	19.5	15.0	5.3	11.2
Propyl acetate	115.1	17.8	15.5	4.5	7.6
Ethyl acetate	98.5	18.6	15.8	5.3	7.2
n-Butyl acetate	132.5	17.4	15.8	3.7	6.3
n-Amyl acetate	149.4	17.3	15.6	3.3	6.7
Isobutyl acetate	133.5	17.0	15.1	3.7	6.3
Isopropyl acetate	117.1	17.3	14.4	6.1	7.4
Diethyl malonate	151.8	19.5	15.5	4.7	10.8
Diethyl oxalate	135.4	22.5	15.5	5.1	15.5
Isoamyl acetate	148.8	16.0	15.3	3.1	7.0
Dimethyl phthalate	163	21.9	18.6	10.8	4.9
Diethyl phthalate	198	20.5	17.6	9.6	4.5
Dibutyl phthalate	266	19.0	17.8	8.6	4.1
Dioctyl phthalate	377	16.8	16.6	7.0	3.1
Phosphorous compounds					
Trimethyl phosphate	116.7	25.2	16.7	15.9	10.2
Triethyl phosphate	169.7	22.2	16.7	11.4	9.2
Tricresyl phosphate	316	23.1	19.0	12.3	4.5
Nitrogen compounds					
Acetonitrile	52.6	24.3	15.3	17.9	6.1
n-Butyronitrile	86.7	20.4	15.3	12.5	5.1

Solvent	V_1, Kmol/m^3	δ, $(MJ/m^3)^{1/2}$	δ_d, $(MJ/m^3)^{1/2}$	δ_p, $(MJ/m^3)^{1/2}$	δ_h, $(MJ/m^3)^{1/2}$
Propionitrile	70.9	22.1	15.3	14.3	5.5
Benzonitrile	102.6	19.9	17.4	9.0	3.3
Nitromethane	54.3	25.1	15.7	18.8	5.1
Nitroethane	71.5	22.6	15.9	15.9	4.5
2-Nitropropane	86.9	20.4	16.1	12.0	4.1
Nitrobenzene	102.7	20.5	20.0	8.6	4.1
Ethylenediamine	67.3	25.2	16.6	8.8	17.0
2-Pyrrolidinone	76.4	30.1	19.4	17.4	11.3
Pyridine	80.9	21.9	19.0	8.8	5.9
Morpholine	87.1	22.1	18.8	4.9	9.2
Aniline	91.5	21.1	19.4	5.1	10.2
n-Butylamine	99.0	17.8	16.2	4.5	8.0
2-Aminoethanol	59.7	31.3	17.1	15.5	21.2
Di-n-propyl amine	136.8	15.9	15.3	1.4	4.1
Diethylamine	103.2	16.4	14.9	2.3	6.1
Quinoline	118.0	22.1	19.4	7.0	7.6
Formamide	39.8	39.3	17.2	26.2	19.0
N,N-Dimethylformamide	77.0	24.8	17.4	13.7	11.2
Sulfur compounds					
Carbon disulfide	60.0	20.3	20.3	0	0
Dimethyl sulfoxide	71.3	26.4	18.4	16.3	10.2
Diethyl sulfide	107.6	17.2	16.8	3.1	2.0
Dimethyl sulfone	75	29.7	19.0	19.4	12.3
Monohydric alcohols and phenols					
Methanol	40.7	29.1	15.1	12.2	22.2
Ethanol	66.8	26.4	15.8	8.8	19.4
Allyl alcohol	68.4	24.1	16.2	10.8	16.8
1-Propanol	75.2	24.4	15.8	6.7	17.3
2-Propanol	76.8	23.5	15.8	6.1	16.4
Furfuryl alcohol	86.5	25.6	17.4	7.6	15.1
1-Butanol	91.5	23.1	15.9	5.7	15.7
2-Butanol	92.0	22.1	15.8	5.7	14.5

Solvent	V_1, Kmol/m^3	δ, (MJ/m^3)$^{1/2}$	δ_d, (MJ/m^3)$^{1/2}$	δ_p, (MJ/m^3)$^{1/2}$	δ_h, (MJ/m^3)$^{1/2}$
1-Pentanol	108.3	21.6	15.9	4.5	13.9
Benzyl alcohol	103.6	24.8	18.4	6.3	13.7
Cyclohexanol	106.0	23.3	17.3	4.1	13.5
Ethylene glycol monomethyl ether	79.1	23.3	16.2	9.2	16.4
Ethylene glycol monoethyl ether	97.8	21.5	16.2	9.2	14.3
Ethylene glycol monobutyl ether	142.1	20.8	15.9	4.5	12.7
1-Octanol	157.7	21.1	17.0	3.3	11.9
m-Cresol	104.7	22.7	18.0	5.1	12.9
Carboxylic acids					
Formic acid	37.8	24.8	14.3	11.9	16.6
Acetic acid	57.1	20.7	14.5	8.0	13.5
n-Butyric acid	110	21.5	14.9	4.1	10.6
Polyhydric alcohols					
Ethylene glycol	55.8	33.2	16.8	11.0	25.9
Glycerol	73.3	43.8	17.3	12.0	29.2
Diethylene glycol	95.3	29.8	16.0	14.7	20.4
Triethylene glycol	114.0	21.9	16.0	12.5	18.6
Water	18.0	47.9	15.5	16.0	42.3

4.1.3 MULTI-DIMENSIONAL APPROACHES

These approaches can be divided into three types:

1 H-bonds are not considered. This approach can be applied only for nonpolar and weak polar liquids.
2 H-bonds taken into account by one parameter.
3 H-bonds taken into account by two parameters.

Blanks and Prausnitz[8,9] proposed two-component solubility parameters. They decomposed the cohesion energy into two contributions of polar and non-polar components:

$$-\frac{E}{V_1} = -\frac{E_{nonpolar}}{V_1} - \frac{E_{polar}}{V_1} = \lambda^2 + \tau^2 \qquad [4.1.15]$$

where:

λ non-polar contribution to solubility parameter
τ polar contribution to solubility parameter

This approach has become a constituent of the Hansen approach and has not received a separate development.

Polar interactions can themselves be divided into two types:

- Polar interactions where molecules having permanent dipole moments interact in solution with the dipole orientation in a symmetrical manner. It follows that the geometric mean rule is obeyed for orientation interactions and the contribution of dipole orientations to the cohesive energy and dispersion interactions.
- Polar interactions accompanied by the dipole induction. These interactions are asymmetrical.

Thus for a pure polar liquid without hydrogen bonds:[10]

$$\delta^2 = \delta_d^2 + \delta_{or}^2 + 2\delta_d \delta_{in} \qquad [4.1.16]$$

where:

δ_d dispersion contribution to the solubility parameter
δ_{or} orientation contribution to the solubility parameter
δ_{in} induction contribution to the solubility parameter.

A more traditional approach of contribution of the induction interaction was published elsewhere;[11] however, it was used only for the estimation of the common value of the δ parameter rather than for evaluation of solubility:

$$\delta^2 = \delta_d^2 + \delta_p^2 + \delta_i^2 \qquad [4.1.17]$$

The first method taking into account the hydrogen bonding was proposed by Beerbower et al.,[12] who expressed hydrogen bonding energy through the hydrogen bonding number $\Delta\nu$. The data for various solvents were plotted into a diagram with the solubility parameter along the horizontal axis and the hydrogen bonding number $\Delta\nu$ along the vertical axis. Data were obtained for a given polymer for suitable solvents. All solvents in which a given polymer was soluble got a certain regions. Lieberman also plotted two-dimensional graphs of solubility parameters versus hydrogen-bonding capabilities.[13]

On the base of work by Gordy and Stanford, the spectroscopic criterion, related to the extent of the shift to lower frequencies of the OD infrared absorption of deuterated methanol, was selected. It provides a measure of the hydrogen-bonding acceptor power of a solvent.[14,15] The spectrum of a deuterated methanol solution in the test solution was compared with that of a solution in benzene and the hydrogen-bonding parameter was defined as

$$\gamma = \Delta\nu / 10 \qquad [4.1.18]$$

where:

$\Delta\nu$ OD absorption shift (in wavenumber).

Crowley et al.[16] used an extension of this method by including the dipole moment of the solvents. One of the axis represented solubility parameter, the second the dipole moment, and the third hydrogen bonding expressed by spectroscopic parameter γ. Because this method involved an empirical comparison of a number of solvents it was impractical. Nelson et al.[17] utilized this approach to hydrogen bond solubility parameters. Hansen (see the next section) developed this method.

Chen introduced a quantity χ_H[18]

$$\chi_H = \frac{V_S}{RT}\left[\left(\delta_{d.S} - \delta_{d.P}\right)^2 + \left(\delta_{p.S} - \delta_{p.P}\right)^2\right] \qquad [4.1.19]$$

where $\delta_{d.S}$, $\delta_{d.P}$, $\delta_{p.S}$, $\delta_{p.P}$ are Hansen's parameters of solvent and polymer (see the next section).

Chen implied that χ_H was the enthalpy contribution to the Flory-Huggins parameter χ_1 and plotted the solubility data in a $\delta_h - \chi_H$ diagram where δ_h was the H-bond parameter in the Hansen approach. In these diagrams sphere-like volumes of Hansen's solubility have degenerated to circles.

The disadvantage of this method lies in the beforehand estimating characteristics of the polymer. Among other two-dimensional methods used for the representation of solubility data was the δ_p-δ_h diagram proposed by Henry[19] and the δ-δ_h diagram proposed by Hoernschemeyer,[20] but their representations of the solubility region were less correct. All these approaches involving hydrogen bond parameter ignored the fact that hydrogen bond interaction was the product of hydrogen bonding donating and accepting capability.[21-23]

On the basis of chemical approach to hydrogen bonding, Rider proposed a model of solubility for liquids in which the enthalpy limited the miscibility of polymers and solvents.[24,25] For substances capable to form hydrogen bonds, Rider proposed a new factor relating miscibility with an enthalpy of mixing which depends on an enthalpy of the hydrogen bond formation. He has introduced the quantity of a hydrogen bond potential (HBP). If the quantity of HBP is positive it promotes miscibility and if it is negative it decreases miscibility.

$$HBP = (b_1 - b_2)(C_1 - C_2) \qquad [4.1.20]$$

where:

b_1,b_2	donor parameters of solvent and solute, respectively
C_1, C_2	acceptor parameters of solvent and solute, respectively

For certain polymers Rider has drawn solubility maps. Thus the area of solubility was represented by a pair of symmetric quarters of a plane lying in coordinates b,C.[24] Values of parameters were defined from data for enthalpies of hydrogen bonds available from the earlier works. The model is a logical development of the Hansen method. A shortcoming of this model is in neglecting all other factors influencing solubility, namely dispersion and polar interactions, change of entropy, molecular mass of polymer and its phase condition. The model was developed as a three-dimensional dualistic model (see Section 4.1.5).

4.1.4 HANSEN'S SOLUBILITY

The Hansen approach[26-30] assumed that the cohesive energy can be divided into contributions of dispersion interactions, polar interactions, and hydrogen bonding.

$$E = E_d + E_p + E_h \qquad [4.1.21]$$

where:

E	total cohesive energy
E_d, E_p, E_h	contributions of dispersion forces, permanent dipole-permanent dipole forces, and hydrogen bonds.

Dividing this equation by the molar volume of solvent, V_1, gives:

$$\frac{E}{V_1} = \frac{E_d}{V_1} + \frac{E_p}{V_1} + \frac{E_h}{V_1} \qquad [4.1.22]$$

or

$$\delta^2 = \delta_d^2 + \delta_p^2 + \delta_h^2 \qquad [4.1.23]$$

where:

δ	total solubility parameter
δ_d, δ_p, δ_h	components of the solubility parameter determined by the corresponding contributions to the cohesive energy.

Hansen gave a visual interpretation of his method by means of three-dimensional spheres of solubility, where the center of the sphere has coordinates corresponding to the values of components of solubility parameter of polymer. The sphere can be coupled with a radius to characterize a polymer. All good solvents for particular polymer (each solvent has been represented as a point in a three-dimensional space with coordinates) should be inside the sphere, whereas all non-solvents should be outside the solubility sphere. An example is given in Section 4.1.7.

In the original work these parameters were evaluated by experimental observations of solubility. It was assumed that if each of the solubility parameter components of one liquid is close to the corresponding values of another liquid, then the process of their mixing should readily occur with a more negative free energy. The solubility volume has dimensions δ_d, δ_p, $2\delta_h$. The factor 2 was proposed to account for the spherical form of solubility volumes and had no physical sense. However, it is necessary to notice that, for example, Lee and Lee[31] have evaluated spherical solubility volume of polyimide with good results without using the factor 2. Because of its simplicity, the method has become very popular.

Using the Hansen approach, the solubility of any polymer in solvents (with known Hansen's parameters of polymer and solvents) can be predicted. The determination of polymer parameters requires evaluation of solubility in a great number of solvents with known values of Hansen parameters. Arbitrary criteria of determination are used because Hansen made no attempts of precise calculations of thermodynamic parameters.

The separation of the cohesion energy into contributions of various forces implies that it is possible to substitute energy for parameter and sum contributions proportional to the second power of a difference of corresponding components. Hansen's treatment permits evaluation of the dispersion and polar contribution to cohesive energy. The fitting parameter of the approach (the solubility sphere radius) reflects on the supermolecular structure of polymer-solvent system. Its values should be higher for amorphous polymers and lower for glass or crystalline polymers.

The weak point of the approach is the incorrect assignment of the hydrogen bond contribution in the energy exchange that does not permit its use for polymers forming strong hydrogen bonds.

Table 4.1.2. Solubility parameters and their components for solvents (after refs 37,40)

Polymer	δ, $(MJ/m^3)^{1/2}$	δ_d, $(MJ/m^3)^{1/2}$	δ_p, $(MJ/m^3)^{1/2}$	δ_h, $(MJ/m^3)^{1/2}$
Polyamide-66	22.77	18.5	5.1	12.2

Polymer	δ, $(MJ/m^3)^{1/2}$	δ_d, $(MJ/m^3)^{1/2}$	δ_p, $(MJ/m^3)^{1/2}$	δ_h, $(MJ/m^3)^{1/2}$
Polyacrylonitrile	25.10	18.19	15.93	6.74
Polyvinylchloride	21.41	18.68	10.01	3.06
Polymethylmethacrylate	20.18	17.72	5.72	7.76
Polystyrene	19.81	19.68	0.86	2.04
Polytetrafluoroethylene	13.97	13.97	0.00	0
Polyethyleneterephthalate	21.6	19.5	3.47	8.58

A large number of data were accumulated for different solvents and polymers (see Tables 4.1.1, 4.1.2). A variation of the Hansen method is the approach of Teas.[33] He showed for some polymer-solvent systems that it was possible to use fractional cohesive energy densities plotted on a triangular chart to represent solubility limits:

$$E_d = \frac{\delta_d^2}{\delta_0^2}, \quad E_p = \frac{\delta_p^2}{\delta_0^2}, \quad E_h = \frac{\delta_h^2}{\delta_0^2} \qquad [4.1.24]$$

where $\delta_0^2 = \delta_d^2 + \delta_p^2 + \delta_h^2$

Teas used fractional parameters defined as

$$f_d = \frac{100\delta_d}{\delta_d + \delta_p + \delta_h}, \quad f_p = \frac{100\delta_p}{\delta_d + \delta_p + \delta_h}, \quad f_h = \frac{100}{\delta_d + \delta_p + \delta_h} \qquad [4.1.25]$$

This representation was completely empirical without any theoretical justification.

Some correlations between components of solubility parameters and physical parameters of liquids (surface tension, dipole moment, the refraction index) were generalized elsewhere.[11]

$$\delta_d^2 + 0.632\delta_p^2 + 0.632\delta_h^2 = 13.9V_1^{-1/3}\gamma_l \qquad \text{non-alcohols} \qquad [4.1.26]$$

$$\delta_d^2 + \delta_p^2 + 0.06\delta_h^2 = 13.9V_1^{-1/3}\gamma_l \qquad \text{alcohols} \qquad [4.1.27]$$

$$\delta_d^2 + 2\delta_p^2 + 0.48\delta_h^2 = 13.9V_1^{-1/3}\gamma_l \qquad \text{acids, phenols} \qquad [4.1.28]$$

where:

γ_l surface tension.

Koenhan and Smolder proposed the following equation applicable to the majority of solvents, except cyclic compounds, acetonitrile, carboxylic acids, and multi-functional alcohols.[34]

$$\delta_d^2 + \delta_p^2 = 13.8V_1^{-1/3}\gamma_l \qquad [4.1.29]$$

They also proposed a correlation between polar contribution to the solubility parameter and refractive index:

$$\delta_d = 9.55 n_D - 5.55 \qquad [4.1.30]$$

where:

n_D refractive index

Alternatively Keller et. al.[35] estimated that for nonpolar and slightly polar liquids

$$\delta_d = 62.8x \qquad \text{for } x \le 0.28 \qquad [4.1.31]$$

$$\delta_d = -4.58 + 108x - 119x^2 + 45x^3 \qquad \text{for } x > 0.28 \qquad [4.1.32]$$

where:

$$x = \frac{n_D^2 - 1}{n_D^2 + 2}$$

Peiffer suggested the following expression:[35]

$$\delta_d^2 = K\left(4\pi\pi I^2 / 3d\right)\left(N / V_1\right)^3 \qquad [4.1.33]$$

where:

K	packing parameter
I	ionization potential
α	molecular polarizability
N	number of molecules in the volume unit
V_1	$=Nr^{*3}/K$
r*	the equilibrium distance between molecules.

For the estimation of nonpolar component of δ Brown et al.[36] proposed the homomorph concept. The homomorph of a polar molecule is the nonpolar molecule most closely resembling it in the size and the structure (e.g., n-butane is the homomorph of n-butyl alcohol). The nonpolar component of the cohesion energy of a polar solvent is taken as the experimentally determined total vaporization energy of the corresponding homomorph at the same reduced temperature (the actual temperature divided by the critical temperature in Kelvin's scale). For this comparison the molar volumes must also be equal. Blanks and Prausnitz proposed plots of dependencies of dispersion energy density on a molar volume for straight-chain, alicyclic and aromatic hydrocarbons. If the vaporization energies of appropriate hydrocarbons are not known they can be calculated by one of the methods of group contributions (See Chapter 5).

Hansen and Scaarup[28] calculated the polar component of solubility parameter using Bottcher's relation to estimating the contribution of the permanent dipoles to the cohesion energy:

$$\delta_p^2 = \frac{12108}{V_1^2} \frac{\varepsilon - 1}{2\varepsilon - n_D^2} \left(n_D^2 + 2\right)\mu^2 \qquad [4.1.34]$$

where:

ε	dielectric constant,
μ	dipole moment

$$\delta_p = 50.1\frac{\mu}{V_1^{3/4}} \qquad [4.1.35]$$

Peiffer[11] proposed the expressions which separates the contributions of polar forces and induction interactions to the solubility parameters:

$$\delta_p^2 = K\left(2\pi\mu^4 / 3kTp\right)\left(N / V_1\right)^3 \qquad [4.1.36]$$

$$\delta_i^2 = K\left(2\pi\alpha\mu / i\right)\left(N / V_1\right)^3 \qquad [4.1.37]$$

where:

ε*	interaction energy between two molecules at the distance r*
N	number of hydroxyl groups in molecule

$$p = 2\mu^4 / 3kT\varepsilon^* \qquad [4.1.38]$$

$$i = 2\alpha\mu^2 / \varepsilon^* \qquad [4.1.39]$$

It should be noted that in Hansen's approach these contributions are cumulative:

$$\delta_p^2 = \delta_p^2 + \delta_i^2 \qquad [4.1.40]$$

For the calculation of hydrogen-bonding component, δ_h, Hansen and Scaarup[28] proposed an empirical expression based on OH-O bond energy (5000 cal/mol) applicable to alcohols only:

$$\delta_h = \left(20.9N / V_1\right)^{1/2} \qquad [4.1.41]$$

In Subchapter 5.3, the values of all the components of a solubility parameter are calculated using group contributions.

4.1.5 THREE-DIMENSIONAL DUALISTIC MODEL

The heat of mixing of two liquids is expressed by the classical theory of regular polymer solutions using Eq. [4.1.10]. This expression is not adequate for systems with specific interactions. Such interactions are expressed as a product of the donor parameter and the acceptor parameter. The contribution of H-bonding to the enthalpy of mixing can be written in terms of volume units as follows:[21]

$$\Delta H'_{mix} = \left(A_1 - A_2\right)\left(D_1 - D_2\right)\varphi_1\varphi_2 \qquad [4.1.42]$$

where:

A_1, A_2	effective acceptor parameters
D_1, D_2	donor parameters,
φ_1, φ_2	volume fractions,

Hence enthalpy of mixing of two liquids per volume unit can be expressed by:[32]

$$\Delta H_{mix} = \left[\left(\delta'_1 - \delta'_2\right)^2 + \left(A_1 - A_2\right)\left(D_1 - D_2\right)\right]\varphi_1\varphi_2 = B\varphi_1\varphi_2 \qquad [4.1.43]$$

This equation is used for the calculation of the enthalpy contribution to the Huggins parameter (see Subchapter 4.2) for a polymer-solvent system:

$$\chi_H = V_1 \left[(\delta'_1 - \delta'_2)^2 + (A_1 - A_2)(D_1 - D_2) \right] / RT \qquad [4.1.44]$$

where:

δ'_1, δ'_2 dispersion-polar components of solubility parameters (values of solubility parameters excluding H-bonds contributions).

Results of calculations using Eq. [4.1.44] of three-dimension dualistic model coincide with the experimental values of χ_H and the χ_H values calculated by other methods.[37] Values A, D, and δ' can been obtained from IR-spectroscopy evaluations and Hansen's parameters.[24,25] Values of the TDM parameters are presented in Tables 4.1.3, 4.1.4. It should be noted that Hansen parameters are used for estimation of values of TDM parameters from equation $\delta_{di}^2 + \delta_{pi}^2 = \delta_i'^2$, $\delta_{hi}^2 = A_i D_i$.

Table 4.1.3. TDM parameters of some solvents. [Adapted, by permission, from V.Yu. Senichev, V.V. Tereshatov , *Vysokomol . Soed* ., B31 , 216 (1989).]

#	Solvent	D	A	δ′	δ	$V_1 \times 10^6$ m^3/mol
		$(MJ/m^3)^{1/2}$				
1	Isopropanol	11.8	13.3	20.0	23.6	76.8
2	Pentanol	9.9	11.2	19.7	22.3	108.2
3	Acetone	3.8	13.1	18.5	19.8	74.0
4	Ethyl acetate	4.9	10.4	17.0	18.3	98.5
5	Butyl acetate	4.8	9.0	16.4	17.6	132.5
6	Isobutyl acetate	4.8	8.4	15.7	16.9	133.3
7	Amyl acetate	4.7	7.8	16.2	17.3	148.9
8	Isobutyl isobutyrate	4.7	7.4	14.6	15.7	165.0
9	Tetrahydrofuran	5.2	12.2	17.7	19.4	81.7
10	o-Xylene	0.5	7.4	18.3	18.4	121.0
11	Chlorobenzene	0.6	7.3	19.3	19.4	102.1
12	Acetonitrile	2.7	14.0	24.4	24.5	52.6
13	n-Hexane	0	0	14.9	14.9	132.0
14	Benzene	0.6	8.5	18.6	18.8	89.4
15	N,N-Dimethylformamide	8.2	15.4	22.0	27.7	77.0
16	Toluene	0.6	7.8	18.1	18.2	106.8
17	Methanol	18.2	17.0	23.5	29.3	41.7
18	Ethanol	14.4	14.7	21.7	26.1	58.5

#	Solvent	D	A	δ′	δ	$V_1 \times 10^6$ m^3/mol
		$(MJ/m^3)^{1/2}$				
19	1-Propanol	11.9	13.4	21.0	24.5	75.2
20	Methyl ethyl ketone	2.3	11.6	18.3	19.0	90.1
21	Cyclohexanone	2.7	11.1	19.5	20.3	104.0
22	Diethyl ether	7.6	12.4	12.0	15.4	104.8
23	Ethylbenzene	0.3	7.3	17.9	18.0	123.1
24	Pyridine	1.9	19.6	21.0	21.8	80.9
25	Propyl acetate	4.8	9.6	16.4	17.8	115.2
26	1,4-Dioxane	8.3	12.9	17.7	20.5	85.7
27	Aniline	6.2	16.8	20.0	22.5	91.5

Table 4.1.4. TDM parameters of some polymers, $(MJ/m^3)^{1/2}$. [Adapted, by permission, from V.Yu. Senichev, V.V. Tereshatov , *Vysokomol . Soed .*, B31 , 216 (1989)]

Polymer	D	A	δ′	δ
Polymethylmethacrylate	2.5	6.5	18.6	19.8
Polyvinylacetate	4.9	10.4	17.8	19.2
Polystyrene	0.3	7.3	17.9	18.0
Polyvinylchloride	11.6	10.6	16.1	19.5

δ_h can be separated into donor and acceptor components using values of enthalpies of the hydrogen bond formation between proton-donors and proton-acceptors. In the absence of such data it is possible to evaluate TDM parameters by means of analysis of parameters of compounds similar in the chemical structure. For example, propyl acetate parameters can been calculated by the interpolation of corresponding parameters of butyl acetate and ethyl acetate,[24] parameters of benzene can be calculated by decomposition of δ_h into acceptor and donor components in the way used for toluene elsewhere.[25]

The solubility prediction can be made using the relationship between solubility and the χ_1 parameter (see Subchapter 4.2). The total value of the χ_1 parameter can be evaluated by adding the entropy contribution:

$$\chi_1 = \chi_S + \chi_H \qquad [4.1.45]$$

where:

χ_S an empirical value. Usually it is 0.2-0.4 for good solvents.

The value of the parameter is inversely proportional to coordination number that is number of molecules of a solvent interacting with a segment of polymer. The value of the entropy contribution to the parameter should be included in solubility calculations. The value $\chi_S = 0.34$ is then used in approximate calculations.

4.1.6 SOLUBILITY CRITERION

The polymer superstructure influences its solubility. Askadskii and Matveev proposed a new criterion of solubility for linear polymers based on interaction of forces of a surface tension on wetting.[38] The solubility parameter of polymer should be lower or equal to the work of rupture by solvent of a bond relative to a volume unit of the bond element. The condition of solubility can be expressed as follows:

$$\mu \le 2\rho\Phi\left(\frac{\gamma_p}{\gamma_s}\right)^{1/2} \qquad [4.1.46]$$

where:

μ $= \delta_p^2 / \delta_s^2$
δ_p, δ_s solubility parameters for polymer and solvent accordingly.

$$\rho = \frac{\varepsilon_{max}^{p} r_s}{\varepsilon_{max}^{s} r_p} \qquad [4.1.47]$$

$$\Phi = \frac{4\left(V_p V_s\right)^{1/2}}{\left(V_p^{1/2} + V_s^{1/2}\right)^2} \qquad [4.1.48]$$

where:

$\varepsilon_{max}^{p}, \varepsilon_{max}^{s}$ maximum deformations of polymer and solvent at rupture
r_s, r_p characteristic sizes of Frenkel's swarms for solvent and and small radius of globule of bond for polymer, respectively
V_p, V_s molar volumes of polymer and solvent (per unit)
$\Phi \approx 1$
$\rho \approx \text{const}$

The above expression was obtained with neglecting the preliminary swelling. Consideration of swelling requires correction for surface tension of swelled surface layers:

$$\mu < 2\rho\Phi\left[\Phi - \left(\Phi^2 - 1 + a\right)^{1/2}\right] \qquad [4.1.49]$$

where:

$$a = \gamma_{ps} / \gamma_p \qquad [4.1.50]$$

$$\gamma_{ps} = \gamma_p + \gamma_s - 2\Phi\left(\gamma_p \gamma_s\right)^{1/2} \qquad [4.1.51]$$

For practical purposes, the magnitude of ρ estimated graphically is 0.687. Thus

$$\mu < 1.374\beta \qquad [4.1.52]$$

$$\text{for } \beta = \Phi\left[\Phi - \left(\Phi^2 - 1 + a\right)^{1/2}\right]$$

For both polymers and solvents, the values of solubility parameters can be obtained experimentally (see Subchapters 5.1, 5.3). The surface tension of polymer can be calculated using parahor:

$$\gamma = (P / V)^4 \qquad [4.1.53]$$

where:

V molar volume of a repeated polymer unit

Then the value of V_p is calculated:

$$V_p = \frac{N_A \sum_i \Delta V_i}{k_{av}} \qquad [4.1.54]$$

where:

k_{av} = 0.681

If the density of polymer d_p is known, then $V_p = M/d_p$, where M is the molecular mass of a repeating unit. The values of parahors are given in Table 4.1.5.

Table 4.1.5. Values of parahors

Atom	C	H	O	O_2	N	S	F	Cl	Br	I
P	4.8	17.1	20.0	60.0	12.5	48.2	27.5	54.3	68.0	91.0

Increment	Double bond	Triple bond	3-member ring	4-member ring	5-member ring	6-member ring
P	23.2	46.4	16.7	11.6	8.5	6.1

The value of Φ is calculated from Eq. [4.1.48]. V_p, V_s are defined from ratios $V_p=M/d_p$ and $V_s=M/d_s$ where d_p, d_s are the densities of polymer and solvent, respectively. Then μ is calculated from Eq. [4.1.49]. The obtained value of μ from Eq. [4.1.49] is compared with value of $\mu = \delta_p^2 / \delta_s^2$ if the last value is lower or equal to the value of μ calculated from Eq. [4.1.49], polymer should dissolve in a given solvent with probability of 85 %.

4.1.7 SOLVENT SYSTEM DESIGN

One-component system. Solvents can be arranged in accordance to their solubility parameter as shown in Figure 4.1.1. It is apparent that a set of compatible solvents can be selected for polymer, determining their range based on the properties of polymer.

The simplest case is expressed by the Gee's equation for equilibrium swelling:[41]

$$Q = q_{max} \exp\left[-V_s \left(\delta_s - \delta_p\right)^2\right] \qquad [4.1.55]$$

where:

δ_s, δ_p solubility parameters for solvent and polymer.

The value of solubility parameter of solvent mixture with components having similar molar volumes is relative to their volume fractions and solubility parameters:

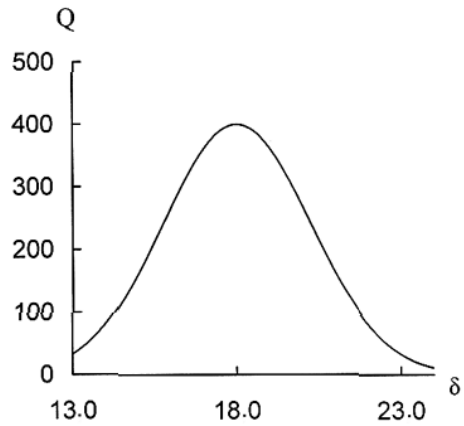

Figure 4.1.1. Representation of the one-component solubility parameter system. The curve represents Eq. [4.1.56] for polymer with $\delta = 18$ $(MJ/m^3)^{1/2}$.

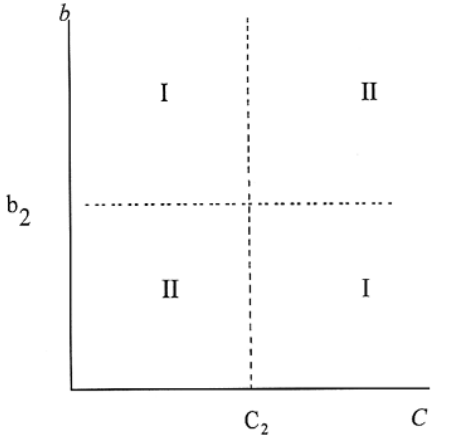

Figure 4.1.2. Representation of the two-component solubility parameter system in the Rider's approach. b_2, C_2 are the values of Rider's parameters for polymer.

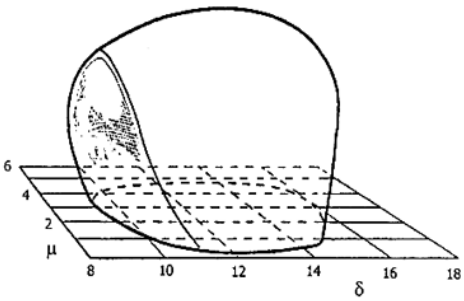

Figure 4.1.3. The solubility volume for cellulose acetate butyrate in terms of one-component solubility parameter, δ, dipole moment, μ, and (on vertical axis) the spectroscopic parameter, γ, from the approach developed by Crowley et.al.[2] [Adapted, by permission, from J.D. Crowley, G.S. Teague and J.W. Lowe, *J. Paint Technol.*, **38**, 269 (1966)]

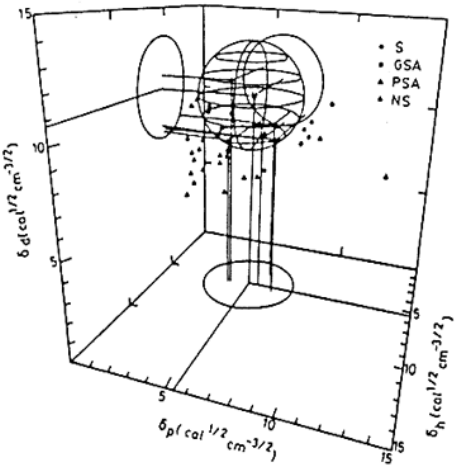

Figure 4.1.4. Hansen's solubility volume of polyimide synthesized from 3,3'4,4'-benzophenone tetracarboxylic dianhydride and 2,3,5,6-tetramethyl-p-phenylene diamine (after Lee[31]). [Adapted, by permission, from H.-R. Lee, Y.-D. Lee, *J. Appl. Polym. Sci*., **40**, 2087 (1990)]

$$\bar{\delta} = \sum_i \delta_i \varphi_i \qquad [4.1.56]$$

Solute is frequently soluble in a mixture of two non-solvents, for example, the mixture of diisopropyl ether ($\delta = 15.6$ $(MJ/m^3)^{1/2}$) and ethanol ($\delta = 26.4$ $(MJ/m^3)^{1/2}$) is a solvent for nitrocellulose ($\delta = 23$ $(MJ/m^3)^{1/2}$).

Two-component systems. Two parametrical models of solubility use two-dimensional graphs of solubility area. Two-dimensional solubility areas may be closed or open.

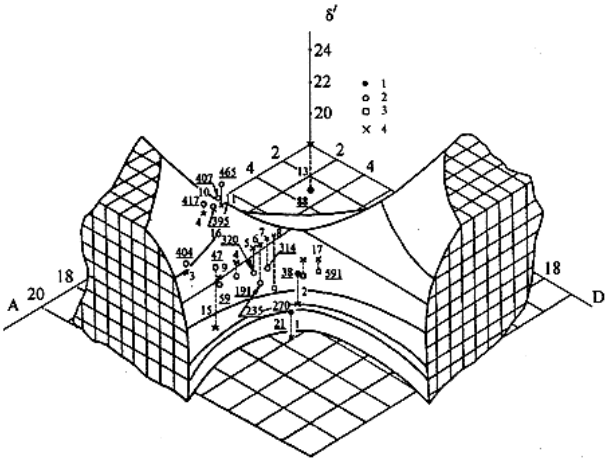

Figure 4.1.5. Volume of the increased swelling of crosslinked polybutadiene urethane elastomer, $\chi_H \le 0.85$. Labels of points: 1-outside volume, points with coordinates corresponding to solvents; 2-inside volume, points with coordinates corresponding to solvents; 3-the points with coordinates corresponding to polymer. This is the center of the volume. 4- points placed on a plane with coordinate $\delta = 18$ $(MJ/m^3)^{1/2}$. Number of solvent (not underlined number) corresponds to their position in the Table 4.1.3. The underlined number corresponds to swelling ratio at the equilibrium.

In accordance to the approach of Blanks and Prausnitz, the solubility area is displayed as a plane with two coordinates, λ, τ.[8,9] The parameters are related to Hansen's parameters by

$$\lambda = \delta_d, \quad \tau = \left(\delta_p^2 + \delta_h^2\right)^{1/2}$$

Solubility areas in this approach are closed because they are degenerated from Hansen's spheres (see below). Another example of application of degenerate Hansen's spheres was given by Chen.[18] Instead of parameters δ_p, δ_d the value χ_H is used which is calculated from the difference of the polar and dispersing contributions, δ_p, δ_d. The zone of solubility is a circle.

Lieberman[13] uses planes with coordinates δ, γ where γ is spectroscopic parameter (see Section 4.1.3). These planes are open and have the areas of solubility, non-solubility and intermediate.

In Rider's approach, the solubility area is a system of two quarters on a plane; two other quarters are the areas of non-solubility (Figure 4.1.2). Coordinates of this plane are accepting and donating abilities. Rider's approach finds application for solvents with high H-bond interactions.

Three-component systems. Crowley et. al.[2] proposed the three-dimensional solubility volumes (Figure 4.1.3). Better known are Hansen's three-dimensional solubility volumes (Figure 4.1.4). In Hansen's approach, the components of solubility parameters for mixed solvents δ_j are calculated from Eq. [4.1.56]:

$$\overline{\delta}_j = \sum_i \delta_{ji} \varphi_i \qquad [4.1.57]$$

The choice of a solvent for polymer is based on coordinates of polymer in space of coordinates δ_d, δ_p, δ_h and the radius of a solubility volume. For mixed solvents, their coordinates can be derived by connecting coordinates of individual solvents. This can be used to determine synergism in solvents for a particular polymer but it cannot demonstrate antisynergism of solvent mixtures (a mixture is less compatible with polymer than the individual solvents).

In the TDM approach, the solubility volume has also three coordinates, but the H-bond properties are taken into account. For this reason solubility volume can be represented by hyperbolic paraboloid (Figure 4.1.5). The use of this model permits to evaluate potential of synergism and antisynergism of solvent mixtures. It can be demonstrated by position of a point of a solvent mixture moving from a zone of good compatibility into the similar zone through the zone of inferior compatibility or, on the contrary, from a zone of an incompatibility into a similar zone through the zone of the improved compatibility. In the case of polymers that have no hydrogen bond forming abilities, this approach is equivalent to the Hansen or Blanks-Prausnitz approaches.

The above review of the methods of solvent evaluation shows that there is a broad choice of various techniques. Depending on the complexity of solvent-polymer interactions, the suitable method can be selected. For example, if solvents and/or polymer do not have functional groups to interact with as simple method as one-dimensional model is adequate. If weak hydrogen bonding is present, Hansen's approach gives good results (see further applications in Subchapter 5.3). In even more complex interactions, TDM model is always the best choice.

REFERENCES

1 W.W. Reynolds and E.C. Larson, *Off. Dig. Fed. Soc. Paint Technol*., **34**, 677 (1972).
2 J.D. Crowley, G.S.Teague and J.W. Lowe, J. Paint Technol., **38**, 269 (1966).
3 H. Burrel, *Off. Dig. Fed. Paint. Varn. Prod. Clubs*, **27**, 726 (1955).
4 P.L. Huyskens, M.C.Haulait-Pirson, *Org. Coat. Sci. Technol.*, **8**, 155 (1986).
5 I.H. Hildebrand , *J. Amer. Chem. Soc*., **38**, 1452, (1916).
6 G. Scatchard, *J. Amer. Chem. Soc.*, **56**, 995 (1934).
7 A.A. Tager, L.K. Kolmakova, *Vysokomol. Soed*., **A22**, 483 (1980).
8 R.F. Blanks, J.M. Prausnitz, *Ind. Eng. Chem., Fundam*., **3**, 1, (1964).
9 R.F. Weimer and J.M. Prausnitz, *Hydrocarbon Process*., **44**, 237 (1965).
10 R.A Keller, B.L.Karger and L.R. Snyder, *Gas Chromatogr., Proc. Int Symp. (Eur)*, **8**, 125 (1971).
11 D.G. Peiffer, *J. Appl. Polym. Sci.*, **25**, 369 (1980).
12 A. Beerbower, L.A. Kaye and D.E. Pattison, *Chem. Eng*., 118 (1967).
13 E.P. Lieberman, *Off. Dig. Fed. Soc. Paint Technol*., **34**, 30 (1962).
14 W.Gordy and S.C. Stanford, *J. Chem. Phys*., **8**, 170 (1940).
15 W.Gordy and S.C. Stanford, *J. Chem. Phys.*, **9**, 204 (1941).
16 J.D. Crowley, G.S. Teague and J.W. Lowe, *J. Paint Technol.*, **39**, 19 (1967).
17 R.C. Nelson, R.W. Hemwall and G.D Edwards, *J. Paint Technol.*, **42**, 636 (1970).
18 S.-A. Chen, *J. Appl. Polym. Sci*., **15**, 1247 (1971).
19 L.F. Henry, *Polym. Eng. Sci*., **14**, 167 (1974)
20 D. Hoernschemeyer, *J. Appl. Polym. Sci.*, **18**, 61 (1974).
21 P.A. Small, *J. Appl. Chem.*, **3**, 71 (1953).
22 H. Burrel, *Adv. Chem. Ser.*, No. 124, 1 (1973).
23 H. Renon, C.A Reckert and J.M. Prausnitz, *Ind. Eng. Chem*., **3**, 1(1964).
24 P.M Rider, *J. Appl. Polym. Sci.*, **25**, 2975 (1980).
25 P.M Rider, *Polym. Eng. Sci.*, **23**, 180 (1983).
26 C.M. Hansen, *J. Paint. Technol*., **39**, 104 (1967).
27 C.M. Hansen, *J. Paint. Technol*., **39**, 505 (1967).
28 C.M. Hansen and K. Scaarup, *J. Paint. Technol*., **39**, 511 (1967).
29 C.M. Hansen, **Three Dimensional Solubility Parameters and Solvent Diffusion Coefficient**, *Danish Technical Press*, Copenhagen, 1967.
30 C.M. Hansen and A. Beerbower in **Kirk-Othmer Encyclopedia of Chemical Technology**, Suppl. Vol., 2nd ed., A.Standen Ed., 889, 1971.
31 H.-R. Lee, Y.-D. Lee, *J. Appl. Polym.Sci*., **40**, 2087 (1990).
32 V.Yu. Senichev, V.V. Tereshatov, *Vysokomol. Soed*., **B31**, 216 (1989).
33 J.P.Teas, J. Paint Technol., **40**, 19 (1968).
34 D.M. Koenhen, C.A. Smolder, *J. Appl. Polym. Sci*., **19**, 1163 (1975).

35 R.A Keller, B.L. Karger and L.R. Snyder, *Gas Chromtogr., Proc. Int Symp. (Eur)*, **8**, 125(1971).
36 H.C. Brown, G.K. Barbaras, H.L. Berneis, W.H. Bonner, R.B. Johannesen, M. Grayson and K.L. Nelson, *J. Amer. Chem. Soc.*, **75**, 1 (1953).
37 A.E. Nesterov, **Handbook on physical chemistry of polymers. V. 1. Properties of solutions**, *Naukova Dumka*, Kiev, 1984.
38 A.A. Askadskii, Yu.I. Matveev, M.S. Matevosyan, *Vysokomol. Soed.* **32**, 2157 (1990).
39 Yu.I. Matveev, A.A. Askadskii, *Vysokomol. Soed.*, **36**, 436 (1994).
40 S.A. Drinberg, E.F. Itsko, **Solvents for paint technology**, *Khimiya*, Leningrad, 1986.
41 A.F. Barton, *Chem Rev.*, **75**, 735 (1975).

4.2 EFFECT OF SYSTEM VARIABLES ON SOLUBILITY

Valery Yu. Senichev, Vasiliy V. Tereshatov
Institute of Technical Chemistry
Ural Branch of Russian Academy of Sciences, Perm, Russia

Solubility in solvents depends on various internal and external factors. Chemical structure, molecular mass of solute, and crosslinking of polymer fall into the first group of factors, in addition to temperature and pressure in the second group of factors involved.

4.2.1 GENERAL CONSIDERATIONS

The process of dissolution is determined by a combination of enthalpy and entropy factors. The dissolution description can be based on the Flory-Huggins equation. Flory[1-3] and Huggins[4] calculated the entropy of mixing of long-chain molecules under the assumption that polymer segments occupy sites of a "lattice" and solvent molecules occupy single sites.

The theory implies that the entropy of mixing is combinatorial, i.e., it is stipulated by permutations of molecules into solution in which the molecules of mixed components differ greatly in size. The next assumption is that $\Delta V_{mix} = 0$ and that the enthalpy of mixing does not influence the value of ΔS_{mix}. The last assumptions are the same as in the Hildebrand theory of regular solutions.[5] The expression for the Gibbs energy of mixing is

$$\frac{\Delta G}{RT} = x_1 \ln \varphi_1 + x_2 \ln \varphi_2 + \chi_1 \varphi_1 \varphi_2 \left(x_1 + x_2 \frac{V_2}{V_1} \right) \qquad [4.2.1]$$

where:

x_1, x_2 molar fractions of solvent and polymer, respectively
χ_1 Huggins interaction parameter

The first two terms result from the configurational entropy of mixing and are always negative. For ΔG to be negative, the χ_1 value must be as small as possible. The theory assumes that the χ_1 parameter does not depend on concentration without experimental confirmation.

χ_1 is a dimensionless quantity characterizing the difference between the interaction energy of solvent molecule immersed in the pure polymer compared with interaction energy in the pure solvent. It is a semi-empirical constant. This parameter was introduced by Flory and Huggins in the equation for solvent activity to extend their theory for athermic processes to the non-athermic processes of mixing:

$$\ln a_1 = \frac{\Delta\mu_1}{RT} = \ln(1-\varphi_2) + \varphi_2 + \chi_1\varphi_2^2 \qquad [4.2.2]$$

where:

$$\chi_1 = z\Delta\varepsilon_{12}^* / kT \qquad [4.2.3]$$

$\Delta\varepsilon_{12}^* = 0.5(\varepsilon_{11}^* + \varepsilon_{22}^*) - \varepsilon_{12}^*$, a_1 - solvent activity, ε_{11}, ε_{22} - energy of 1-1 and 2-2 contacts formation in pure components, ε_{12}- energy of 1-2 contacts formation in the mixture, μ_1- chemical potential of solvent.

The critical value of χ_1 sufficient for solubility of polymer having large molecular mass is 0.5. Good solvents have a low χ_1 value. χ_1 is a popular practical solubility criterion and comprehensive compilations of these values have been published.[6-9]

Temperature is another factor. It defines the difference between polymer and solvent. Solvent is more affected than polymer. This distinction in free volumes is stipulated by different sizes of molecules of polymer and solvent. The solution of polymer in chemically identical solvent should have unequal free volumes of components. It causes important thermodynamic consequences. The most principal among them is the deterioration of compatibility between polymer and solvent at high temperatures leading to phase separation.

The theory of regular solutions operates with solutions of spherical molecules. For the long-chain polymer molecules composed of segments, the number of modes of arrangement in a solution lattice differs from a solution of spherical molecules, and hence it follows the reduction in deviations from ideal entropy of mixing. It is clear that the polymer-solvent interactions differ qualitatively because of the presence of segments.

Some novel statistical theories of solutions of polymers use the χ_1 parameter, too. They predict the dependence of the χ_1 parameter on temperature and pressure. According to the Prigogine theory of deformable quasi-lattice, a mixture of a polymer with solvents of different chain length is described by the equation:[10]

$$R\chi_1 = A(r_A / T) + (BT / r_A) \qquad [4.2.4]$$

where:

A, B	constants
r_A	number of chain segments in homological series of solvents.

These constants can be calculated from heats of mixing, values of parameter χ_1, and from swelling ratios. The Prigogine theory was further developed by Patterson, who proposed the following expression:[11]

$$\chi_1 = \left(\frac{U_1}{RT}\right)\nu^2 + \left(\frac{C_{P1}}{2R}\right)\tau^2 \qquad [4.2.5]$$

where:

U_1	configuration energy ($-U_1$ - enthalpy energy)
C_{P1}	solvent thermal capacity
ν, τ	molecular parameters

The first term of the equation characterizes distinctions in the fields of force of both sizes of segments of polymer and solvent. At high temperatures, in mixtures of chemically similar components, its value is close to zero. The second term describes the structural con-

tribution to χ_1 stipulated by the difference in free volumes of polymer and solvent. Both terms of the equation are larger than zero, and as temperature increases the first term decreases and the second term increases. The expression can be given in a reduced form (with some additional substitutions):[12]

$$\frac{\chi_1}{V_1^*} = \frac{P_1^*}{RT_1^*}\left[\frac{\tilde{V}_1^{1/3}}{\tilde{V}_1^{1/3}-1}\left(\frac{X_{12}}{P_1^*}\right)+\frac{\tilde{V}_1^{1/3}}{2\left(4/3-\tilde{V}_1^{1/3}\right)}\tau^2\right] \qquad [4.2.6]$$

where:

$\tilde{V}_1$, P_1^*, T_1^* reduced molar volume of solvent, pressure and temperature consequently

X_{12} contact interaction parameter.

These parameters can be calculated if factors of the volumetric expansion, isothermal compressibility, thermal capacity of a solvent and enthalpy of mixing of solution components are known.

With temperature decreasing, the first term of the right side of the expression [4.2.6] increases and the second term decreases. Such behavior implies the presence of the upper and lower critical temperatures of mixing. Later Flory developed another expression for χ_1 that includes the parameter of contact interactions, X_{12}:[13,14]

$$\chi_1 = \frac{P_1^* V_1^*}{\tilde{V}_1 RT}\left[\left(\frac{s_2}{s_1}\right)^2 \frac{X_{12}}{P_1^*}+\frac{\alpha_1 T}{2}\left\{\left(\frac{P_2^*}{P_1^*}\right)\tau-\frac{s_2}{s_1}\frac{X_{12}}{P_1^*}\right\}^2\right] \qquad [4.2.7]$$

where:

s_1, s_2 ratios of surfaces of molecules to their volumes obtained from structural data.

The large amount of experimental data is then an essential advantage of the Flory's theory.[9] Simple expressions exist for parameter X_{12} in the terms of X_{ij} characteristic parameters for chemically different segments of molecules of components 1 and 2. Each segment or chemical group has an assigned value of characteristic length (α_i, α_j) or surface area as a fraction of the total surface of molecule:[15]

$$X_{12} = \sum_{i,j}\left(\alpha_{i,1}-\alpha_{i,2}\right)\left(\alpha_{j,1}-\alpha_{j,2}\right)X_{ij} \qquad [4.2.8]$$

Bondi's approach may be used to obtain surface areas of different segments or chemical groups.[16] To some extent Huggins' new theory[17-21] is similar to Flory's theory.

4.2.2 CHEMICAL STRUCTURE

Chemical structure and the polarity determine dissolution of polymers. If the bonds in polymer and solvent are similar, then the energy of interaction between homogeneous and heterogeneous molecules is nearly identical which facilitates solubility of polymer. If the chemical structure of polymer and solvent molecule differ greatly in polarity, then swelling and dissolution does not happen. It is reflected in an empirical rule that "like dissolves like".

Nonpolar polymers (polyisoprene, polybutadiene) mix infinitely with alkanes (hexane, octane, etc.) but do not mix with such polar liquids as water and alcohols. Polar polymers (cellulose, polyvinylalcohol, etc.) do not mix with alkanes and readily swell in water. Polymers of the average polarity dissolve only in liquids of average polarity. For example, polystyrene is not dissolved or swollen in water and alkanes but it is dissolved in aromatic hydrocarbons (toluene, benzene, xylene), methyl ethyl ketone and some ethers. Polymethylmethacrylate is not dissolved nor swollen in water nor in alkanes but it is dissolved in dichloroethane. Polychloroprene does not dissolve in water, restrictedly swells in gasoline and dissolves in 1,2-dichloroethane and benzene. Solubility of polyvinylchloride was considered in terms of relationship between the size of a solvent molecule and the distance between polar groups in polymer.[22]

The above examples are related to the concept of the one-dimensional solubility parameter. However the effects of specific interactions between some functional groups can change compatibility of the system. Chloroalkanes compared with esters are known to be better solvents for polymethylmethacrylate. Aromatic hydrocarbons although having solubility parameters much higher than those of alkanes, dissolve some rubbers at least as well as alkanes. Probably it is related to increase in entropy change of mixing that has a positive effect on solubility.

The molecular mass of polymer significantly influences its solubility. With molecular mass of polymer increasing, the energy of interaction between chains also increases. The separation of long chains requires more energy than with short chains.

4.2.3 FLEXIBILITY OF A POLYMER CHAIN

The dissolution of polymer is determined by chain flexibility. The mechanism of dissolution consists of separating chains from each other and their transfer into solution. If a chain is flexible, its segments can be separated without a large expenditure of energy. Thus functional groups in polymer chain may interact with solvent molecules.

Thermal movement facilitates swelling of polymers with flexible chains. The flexible chain separated from an adjacent chain penetrates easily into solvent and the diffusion occurs at the expense of sequential transition of links.

The spontaneous dissolution is accompanied by decrease in free energy ($\Delta G < 0$) and that is possible at some defined values of ΔH and ΔS. At the dissolution of high-elasticity polymers $\Delta H \geq 0$, $\Delta S > 0$ then $\Delta G < 0$. Therefore high-elasticity polymers are dissolved in solvents completely.

The rigid chains cannot move gradually because separation of two rigid chains requires large energy. At usual temperatures the value of interaction energy of links between polymer chains and molecules of a solvent is insufficient for full separation of polymer chains. Amorphous linear polymers with rigid chains having polar groups swell in polar liquids but do not dissolve at normal temperatures. For dissolution of such polymers, the interaction between polymer and solvent (polyacrylonitrile in N,N-dimethylformamide) must be stronger.

Glassy polymers with a dense molecular structure swell in solvents with the heat absorption $\Delta H > 0$. The value of ΔS is very small. Therefore $\Delta G > 0$ and spontaneous dissolution is not observed and the limited swelling occurs. To a greater degree this concerns crystalline polymers which are dissolved if $\Delta H < 0$ and $|\Delta H| > |T\Delta S|$.

When molecular mass of elastic polymers is increased, ΔH does not change but ΔS decreases. The ΔG becomes less negative. In glassy polymers, the increase in molecular mass

is accompanied by a decrease in ΔH and ΔS. The ΔS value changes faster than the ΔH value, therefore the ΔG value becomes more negative, which means that the dissolution of polymeric homologues of the higher molecular weight becomes less favorable.

Crystalline polymers dissolve usually less readily than amorphous polymers. Dissolution of crystalline polymers requires large expenditures of energy for chain separation. Polyethylene swells in hexane at the room temperature and dissolves at elevated temperature. Isotactic polystyrene does not dissolve at the room temperature in solvents capable to dissolve atactic polystyrene. To be dissolved, isotactic polystyrene must be brought to elevated temperature.

4.2.4 CROSSLINKING

The presence of even a small amount of crosslinks hinders chain separation and polymer diffusion into solution. Solvent can penetrate into polymer and cause swelling. The swelling degree depends on crosslink density and compatibility of polymer and solvent.

The correlation between thermodynamic parameters and the value of an equilibrium swelling is given by Flory-Rehner equation[23] used now in a modified form:[24]

$$\ln(1-\varphi_2) + \varphi_2 + \chi_1\varphi_2^2 = -\frac{\nu_2}{V} V_s \left(\varphi_2^{1/3} - \frac{2\varphi_2}{f} \right) \qquad [4.2.9]$$

where:

φ_2	polymer volume fraction in a swollen sample
ν_2/V	volume concentration of elastically active chains
f	the functionality of polymer network

The value of ν_2/V is determined by the concentration of network knots. These knots usually have a functionality of 3 or 4. This functionality depends on the type of curing agent. Crosslinked polyurethanes cured by polyols with three OH-groups are examples of the three-functional network. Rubbers cured through double bond addition are examples of four-functional networks.

Eq. [4.2.9] has different forms depending on the form of elasticity potential but for practical purposes (evaluation of crosslinking density of polymer networks) it is more convenient to use the above form. The equation can be used in a modified form if the concentration dependence of the parameter χ_1 is known.

The value of equilibrium swelling can be a practical criterion of solubility. Good solubility of linear polymers is expected if the value of equilibrium swelling is of the order of 300-400%. The high resistance of polymers to solvents indicates that the equilibrium swelling does not exceed several percent.

In engineering data on swelling obtained at non-equilibrium conditions (for example, for any given time), swelling is frequently linked to the diffusion parameters of a system (see more on this subject in Subchapter 6.1).[25]

An interesting effect of swelling decrease occurs when swollen polymer is placed in a solution of linear polymer of the same structure as the crosslinked polymer. The decrease of solvent activity causes this effect. The quantitative description of these processes can be made by the scaling approach.[26]

4.2.5 TEMPERATURE AND PRESSURE

The temperature effect on solubility may have different characters depending on the molecular structure of solute. For systems of liquid-amorphous polymer or liquid-liquid, the tem-

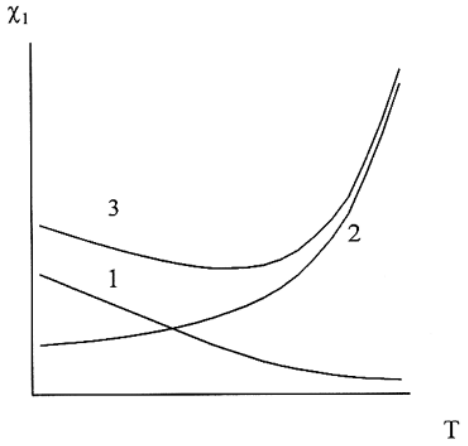

Figure 4.2.1 Two contributions to the χ_1 parameter. 1-χ_H, 2 -χ_S, 3 - the total value of χ_1.

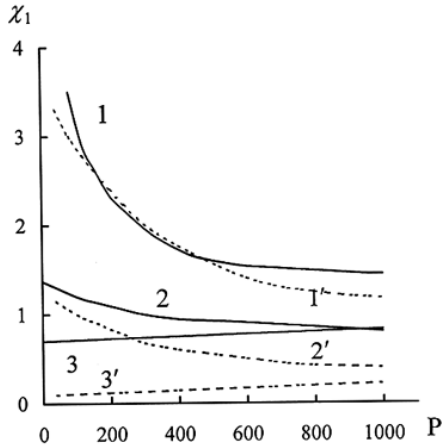

Figure 4.2.2 The χ_1 parameter as a function of pressure at T = 300K, r_1 = 3.5. The curves are for the following values of ε_{11}^* / ε_{22}^* = 0.85; 1.0 and 1.3 (After refs.[9,28]).

perature raise can cause improvement of compatibility. Such systems are considered to have the upper critical solution temperature (UCST). If the system of two liquids becomes compatible at any ratio at the temperature below the defined critical point, the system is considered to have the lower critical solution temperature (LCST). Examples of a system with UCST are mixtures of methyl ethyl ketone-water (150°C) and phenol-water (65.8°C). An example of a system with LCST is the mixture of water-triethylamine (18°C). There are systems with both critical points, for example, nicotine-water and glycerol-benzyl-ethylamine.

Presence of UCST in some cases means a rupture of hydrogen bonds on heating; however, in many cases, UCST is not determined by specific interactions, especially at high temperatures, and it is close to critical temperature for the liquid-vapor system.

There are suppositions that the UCST is the more common case but one of the critical points for polymer-solvent system is observed only at high temperatures. For example, polystyrene (M = 1.1×10^5) with methylcyclopentane has LCST 475K and UCST 370K. More complete experimental data on the phase diagrams of polymer-solvent systems are published elsewhere.[27]

The solubility of crystalline substances increases with temperature increasing. The higher the melting temperature of the polymer, the worse its solubility. Substances having higher melting heat are less soluble, with other characteristics being equal. Many crystalline polymers such as polyethylene or polyvinylchloride are insoluble at the room temperature (only some swelling occurs); however, at elevated temperature they dissolve in some solvents.

The experimental data on the temperature dependence of χ_1 of polymer-solvent systems are described by the dependence $\chi_1 = \alpha + \beta / T$. Often in temperatures below 100°C, $\beta < 0$.[9] In a wide temperature range, this dependence decreases non-linearly. The negative contribution to ΔS and positive contribution to the χ_1 parameter are connected with the difference of free volume. On heating the difference in free volumes of polymer and solvent in-

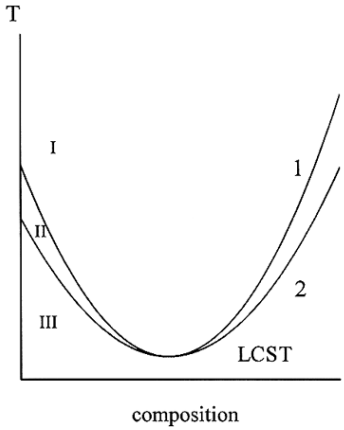

Figure 4.2.3. A phase diagram with the lower critical solution temperature (LCST).1-binodal, 2-spinodal; I- zone of non-stable conditions, II- zone of metastable conditions, III- zone of the one phase conditions.

creases as does the contribution into χ_S (Figure 4.2.1). For example, polyvinylchloride with dibutyl phthalate, tributylphosphate and some other liquids have values $\beta > 0$.

The dependence of solubility on pressure can be described only by modern theories taking into account the free volume of components.[28] The corresponding states theory predicts[12] a pressure dependence of the χ_1 parameter through the effect on the free volume of the solution components. This dependence is predicted by the so-called solubility parameters theory as well,[28] where the interaction between solvent and solute is described by solubility parameters with their dependencies on temperature and pressure (Fig. 4.2.2). When $\varepsilon_{11}^{*} / \varepsilon_{22}^{*} \le 1$ then $\delta_1 < \delta_2$ and hence $\partial\chi_1 / \partial P < 0$ in the solubility parameters theory and in the corresponding states theory. When $\varepsilon_{11}^{*} / \varepsilon_{22}^{*}$ is greater than unity $\delta_1 > \delta_2$ and the solvent becomes less compressible than the polymer. Then pressure can increase the $(\delta_1 - \delta_2)$ value, giving $\partial\chi_1 / \partial P > 0$.

4.2.6 METHODS OF CALCULATION OF SOLUBILITY BASED ON THERMODYNAMIC PRINCIPLES

Within the framework of the general principles of thermodynamics of solutions, the evaluation of solubility implies the evaluation of value of the Gibbs energy of mixing in the whole range of concentrations of solution. However, such evaluation is difficult and for practical purposes frequently unnecessary. The phase diagrams indicate areas of stable solutions. But affinity of solvent to polymer in each of zone of phase diagram differs. It is more convenient to know the value of the interaction parameter, possibly with its concentration dependence. Practical experience from solvent selection for rubbers gives foundations for use of equilibrium swelling of a crosslinked elastomer in a given solvent as a criterion of solubility. The equilibrium swelling is related to χ_1 parameter by Eq. [4.2.9]. As previously discussed in Subchapter 4.1, the value of the χ_1 parameter can be determined as a sum of entropy and enthalpy contributions. In the one-dimensional solubility parameter approach, one may use the following equation:

$$\chi_1 = \chi_S + \frac{(\delta_1 - \delta_2)^2 V_1}{RT} \qquad [4.2.10]$$

where:

χ_S the entropy contribution

In TDM approach, Eq. [4.1.45] can be used. Similar equations can be derived for the Hansen approach. All existing systems of solubility imply some constancy of the entropy contribution or even constancy in some limits of a change of cohesion characteristics of polymers. Frequently $\chi_1 = 0.34$ is used in calculations.

Phase diagrams are characterized by critical temperatures, spinodals and binodals. A binodal is a curve connecting equilibrium structures of a stratified system. A spinodal is a curve defining boundary of metastables condition (Fig.4.2.3).

Binodals are evaluated experimentally by light scattering at cloud point,[29] by volume changes of coexisting phases,[30] or by the electron probe R-spectral analysis.[31]

It is possible to calculate phase behavior, considering that binodals correspond to a condition:

$$(\Delta\mu_i)' = (\Delta\mu_i)'' \qquad [4.2.11]$$

where:

i a component of a solution

$(\Delta\mu_i)', (\Delta\mu_i)''$ changes of a chemical potential in phases of a stratified system

The equation of the spinodal corresponds to the condition

$$\frac{\partial^2(\Delta G)}{\partial\varphi_i^2} = \frac{\partial(\Delta\mu_i)}{\partial\varphi_i} = 0 \qquad [4.2.12]$$

where:

ΔG the Gibbs free mixing energy

φ_i volume fraction of a component of a solvent.

At a critical point, binodal and spinodal coincide

$$\frac{\partial^2(\Delta G)}{\partial\varphi_i^2} = \frac{\partial^3(\Delta G)}{\partial\varphi_i^3} \qquad [4.2.13]$$

In the elementary case of a two-component system, the Flory-Huggins theory gives the following solution:[3]

$$\Delta\mu_i = RT\left[\ln\varphi_i + \left(1-\frac{r_i}{r_j}\right)(1-\varphi_i) + r_i\chi_1\varphi_i^2\right] \qquad [4.2.14]$$

where:

r_i, r_j numbers of segments of corresponding component.

The last equation can be solved if one takes into account the equality of chemical potentials of a component in two co-existing phases of a stratified system.

$$\ln\varphi_i' + \left(1-\frac{x_i}{x_j}\right)\varphi_j' + x_i\chi_{ij}(\varphi_i')^2 = \ln\varphi_i'' + \left(1-\frac{x_i}{x_j}\right)\varphi_j'' + x_i\chi_{ij}(\varphi_i'')^2 \qquad [4.2.15]$$

REFERENCES

1 P.J. Flory, *J. Chem. Phys*., **9**, 660, (1941).
2 P.J. Flory, *J. Chem. Phys.*, **10**, 51 (1942).
3 P.J. Flory, **Principles of polymer chemistry**, *Cornell University Press*, Ithaca, 1953.
4 M.L. Huggins, *J. Chem. Phys.*, **9**, 440 (1941).

5 J.H. Hildebrand and R.L. Scott, **Solubility of none-electrolytes**. 3rd ed., *Reinhold*, New-York, 1950.
6 R.M.Masegosa, M.G. Prolonga, A. Horta, *Macromolecules*, **19**, 1478 (1986)
7 G.M. Bristow, *J. Polym. Sci.*, **36**, 526 (1959).
8 J. Rehner, *J. Polym. Sci.*, **46**, 550 (1960).
9 A.E. Nesterov, **Handbook on physical chemistry of polymers. V. 1. Properties of solutions**, *Naukova Dumka*, Kiev, 1984.
10 I. Prigogine, **The molecular theory of solutions**, New York, **Interscience**, 1959.
11 D. Patterson, G. Delmas, T. Somsynsky, *J. Polym. Sci.*, **57**, 79 (1962).
12 D. Patterson, *Macromolecules*, **2**, 672 (1969).
13 P.J. Flory, R.A. Orwoll, A Vrij, *J. Amer. Chem. Sci*., **86**, 3507 (1968).
14 P.J. Flory, *J. Amer. Chem. Sci*., **87**, 1833 (1965).
15 A. Abe, P.J Flory, *J. Amer. Chem. Sci.*, **87**, 1838 (1965).
16 V. Crescenzi, G. Manzini, *J. Polym. Sci., C*, **54**, 315 (1976).
17 A. Bondi, **Physical properties of molecular crystals, liquids and glasses**. New York, *Wiley*, 1968
18 M.L. Huggins, *J. Phys. Chem*., **74**, 371 (1970).
19 M.L. Huggins, *Polymer*, **12**, 389 (1971).
20 M.L. Huggins, *J. Phys. Chem.*, **75**, 1255 (1971).
21 M.L. Huggins, *Macromolecules*, **4**, 274 (1971).
22 K. Thinius, *Chem. Techn*., **6**, 330 (1954).
23 P.J. Flory, J. Rehner, *J. Chem. Phys.*, **11**, 512 (1943).
24 A.E. Oberth, R.S. Bruenner, *J. Polym. Sci*., **8**, 605 (1970).
25 U.S. Aithal, T.M. Aminabhavi, *Polymer*, **31**, 1757 (1990).
26 J. Bastide, S. Candau, L. Leibner, *Macromolecules*, **14**, 319 (1981).
27 A.E.Nesterov, Y.S. Lipatov, **Phase condition of polymer solutions and mixtures**, *Naukova dumka,* Kiev, 1987.
28 J. Biros, L. Zeman, D.Patterson, *Macromolecules*, **4**, 30 (1971).
29 J.W. Kennedy , M. Gordon, G.A. Alvarez, *J. Polym. Sci.*, **20**, 463 (1975).
30 R. Konningsveld, *Brit. Polym. J*., **7**, 435 (1975).
31 N.N. Avdeev, A.E. Chalych, Y.N. Moysa, R.C. Barstein, *Vysokomol. soed*., **A22**, 945 (1980).

4.3 POLAR SOLVATION DYNAMICS: THEORY AND SIMULATIONS

Abraham Nitzan
School of Chemistry,
The Sackler Faculty of Sciences, Tel Aviv University, Tel Aviv, Israel

4.3.1 INTRODUCTION

When an ion or, more generally, a charge distribution associated with a given solute is placed in a dielectric solvent, the solvent responds to accommodate this solute and to minimize the free energy of the overall system. Equilibrium aspects of this phenomenon are related to macroscopic observables such as solvation free energy and microscopic properties such as the structure of the solvation 'shell'. Dynamical aspects of this process are manifested in the time evolution of this solvent response.[1] A direct way to observe this dynamics is via the time evolution of the spectral line-shifts following a pulse excitation of a solute molecule into an electronic state with a different charge distribution.[1] Indirectly, this dynamics can have a substantial effect on the course and the rate of chemical reactions that involve a redistribution of solute charges in the polar solvent environment.[2] Following a brief introduction to this subject within the framework of linear response and continuum dielectric theories, this chapter describes numerical simulation studies of this process, and con-

trasts the results obtained from such simulations with those obtained from linear response continuum models. In particular we focus on the following issues:

- How well can the solvation process be described by linear response theory?
- To what extent can the dynamics of the solvation process be described by continuum dielectric theory?
- What are the signatures of the solute and solvent structures in the deviation of the observed dynamics from that predicted by continuum dielectric theory?
- What are the relative roles played by different degrees of freedom of the solvent motion, in particular, rotation and translation, in the solvation process?
- How do inertial (as opposed to diffusive) solvent motions manifest themselves in the solvation process?

This chapter is not an exhaustive review of theoretical treatments of solvation dynamics. Rather, it provides, within a simple model, an exposition of the numerical approach to this problem. It should be mentioned that a substantial effort has been recently directed towards developing a theoretical understanding of this phenomenon. The starting point for such analytical efforts is linear response theory. Different approaches include the dynamical mean spherical approximation (MSA),[3,4] generalized transport equations,[5-8] and ad hoc models for the frequency and wavevector dependence of the dielectric response function $\varepsilon(k,\omega)$.[9] These linear response theories are very valuable in providing fundamental understanding. However, they cannot explore the limits of validity of the underlying linear response models. Numerical simulations can probe non-linear effects, but are very useful also for the direct visualization and examination of the interplay between solvent and solute properties and the different relaxation times associated with the solvation process. A substantial number of such simulations have been carried out in recent years.[10,11] The present account describes the methodology of this approach and the information it yields.

4.3.2 CONTINUUM DIELECTRIC THEORY OF SOLVATION DYNAMICS

The Born theory of solvation applies continuum dielectric theory to the calculation of the solvation energy of an ion of charge q and radius a in a solvent characterized by a static dielectric constant, ε_s. The well known result for the solvation free energy, i.e., the reversible work needed to transfer an ion from the interior of a dielectric solvent to vacuum, is

$$W = \frac{q^2}{2a}\left(\frac{1}{\varepsilon_s} - 1\right) \qquad [4.3.1]$$

Eq. [4.3.1] corresponds only to the electrostatic contribution to the solvation energy. In experiments where the charge distribution on a solute molecule is suddenly changed (e.g. during photoionization of the solute) this is the most important contribution because short range solute-solvent interactions (i.e., solute size) are essentially unchanged in such processes. The origin of W is the induced polarization in the solvent under the solute electrostatic field.

The time evolution of this polarization can be computed from the dynamic dielectric properties of the solvent expressed by the dielectric response function $\varepsilon(\omega)$.[12] Within the usual linear response assumption, the electrostatic displacement and field are related to each other by

$$D(t) = \int_{-\infty}^{t} dt' \varepsilon(t-t') E(t') \qquad [4.3.2]$$

and their Fourier transforms (e.g. $E(\omega) = \int_{-\infty}^{\infty} dt e^{-i\omega t} E(t)$) satisfy

$$D(\omega) = \varepsilon(\omega) E(\omega) \qquad [4.3.3]$$

where

$$\varepsilon(\omega) \equiv \int_{0}^{\infty} dt e^{-i\omega t} \varepsilon(t) \qquad [4.3.4]$$

rewriting ε(t) in the form

$$\varepsilon(t) = 2\varepsilon_e \delta(t) + \tilde{\varepsilon}(t) \qquad [4.3.5]$$

we get

$$D(t) = \varepsilon_e E(t) + \int_{-\infty}^{t} dt' \tilde{\varepsilon}(t-t') E(t') \qquad [4.3.6]$$

$$D(\omega) = \varepsilon_e E(\omega) + \tilde{\varepsilon}(\omega) E(\omega) \qquad [4.3.7]$$

In Eq. [4.3.5] ε_e is the "instantaneous" part of the solvent response, associated with its electronic polarizability. For simplicity we limit ourselves to the Debye model for dielectric relaxation in which the kernel $\tilde{\varepsilon}$ in [4.3.5] takes the form

$$\tilde{\varepsilon}(t) = \frac{\varepsilon_s - \varepsilon_e}{\tau_D} e^{-t/\tau_D} \qquad [4.3.8]$$

This function is characterized by three parameters: the electronic ε_e and static ε_s response constants, and the Debye relaxation time, τ_D. In this case

$$\varepsilon(\omega) = \varepsilon_e + \int_{0}^{\infty} dt \frac{\varepsilon_s - \varepsilon_e}{\tau_D} e^{-t/\tau} e^{-i\omega t} = \varepsilon_e + \frac{\varepsilon_s - \varepsilon_e}{1 + i\omega\tau_D} \qquad [4.3.9]$$

In this model a step function change in the electrostatic field

$$E(t) = 0, t < 0; \quad E(t) = E, t \geq 0 \qquad [4.3.10]$$

leads to

$$D(t) = \varepsilon_e E(t) + \int_{0}^{t} \frac{\varepsilon_s - \varepsilon_e}{\tau_D} e^{-(t-t')/\tau_D} E(t') dt' = \left[\varepsilon_s \left(1 - e^{-t/\tau_D} \right) + \varepsilon_e e^{-t/\tau_D} \right] E \qquad [4.3.11]$$

For $t \to 0$, D(t) becomes $\varepsilon_e E$, and for $t \to \infty$ it is $D = \varepsilon_s E$. The relaxation process which carries the initial response to its final value is exponential, with the characteristic relaxation time, τ_D.

The result [4.3.11] is relevant for an experiment in which a potential difference is suddenly switched on and held constant between two electrodes separated by a dielectric spacer. This means that the electrostatic field is held constant as the solvent polarization relaxes. For this to happen the surface charge density on the electrodes, i.e. the dielectric displacement **D**, has to change under the voltage source so as to keep the field constant.

The solvation dynamics experiment of interest here is different: Here at time t = 0 the charge distribution $\rho(\mathbf{r})$ is switched on and is kept constant as the solvent relaxes. In other words, the dielectric displacement **D**, the solution of the Poisson equation $\nabla \mathbf{D} = 4\pi\rho$ that corresponds to the given ρ is kept constant while the solvent polarization and the electrostatic field relax to equilibrium. To see how the relaxation proceeds in this case we start again from

$$D(t) = \varepsilon_e E(t) + \int_{-\infty}^{t} dt' \tilde{\varepsilon}(t-t') E(t') \qquad [4.3.12]$$

take the time derivative of both sides with respect to t

$$\frac{dD}{dt} = \varepsilon_e \frac{dE}{dt} + E(t)\tilde{\varepsilon}(0) + \int_{-\infty}^{t} dt' \left(\frac{d\tilde{\varepsilon}}{dt}\right)_{t-t'} E(t') \qquad [4.3.13]$$

use the relations $\tilde{\varepsilon}(0) = (\varepsilon_s - \varepsilon_e)/\tau_D$ and

$$\int_{-\infty}^{t} dt' \left(\frac{d\tilde{\varepsilon}}{dt}\right)_{t-t'} E(t') = -\frac{1}{\tau_D} \int_{-\infty}^{t} \tilde{\varepsilon}(t-t') E(t') = -\frac{1}{\tau_D} \left(D(t) - \varepsilon_e E(t)\right)$$

(cf Eq. [4.3.8]), to get

$$\frac{d}{dt}(D - \varepsilon_e E) = -\frac{1}{\tau_D}(D - \varepsilon_s E) \qquad [4.3.14]$$

When D evolves under a constant E, Eq. [4.3.14] implies that $(d/dt)D = (-1/\tau_D)D + \text{constant}$, so that D relaxes exponentially with the time constant τ_D, as before. However if E relaxes under a constant D, the time evolution of E is given by

$$\frac{d}{dt} E = -\frac{\varepsilon_s}{\varepsilon_e \tau_D} \left(E - \frac{1}{\varepsilon_s} D\right) \qquad [4.3.15]$$

i.e.

$$E(t) = \frac{1}{\varepsilon_s} D + A e^{-t/\tau_L} \qquad [4.3.16]$$

where A is an integration constant and τ_L is the longitudinal Debye relaxation time

$$\tau_L = \frac{\varepsilon_e}{\varepsilon_s}\tau_D \qquad [4.3.17]$$

The integration constant A is determined from the initial conditions: Immediately following the switch-on of the charge distribution, i.e. of D, E is given by $E(t=0) = D/\varepsilon_e$, so $A = \left(\varepsilon_e^{-1} - \varepsilon_s^{-1}\right) D$. Thus, finally,

$$E(t) = \frac{1}{\varepsilon_s} D + \left(\frac{1}{\varepsilon_e} - \frac{1}{\varepsilon_s}\right) D e^{-t/\tau_L} \qquad [4.3.18]$$

We see that in this case the relaxation is characterized by the time τ_L which can be very different from τ_D. For example, in water $\varepsilon_e / \varepsilon_s \cong 1/40$, and while $\tau_D \cong 10$ps, τ_L is of the order of 0.25ps.

4.3.3 LINEAR RESPONSE THEORY OF SOLVATION DYNAMICS

The continuum dielectric theory of solvation dynamics is a linear response theory, as expressed by the linear relation between the perturbation D and the response of E, Eq. [4.3.2]. Linear response theory of solvation dynamics may be cast in a general form that does not depend on the model used for the dielectric environment and can therefore be applied also in molecular theories.[13,14] Let

$$H = H_0 + H' \qquad [4.3.19]$$

where H_0 describes the unperturbed system that is characterized by a given potential surface on which the nuclei move, and where

$$H' = \sum_j X_j F_j(t) \qquad [4.3.20]$$

is some perturbation written as a sum of products of system variables X_j and external time dependent perturbations $F_j(t)$. The nature of X and F depend on the particular experiment: If for example the perturbation is caused by a point charge q(t) at position r_j, $q(t)\delta(r-r_j)$, we may identify F(t) with this charge and the corresponding X_j is the electrostatic potential operator at the charge position. For a continuous distribution $\rho(\mathbf{r},t)$ of such charge we may write $H' = \int d^3\mathbf{r}\Phi(\mathbf{r})\rho(\mathbf{r},t)$, and for $\rho(\mathbf{r},t) = \sum_j q_j(t)\,\delta(\boldsymbol{r} - \boldsymbol{r}_j)$ this becomes $\sum_j \Phi(\boldsymbol{r}_j)\, q_j(t)$. Alternatively we may find it convenient to express the charge distribution in terms of point moments (dipoles, quadrupoles, etc.) coupled to the corresponding local potential gradient tensors, e.g. H′ will contain terms of the form $\mu\nabla\Phi$ and $\mathbf{Q}{:}\nabla\nabla\Phi$ where μ and $\mathbf{Q}$ are point dipoles and quadrupoles respectively.

In linear response theory the corresponding solvation energies are proportional to the corresponding products $q\langle\Phi\rangle$, $\mu\langle\nabla\Phi\rangle$ and $\mathbf{Q}{:}\langle\nabla\nabla\Phi\rangle$ where $\langle\rangle$ denotes the usual observable average. For example, the average potential $\langle\Phi\rangle$ is proportional in linear response to the perturbation source q. The energy needed to create the charge q is therefore $\int_0^q dq'\langle\Phi\rangle \approx (1/2)q^2 \approx (1/2)q\langle\Phi\rangle$.

Going back to the general expressions [4.3.19] and [4.3.20], linear response theory relates non-equilibrium relaxation close to equilibrium to the dynamics of equilibrium fluctu-

ations: The first fluctuation dissipation theorem states that following a step function change in F:

$$F_j(t) = 0, t < 0; \quad F_j(t) = F_j, t \geq 0 \qquad [4.3.21]$$

the corresponding averaged system's observable relaxes to its final equilibrium value as $t \to \infty$ according to

$$\langle X_j(t)\rangle - \langle X_j(\infty)\rangle = \frac{1}{k_B T}\sum_l F_l\left(\langle X_j X_l(t)\rangle - \langle X_j\rangle\langle X_l\rangle\right) \qquad [4.3.22]$$

where all averages are calculated with the equilibrium ensemble of H_0. Applying Eq. [4.3.22] to the case where a sudden switch of a point charge $q \to q + \Delta q$ takes place, we have

$$\langle \Phi(t)\rangle - \langle \Phi(\infty)\rangle = \frac{\Delta q}{k_B T}\left(\langle \Phi\Phi(t)\rangle - \langle \Phi\rangle^2\right) = \frac{\Delta q}{k_B T}\langle \delta\Phi\delta\Phi(t)\rangle \qquad [4.3.23]$$

The left hand side of [4.3.23], normalized to 1 at t = 0, is a linear approximation to the solvation function

$$S(t) = \frac{E_{solv}(t) - E_{solv}(\infty)}{E_{solv}(0) - E_{solv}(\infty)} \underline{\underline{LR}} \frac{\langle \Phi(t)\rangle - \langle \Phi(\infty)\rangle}{\langle \Phi(0)\rangle - \langle \Phi(\infty)\rangle} \qquad [4.3.24]$$

and Eq. [4.3.23] shows that in linear response theory this non equilibrium relaxation function is identical to the equilibrium correlation function

$$S(t) \underline{\underline{LR}} C(t) \equiv \frac{\langle \delta\Phi(0)\,\delta\Phi(t)\rangle}{\langle \delta\Phi^2\rangle} \qquad [4.3.25]$$

C(t) is the time correlation function of equilibrium fluctuations of the solvent response potential at the position of the solute ion. The electrostatic potential in C(t) will be replaced by the electric field or by higher gradients of the electrostatic potential when solvation of higher moments of the charge distribution is considered.

The time dependent solvation function S(t) is a directly observed quantity as well as a convenient tool for numerical simulation studies. The corresponding linear response approximation C(t) is also easily computed from numerical simulations, and can also be studied using suitable theoretical models. Computer simulations are very valuable both in exploring the validity of such theoretical calculations, as well as the validity of linear response theory itself (by comparing S(t) to C(t)). Furthermore they can be used for direct visualization of the solute and solvent motions that dominate the solvation process. Many such simulations were published in the past decade, using different models for solvents such as water, alcohols and acetonitrile. Two remarkable outcomes of these studies are first, the close qualitative similarity between the time evolution of solvation in different simple solvents, and second, the marked deviation from the simple exponential relaxation predicted by the Debye relaxation model (cf. Eq. [4.3.18]). At least two distinct relaxation modes are

observed, a fast Gaussian-like component and a slower relaxation mode of an exponential character which may correspond to the expected Debye relaxation. In what follows we describe these and other features observed in computer simulations of solvation dynamics using simple generic model dielectric solvents.

4.3.4 NUMERICAL SIMULATIONS OF SOLVATION IN SIMPLE POLAR SOLVENTS: THE SIMULATION MODEL[11a]

The simplest simulated system is a Stockmayer fluid: structureless particles characterized by dipole-dipole and Lennard-Jones interactions, moving in a box (size L) with periodic boundary conditions. The results described below were obtained using 400 such particles and in addition a solute atom A which can become an ion of charge q embedded in this solvent. The long range nature of the electrostatic interactions is handled within the effective dielectric environment scheme.[15] In this approach the simulated system is taken to be surrounded by a continuum dielectric environment whose dielectric constant ε' is to be chosen self consistently with that computed from the simulation. Accordingly, the electrostatic potential between any two particles is supplemented by the image interaction associated with a spherical dielectric boundary of radius R_c (taken equal to L/2) placed so that one of these particles is at its center. The Lagrangian of the system is given by

$$L\left(R,\dot{R},\mu,\dot{\mu}\right)=\frac{1}{2}M_A\dot{R}_A^2+\frac{1}{2}M\sum_{i=1}^{N}\dot{R}_i^2+\frac{1}{2}M\sum_{i=1}^{N}\frac{I}{\mu^2}\dot{\mu}_i^2-\frac{1}{2}\sum_{i\neq j}^{N}V_{ij}^{IJ}\left(R_{ij}\right)-\sum_{i=1}^{N}V_{iA}^{IJ}\left(R_{iA}\right)-$$

$$-\frac{1}{2}\sum_{i\neq j}^{N}V^{DD}\left(R_i,R_j,\mu_i,\mu_j\right)-\sum_{i=1}^{N}V^{AD}\left(R_A,R_i,\mu_i\right)-\sum_{i=1}^{N}\lambda_i\left(\mu_i^2-\mu^2\right) \qquad [4.3.26]$$

where N is the number of solvent molecules of mass M, μ dipole moment, and I moment of inertia. R_A and R_i are positions of the impurity atom (that becomes an ion with charge q) and a solvent molecule, respectively, and R_{ij} is $|R_i - R_j|$. V^{LJ}, V^{DD} and V^{AD} are, respectively, Lennard-Jones, dipole-dipole, and charge-dipole potentials, given by

$$V_{ij}^{LJ}(R)=e\varepsilon_D\left[\left(\sigma_D/R\right)^{12}-\left(\sigma_D/R\right)^{6}\right] \qquad [4.3.27]$$

(V_{ij}^{LJ} is of the same form with σ_A and ε_A replacing σ_D and ε_D) and

$$V^{DD}\left(R_i,R_j,\mu_i,\mu_j\right)=\frac{\mu_i\mu_j-3\left(n\mu_i\right)\left(n\mu_j\right)}{R_{ij}^3}-\frac{2\left(\varepsilon'-1\right)}{\left(2\varepsilon'+1\right)R_C^3}\mu_i\mu_j \qquad [4.3.28]$$

where $n = (R_i - R_j)/R_{ij}$,

$$V^{AD}\left(R_i,\mu_i,R_A\right)=q\left(\frac{1}{R_{ij}^3}-\frac{2\left(\varepsilon'-1\right)}{\left(2\varepsilon'+1\right)R_C^3}\right)\mu_i\left(R_i-R_A\right) \qquad [4.3.29]$$

The terms containing ε' in the electrostatic potentials V^{DD} and V^{AD} are the reaction field image terms.[15,16] The last term in Eq. [4.3.26] is included in the Lagrangian as a constraint, in order to preserve the magnitude of the dipole moments $\left(|\mu_i|=\mu\right)$ with a SHAKE

like algorithm.[17] In this representation the mass, M, and the moment of inertia, I, of the solvent molecules are independent parameters, which makes it possible to study the relative importance of translational and rotational motions in the solvation process without affecting other potentially relevant parameters such as the molecular size. The time evolution is done using the velocity Verlet algorithm, with the value of $\lambda(t)$ determined as in the SHAKE algorithm, and with the Andersen[18] thermalization used to keep the system at constant temperature.

For the Stockmayer solvent, the initial molecular parameters are taken to approximate the CH_3Cl molecule: $\sigma_D = 4.2$ Å, $\varepsilon_D = 195$K, M = 50 amu, I = 33.54 amu Å^2, and $\mu = 1.87$ D. The parameters taken for the solvated ion are $M_A = 25$ amu, $\sigma_A = 3.675$ Å, and $\varepsilon_A = 120$K, q is taken to be one electron charge e. These parameters can be changed so as to examine their effect on the solvation dynamics. Most of the results described below are from simulations done at 240K, and using L = 33.2Å for the edge length of the cubic simulation cell was, corresponding to the density $\rho = 1.09\times10^{-2}$ Å^{-3}, which is the density of CH_3Cl at this temperature. In reduced units we have for this choice of parameters $\rho^* \equiv \rho\sigma_D^3 = 0.81$, $\mu^* \equiv \mu\left(\varepsilon_D\sigma_D^3\right)^{1/2} = 1.32$, $T^* \equiv k_BT/\varepsilon_D = 1.23$, and $I^* \equiv I(M\sigma^2) = 0.038$. A simple switching function

$$f(R) = \begin{cases} 1 & R < R_s \\ (R_c - R)/(R_c - R_s) & R_s < R < R_c \\ 0 & R > R_c \end{cases} \qquad [4.3.31]$$

is used to smoothly cut off this electrostatic potential. R_c and R_s are taken to be $R_c = L/2$ and $R_s = 0.95R_c$. Under these simulation conditions the pressure fluctuates in the range 500±100 At.The dielectric constant is computed from pure solvent simulations, using the expression[33]

$$\frac{(\varepsilon - 1)(2\varepsilon' + 1)}{2\varepsilon' + \varepsilon} = \frac{1}{k_BTR_c^3}\left\langle PP(R_c)\right\rangle \qquad [4.3.32]$$

where

$$P = \sum_{i=1}^{N}\mu_i \qquad [4.3.33]$$

and

$$P(R_c) = \frac{1}{N}\sum_{j=1}^{N}\sum_{k=1}^{N}{}'\mu_k \qquad [4.3.34]$$

where the prime on the inner summation indicates the restriction $R_{jk} < R_c$. The result for our solvent is $\varepsilon = 17$, compared with $\varepsilon(CH_3Cl) = 12.6$ at 253K. After evaluating ε in this way the external dielectric constant ε' is set to ε and the computation is, in principle, repeated until convergence, i.e., until the evaluated ε is equal to the environmental ε'. In fact, we have found that our dynamical results are not sensitive to the magnitude of ε'.

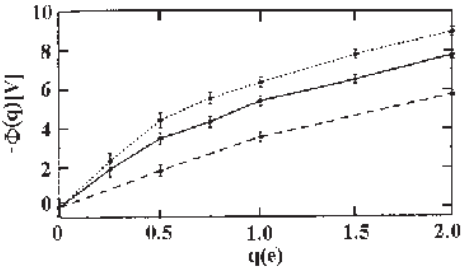

Figure 4.3.1. The electrostatic response potential <Φ> induced by the solvent at the position of the solute ion, as a function of the solute charge. Dashed line - the Stockmayer-CH_3Cl model described in Section 4. Full and dotted lines, model polyether solvents described in the text. [From Ref. 11b].

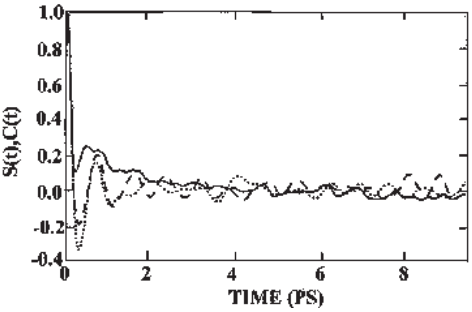

Figure 4.3.2. The linear response relaxation function C(t) (dashed and dotted lines] and the non-equilibrium solvation function S(t) (solid line) computed for the Stockmayer-CH_3Cl model described in Section 4. In the nonequilibrium simulation the ion charge is switched on at t = 0. The dotted and dashed lines represent C(t) obtained from equilibrium simulations with uncharged and charged ion, respectively. [From Ref. 11a].

A typical timestep for these simulation is 3fs. In the absence of thermalization this gives energy conservation to within 10^{-4} over ~80,000 time steps. After equilibrating the system at 240K, the equilibrium correlation function C(t) is evaluated from equilibrium trajectories with both a charged (q = e) and an uncharged (q = 0) impurity atom. The non-equilibrium solvation function S(t) can also be computed from trajectories that follow a step function change in the ion charge from q = 0 to q = e. These calculations are done for the CH_3Cl solvent model characterized by the above parameters and for similar models with different parameters. In particular, results are shown below for systems characterized by different values of the parameter[15]

$$p' = I / 2M\sigma^2 \qquad [4.3.35]$$

which measures the relative importance of rotational and translational solvent motions.

4.3.5 NUMERICAL SIMULATIONS OF SOLVATION IN SIMPLE POLAR SOLVENTS: RESULTS AND DISCUSSION

The dashed line of Figure 4.3.1 shows the equilibrium solvent induced electrostatic potential Φ at the position of the ion, as a function of the ion charge q obtained for the Stockmayer-CH_3Cl model described in Section 4. Clearly the solvent response is linear with q all the way up to q = e, with slight deviations from linearity starting at q > e. The slope (~4) of the linear dependence of the dashed line in Figure 1 (for q < e) is considerably smaller from that obtained from $\Phi = q / a\varepsilon_s$ (taking $a = \sigma_A/2$ gives a slope of 7.4) that is used to get Eq. [4.3.1]. A more advanced theory of solvation based on the mean spherical approximation predicts (using σ_A and σ_D for the diameters of the ion and the solvent, respectively) a slope of 4.6.

The linearity of the response depends on the nature of the solvent. As examples Figure 4.3.1 also shows results obtained for models of more complex solvents, $H(CH_2OCH_2)_nCH_3$

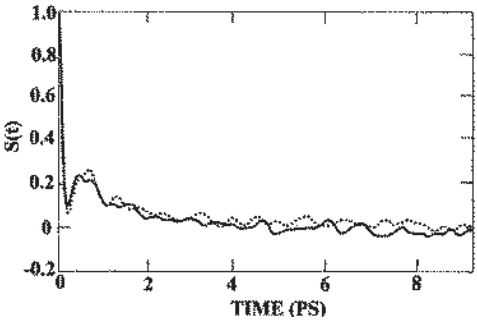

Figure 4.3.3. The function S(t) obtained with $\varepsilon' = 17.0$ (solid line, same as in Figure 4.3.2), together with the same function obtained with $\varepsilon' = 1.0$ (dashed line). ε' is the continuum dielectric constant associated with the reaction field boundary conditions. [From Ref. 11a].

with n = 1 (ethyl methyl ether, full line) and n = 2 (1,2-methoxy ethoxy ethane, dotted line). In these solvents the main contribution to the solvation energy of a positive ion comes from its interaction with solvent oxygen atoms. Because of geometric restriction the number of such atoms in the ion's first solvation shell is limited, leading to a relatively early onset of dielectric saturation.

Figure 4.3.2 shows the time evolution of the solvation functions C(t), Eq. [4.3.25] and S(t) (Eq. [4.3.24]). C(t) is evaluated from an equilibrium trajectory of 220 ps for a system consisting of the solvent and a charged or uncharged atom. The nonequilibrium results for S(t) are averages over 25 different trajectories, each starting from an initial configuration taken from an equilibrium run of an all-neutral system following switching, at t = 0, of the charge on the impurity atom from q = 0 to q = e.

These results show a large degree of similarity between the linear response (equilibrium) and nonequilibrium results. Both consist of an initial fast relaxation mode that, at closer inspection is found to be represented well by a Gaussian, $\exp[-(t/\tau)^2]$, followed by a relatively slow residual relaxation. The initial fast part is more pronounced in C(t). The latter is also characterized by stronger oscillations in the residual part of the relaxation. The fact that the linear response results obtained for equilibrium simulations with an uncharged solute and with a solute of charge q are very similar give further evidence to the approximate validity of linear response theory for this systems.

The sensitivity of these results to the choice of boundary conditions is examined in Figure 4.3.3. We note that the use of reaction field boundary conditions as implemented here is strictly valid only for equilibrium simulations, since the dynamic response of the dielectric continuum at $R > R_c$ is not taken into account. One could argue that for the short-time phenomena considered here, ε' should have been taken smaller than the static dielectric constant of the system. Figure 4.3.3 shows that on the relevant time scale our dynamical results do not change if we take $\varepsilon' = 1$ instead of $\varepsilon' = \varepsilon = 17$. (The absolute solvation energy does depend on ε', and replacing $\varepsilon' = 17$ by $\varepsilon' = 1$ changes it by $\cong 5\%$.)

In the simulations described so far the solvent parameters are given by the aforementioned data. For these, the dimensionless parameter p', Eq. [4.3.35], is 0.019. In order to separate between the effects of the solvent translational and rotational degrees of freedom, we can study systems characterized by other p' values. Figure 4.3.4 shows results obtained for $p' = 0$ (dotted line), 0.019 (solid line), 0.25 (dashed line), and ∞ (dashed-dotted line). Except for $p' = 0$, these values were obtained by changing the moment of inertia I, keeping M=50 amu. The value $p' = 0$ was achieved by taking $M = M_A = \infty$ and I=33.54 amu Å^2. Note that the values $p' = 0$ and $p' = \infty$ correspond to models with frozen translations and frozen rotations, respectively. Figures 4.3.4(a) and 4.3.4(b) show, respectively, the solvation energy $E_{solv}(t)$ and the solvation function S(t) obtained for these different systems. The following points are noteworthy:

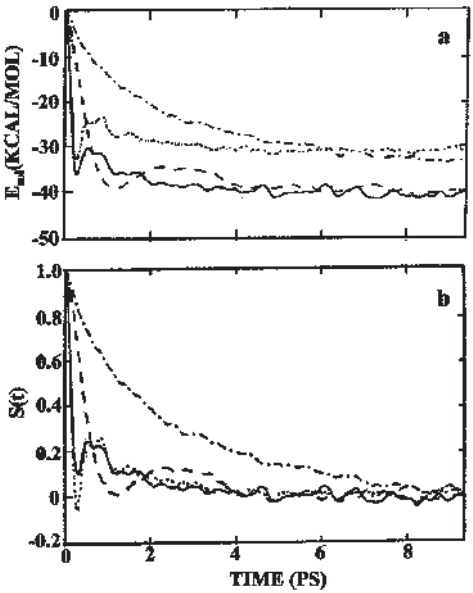

Figure 4.3.4. The solvation energy, E_{solv} (a) and the non-equilibrium solvation function S(t) (b), plotted against time (after switching the ion charge from 0 to e at t = 0) for different solvent models characterized by the parameter p′(Eq. [4.3.35]). Dotted line, p′= 0; solid line, p′=0.019; dashed line, p′=0.25; dashed-dotted line, p′=8. [From Ref. 11a].

Table 4.3.1. Relaxation times τ obtained from fitting the short time component of the solvation function to the function $S(t) = \exp[-(t/\tau)^2]$. The fitting is done for S(t) > 0.3 [From Ref. 11a].

p′	M amu	I amu Å^2	τ ps
0.0	∞	33.54	0.206
0.019	50	33.54	0.170
0.125	50	220.5	0.347
0.250	50	441.0	0.421

(1) The asymptotic ($t\rightarrow\infty$) values of E_{solv} (Figure 4.3.4a) are different for $p' = 0$ ($M = \infty$) and $p' = \infty$ ($I = \infty$) then in the other cases because of the freezing of solvent translations and rotations, respectively. Note, however, that the $I = \infty$ curves converge very slowly (the solvent compensates for the lack of rotations by bringing into the neighborhood of the solute solvent molecules with the "correct" orientation) and probably did not reach its asymptotic value in Figure 3.4.4a.

(2) Except for the rotationless system ($p' = \infty$) all the other systems exhibit a bimodal relaxation, with a fast relaxation component that accounts for most of the solvation energy. The relaxation of the rotationless solvent is exponential (a fit to $\exp(-t/\tau)$ yields $\tau = 2.2$ ps).

(3) A closer look at the fast component in the finite p′ systems shows a Gaussian behavior, a fit to $\exp[-(t/\tau)^2]$ yields the τ values summarized in Table 4.3.1. τ increases with increasing solvent moment of inertia (recall that this is how p′ is changed for $p' > 0$, still for the range of p′ studied, it stays distinct from the long component.

(4) The oscillations and the thermal noise seen in the relatively small slow relaxation component make it difficult to estimate the long relaxation time. A fit of the long time component for the $p' = 0.019$ case to an exponential relaxation $\exp(-t/\tau)$ yields $\tau \cong 2.7 \pm 0.7$ ps. The long-time components in the other systems relax on similar time scales.

The nature of this fast relaxation component of the solvation dynamics has been discussed extensively in the past decade.[19] Carter and Hynes[20] were the first to suggest that this initial relaxation is associated with inertial, as opposed to diffusive, solvent motion. In this mode of motion solvent molecules move under the suddenly created force-field without their mutual interactions and consequent energy exchange having a substantial influence on this fast time scale. Simulations and analytical calculations[19,21,22] have confirmed this assertion for simple polar fluids.

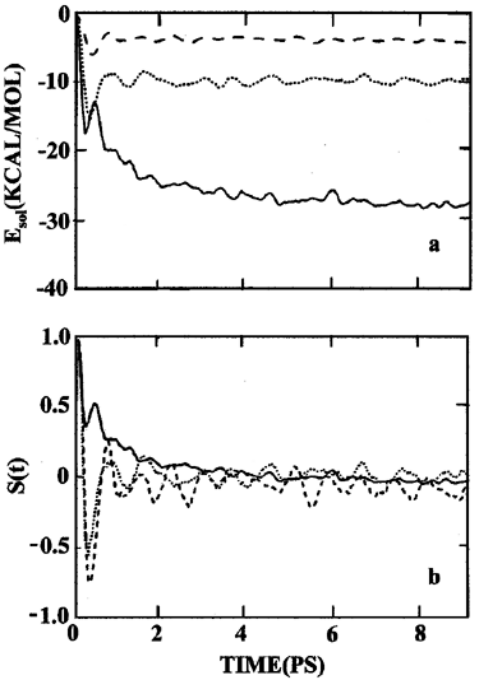

Figure 4.3.5.(a) The solvation energy E(t) and (b) the solvation function S(t) associated with the three solvation shells defined in the text, plotted against time after the ion charge is switched on, for the system with p≒0.019. Solid line, nearest shell; dotted line, second shell, dashed line, outer shell. [From Ref. 11a].

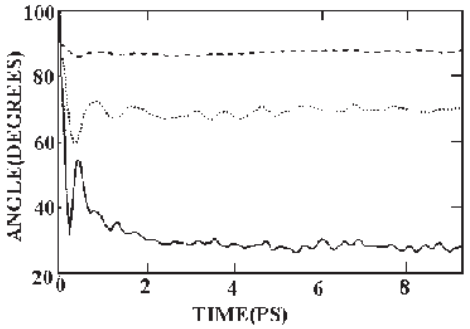

Figure 4.3.6. The time dependence of the average angle between the molecular dipoles and between the corresponding radius vectors to the ion center, associated with molecules in the three different solvation shells defined in the text, plotted against time following the switching on of the ionic charge. [From Ref. 11a].

Next we examine the relative contributions of different solvation shells to the solvation process. This issue is important for elucidating the solvation mechanism, and has been under discussion since an early remark made by Onsager[23] that the shorter time scales are associated mostly with solvent layers further away from the solute, and that the longer $\sim \tau_D$ times are associated with the individual response of solvent molecules nearest to the solute. From the structure of the solute-solvent radial distribution function of the simulated system one can estimate[11a] that the first solvation shell about the solute consists of the eight nearest neighbor solvent particles at distance closer than 5.5 Å from the solute center, and the second solvation shell encompasses the next nearest 26 solvent particles at distance smaller than ~10 Å from the solute center. Taking the rest of the solvent particles in the simulation box as the "third solvation shell", Figure 4.3.5 shows the contributions of these layers to the time evolution of the solvation energy and of the solvation function. It seems that the fast component in these time evolutions is faster for the contribution from the first solvation shell. The same shell also shows a distinct slow component which is much smaller or absent in the contribution from the further shells. Also note that the solvation energy is dominated by the first solvation shell: the first, second, and third shells contribute ~67%, 24%, and 9%, respectively, to the solvation energy. The fast relaxation component accounts for ~80% of the solvation energy. It should be kept in mind, however, that the contribution from outer shell molecules is suppressed by the finite size of the simulated system.

Finally, the nature of the motion that gives rise to the fast relaxation component is seen in Figure 6, which depicts as functions of time the average angles between the molecular dipoles in the different solvation shells and between the corresponding radius vectors to the

ion centers. These results are for the $p' = 0.019$ system; the other systems with $p' < \infty$ show qualitatively similar behavior. Generally, the time evolution of the angular motion is similar to that of the solvation energy. Typical to the present system that represents simple polar solvents, the fast relaxation component is associated with the initial relaxation of the orientational structure in the solvation layers close to the solute.

4.3.6 SOLVATION IN COMPLEX SOLVENTS

The previous sections have focused on a generic model of a very simple solvent, in which solvation dynamics is determined by molecular translations and reorientations only. These in turn are controlled by the solvent molecular mass, moment of inertia, dipole moment and short-range repulsive interactions. When the solvent is more complex we may expect specific structures and interactions to play significant roles. Still, numerical simulations of solvation dynamics in more complex systems lead to some general observations:

(a) In large molecular solvents, solvation may be associated with binding of the solute to particular solvents sites. As seen in Figure 4.3.1, deviations from linearity in the solvent response potential are associated with the fact that the fraction of polar binding sites constitutes a relatively small fraction of the solvent molecule.

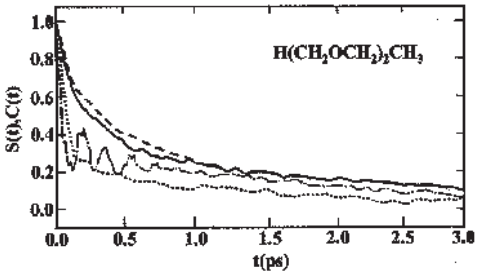

Figure 4.3.7. The solvation and response functions, S(t) and C(t), respectively, for solvation of a spherical ion in a model for the solvent 1,2-methoxy ethoxy ethane, $H(CH_2OCH_2)_2CH_3$. Full line: $S_{0\to1}(t)$; dotted line: $S_{1\to0}(t)$; dashed line: $C(t)|_{q=0}$ and dotted-dashed line: $C(t)|_{q=1}$. [From Ref. 11b].

This deviation from linearity shows itself also in the solvation dynamics. Figure 4.3.7 shows the linear response functions and the non-equilibrium solvation function, C(t) and S(t), respectively, computed as before, for the di-ether $H(CH_2OCH_2)_2CH_3$ solvent. Details of this simulations are given in Ref.11b. If linear response was a valid approximation all the lines in Figure 4.3.7: The two lines for C(t) that correspond to q=0 and q=1, and the two lines for S(t) for the processes $q=0\to q=1$ and the process $q=1\to q=0$, would coalesce. The marked differences between these lines shows that linear response theory fails for this system.

(b) Linear response theory was also shown to fail for low-density solvents (e.g. near and above the liquid-gas critical point[11c,24]). In this case the origin of the non-linearity is the large rearrangement in the solvent structure near the solute during the solvation process. This rearrangement is associated with a local density change in such highly compressible low-density solvents.

(c) Similarly, solvation in mixed solvents usually involve large rearrangement of solvent structure near the solute because the latter usually have a higher affinity for one of the solvent components. Solvation in electrolyte solutions provides a special example.[25,26] In this case the solvent dynamics about the newly created charge distribution is not much different than in the pure dielectric solution, however in addition the mobile ions rearrange about this charge distribution, and on the timescale of this process linear response theory fails.[27]

(d) In the situations discussed in (b) and (c) above, new dynamical processes exist: While the dielectric response in normal simple polar solvents is dominated by molecular ro-

tations, the motions that change the local structure about the solute are usually dominated by solvent translation. This gives rise to a new, usually slower, relaxation components. Solvation in electrolyte solutions clearly shows this effect: In addition to the dielectric response on the picosecond timescale, a much slower relaxation component is observed on the nanosecond scale.[25] Numerical simulations have identified the origin of this relaxation component as the exchange between a water molecule and an ion in the first solvation shell about the solute.[26]

Finally, it is intuitively clear that in large molecule complex solvents simple molecular rotation as seen in Figure 4.3.6 can not be the principal mode of solvation. Numerical simulations with polyether solvents show that instead, hindered intramolecular rotations that distort the molecular structure so as to bring more solvating sites into contact with the ion dominate the solvation dynamics.[11b] The bi-modal, and in fact multi-modal, character of the solvation is maintained also in such solvents, but it appears that the short time component of this solvation process is no longer inertial as in the simple small molecule solvents.[11]

4.3.7 CONCLUSIONS

Numerical simulations of solvation dynamics in polar molecular solvents have been carried out on many models of molecular systems during the last decade. The study described in sections 4.3.4-4.3.5 focused on a generic model for a simple polar solvent, a structureless Stockmayer fluid. It is found that solvation dynamics in this model solvent is qualitatively similar to that observed in more realistic models of more structured simple solvents, including solvents like water whose energetics is strongly influenced by the H-bond network. In particular, the bimodal nature of the dynamics and the existing of a prominent fast Gaussian relaxation component are common to all models studied.

Such numerical simulations have played an important role in the development of our understanding of solvation dynamics. For example, they have provided the first indication that simple dielectric continuum models based on Debye and Debey-like dielectric relaxation theories are inadequate on the fast timescales that are experimentally accessible today. It is important to keep in mind that this failure of simple theories is not a failure of linear response theory. Once revised to describe reliably response on short time and length scales, e.g. by using the full k and ω dependent dielectric response function $\varepsilon(k,\omega)$, and sufficiently taking into account the solvent structure about the solute, linear response theory accounts for most observations of solvation dynamics in simple polar solvents.

Numerical simulations have also been instrumental in elucidating the differences between simple and complex solvents in the way they dynamically respond to a newly created charge distribution. The importance of translational motions that change the composition or structure near the solute, the consequent early failure of linear response theory in such systems, and the possible involvement of solvent intramolecular motions in the solvation process were discovered in this way.

We conclude by pointing out that this report has focused on solvation in polar systems where the solvent molecule has a permanent dipole moment. Recently theoretical and experimental work has started on the dynamics of non-polar solvation.[28] This constitutes another issue in our ongoing effort to understand the dynamics of solvation processes.

REFERENCES

1 For recent reviews see M. Maroncelli, *J. Mol. Liquids*, **57**, 1 (1993); G.R. Fleming and M. Cho, *Ann. Rev. Phys. Chem*., **47**, 109 (1996).

2 See, e.g., J.T. Hynes, in **Ultrafast Dynamics of Chemical Systems**, edited by J.D. Simon, *Kluwer*, Dordrecht, 1994, pp. 345-381; L.D. Zusman, *Zeit. Phys. Chem.*, **186**, 1 (1994); S. Roy and B. Bagchi, *J. Chem. Phys.*, **102**, 6719; 7937 (1995).
3 P. G. Wolynes, *J. Chem. Phys*., **86**, 5133 (1987).
4 I. Rips, J. Klafter and J. Jortner, *J. Chem. Phys.*, **88**, 3246 (1988); **89**, 4288 (1988).
5 D. F. Calef and P. G. Wolynes, *J. Chem. Phys*., **78**, 4145 (1983).
6 B. Bagchi and A. Chandra, *J. Chem. Phys*., **90**, 7338 (1989); **91**, 2594 (1989); **97**, 5126 (1992).
7 F.O Raineri, H. Resat, B-C Perng, F. Hirata and H.L. Friedman, *J. Chem. Phys.*, **100**, 1477 (1994)
8 R. F. Loring and S. Mukamel, *J. Chem. Phys.*, **87**, 1272 (1987); L. E. Fried and S. Mukamel, *J. Chem. Phys.*, **93**, 932 (1990).
9 A. A. Kornyshev. A. M. Kuznetsov, D. K. Phelps and M. J. Weaver, *J. Chem. Phys.*, **91**, 7159 (1989).
10 See, e.g. M. Maronelli and G.R. Fleming *JCP*, **89**, 5044 (1988); M. Maroncelli, *J. Chem. Phys*., **94**, 2084 (1991); Perera and Berkowitz, *J. Chem. Phys.*, **96**, 3092 (1992); P.V. Kumar and M. Maroncelli, *J. Chem. Phys*., **103**, 3038 (1995).
11 (a) E. Neria and A. Nitzan, *J. Chem. Phys*., **96**, 5433 (1992).
(b) R. Olender and A. Nitzan, *J. Chem. Phys*., **102**, 7180 (1995).
(c) P. Graf and A. Nitzan, *Chem. Phys*., **235**, 297(1998).
12 A. Mozumder in **Electron-solvent and anion- solvent interactions**, L. Kevan and B. Webster, Editors, *Elsevier*, Amsterdam, 1976.
13 M. Maronelli and G.R. Fleming in Ref. 11.
14 E.A. Carter and J.T. Hynes, *JCP,* **94**, 2084 (1991).
15 J. W. de Leeuw, J. W. Perram and E. R. Smith, *Annu. Rev. Phys. Chem*., **37**, 245 (1986).
16 C. J. F. Böttcher and P. Bordewijc, **Theory of Electric Polarization**, 2nd. ed. *Elsevier,* Amsterdam, 1978, Vol. 2, Chap. 10.
17 M. P. Allen and D. J. Tildesely, **Computer Simulation of Liquids**, *Oxford*, London, 1989).
18 H. C. Andersen, *J. Chem. Phys*., **72**, 2384 (1980).
19 See, e.g. M. Maroncelli, in Ref. 11.
20 E. A. Carter and J.T. Hynes, *J. Chem. Phys*., **94**, 5961 (1991).
21 M. Maroncelli, V.P. Kumar and A. Papazyan, *J. Phys. Chem.*, **97**, 13 (1993).
22 L. Perera and M.L. Berkowitz, *J. Chem. Phys.*, **97**, 5253 (1992).
23 L. Onsager, *Can. J. Chem*., **55**, 1819 (1977).
24 R. Biswas and B. Bagchi, *Chem. Phys. Lett*., 290 (1998).
25 V. Itah and D. Huppert, *Chem. Phys. Lett.*, **173**, 496 (1990); E. Bart and D. Huppert, *ibid*. **195**, 37 (1992).
26 C.F. Chapman and M. Maroncelli, *J. Phys. Chem*., **95**, 9095 (1991).
27 E. Neria and A. Nitzan, *J. Chem. Phys*., **100**, 3855 (1994).
28 B.M. Ladanyi and M. Maroncelli, *J. Chem. Phys.*, **109**, 3204 (1998); M. Berg, *J. Phys. Chem*., **A102,** 17 (1998); *Chem. Phys*., **233**, 257, (1998).

4.4 METHODS FOR THE MEASUREMENT OF SOLVENT ACTIVITY OF POLYMER SOLUTIONS

Christian Wohlfarth
Martin-Luther-University Halle-Wittenberg, Institute of Physical Chemistry, Merseburg, Germany, e-mail: Wohlfarth@chemie.uni-halle.de

4.4.1 INTRODUCTION

Knowledge of solvent activities in polymer solutions is a necessity for a large number of industrial and laboratory processes. Such data are an essential tool for understanding the thermodynamic behavior of polymer solutions, for studying their intermolecular interactions and for getting insights into their molecular nature. Besides, they are the necessary basis for any development of theoretical thermodynamic models. Scientists and engineers in academic and industrial research need such data.

Solvent activities of polymer solutions have been measured for about 60 years now. However, the database for polymer solutions is still modest, in comparison with the enormous amount of data available for mixtures of low-molecular substances. Three explicit databases have been published in the literature up to now.[1-3] The database prepared by Wen Hao et al.[1] is summarized in two parts of the DECHEMA Chemistry Data Series. Danner and High[2] provided a database and some calculation methods on a floppy disk with their book. Wohlfarth[3] prepared the most complete data collection regarding vapor-liquid equilibrium data of polymer solutions. His annually updated electronic database is not commercially available; however, personal requests can be made via his e-mail address given above.

Some implicit databases are provided within the Polymer Handbook[4] by Schuld and Wolf[5] or by Orwoll[6] and in two papers prepared earlier by Orwoll.[7,8] These four sources list tables of Flory's χ-function and tables where enthalpy, entropy or volume changes, respectively, are given in the literature for a large number of polymer solutions. The tables of second virial coefficients of polymers in solution, which were prepared by Lechner and coworkers[9] (also provided in the Polymer Handbook), are a valuable source for estimating the solvent activity in the dilute polymer solution. Bonner reviewed vapor-liquid equilibria in concentrated polymer solutions and listed tables containing temperature and concentration ranges of a certain number of polymer solutions.[10] Two CRC-handbooks prepared by Barton list a larger number of thermodynamic data of polymer solutions in form of polymer-solvent interaction or solubility parameters.[11,12]

An up-to-date list of all polymer-solvent systems for which solvent activities or vapor pressures from vapor-liquid equilibrium measurements were published in the literature is provided in Appendix 4.4.A of this Subchapter 4.4 (please see below).

Solvent activities in polymer solutions can be determined by rather different techniques. However, no one is really a universal method but covers a certain concentration range of the polymer solution. Figure 4.4.1 explains in short the situation.

Corresponding to the different regions in the diagram, different experimental techniques were used for the measurement of the solvent activity in a homogeneous polymer solution:

(i) Solvent activities of highly diluted polymer solutions can be obtained from scattering methods such as light scattering, small angle X-ray scattering and small angle neutron scattering via the second osmotic virial coefficient, which is often related to investigations for polymer characterization. These methods are able to resolve the very small difference between the thermodynamic limit of 1.0 for the activity of the pure solvent and the actual value of perhaps 0.9999x at the given (very low) polymer concentration.

(ii) Solvent activities of polymer solutions with polymer concentrations up to about 30 wt% can be measured by osmometry (membrane as well as vapor-pressure osmometry), light scattering, ultracentrifuge (of course, all these methods can also be applied for polymer characterization and can be extrapolated to zero polymer concentration to obtain the second virial coefficient), and differential vapor pressure techniques. Cryoscopy and ebulliometry can also be used to measure solvent activities in dilute and semidilute polymer solutions, but with limited success only.

(iii) The concentrated polymer solution between 30 and 85 wt% is covered by vapor pressure measurements which were usually performed by various isopiestic sorption meth-

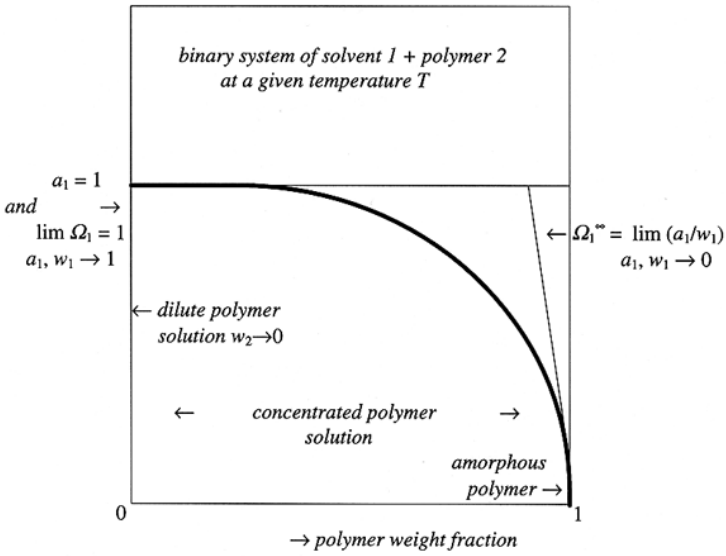

Figure 4.4.1. Typical isotherm for the solvent activity of a homogeneous binary polymer solution.

ods. The ultracentrifuge can also be applied for solutions up to 80 wt% polymer, but this was only scarcely done in the literature.

(iv) A special problem are polymer solutions with concentrations higher than 90 wt% up to the limit of the region of Henry's law. For this purpose, the inverse gas-liquid chromatography (IGC) is the most useful method. Measurements can be made at infinite dilution of the solvent for determining the activity coefficient at infinite dilution or Henry's constant, but IGC can also be performed at finite solvent concentrations up to 10-15 wt% of the solvent to get solvent activities for highly concentrated polymer solutions. Some sorption experiments in this concentration range were reported by piezoelectric quartz crystal technique; however, thermodynamic equilibrium absorption is difficult to obtain, as discussed below. At least, melting point depression can be applied in some cases for small amounts of solvents in semicrystalline polymers, but obtaining reliable results seems to be difficult.

(v) There is another possibility to measure solvent activities in polymer solutions if the state of the solution is inhomogeneous, i.e., for the region of liquid-liquid equilibrium. Binodal and/or spinodal curves can be reduced to solvent activity data by means of a thermodynamic ansatz for the Gibbs free energy of mixing in dependence on temperature, concentration (and pressure if necessary), which has to be solved according to thermodynamic equilibrium conditions. In the case of polymer networks, swelling equilibria can be measured instead. The solvent activity in a swollen network arises from two parts, a mixing part with the (virtually) infinite-molar-mass polymer, and a contribution from elastic network deformation. The second follows from statistical theory of rubber elasticity and also needs certain model approximations for data reduction.

In summary, investigations on vapor-liquid equilibrium of polymer solutions are the most important source for obtaining solvent activities in polymer solutions. Therefore, emphasis is laid in this subchapter on the experimental methods, which use this equilibrium.

Reviews on experimental methods, sometimes including tables with thermodynamic data were prepared more or less continuously during the last three decades. Especially methods and results of the application of IGC to polymers and polymer solutions are carefully reviewed.[13-25] Special reviews on determining solvent activities from various scattering techniques could not be found. However, there is a large number of reviews and books on scattering methods and their applications. Some references may give a starting point for the interested reader.[26-32] Experimental techniques for vapor-pressure measurements were reviewed in the paper by Bonner.[10] Ebulliometry, cryoscopy and vapor-pressure osmometry were reviewed by Cooper,[33] Glover,[34] Mays and Hadjichristidis,[40] and a recent summary can be found in a new book edited by Pethrick and Dawkins.[26] Reviews that account for the measurement of thermodynamic data from sedimentation equilibria using the ultracentrifuge are given by Fujita,[35] Harding et al.[36] or Munk.[37] An overview on membrane osmometry was given by Adams,[38] Tombs and Peacock[39] or Mays and Hadjichristidis,[40] and a recent summary can again be found in the book edited by Pethrick and Dawkins.[26] Reviews on liquid-liquid demixing of polymer solutions will not be summarized in detail here, some references should be enough for a well-based information.[41-45] A short summary on equipment and thermodynamic equations of most techniques was given in Danner's handbook.[2] Finally, the classical books on polymer solutions written by Flory,[46] by Huggins,[47] and by Tompa[48] must not be forgotten for the historical point of view on the topic of this subchapter.

4.4.2 NECESSARY THERMODYNAMIC EQUATIONS

Here, the thermodynamic relations are summarized which are necessary to understand the following text. No derivations will be made. Details can be found in good textbooks, e.g., Prausnitz et al.[49]

The activity of a component i at a given temperature, pressure, and composition can be defined as the ratio of the fugacity of the solvent at these conditions to the solvent fugacity in the standard state; that is, a state at the same temperature as that of the mixture and at specified conditions of pressure and composition:

$$a_i(T,P,x) \equiv f_i(T,P,x) / f_i\left(T,P^0,x^0\right) \qquad [4.4.1a]$$

where:

a_i	activity of component i
T	absolute temperature
P	pressure
x	mole fraction
f_i	fugacity of component i

In terms of chemical potential, the activity of component i can also be defined by:

$$a_i(T,P,x) \equiv \exp\left\{\frac{\mu_i(T,P,x) - \mu_i\left(T,P^0,x^0\right)}{RT}\right\} \qquad [4.4.1b]$$

where:

μ_i chemical potential of component i
R gas constant

P^0 and x^0 denote the standard state pressure and composition. For binary polymer solutions the standard state is usually the pure liquid solvent at its saturation vapor pressure at T. The standard state fugacity and the standard state chemical potential of any component i are abbreviated in the following text by their symbols f_i^0 and μ_i^0, respectively.

Phase equilibrium conditions between two multi-component phases I and II require thermal equilibrium,

$$T^I = T^{II} \qquad [4.4.2a]$$

mechanical equilibrium,

$$P^I = P^{II} \qquad [4.4.2b]$$

and the chemical potential of each component i must be equal in both phases I and II.

$$\mu_i^I = \mu_i^{II} \qquad [4.4.3]$$

For Equation [4.4.3] to be satisfied, the fugacities of each component i must be equal in both phases.

$$f_i^I = f_i^{II} \qquad [4.4.4]$$

Applying fugacity coefficients, the isochemical potential expression leads to:

$$\phi_i^I x_i^I = \phi_i^{II} x_i^{II} \qquad [4.4.5]$$

where:

ϕ_i fugacity coefficient of component i.

Fugacity coefficients can be calculated from an equation of state by:

$$\ln \phi_i = \frac{1}{RT} \int_V^\infty \left[\left(\frac{\partial P}{\partial n_i} \right)_{T,V,n_j} - \frac{RT}{V} \right] dV - \ln \frac{PV}{RT} \qquad [4.4.6]$$

where a pressure explicit equation of state is required to use Equation [4.4.6]. Not all equations of state for polymers and polymer solutions also are valid for the gaseous state (see section in Subchapter 4.4.4), however, and a mixed gamma-phi approach is used by applying Equation [4.4.7]. Applying activity coefficients in the liquid phase, the isochemical potential expression leads, in the case of the vapor-liquid equilibrium (superscript V for the vapor phase and superscript L for the liquid phase), to the following relation:

$$\phi_i^V y_i P = \gamma_i x_i^L f_i^0 \qquad [4.4.7]$$

where:

y_i mole fraction of component i in the vapor phase with partial pressure $P_i = y_i P$
γ_i activity coefficient of component i in the liquid phase with activity $a_i = x_i^L \gamma_i$

or in the case of liquid-liquid equilibrium to

$$\gamma_i^{I} x_i^{I} f_i^{0I} = \gamma_i^{II} x_i^{II} f_i^{0II} \qquad [4.4.8]$$

If the standard state in both phases is the same, the standard fugacities cancel out in Equation [4.4.8]. Equation [4.4.8] also holds for solid-liquid equilibria after choosing appropriate standard conditions for the solid state, but they are of minor interest here.

All expressions given above are exact and can be applied to small molecules as well as to macromolecules. The one difficulty is having accurate experiments to measure the necessary thermodynamic data and the other is finding correct and accurate equations of state and/or activity coefficient models to calculate them.

Since mole fractions are usually not the concentration variables chosen for polymer solutions, one has to specify them in each case. The following three quantities are most frequently used:

mass fractions $$w_i = m_i / \sum m_k \qquad [4.4.9a]$$

volume fractions $$\varphi_i = n_i V_i / \sum n_k V_k \qquad [4.4.9b]$$

segment (hard-core volume) fractions $$\psi_i = n_i V_i^* / \sum n_k V_k^* \qquad [4.4.9c]$$

where:

m_i	mass of component i
n_i	amount of substance (moles) of component i
V_i	molar volume of component i
V_i^*	molar hard-core (characteristic) volume of component i.

With the necessary care, all thermodynamic expressions given above can be formulated with mass or volume or segment fractions as concentration variables instead of mole fractions. This is the common practice within polymer solution thermodynamics. Applying characteristic/hard-core volumes is the usual approach within most thermodynamic models for polymer solutions. Mass fraction based activity coefficients are widely used in Equations [4.4.7 and 4.4.8] which are related to activity by:

$$\Omega_i = a_i / w_i \qquad [4.4.10]$$

where:

Ω_i	mass fraction based activity coefficient of component i
a_i	activity of component i
w_i	mass fraction of component i

Classical polymer solution thermodynamics often did not consider solvent activities or solvent activity coefficients but usually a dimensionless quantity, the so-called Flory-Huggins interaction parameter χ.[44,45] χ is not only a function of temperature (and pressure), as was evident from its foundation, but it is also a function of composition and polymer molecular mass.[5,7,8] As pointed out in many papers, it is more precise to call it χ-function (what is in principle a residual solvent chemical potential function). Because of its widespread use and its possible sources of mistakes and misinterpretations, the necessary relations must be included here. Starting from Equation [4.4.1b], the difference between the chemical potentials of the solvent in the mixture and in the standard state belongs to the first

derivative of the Gibbs free energy of mixing with respect to the amount of substance of the solvent:

$$\Delta\mu_1 = \mu_1 - \mu_1^0 = \left(\frac{\partial n \Delta_{mix} G}{\partial n_1} \right)_{T,p,n_{j\neq1}} \qquad [4.4.11]$$

where:

n_i	amount of substance (moles) of component i
n	total amount of substance (moles) of the mixture: $n = \Sigma n_i$
$\Delta_{mix}G$	molar Gibbs free energy of mixing.

For a truly binary polymer solutions, the classical Flory-Huggins theory leads to:[46,47]

$$\Delta_{mix} G / RT = x_1 \ln\varphi_1 + x_2 \ln\varphi_2 + g x_1 \varphi_2 \qquad [4.4.12a]$$

or

$$\Delta_{mix} G / RTV = (x_1 / V_1)\ln\varphi_1 + (x_2 / V_2)\ln\varphi_2 + BRT\varphi_1\varphi_2 \qquad [4.4.12b]$$

where:

x_i	mole fraction of component i
φ_i	volume fraction of component i
g	integral polymer-solvent interaction function that refers to the interaction of a solvent molecule with a polymer segment, the size of which is defined by the molar volume of the solvent V_1
B	interaction energy-density parameter that does not depend on the definition of a segment but is related to g and the molar volume of a segment V_{seg} by $B = RTg/V_{seg}$
V	molar volume of the mixture, i.e. the binary polymer solution
V_i	molar volume of component i

The first two terms of Equation [4.4.12] are named combinatorial part of $\Delta_{mix}G$, the third one is then a residual Gibbs free energy of mixing. Applying Equation [4.4.11] to [4.4.12], one obtains:

$$\Delta\mu_1 / RT = \ln(1-\varphi_2) + \left(1 - \frac{1}{r}\right)\varphi_2 + \chi\varphi_2^2 \qquad [4.4.13a]$$

or

$$\chi = \left[\Delta\mu_1 / RT - \ln(1-\varphi_2) - \left(1 - \frac{1}{r}\right)\varphi_2\right] / \varphi_2^2 \qquad [4.4.13b]$$

or

$$\chi = \left[\ln a_1 - \ln(1-\varphi_2) - \left(1 - \frac{1}{r}\right)\varphi_2\right] / \varphi_2^2 \qquad [4.4.13c]$$

where:

r	ratio of molar volumes V_2/V_1, equal to the number of segments if $V_{seg} = V_1$

χ Flory-Huggins interaction function of the solvent

The segment number r is, in general, different from the degree of polymerization or from the number of repeating units of a polymer chain but proportional to it. One should note that Equations [4.4.12 and 4.4.13] can be used on any segmentation basis, i.e., also with $r = V_2^* / V_1^*$ on a hard-core volume segmented basis and segment fractions instead of volume fractions, or with $r = M_2/M_1$ on the basis of mass fractions. It is very important to keep in mind that the numerical values of the interaction functions g or χ depend on the chosen basis and are different for each different segmentation!

From the rules of phenomenological thermodynamics, one obtains the interrelations between both parameters at constant pressure and temperature:

$$\chi = g + \varphi_1 \frac{\partial g}{\partial \varphi_1} = g - (1-\varphi_2)\frac{\partial g}{\partial \varphi_2} \qquad [4.4.14a]$$

$$g = \frac{1}{\varphi_1}\int_0^{\varphi_1} \chi d\varphi_1 \qquad [4.4.14b]$$

A recent discussion of the g-function was made by Masegosa et al.[50] Unfortunately, g- and χ-functions were not always treated in a thermodynamically clear manner in the literature. Sometimes they were considered to be equal, and this is only true in the rare case of composition independence. Sometimes, and this is more dangerous, neglect or misuse of the underlying segmentation basis is formed. Thus, numerical data from literature has to be handled with care (using the correct data from the reviews[5-8,11] is therefore recommended).

A useful form for their composition dependencies was deduced from lattice theory by Koningsveld and Kleintjens:[51]

$$g = \alpha + \frac{\beta}{(1-\gamma\varphi_2)} \quad and \quad \chi = \alpha + \frac{\beta(1-\gamma)}{(1-\gamma\varphi_2)^2} \qquad [4.4.15]$$

where:

α acts as constant within a certain temperature range
β describes a temperature function like $\beta = \beta_0 + \beta_1 / T$
γ is also a constant within a certain temperature range.

Quite often, simple power series are applied only:

$$\chi = \sum_{i=0}^{n} \chi_i \varphi_2^i \; and \; g = \sum_{i=0}^{n} \left(\frac{\chi_i}{i+1}\right)\left(\frac{1-\varphi_2^{i+1}}{1-\varphi_2}\right) \qquad [4.4.16]$$

where:

χ_i empirical fitting parameters to isothermal-isobaric data

Both interaction functions are also functions of temperature and pressure. An empirical form for these dependencies can be formulated according to the rules of phenomenological thermodynamics:

$$g = \beta_{00} + \beta_{01}/T + (\beta_{10} + \beta_{11}/T)P \; or \; \chi = a + b/T + (c + d/T)P \qquad [4.4.17]$$

where:

a,b,c,d	empirical fitting parameters for the χ-function
$\beta_{00}, \beta_{01}, \beta_{10}, \beta_{11}$	empirical fitting parameters for the g-function
T	absolute temperature
P	pressure

All these fitting parameters may be concentration dependent and may be included into Equations [4.4.15 or 4.4.16]. Details are omitted here. More theoretical approaches will be discussed shortly in Subchapter 4.4.4.

The χ-function can be divided into an enthalpic and an entropic parts:

$$\chi = \chi_H + \chi_S \text{ with } \chi_H = -T\left(\frac{\partial \chi}{\partial T}\right)_{p,\varphi} \text{ and } \chi_S = \left(\frac{\partial \chi T}{\partial T}\right)_{P,\varphi} \qquad [4.4.18]$$

where:

χ_H	enthalpic part
χ_S	entropic part

An extension of all these equations given above to multi-component mixtures is possible. Reviews of continuous thermodynamics which take into account the polydisperse character of polymers by distribution functions can be found elsewhere.[52-54]

4.4.3 EXPERIMENTAL METHODS, EQUIPMENT AND DATA REDUCTION

4.4.3.1 Vapor-liquid equilibrium (VLE) measurements

Investigations on vapor-liquid equilibrium of polymer solutions are the most important source for obtaining solvent activities in polymer solutions. Therefore, emphasis is laid to the experimental methods which use this equilibrium. These methods are:

(i) absolute vapor pressure measurement,
(ii) differential vapor pressure measurement,
(iii) isopiestic sorption/desorption methods, i.e. gravimetric sorption, piezoelectric sorption, or isothermal distillation,
(iv) inverse gas-liquid chromatography (IGC) at infinite dilution, IGC at finite concentrations, and head-space gas-chromatography (HSGC),
(v) ebulliometry and
(vi) the non-equilibrium steady-state method vapor-pressure osmometry (VPO).

The measurement of vapor pressures for polymer solutions is generally more difficult and more time-consuming than that of low-molecular mixtures. The main difficulties can be summarized as follows: Polymer solutions exhibit strong negative deviations from Raoult's law. These are mainly due to the large entropic contributions caused by the difference between the molar volumes of solvents and polymers, as was explained by the classical Flory-Huggins theory[46,47] about 60 years ago, Equation [4.4.12]. However, because of this large difference in molar mass, vapor pressures of dilute solutions do not differ markedly from the vapor pressure of the pure solvent at the same temperature, even at polymer concentrations of 10-20 wt%. This requires special techniques to measure very small differences in solvent activities. Concentrated polymer solutions are characterized by rapidly increasing viscosities with increasing polymer concentration. This leads to a strong increase in time required to obtain real thermodynamic equilibrium caused by a slow solvent diffu-

sion effects (in or out of a non-equilibrium-state polymer solution). Furthermore, only the solvent coexists in both phases because polymers do not evaporate. The experimental techniques used for the measurement of vapor pressures of polymer solutions have to take into account all these effects.

Vapor pressures of polymer solutions are usually measured in the isothermal mode by static methods. Dynamic methods are seldom applied, see under ebulliometry below. At least, one can consider measurements by VPO to be dynamic methods, where a dynamic (steady-state) balance is obtained. However, limits for the applicable ranges of polymer concentration and polymer molar mass, limits for the solvent vapor pressure and the measuring temperature and some technical restrictions prevent its broader application, see below. Static techniques usually work at constant temperature. The three different methods (i)-(iii) were used to determine most of the vapor pressures of polymer solutions in the literature. All three methods have to solve the problems of establishing real thermodynamic equilibrium between liquid polymer solution and solvent vapor phase, long-time temperature constancy during the experiment, determination of the final polymer concentration and determination of pressure and/or activity. Methods (i) and (ii) were mostly used by early workers. The majority of recent measurements was done with the isopiestic sorption methods. Gas-liquid chromatography as IGC closes the gap at high polymer concentrations where vapor pressures cannot be measured with sufficient accuracy. HSGC can be considered as some combination of absolute vapor pressure measurement with GLC. The following text will now explain some details of experimental equipment and measuring procedures as well as of data reduction procedures to obtain solvent activities. A recent review by Williamson[55] provides corresponding information related to low-molecular mixtures.

4.4.3.1.1 Experimental equipment and procedures for VLE-measurements

(i) Absolute vapor pressure measurement

Absolute vapor pressure measurement may be considered to be the classical technique for our purposes, because one measures directly the vapor pressure above a solution of known polymer concentration. Refs. 56-65 provide a view of the variety of absolute vapor pressure apparatuses developed and used by different authors. The common principle of an absolute vapor pressure apparatus is shown in Figure 4.4.2.

Vapor pressure measurement and solution equilibration were made separately: A polymer sample is prepared by weighing, the sample flask is evacuated, degassed solvent is introduced into the flask and the flask is sealed thereafter. All samples are equilibrated at elevated temperature in a thermostat for some weeks (!). The flask with the equilibrated polymer solution is connected to the pressure measuring device (in Figure 4.4.2 a Hg-manometer) at the measuring temperature. The vapor pressure is measured after reaching equilibrium and the final polymer concentration is obtained after correcting for the amount of evaporated solvent. Modern equipment applies electronic pressure sensors and digital techniques to measure the vapor pressure, e.g. Schotsch and Wolf[57] or Killmann et al.[58] Data processing can be made online using computers. Figure 4.4.3 shows a schematic diagram of the equipment used by Killmann and coworkers.[58]

A number of problems have to be solved during the experiment. The solution is usually in an amount of some cm^3 and may contain about 1 g of polymer or even more. Degassing is absolutely necessary. For example, Killmann et al.[58] included special degassing units for each component of the entire equipment. All impurities in the pure solvent have to

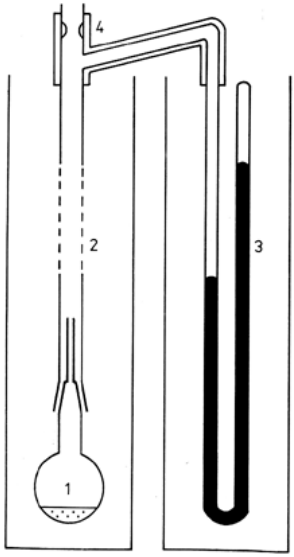

Figure 4.4.2. Schematic of the common principle of an absolute vapor pressure apparatus: 1 - polymer solution, 2 - connection to the manometer, 3 - Hg-manometer, 4 - heating coils. The whole construction is thermostated at the measuring temperature, the connection to the manometer is kept slightly above the measuring temperature to avoid condensation.

be eliminated. Equilibration of all prepared solutions is very time-consuming (liquid oligomers need not so much time, of course). Increasing viscosity makes the preparation of concentrated solutions more and more difficult with further increasing amount of polymer. Solutions above 50-60 wt% can hardly be prepared (depending on the solvent/polymer pair under investigation). The determination of the volume of solvent vaporized in the unoccupied space of the apparatus is difficult and can cause serious errors in the determination of the final solvent concentration. To circumvent the vapor phase correction, one can measure the concentration directly by means, for example, of a differential refractometer. The contact of solvent vapor with the Hg-surface in older equipment may cause further errors. Complete thermostating of the whole apparatus is necessary to avoid condensation of solvent vapors at colder spots. Since it is disadvantageous to thermostat Hg-manometers at higher temperatures, null measurement in-

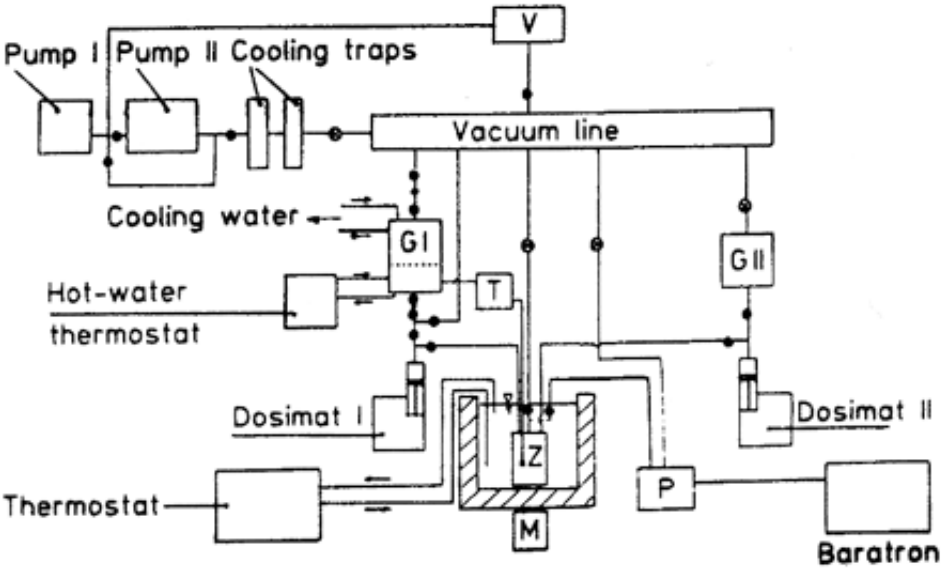

Figure 4.4.3. Schematic diagram of a modern absolute vapor pressure apparatus: T - temperature meter, P - vapor-pressure meter, V - vacuum meter, Z - measuring cell, M - magnetic stirrer, GI and GII - degassing units for the solvent and for the polymer. [Reprinted with permission from Ref. 58, Copyright 1990,Wiley-VCH].

struments with pressure compensation were sometimes used, e.g., Baxendale et al.[59] Modern electronic pressure sensors can be thermostated within certain temperature ranges. If pressure measurement is made outside the thermostated equilibrium cell, the connecting tubes must be heated slightly above the equilibrium temperature to avoid condensation.

The measurement of polymer solutions with lower polymer concentrations requires very precise pressure instruments, because the difference in the pure solvent vapor pressure becomes very small with decreasing amount of polymer. At least, no one can really answer the question if real thermodynamic equilibrium is obtained or only a frozen non-equilibrium state. Non-equilibrium data can be detected from unusual shifts of the χ-function with some experience. Also, some kind of hysteresis in experimental data seems to point to non-equilibrium results. A common consistency test on the basis of the integrated Gibbs-Duhem equation does not work for vapor pressure data of binary polymer solutions because the vapor phase is pure solvent vapor. Thus, absolute vapor pressure measurements need very careful handling, plenty of time, and an experienced experimentator. They are not the method of choice for high-viscous polymer solutions.

(ii) Differential vapor pressure measurement

The differential method can be compared under some aspects with the absolute method, but there are some advantages. The measuring principle is to obtain the vapor pressure difference between the pure solvent and the polymer solution at the measuring temperature. Figure 4.4.4 explains the basic principle as to how it is used by several authors. References[66-75] provide a view of a variety of differential vapor pressure apparatuses developed and used by different authors.

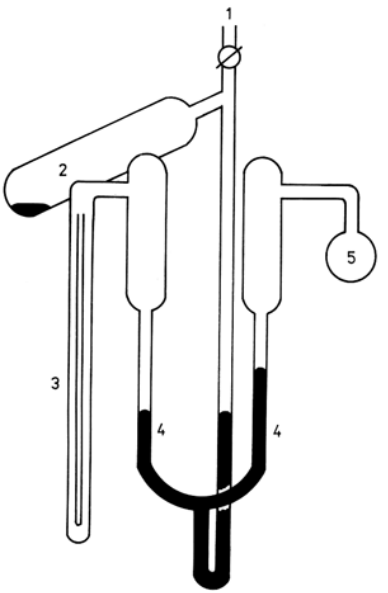

Figure 4.4.4. Schematic diagram of a differential vapor-pressure apparatus: 1 - connection to vacuum pump, 2 - Hg-storage bulb, 3 - burette, 4 - Hg-manometer, 5 - polymer solution. The whole apparatus is kept constant at the measuring temperature within a thermostat.

The polymer sample is put, after weighing, into the sample flask and the apparatus is evacuated. Degassed solvent is distilled into the measuring burette and from there a desired amount of solvent is distilled into the sample flask. The Hg-manometer is filled from the storage bulb and separates the polymer solution from the burette. Care must be taken to avoid leaving any solvent in the manometer. The apparatus is kept at constant measuring temperature, completely immersed in a thermostat for several days. After reaching equilibrium, the pressure is read from the manometer difference and the concentration is calculated from the calibrated burette meniscus difference corrected by the amount of vaporized solvent in the unoccupied space of the equipment. The pure solvent vapor pressure is usually precisely known from independent experiments.

Difference/differential manometers have some advantages from their construction: They are comparatively smaller and their resolution is much higher (modern pressure transducers can resolve differences of 0.1 Pa and less). However, there are the same disadvantages with sample/solution preparation (solutions of grams of polymer in some cm^3 vol-

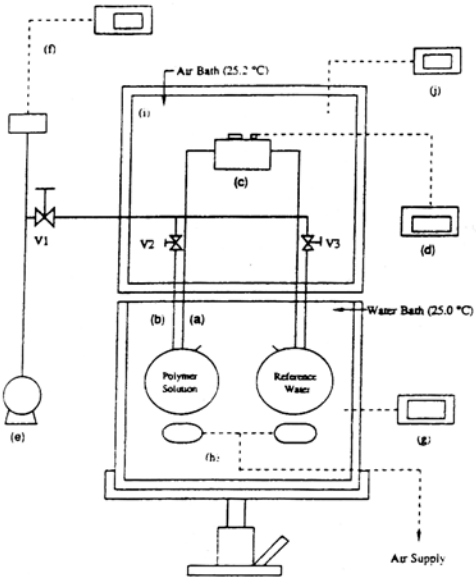

Figure 4.4.5. Differential vapor-pressure apparatus. 100 ml Pyrex flasks connected (a) to a differential pressure transducer (c) with digital readout (d) and (b) to vacuum pump (e) and absolute pressure vacuum thermocouple gauge (f). The constant temperature in the water bath is maintained by a temperature controller (g). The transducer and connecting glassware are housed in an insulated box (i) and kept at constant temperature slightly above the measuring temperature by controller (j). Polymer solution and pure solvent (here water) are stirred by underwater magnetic stirrers (h). [Reprinted with permission from Ref. 66, Copyright 1989, American Chemical Society].

ume, degassing, viscosity), long-time thermostating of the complete apparatus because of long equilibrium times (increasing with polymer molar mass and concentration/viscosity of the solution), correction of unoccupied vapor space, impurities of the solvent, connection to the Hg-surface in older equipment and there is again the problem of obtaining real thermodynamic equilibrium (or not) as explained above.

Modern equipment uses electronic pressure sensors instead of Hg-manometers and digital technique to measure the vapor pressure. Also thermostating is more precise in recent apparatuses. The apparatus developed by Haynes et al.[66] is shown in Figure 4.4.5 as example.

Problems caused by the determination of the unoccupied vapor space were avoided by Haynes et al., since they measure the pressure difference as well as the absolute vapor pressure. Also, the concentration is determined independently by using a differential refractometer and a normalized relation between concentration and refractive index. Degassing of the liquids remains a necessity. Time for establishing thermodynamic equilibrium could be somewhat shortened by intensive stirring (slight problems with increasing polymer concentration and solution viscosity were reported).

In comparison to absolute vapor-pressure measurements, differential vapor-pressure measurements with a high resolution for the pressure difference can be applied even for dilute polymer solutions where the solvent activity is very near to 1. They need more time than VPO-measurements, however.

(iii) Isopiestic sorption/desorption methods

Isopiestic measurements allow a direct determination of solvent activity or vapor pressure in polymer solutions by using a reference system (a manometer has not necessarily to be applied). There are two general principles for lowering the solvent activity in the reference system: concentration lowering or temperature lowering. Isopiestic measurements have to obey the condition that no polymer can vaporize (as it might be the case for lower-molecular oligomers at higher temperatures).

Concentration lowering under isothermal conditions is the classical isopiestic technique, sometimes also called isothermal distillation. A number of solutions (two as the minimum) are in contact with each other via their common solvent vapor phase and solvent

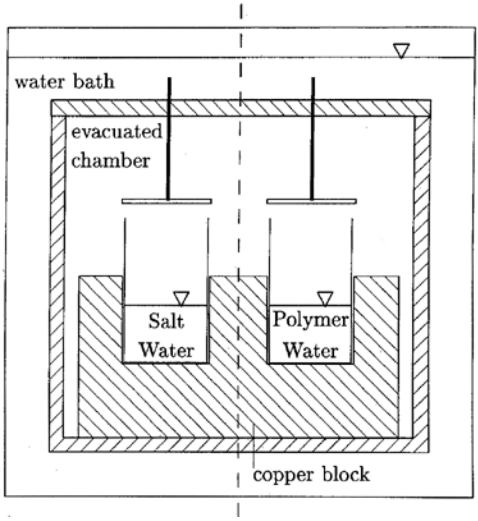

Figure 4.4.6. Schematic of the experimental arrangement for an isopiestic measurements. [Reprinted with permission from Ref. 77, Copyright 1995, Elsevier Science].

evaporates and condenses (this is the isothermal "distillation" process) between them as long as the chemical potential of the solvent is equal in all solutions. At least one solution serves as reference system, i.e., its solvent activity vs. solvent concentration dependence is precisely known. After an exact determination of the solvent concentration in all equilibrated solutions (usually by weighing), the solvent activity in all measured solutions is known from and equal to the activity of the reference solution, Equations [4.4.1 to 4.4.5]. This method is almost exclusively used for aqueous polymer solutions, where salt solutions can be applied as reference systems. It is a standard method for inorganic salt systems. Examples of this technique are given elsewhere.[76-80] Figure 4.4.6 provides a scheme of the experimental arrangement for isopiestic measurements as used by Grossmann et al.[77] to illustrate the common principle.

The complete apparatus consists of six removable stainless steel cells placed in hexagonal pattern in a copper block. The copper block is mounted in a chamber which is thermostated. Each cell has a volume of about 8 cm^3 and is closed by a removable lid. During the experiment, the cells are filled with about 2 cm^3 polymer solution (or reference solution) and placed into the copper block. The chamber is sealed , thermostated and evacuated. The lids are then opened and solvent is allowed to equilibrate between the cells as explained above. After equilibration, the cells are closed, removed from the chamber and weighed precisely. Equilibrium requires usually a couple of days up to some weeks. During this time, the temperature of the thermostat does not fluctuate by less than ±0.1 K, which is realized by the copper block that works as a thermal buffer.

Temperature lowering at specified isobaric or isochoric conditions is the most often used technique for the determination of solvent vapor pressures or activities in polymer solutions. The majority of all measurements is made using this kind of an isopiestic procedure where the pure solvent is used as reference system. The equilibrium condition of equal chemical potential of the solvent in the polymer solution as well as in the reference system is realized by keeping the pure solvent at a lower temperature (T_1) than the measuring temperature (T_2) of the solution. At equilibrium, the vapor pressure of the pure solvent at the lower temperature is then equal to the partial pressure of the solvent in the polymer solution, i.e., $P_1^s(T_1) = P_1(T_2)$. Equilibrium is again established via the common vapor phase for both subsystems. The vapor pressure of the pure solvent is either known from independent data or measured additionally in connection with the apparatus. The composition of the polymer solution can be altered by changing T_1 and a wide range of compositions can be studied (between 30-40 and 85-90 wt% polymer, depending on the solvent). Measurements above 85-90 wt% polymer are subject to increasing errors because of surface adsorption effects.

There is a broad variety of experimental equipment that is based on this procedure (see below). This isopiestic technique is the recommended method for most polymer solutions since it is advantageous in nearly all aspects of measurement: It covers the broadest concentration range. Only very small amounts of polymer are needed (about 30-50 mg with the classical quartz spring balance, about 100 µg with piezoelectric sorption detector or microbalance techniques - see below). It is much more rapid than all other methods explained above, because equilibrium time decreases drastically with such small amounts of polymer and polymer solution (about 12-24 hours for the quartz spring balance, about 3-4 hours for piezoelectric or microbalance techniques). The complete isotherm can be measured using a single loading of the apparatus. Equilibrium is easier to obtain since comparatively small amounts of solvent have to diffuse into the bulk sample solution. Equilibrium can better be tested by measuring sorption and desorption runs which must lead to equal results for thermodynamic absorption equilibrium. Supercritical solvents can be investigated if the piezoelectric detector is used (otherwise buoyancy in dense fluids may cause serious problems). Much broader pressure and temperature ranges can be covered with relatively simple equipment, what may again be limited by the weighing system. Isopiestic sorption measurements can be automated and will allow also kinetic experiments. There are two disadvantages: First, isopiestic sorption measurements below about 30 wt% polymer are subject to increasing error because very small temperature differences (vapor pressure changes) are connected with large changes in concentration. Second, problems may arise with precise thermostating of both the solvent and the solution at different constant temperatures over a longer period of time.

Because of their importance, several technical solutions will now be presented in some detail. The classical concept is the sorption method using a quartz spring balance. Refs. 81-90 provide some examples, where the concentration (mass) of the solution is measured by the extension of the quartz spring according to Hook's law (linear relationship, no hysteresis). It was not originally developed for polymer solutions but for gas-solid adsorption measurements by McBain.[91] The principle was introduced into the investigation of polymer solutions by van der Waals and Hermans[84] and became popular after the work of Bonner and Prausnitz.[85] In this method, a weighed quantity of the (non-volatile) polymer is placed on the pan of the quartz spring balance within a measuring cell. The determination of spring extension vs. mass has to be made in advance as a calibration procedure. Reading of the spring extension is usually made by means of a cathetometer. The cell is sealed, evacuated and thermostated to the measuring temperature (T_2), and the solvent is then introduced into the measuring cell as solvent vapor. The solvent vapor is absorbed by the polymer sample to form the polymer solution until thermodynamic equilibrium is reached. The solvent vapor is provided from a reservoir either of pure liquid solvent thermostated at a lower temperature (T_1) or of a reference liquid solution of known concentration/solvent partial pressure like in the case of the isothermal distillation procedure as described above. A compact version of such an apparatus was developed by Illig[82] and widely used within the author's own work (see Appendix 4.4A for the corresponding references). Figure 4.4.7a shows the details of the equilibrium cell, which has a vacuum double-walled jacket.

The following problems have to be solved during the experiment: The equilibrium cell has to be sealed carefully to avoid any air leakage over the complete duration of the measurements (to measure one isotherm lasts about 14 days). Specially developed thin Teflon sealing rings were preferred to grease. The polymer sample has to withstand the tempera-

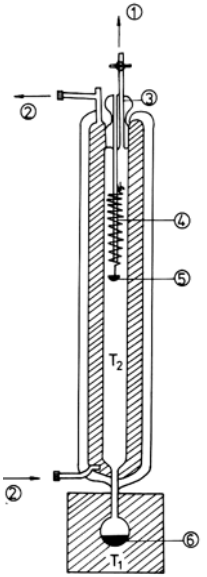

Figure 4.4.7a. Isopiestic vapor - sorption apparatus using a quartz spring: 1 - connection to the vacuum line, 2 - connection to the thermostating unit which realizes the constant measuring temperature T_2 (the correct value of T_2 is obtained by a Pt-100 resistance thermometer within the cell that is not shown), 3 - closing plug, 4 - quartz spring (reading of its extension is made by a cathetometer), 5 - sample pan with the polymer solution, 6 - pure solvent reservoir at temperature T_1. [Reprinted with permission from Ref. 82, Copyright 1982, Wiley-VCH].

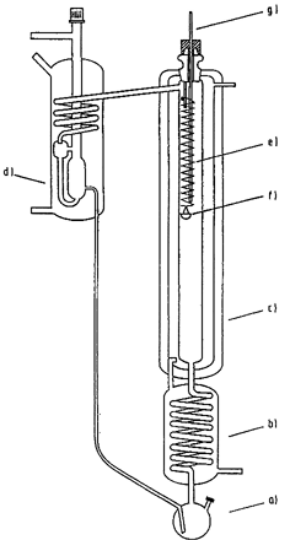

Figure 4.4.7b. Dynamic isopiestic vapor-sorption apparatus using a quartz spring (drawing provided by G. Sadowski): a) evaporator, b) superheater, c) measuring cell, d) condenser, e) quartz spring, f) polymer sample/solution, g) Pt-100 resistance thermometer. [Reprinted with permission from Ref. 87, Copyright 1995, Wiley-VCH].

ture. Changes by thermal ageing during the experiment must be avoided. The temperatures provided by the thermostats must not fluctuate more than ±0.1 K. Condensation of solvent vapor at points that become colder than T_2 has to be avoided by slight overheating (this problem may arise at the closing plug and at the connection between the pure solvent reservoir flask and the double-walled jacket). An intelligent improvement of this compact apparatus was made by Sadowski,[87] see Figure 4.4.7b, where this vapor-sorption apparatus is combined with technical solutions from ebulliometry (more about ebulliometers can be found below).

In comparison to the usual ebulliometric equipment where the polymer solution is placed into the evaporator, only pure solvent is evaporated. The vapor flows through the cell and is condensed at its head-condenser to flow back into the reservoir at the bottom. The vapor pressure is kept constant using a manostat and is measured additionally outside the apparatus after the condenser. Equilibrium times decrease somewhat, degassing of the solvent is not necessary, air leakage does not play any role.

As was stated by different authors, additional measurement of the vapor pressure inside the isopiestic sorption apparatus seems to be necessary if there is some doubt about the real pressure or if no reliable pure solvent vapor pressure data exist for the investigated temperature range. Figure 4.4.8 shows an apparatus used by the author for measurements between room temperature and 70°C and pressures up to 1.5 bar. It combines mercury float valves with Hg-manometers to avoid the use of any grease within the measuring system, a kind of equipment proposed earlier by Ashworth and Everett.[88] Up to four quartz springs can be inserted into the equilibrium cell (only one is shown). Reading of the manometer and of the extension of the quartz spring was made using a cathetometer.

The direct pressure measurement has the advantage that absolute pressures can be obtained and pressure fluctuations can be observed. More modern equipment applies electronic pressure sensors instead of Hg-manometers to avoid the problems caused by the

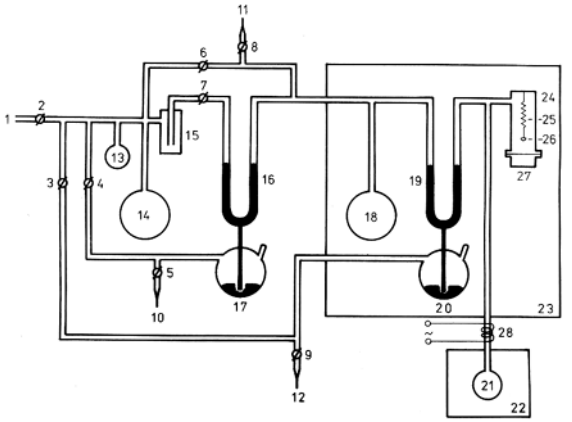

Figure 4.4.8. Isopiestic vapor-sorption apparatus with built-in manometer using a quartz spring: 1 - connection to the vacuum, 2-9 - stop corks, 10, 11, 12 - connections to nitrogen, 13 - degassing flask for the pure solvent, 14, 18 - buffers, 15 - cold trap, 16, 19 - Hg-manometers, 17, 20 - mercury float valves, 21 - pure solvent reservoir at temperature T_1 provided by 22 - thermostat, 23 - temperature controlled air box, 24 - measuring cell, 25 - quartz spring (four quartz springs can be inserted into the equilibrium cell, only one is shown), 26 - pan with the polymer solution, 27 - closing plug sealed with epoxy resin, 28 - heating to avoid solvent condensation.

contact of solvent vapor with the mercury surface and to get a better resolution of the measuring pressure.

Isopiestic vapor sorption can be made using an electronic microbalance instead of the quartz spring balance. Again, this was not originally developed for polymer solutions but for gas-solid adsorption measurements where this is a widespread application. Electronic microbalances are commercially available from a number of producers. Their main advantages are their high resolution and their possibility to allow kinetic measurements. Additionally, experiments using electronic microbalances can easily be automated and provide computing facilities. The major disadvantage with some of these microbalances is that they cannot be used at high solvent vapor pressures and so are limited to a relatively small concentration range. However, since thin polymer films can be applied, this reduces both the time necessary to attain equilibrium (some hours) and the amount of polymer required and equilibrium solvent absorption can be obtained also at polymer mass fractions approaching 1 (i.e., for small solvent concentrations). Depending on their construction, the balance head is situated inside or outside the measuring apparatus. Problems may arise when it is inside where the solvent vapor may come into contact with some electronic parts. Furthermore, all parts of the balance that are inside the apparatus have to be thermostated to the measuring temperature to enable the correct equilibration of the polymer solution or even slightly above to avoid condensation of solvent vapor in parts of the balance. The allowed temperature range of the balance and its sensitivity to solvent corrosion determine then the accessible measuring range of the complete apparatus. Yoo and coworkers[92,93] have recently measured various polymer solutions with such equipment and Figure 4.4.9 shows some details of their apparatus.

Two thermostats maintain the pure solvent temperature T_1 and the measuring temperature T_2 as described above for the spring balance technique, thermostat three protects the essential part of the balance for solvent vapor condensation and damage. A calibrated weight was loaded on the left side of the balance. A granular type of quartz was used as reference weight in order to prevent possible solvent vapor condensation. A dish-type quartz sorption cell was used to load the polymer sample. Platinum wire was used to link both arms to the balance to prevent possible oxidative corrosion of the arm by the solvent. The vapor pressure is measured directly by applying a W-tube Hg-Manometer. The manome- ter reading was made using a cathetometer.

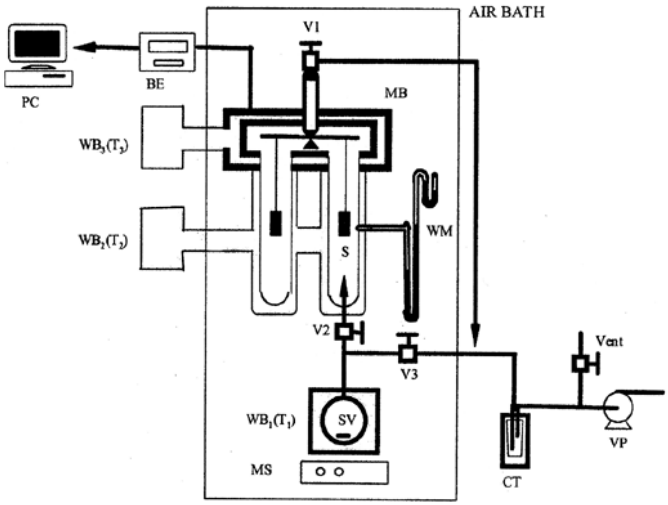

Figure 4.4.9. Schematic diagram of an isopiestic vapor sorption apparatus using an electronic microbalance: PC - personal computer, MB - microbalance, WB1-3 - water bath thermostats with $T_3>T_2>T_1$, V1-3 - valves, WM - W-tube mercury manometer, S - polymer sample/solution, SV - solvent reservoir, MS - magnetic stirrer, CT - cold trap, VP - vacuum pump. [Reprinted with permission from Ref. 92, Copyright 1998, American Chemical Society].

Comparable apparatuses were constructed and used, for example, by Bae et al.[94] or by Ashworth,[95] Ashworth and Price[96] applied a magnetic suspension balance instead of an electronic microbalance. The magnetic suspension technique has the advantage that all sensitive parts of the balance are located outside the measuring cell because the balance and the polymer solution measuring cell are in separate chambers and connected by magnetic coupling only. This allows its application even at very high temperatures of some hundred degrees as well as pressures up to hundreds of MPa.

The most sensitive solvent vapor sorption method is the piezoelectric sorption detector. The amount of solvent vapor absorbed by a polymer is detected by a corresponding change in frequency of a piezoelectric quartz crystal coated with a thin film of the polymer because a frequency change is the response of a mass change at the surface of such a crystal. The frequency of the crystal decreases as mass increases when the crystal is placed in a gas or vapor medium. The frequency decrease is fairly linear. The polymer must be coated onto the crystal from a solution with some care to obtain a fairly uniform film. Measurements can be made at dynamic (vapor flow) or static conditions. With reasonable assumptions for the stability of the crystal's base frequency and the precision of the frequency counter employed, the piezoelectric method allows the detection of as little as 10 nanograms of solvent using a 10 MHz crystal. This greatly reduces both the time necessary to attain equilibrium (3-4 hours) and the amount of polymer required. Saeki et al.[97-99] extensively applied this method to various polymer solutions in a concentration range between 60 and 100 wt% polymer. Recently, Wong et al.[100] and Mikkilineni et al.[101] presented some new investigations with this method. Figure 4.4.10 shows a schematic diagram of the general equipment.

A resolution of nanograms could be realized by Mikkilineni et al.[101] Measurements were also made as a function of time to obtain diffusion coefficients. Comparison with gravimetric sorption measurements demonstrated the accuracy of the experiment. Ref.[100] presents some details about the electronic circuit, the mounting arrangements for the quartz crystals and the sorption cell. Because very thin films are applied, equilibrium solvent absorption also can be obtained at polymer mass fractions approaching 1 (i.e., for small sol-

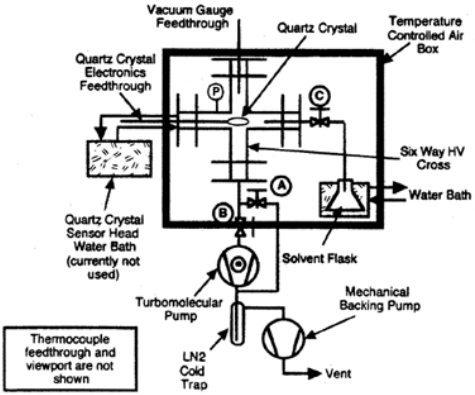

Figure 4.4.10. Schematic diagram of an isopiestic vapor sorption apparatus using a piezoelectric crystal detector. [Reprinted with permission from Ref. 101, Copyright 1995, American Chemical Society].

vent concentrations). Sorption- desorption hysteresis has never been observed when using piezoelectric detectors. Bonner and Prausnitz[85] reported some hysteresis results when applying their quartz spring sorption balance for polymer concentrations above 85 wt%. This demonstrates the effect of reducing the amount of polymer from about 50 mg for the quartz spring sorption technique by an order of 10^3 for the piezoelectric detector. However, measurements are limited to solvent concentrations well below the region where solution drops would be formed. On the other hand, measurements also can be made at higher temperatures and pressures. Limits are set by the stability of the electrical equipment and the construction of the measuring cell.

(iv) Gas-liquid chromatography (GLC)

In 1969 Smidsrod and Guillet[102] demonstrated that GLC could be used to determine the activity coefficient of a solute in a (molten) polymer at essentially zero solute concentration. This type of activity coefficient is known as an infinite-dilution activity coefficient. Smidsrod and Guillet also introduced the term "inverse" gas-liquid chromatography (IGC) because in IGC the liquid polymer in the stationary phase acts as a solvent for the very small amount of an injected solvent sample like the solute in this case. Methods and results of the application of IGC to polymers and polymer solutions have been reviewed continuously[13-25] so that an extensive discussion is not required here. The equipment in principle does not differ very much from that used in analytical GLC. Figure 4.4.11 is a schematic of a simple IGC unit.

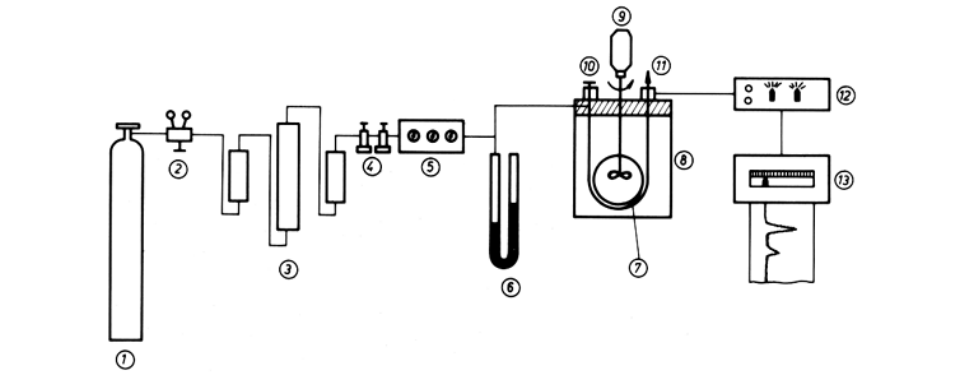

Figure 4.4.11. Schematic diagram of an IGC apparatus: 1 - carrier gas, 2 - pressure reducer, 3 - gas cleaning unit (if necessary) , 4+5 - gas-pressure regulation and control unit, 6 - manometer, 7 - column, 8 - thermostat, 9 - mechanical mixer, 10 - inlet syringe, 11 - detector (the gas flows after the detector through a bubble flow meter that is not shown here), 12 - electronics, 13 - recorder.

For infinite dilution operation the carrier gas flows directly to the column which is inserted into a thermostated oil bath (to get a more precise temperature control than in a conventional GLC oven). The output of the column is measured with a flame ionization detector or alternately with a thermal conductivity detector. Helium is used today as carrier gas (nitrogen in earlier work). From the difference between the retention time of the injected solvent sample and the retention time of a non-interacting gas (marker gas), the thermodynamic equilibrium behavior can be obtained (equations see below). Most experiments were made up to now with packed columns, but capillary columns were used, too. The experimental conditions must be chosen so that real thermodynamic data can be obtained, i.e., equilibrium bulk absorption conditions. Errors caused by unsuitable gas flow rates, unsuitable polymer loading percentages on the solid support material and support surface effects as well as any interactions between the injected sample and the solid support in packed columns, unsuitable sample size of the injected probes, carrier gas effects, and imprecise knowledge of the real amount of polymer in the column, can be sources of problems, whether data are nominally measured under real thermodynamic equilibrium conditions or not, and have to be eliminated. The sizeable pressure drop through the column must be measured and accounted for.

Column preparation is the most difficult task within the IGC-experiment. In the case of packed columns, the preparation technique developed by Munk and coworkers[103,104] is preferred, where the solid support is continuously soaked with a predetermined concentration of a polymer solution. In the case of capillary IGC, columns are made by filling a small silica capillary with a predetermined concentration of a degassed polymer solution. The one end is then sealed and vacuum is applied to the other end. As the solvent evaporates, a thin layer of the polymer is laid down on the walls. With carefully prepared capillary surfaces, the right solvent in terms of volatility and wetting characteristics, and an acceptable viscosity in the solution, a very uniform polymer film can be formed, typically 3 to 10 µm thick. Column preparation is the most time-consuming part of an IGC-experiment. In the case of packed columns, two, three or even more columns must be prepared to test the reproducibility of the experimental results and to check any dependence on polymer loading and sometimes to filter out effects caused by the solid support. Next to that, various tests regarding solvent sample size and carrier gas flow rate have to be done to find out correct experimental conditions.

There is an additional condition for obtaining real thermodynamic equilibrium data that is caused by the nature of the polymer sample. Synthetic polymers are usually amorphous or semi-crystalline products. VLE-based solvent activity coefficients require the polymer to be in a molten state, however. This means that IGC-measurements have to be performed for our purpose well above the glass transition temperature of the amorphous polymer or even above the melting temperature of the crystalline parts of a polymer sample. On the other hand IGC can be applied to determine these temperatures. The glass transition of a polymer does not take place at a fixed temperature but within a certain temperature range depending on the probing technique applied because it is a non-equilibrium effect. Figure 4.4.12 demonstrates the appearance of the glass transition region in an IGC-experiment.

The S-shaped part of the curves in Figure 4.4.12 is the glass transition region. Its minimum describes the glass transition temperature as obtained by IGC. Only data from the straight line on the left side at temperatures well above the glass transition temperature lead

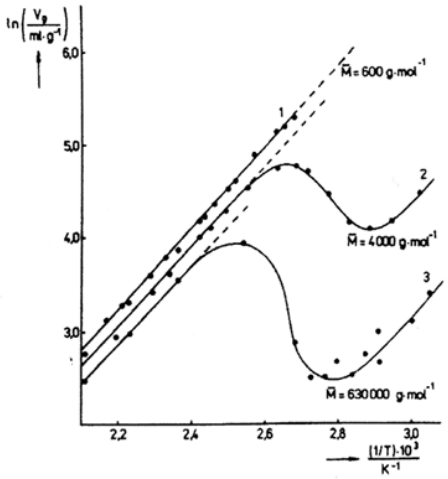

Figure 4.4.12. Temperature dependence of the specific retention volume V_g of p-xylene in polystyrenes of varying molar masses, experimental data were measured by Glindemann.[105]

to real thermodynamic vapor-liquid equilibrium data. As a rule of thumb, the experimental temperature must exceed the glass transition temperature by about 50K. Form and width of the S-shaped region depend somewhat on the solvent used and, as can be seen from the picture, there is a certain dependence on molar mass of the polymer. Data on the right side at temperatures below the glass transition describe mainly surface adsorption effects.

Brockmeier et al.[106,107] showed that GLC can also be used to determine the partial pressure of a solute in a polymer solution at concentrations as great as 50 wt% solute. In this case of finite concentration IGC, a uniform background concentration of the solute is established in the carrier gas. The carrier gas is diverted to a saturator through a metering valve. In the saturator it passes through a diffuser in a well-stirred, temperature-controlled liquid bath. It leaves the separator with the solute equilibrium vapor pressure in the carrier gas. The solute concentration is varied by changing the saturator temperature. Precise control of the temperature bath is needed in order to obtain a constant plateau concentration. Upon leaving the saturator the gas flows to the injector block and then to the column. As in the infinite dilute case a small pulse of the solvent is then injected. This technique is known as elution on a plateau, Conder and Purnell.[108,109] Because finite concentration IGC is technically more complicated, only few workers have applied it. Price and Guillet[110] demonstrated that results for solvent activity, activity coefficient or χ-function are in good agreement with those obtained by traditional isopiestic vapor sorption methods. Whereas the vapor sorption results are more accurate at higher concentrations, the reverse is true for finite concentration IGC since larger injection volumes have to be used, which strains the theory on which the calculations are based. Also, at large vapor concentrations the chromatographic peaks become more spread out, making the measurement of retention times less precise. Additionally, the concentration range is limited by the requirement that the saturator temperature must be below that of the column. Clearly, at higher measuring temperatures, higher solvent concentrations may be used. Finite concentration IGC can be extended to multi-component systems. Especially ternary polymer solutions were investigated to some extend with this technique, e.g., Bonner and coworkers[111,112] or Glover and coworkers.[113-115] Data reduction is somewhat complicated, however.

Danner et al.[116] tested the frontal analysis by characteristic point (FACP) technique to measure thermodynamic data for polymer-solvent systems at finite concentrations. In the FACP technique, a complete isotherm can be derived from the shape of one breakthrough profile. A point on an isotherm is obtained by measuring the retention volume of the characteristic point at the corresponding concentration. The methods to determine thermodynamic data by FACP technique were discussed in detail by Conder and Young.[117]

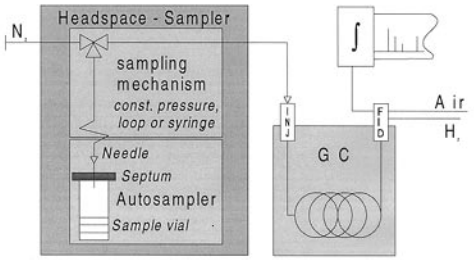

Figure 4.4.13. Schematic of applying head-space gas-chromatography (HSGC) to VLE-measurements in polymer solutions (drawing provided by B. A. Wolf, Univ. Mainz, Germany).

Wolf and coworkers[118,119] applied another GLC technique to VLE-measurements for polymer-solvent systems, the so-called head-space gas-chromatography (HSGC). This is practically a combination of static vapor pressure measurement with gas-chromatographic detection. HSGC experiments were carried out with an apparatus consisting of a head-space-sampler and a normal gas chromatograph. Figure 4.4.13 shows a schematic diagram of the equipment.

The pneumatically driven thermostated headspace-sampler samples a constant amount of gas phase (that must be in equilibrium with the liquid polymer solution, of course) and injects this mixture into the gas chromatograph. Helium is used as carrier gas. After separation of the components of the gaseous mixture in a capillary column they are detected individually by a thermal conductivity detector. The signals are sent to an integrator which calculates the peak areas, which are proportional to the amount of gas in the sample volume and consequently to the vapor pressure. Calibration can be made by measuring the pure solvent in dependence on temperature and to compare the data with the corresponding vapor pressure vs. temperature data. Measurements can be done between about 25 and 85 wt% polymer in the solution (again depending on temperature, solvent and polymer investigated). In order to guarantee thermodynamic equilibrium, solutions have to be conditioned for at least 24 h at constant temperature in the head-space-sampler before measurement. Degassing is not necessary and solvents have to be purified only to the extent necessary to prevent unfavorable interactions in the solution. The experimental error in the vapor pressures is typically of the order of 1-3%. Details about theory and practice of HSGC were discussed by Kolb and Ettre.[120] One great advantage of HSGC is its capability to measure VLE-data, not only for binary polymer solutions but also for polymer solutions in mixed solvents, since it provides a complete analysis of the vapor phase in equilibrium. This is usually not the case with the classical isopiestic sorption balances where PVT-data and a material-balance calculation must be included into the data reduction to calculate vapor phase concentrations, e.g., Refs.[121-123]

(v) Ebulliometry (boiling point elevation of the solvent)

As pointed out above, dynamic vapor-liquid equilibrium measurement methods are not very suitable for concentrated polymer solutions, especially due to their heavy foaming behavior. For dilute polymer solutions, however, there is continuing application of ebulliometry as an absolute method for the direct determination of the number-average molecular mass M_n. Dedicated differential ebulliometers allow the determination of values up to an order of 100,000 g/mol. Ebulliometry as a method for molar mass determination was recently reviewed by Cooper,[33] Glover,[34] and Mays and Hadjichristidis.[40]

The major requirements for a successful ebulliometry experiment are thermal stability, equilibration of both concentration and temperature, temperature measurement and control and pressure measurement and control. It is an advantage of ebulliometry to know very exactly the constant pressure applied since pressure constancy is a prerequisite of any

successful experiment. Commercially sold ebulliometers have seldom been used for polymer solutions. For application to polymer solutions, the operating systems have been individually constructed. The above-mentioned reviews explain some of these in detail which will not be repeated here as ebulliometry is not really a practiced method to obtain solvent activities and thermodynamic data in polymer solutions. However, ebulliometry is a basic method for the investigation of vapor-liquid equilibrium data of common binary liquid mixtures, and we again point to the review by Williamson,[55] where an additional number of equilibrium stills is shown.

Ebulliometers have traditionally been classified as either simple, in which only a single temperature is measured, or differential, in which the boiling temperatures of the pure solvent and of the solution were measured simultaneously. In differential ebulliometers, two independent temperature sensors can work, or a single differential temperature measurement is done. Essentially, all ebulliometers for polymer solutions are of the differential type. The manner in which the reference boiling temperature of the pure solvent is provided differs, however. Establishment and maintenance of both temperature and concentration equilibrium are accomplished in a variety of ways. The common method is the use of a vapor lift pump (a Cottrell pump) where the boiling liquid is raised to a position from which it can flow in a thin film until superheat is dissipated and its true boiling temperature can be measured. This technique has one disadvantage: the pumping rate depends on the heat input. This is of particular importance with polymer solutions in which problems due to foaming occur. To overcome this problem mechanical pumps were sometimes applied. Other ebulliometer types have been reported that use the methods of surface volatilization, spray cooling, two-stage heating, or rotating ebulliometer; for more details please see Refs.[33,34,40] Methods of temperature measurement within ebulliometer experiments will not be discussed here, as they change rapidly with continuing progress of electronics and computerization. Pressure control is important for single temperature ebulliometers, as the boiling temperature depends on pressure. It is not so important in differential type ebulliometers, owing to the simultaneous and compensating change in reference temperatures. Therefore, direct changes in boiling temperatures present no serious problem if sufficient time is allowed for calibration. It is usually recommended that the ebulliometer be thoroughly cleaned and dried between experiments. Small amounts of polymer adsorbed on the surface must be avoided.

(vi) Vapor-pressure osmometry (VPO)

Vapor-pressure osmometry is, from its name, compared with membrane osmometry by considering the vapor phase to act like the semipermeable membrane, however, from its principles it is based on vapor pressure lowering or boiling temperature elevation. Since the direct measure of vapor pressure lowering of dilute polymer solutions is impractical because of the extreme sensitivity that is required, VPO is in widespread use for oligomer solutions (M_n less than 20,000 g/mol) by employing the thermoelectric method as developed by Hill in 1930.[124] In the thermoelectric method, two matched temperature-sensitive thermistors are placed in a chamber that is thermostated to the measuring temperature and where the atmosphere is saturated with solvent vapor. If drops of pure solvent are placed on both thermistors, the thermistors will be at the same temperature (zero point calibration). If a solution drop is placed on one thermistor, a temperature difference ΔT occurs which is caused by condensation of solvent vapor onto the solution drop. From equilibrium thermodynamics follows that this temperature increase has its theoretical limit when the vapor pressure of

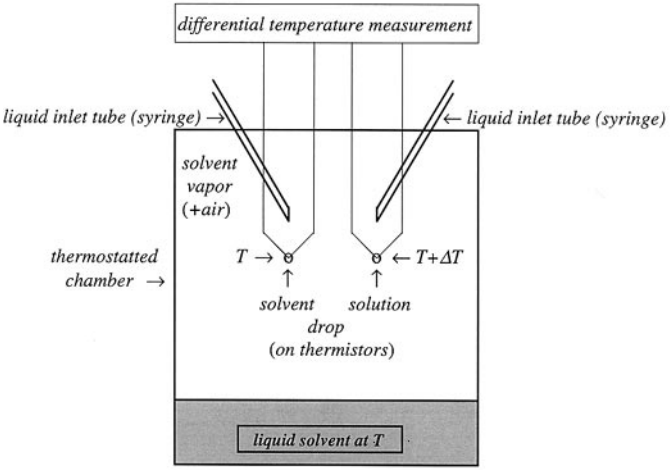

Figure 4.4.14. Principle scheme of a vapor-pressure osmometer of the hanging drop type. T - measuring temperature, ΔT - obtained temperature difference (time dependent), measurements are made at atmospheric pressure where T determines the partial vapor pressure of the solvent P_1 in air.

the solution is equal to that of the pure solvent, i.e., at infinite dilution. The obtained temperature difference is very small, about 10^{-5}K. Because solvent transfer effects are measured, VPO is a dynamic method. This leads to a time-dependent measurement of ΔT. The principle scheme of a VPO apparatus is given in Figure 4.4.14.

Today, vapor-pressure osmometers are commercially available from a number of producers. They can be divided into two basic types: those that employ conventional hanging drop thermistors as in Figure 4.4.14 and those that use vertical thermistors. The vertical thermistors automatically control drop size to ensure more reproducible response. The hanging drop design requires the operator to manually monitor and control drop size. Furthermore, commercial instruments have been developed which utilize vertical thermistors having cups or pieces of platinum gauze to control drop size in a highly reproducible manner. More details about instrumentation and techniques can be found in the reviews given by Glover,[34] Mays and Hadjichristidis.[40] A very recent presentation can be found in a new book edited by Pethrick and Dawkin.[26]

Depending on technical details of the equipment, on the sensitivity of the temperature detector, on measuring temperature, solvent vapor pressure and polymer concentration in the solution drop, a steady state for ΔT can be obtained after some minutes. The value of ΔT^{st} is the basis for thermodynamic data reduction (see below). If measuring conditions do not allow a steady state, an extrapolation method to ΔT at zero measuring time can be employed for data reduction. Sometimes a value is used that is obtained after a predetermined time; however, this may lead to some problems with knowing the exact polymer concentration in the solution. The extrapolation method is somewhat more complicated and needs experience of the experimentator but gives an exact value of polymer concentration. Both methods are used within solvent activity measurements when polymer concentrations are higher and condensation is faster than in common polymer characterization experiments. A way to avoid these problems is discussed below.

Experience has shown that careful selection of solvent and temperature is critical to the success of the VPO experiment. Nearly all common solvents, including water (usually, there are different thermistor sensors for organic solvents and for water), can be used with VPO. The measuring temperature should be chosen so that the vapor pressure of the solvent will be greater than 6,000 Pa, but not so high as to lead to problems with evaporation from the chamber. Solvent purity is critical, especially volatile impurities, and water must be

avoided. Greater sensitivity can be achieved by using solvents with low enthalpies of vaporization. This means, for our task, that not all desirable polymer-solvent pairs and not all temperature (pressure) ranges can be investigated by VPO. Additionally, VPO has some inherent sources of error. These belong to the possible existence of surface films, to differences in diffusion coefficients in solutions, to appreciably different solution concentrations, to differences in heat conductivity, to problems with drop size and shape, to the occurrence of reactions in the solution, and to the presence of volatile solutes. Of course, most of them can be avoided by laboratory practice and/or technical improvements, but it must be taken into account when measuring solvent activities.

Regener and Wohlfarth[125] developed a way to enlarge the applicability range of VPO to polymer concentrations ≤40wt% for the purpose of measuring solvent activities. An increase of polymer concentration over the linear steady state working range of VPO causes some problems. First, no thermodynamically defined ΔT can be obtained and, second, the calibration constant may become dependent on concentration. Thus, the only way to achieve higher concentrations is to find methods to minimize the increasing chemical potential difference of the solvent between the two drops. This can be achieved by using a reference solution of known solvent activity instead of the pure solvent. The instrument is then used as a zero-point detector comparing the solvent activity of the reference solution with solvent activity of the polymer solution. The reference concentration has to be varied until $\Delta T = 0$ is found. The only assumption involved in this method is equal solvent condensation and diffusion. The extrapolation method to ΔT at zero measuring time can be used to minimize these influences. It is not really necessary to find the reference solution at exactly $\Delta T=0$, but it is sufficient to measure a small $\Delta T < 0$ and small $\Delta T > 0$ and to interpolate between both known solvent activities. An example is shown in Figure 4.4.15, where benzene was used as solute for the reference solutions.

Since the polymer solution remains quasi unchanged in concentration, this modified VPO-method is faster than isopiestic isothermal distillation experiments with organic solvents and polymer solutions. Difficulties with the increasing viscosity of concentrated polymer solutions set limits to its applicability, because solutions should flow easily to form drops.

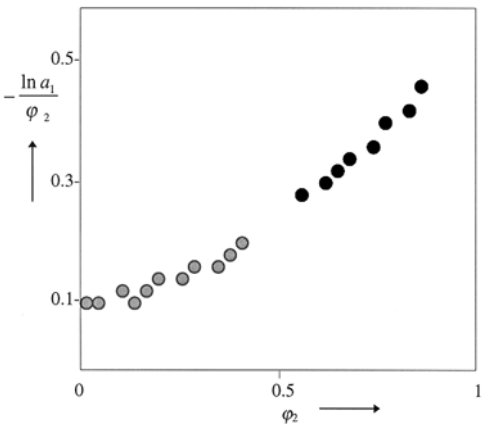

Figure 4.4.15. Experimental data of the system toluene + polystyrene, M_n = 1380 g/mol, at 323.15K, isopiestic vapor pressure/sorption measurement (full circles), VPO at higher concentrations (gray circles), data from authors own work.

Recently, Gaube et al.[126,127] or Eliassi et al.[128] measured water activities in aqueous solutions of poly(ethylene glycol) and showed that the conventional VPO method also can be used for higher polymer concentrations with good success.

4.4.3.1.2 Primary data reduction

Equation [4.4.7] is the starting relation for data from VLE-measurements. Two relations are necessary to obtain the solvent activity a_1: one for the fugacity coefficient of the solvent vapor and one for the standard state fugacity of the liquid solvent. In principle, every kind of equation of state can be

applied to calculate the solvent vapor fugacity coefficient. This is done if dedicated equations of state are applied for further modeling. However, in most cases it is common practice to use the virial equation of state for the purpose of reducing primary VLE-data of polymer solutions. This procedure is sufficient for vapor pressures in the low or medium pressure region where most of the VLE-measurements are performed. The virial equation is truncated usually after the second virial coefficient, and one obtains from Equation [4.4.6]:

$$\ln \phi_i = \left(2\sum_{j=1}^{m} y_i B_{ij} - \sum_{i=1}^{m}\sum_{j=1}^{m} y_i y_j B_{ij} \right) \frac{P}{RT} \qquad [4.4.19]$$

where:

B_{ii} second virial coefficient of pure component i at temperature T
B_{jj} second virial coefficient of pure component j at temperature T
B_{ij} second virial coefficient corresponding to i-j interactions at temperature T.

In the case of a strictly binary polymer solutions Equation [4.4.19] reduces simply to:

$$\ln \phi_1 = \frac{B_{11} P}{RT} \qquad [4.4.20]$$

To calculate the standard state fugacity, we consider the pure solvent at temperature T and saturation vapor pressure P^s for being the standard conditions. The standard state fugacity is then calculated as:

$$f_1^0 = P_1^s \exp\left[\frac{V_1^L \left(P - P_1^s \right) + B_{11} P_1^s}{RT} \right] \qquad [4.4.21]$$

where:

P_1^s saturation vapor pressure of the pure liquid solvent 1 at temperature T
V_1^L molar volume of the pure liquid solvent 1 at temperature T

The so-called Poynting correction takes into account the difference between the chemical potentials of the pure liquid solvent at pressure P and at saturation pressure P_1^s assuming that the liquid molar volume does not vary with pressure. Combining Equations [4.4.7, 4.4.20 and 4.4.21] one obtains the following relations:

$$a_1 = \phi_1^V y_1 P / f_1^0 = \left(P_1 / P_1^s \right) \exp\left[\frac{\left(B_{11} - V_1^L \right)\left(P - P_1^s \right)}{RT} \right] \qquad [4.4.22a]$$

$$\gamma_1 = a_1 / x_1^L = \left(P_1 / x_1^L P_1^s \right) \exp\left[\frac{\left(B_{11} - V_1^L \right)\left(P - P_1^s \right)}{RT} \right] \qquad [4.4.22b]$$

$$\Omega_1 = a_1 / w_1^L = \left(P_1 / w_1^L P_1^s\right) \exp\left[\frac{\left(B_{11} - V_1^L\right)\left(P - P_1^s\right)}{RT}\right] \qquad [4.4.22c]$$

These relations can be applied to VLE-data from all experimental methods.

The data reduction for infinite dilution IGC starts with the usually obtained terms of retention volume or net retention volume.

$$V_{net} = V_r - V_{dead} \qquad [4.4.23]$$

where:

V_{net}	net retention volume
V_r	retention volume
V_{dead}	retention volume of the (inert) marker gas, dead retention, gas holdup

These retention volumes are reduced to specific ones by division of Equation [4.4.23] with the mass of the liquid (here the liquid, molten polymer), corrected for the pressure difference between column inlet and outlet pressure and reduced to $T_0 = 273.15K$.

$$V_g^0 = \left(\frac{V_{net}}{m_2}\right)\left(\frac{T_0}{T}\right)\frac{3\left(P_{in} / P_{out}\right)^2 - 1}{2\left(P_{in} / P_{out}\right)^3 - 1} \qquad [4.4.24]$$

where:

V_g^0	specific retention volume corrected to 0°C
m_2	mass of the polymer in the liquid phase within the column
P_{in}	column inlet pressure
P_{out}	column outlet pressure

Theory of GLC provides the relation between V_g^0 and thermodynamic data for the low-molecular component (solvent) 1 at infinite dilution:

$$\left(\frac{P_1}{x_1^L}\right)^{\infty} = \frac{T_0 R}{V_g^0 M_2} \quad or \quad \left(\frac{P_1}{w_1^L}\right)^{\infty} = \frac{T_0 R}{V_g^0 M_1} \qquad [4.4.25]$$

where:

M_2	molar mass of the liquid (molten) polymer
M_1	molar mass of the low-molecular component (solvent).

The activity coefficients at infinite dilution follow immediately from Equation [4.4.22] by introducing the above result, if we neglect interactions to and between carrier gas molecules (which is normally helium):

$$\gamma_1^{\infty} = \left(\frac{T_0 R}{V_g^0 M_2 P_1^s}\right) \exp\left[\frac{\left(B_{11} - V_1^L\right)\left(P - P_1^s\right)}{RT}\right] \qquad [4.4.26a]$$

$$\Omega_1^{\infty} = \left(\frac{T_0 R}{V_g^0 M_2 P_1^s} \right) \exp \left[\frac{P_1^s \left(V_1^L - B_{11} \right)}{RT} \right] \qquad [4.4.26b]$$

The standard state pressure P has to be specified. It is common practice by many authors to define here zero pressure as standard pressure since pressures are usually very low during GLC-measurements. Then, Equations [4.4.26a and b] change to:

$$\gamma_1^{\infty} = \left(\frac{T_0 R}{V_g^0 M_2 P_1^s} \right) \exp \left[\frac{P_1^s \left(V_1^L - B_{11} \right)}{RT} \right] \qquad [4.4.27a]$$

$$\Omega_1^{\infty} = \left(\frac{T_0 R}{V_g^0 M_1 P_1^s} \right) \exp \left[\frac{P_1^s \left(V_1^L - B_{11} \right)}{RT} \right] \qquad [4.4.27b]$$

One should keep in mind that mole fraction-based activity coefficients become very small values for common polymer solutions and reach the value of 0 for $M_2 \rightarrow \infty$, which means a limited applicability to at least oligomer solutions. Therefore, the common literature provides only mass fraction-based activity coefficients for (high-molecular) polymer/(low-molecular) solvent pairs. Furthermore, the molar mass M_2 of the polymeric liquid is an average value according to the usual molar-mass distribution of polymers. Additionally, it is a second average if mixed stationary liquid phases are applied.

Furthermore, thermodynamic VLE-data from GLC-measurements are provided in the literature as values for $(P_1/w_1)^{\infty}$, see Equation [4.4.25], i.e., classical mass fraction based Henry's constants (if assuming ideal gas phase behavior):

$$H_{1,2} = \left(\frac{P_1}{w_1^L} \right)^{\infty} = \frac{T_0 R}{V_g^0 M_1} \qquad [4.4.28]$$

Thus, Equation (4.4.27b) reduces to

$$\Omega_1^{\infty} = \frac{H_{1,2}}{P_1^s} \exp \left[\frac{P_1^s \left(V_1^L - B_{11} \right)}{RT} \right] \qquad [4.4.29]$$

The data reduction for finite concentration IGC by elution on a plateau is more complicated than for infinite dilution IGC via Equations [4.4.24 to 26] and will not be explained here. A detailed analysis of the elution on plateau mode was made by Conder and Purnell.[108,109] For the determination of thermodynamic properties of polymer solutions by finite-concentration IGC the reader is referred to the paper by Price and Guillet[110] who provide a comprehensive derivation of all necessary equations.

The data reduction of ebulliometric measurements can be made either by using Equations [4.4.22] or by applying the relation for the boiling point elevation of a binary mixture:

$$\Delta T^{ebull} = -\frac{RT^2}{\Delta_{vap}H_1^0}\ln a_1 \qquad [4.4.30]$$

where:

T	measuring temperature (= boiling point temperature of the pure solvent)
ΔT^{ebull}	temperature difference of boiling point elevation
$\Delta_{vap}H_1^0$	molar enthalpy of vaporization of the pure solvent 1 at temperature T.

The ratio $M_1RT^2/\Delta_{vap}H_1^0$ is called the ebulliometric constant. For the determination of solvent activities from ebulliometric data, tabulated ebulliometric constants should not be used, however. On the other side, it is sometimes recommended to use reference solutes to establish an experimental relationship for the equipment in use, i.e., unprecise data for the enthalpy of vaporization or perhaps some non-equilibrium effects cancel out of the calculation. Enthalpies of vaporization are provided by several data collections, e.g., by Majer and Svoboda,[129] or through the DIPPR database.[130]

The data reduction of vapor-pressure osmometry (VPO) follows to some extent the same relations as outlined above. However, from its basic principles, it is not an equilibrium method, since one measures the (very) small difference between the boiling point temperatures of the pure solvent drop and the polymer solution drop in a dynamic regime. This temperature difference is the starting point for determining solvent activities. There is an analogy to the boiling point elevation in thermodynamic equilibrium. Therefore, in the steady state period of the experiment, the following relation can be applied if one assumes that the steady state is sufficiently near the vapor-liquid equilibrium and linear non-equilibrium thermodynamics is valid:

$$\Delta T^{st} = -k_{VPO}\frac{RT^2}{\Delta_{vap}H_1^0}\ln a_1 \qquad [4.4.31]$$

where:

T	measuring temperature (= temperature of the pure solvent drop)
ΔT^{st}	temperature difference between solution and solvent drops in the steady state
k_{VPO}	VPO-specific constant
$\Delta_{vap}H_1^0$	molar enthalpy of vaporization of the pure solvent 1 at temperature T .

Recent examples of solvent activity measurements by VPO in aqueous solutions of poly(ethylene glycol) by Eliassi et al.[128] and of poly(ethylene glycol) or dextran by Gaube et al.[126,127] demonstrate the obtainable high quality if precise experiments were made.

The so-called VPO-specific constant contains all deviations from equilibrium state and it is to be determined experimentally. It depends on certain technical details from the equipment used and also on the temperature and solvent applied. It is assumed not to depend on the special solute under investigation and can therefore be obtained by calibration. Equation [4.4.31] can also be used if not the steady state, but the temperature difference extrapolated to a measuring time of zero is determined by the experimentator. However, the values of k_{VPO} are different for both methods. A more detailed discussion about calibration problems can be found in the papers of Bersted,[131,132] or Figini.[133-135]

Usually, VPO-data are reduced to virial coefficients and not to solvent activities. Power series expansion of Equation [4.4.31] leads to the following relations:

$$\frac{\Delta T^{st}}{c_2} = k_{VPO}\,\frac{RT^2V_1}{\Delta_{LV}H_1^0}\left[\frac{1}{M_2} + \Gamma_2 c_2 + \Gamma_3 c_2^2 + \ldots\right] \qquad [4.4.32a]$$

or

$$\frac{\Delta T^{st}}{c_2'} = k_{VPO}\,\frac{RT^2V_1}{\Delta_{LV}H_1^0}\left[\frac{1}{M_2} + \Gamma_2' c_2' + \Gamma_3' c_2'^2 + \ldots\right] \qquad [4.4.32b]$$

where:

c_2	mass by volume concentration $c_2 = m_2/v$
c_2'	mass by mass concentration $c_2' = m_2/m_1$
v	volume of the polymer solution
m_i	mass of component i
V_1	molar volume of the solvent
M_1	molar mass of the solvent
M_2	molar mass of the polymer
Γ_2, Γ_3, ...	second, third, ... VPO-virial coefficients based on g/cm^3 concentrations
Γ_2', Γ_3', ..	second, third, ... VPO-virial coefficients based on g/g concentrations

In the dilute concentration region, these virial equations are usually truncated after the second virial coefficient which leads to a linear relationship. These truncated forms of Equation [4.4.32] are the basis for applying VPO to polymer characterization, which will not be discussed here - please see Refs.[26,34,40] Solvent activities can be estimated from second virial coefficients with some care regarding the necessary accuracy of all numerical values included. The molar mass of the polymer, M_2, is the number-average, M_n, if polydisperse samples are investigated. Corresponding averages of the virial coefficients can be introduced, too. The estimation of higher virial coefficients than the second one is difficult and hardly leads to satisfying results, because measurements at high polymer concentrations cause a lot of problems. In some cases, however, as in the above-mentioned paper by Gaube et al.,[126,127] precise measurements were done for polymer concentrations up to 30-40 wt% and second and third virial coefficients were obtained in good quality.

As pointed out above, there is another way VPO can be applied to measure activity differences between two polymer solution drops that differ slightly in concentration (in the same solvent, of course). In this case, VPO is quasi an isopiestic experiment and the unknown activity can be determined by using reference solutions with known solvent activity values:[125]

$$a_1(T, w_{polymer}) = a_1(T, w_{reference}) \qquad [4.4.33]$$

Reference solutions can be made with the same organic solutes that are used for calibration. In the case of water, NaCl or KCl solutions may be applied as it is done for many isopiestic (isothermal distillation) measurements with aqueous solutions.

4.4.3.1.3 Comparison of experimental VLE-methods

The general aim of all experiments is to measure solvent activities in polymer solutions over the complete concentration range and for all desired temperatures (and pressures). Additionally, the dependence on molar mass of the polymer has to be taken into account. As is clear from all explanations above, there is no really universal method to fulfill all purposes.

Vapor pressure/vapor sorption measurements cover nearly the complete concentration range if different apparatuses are used. Measurements can be made with good accuracy. Principal limits with respect to temperature or pressure do not exist, but most apparatuses in the literature are constructed only for temperatures between 20 and 100°C, sometimes up to 150°C, and pressures between 1 and 100 - 200 kPa. Vapor pressure/vapor sorption measurements are very time-consuming experiments. To obtain a complete isotherm one needs usually about a month with conventional techniques or, at least, some days with microbalances or piezoelectric sensors. This demands long-time stability for thermostating and precise temperature control. Furthermore, the equilibrium cell has to be sealed in such a way that air leakage is avoided for the complete duration of the measurement. Experimentators need quite a lot of experience until they observe really good data. Experiments can only partially be automated depending on the method and equipment applied. The accuracy of the final data depends on the method applied, the temperature or pressure investigated, and also the given concentration. Measurements above about 85 wt% polymer showed sometimes sorption-desorption hysteresis. Solvent degassing is absolutely necessary with the exception of the apparatus proposed by Sadowski where degassing takes place automatically during the experiment (see above). The solvent must be purified from all other impurities. This is true of course also for the polymer investigated. According to their capabilities, different apparatuses should be used: differential pressure measurements for 5-30 wt% polymer in the solution, isopiestic sorption techniques for 30-85 wt% polymer, piezoelectric or microbalance detection for 60-99 wt% polymer. These limits can change somewhat with molar mass of the polymer. Oligomer solutions are easier to handle and can be measured even with conventional VLE-technique as developed for low-molecular liquid mixtures. There may be limits in temperature and pressure that depend on the nature of the solvent/polymer pair. Usually, the solutions investigated should not show liquid-liquid demixing and solutions should not become solid. Thermodynamic equilibrium data can only be obtained if the polymer is investigated well above its glass transition temperature. There is a depression of the glass transition temperature with increasing solvent concentration, but there are polymers that can be investigated only at temperatures above 100°C and more, even in concentrated solutions.

VPO is more limited with respect to the measurement of solvent activities. It is designed only for dilute polymer solutions (in the maximum up to 40 wt% polymer), optimum temperature and pressure (well below normal pressure) ranges and molar masses up to about 20,000 g/mol for the polymer. Not all solvents can be applied. On the other hand, VPO is a well-established method, commercially available, possessing a high resolution for very small differences of solvent activities with respect to the pure solvent and does not need much time. Steady-state conditions are obtained within minutes and quite a lot of measurements can be made during a working day. There are no problems with external thermostating or long-time stability. Experimental results from VPO are in good agreement with measurements from scattering techniques. VPO measurements close the gap between 0 and 30 wt% polymer in the solution with respect to conventional vapor pressure/vapor sorption measurements (of course, only within its limits explained). Experimentators easily acquire the necessary experience with the measuring equipment.

The piezoelectric sorption technique is a method that is especially suitable for the low solvent concentration range. It is the most sensitive solvent vapor sorption method. A resolution of nanograms can be realized. Measurements can also be made as a function of time

to obtain diffusion coefficients. Comparison with gravimetric sorption measurements demonstrated the accuracy of the experiment. Because very thin films are applied, equilibrium solvent absorption also can be obtained at polymer mass fractions approaching 1, as with the IGC experiment. Comparison to IGC-data gives good agreement. Sorption-desorption hysteresis has never been observed when using piezoelectric detectors. Measurements are limited to a concentration range where the swollen polymer film is still stable at the crystal surface. Equilibrium is rather quickly established, usually after 3-4 hours, i.e., an isotherm can be measured within some days. With the corresponding equipment, high pressures and high temperatures can be applied, too.

IGC is the most rapid method and it is the recommended technique for the infinite dilution range of the solvent in the (liquid, molten) polymer. Measurements can also be made to obtain diffusion coefficients. Column preparation and finding optimum experimental conditions are the most time-consuming tasks. These tasks require quite a lot of experience. The final measurements can be automated and provide quick, reliable and reproducible results. Temperature and solvent dependencies can easily be investigated. The common accuracy is 1-3% with respect to data of the χ-function or Henry's constant. There is no need to degas the solvents or to purify them except from impurities which may react with the polymer. Limits are mainly given by the glass transition temperature of the polymer as explained above. Due to this problem, most IGC measurements are made at temperatures well above 100°C. On the other hand, temperatures well above 100°C can cause the problem of thermal ageing and degradation of the polymer sample if temperatures are too high. In comparison to IGC, vapor pressure measurements were made in most cases below 100°C. There were some special investigations in earlier literature to compare IGC-data at infinite dilution with those from vapor pressure measurements at concentrated solutions, e.g., Refs.[110,136-138] Differences between IGC-data and vapor pressure measurements reported in older papers are mainly caused by errors with the IGC technique. Temperatures were used too near or even within the glass transition region, unsuitable polymer loading was applied, non-equilibrium conditions were used. But, there are also errors from/within vapor pressure data, mainly sorption/desorption hysteresis at too high polymer concentrations because of non-equilibrium conditions. Today it is accepted that there are no differences between IGC-data and vapor pressure measurements if all thermodynamic equilibrium conditions are carefully obeyed. In contrast to vapor pressure measurements, IGC can also be applied with thermodynamically bad solvents. It is the only method to obtain limiting activity coefficients for strong non-solvents. Even mass fraction based activity coefficients above 25 or χ-values of 2 or more can be measured.

Finite concentration IGC provides the possibility to connect advantages from IGC and vapor pressure measurements because it can be applied between 50 and 100 wt% polymer. However, the experimental technique is more sophisticated, data reduction is more complicated, and only few workers have applied it. On the other hand, much experimental time can be saved since finite concentration IGC is a rapid method. One isotherm can be observed within one day (or two). Price and Guillet[110] or Danner et al.[116] demonstrated that results for solvent activity coefficients and χ-functions or sorption isotherms are in good agreement with those obtained by traditional isopiestic vapor sorption methods. The concentration range of finite concentration IGC is limited by the requirement that the saturator temperature must be below that of the column. Clearly, at higher measuring temperatures, higher

solvent concentrations may be used. Finite concentration IGC can be extended to multi-component systems.

Head-space gas chromatography is a modern tool for the measurement of vapor pressures in polymer solutions that is highly automated. Solutions need time to equilibrate, as is the case for all vapor pressure measurements. After equilibration of the solutions, quite a lot of data can be measured continuously with reliable precision. Solvent degassing is not necessary. Measurements require some experience with the equipment to obtain really thermodynamic equilibrium data. Calibration of the equipment with pure solvent vapor pressures may be necessary. HSGC can easily be extended to multi-component mixtures because it determines all components in the vapor phase separately.

In summary, the decision for a special equipment depends to some extend on concentration, temperature and pressure ranges one is interested in. From the experience of the author, the combination of isopiestic vapor pressure/vapor sorption measurements for the determination of solvent activities with infinite dilution IGC for the determination of Henry's constants provides good experimental data and covers a temperature range that is broad enough to have a sufficient data basis for thermodynamic modeling. If one is interested in both solvent solubility and diffusion data, finite concentration IGC or piezoelectric sorption techniques should be applied.

4.4.3.2 Other measurement methods

This subchapter summarizes all other experimental methods mentioned in subchapter 4.4.1 in order of their special importance and use regarding the determination of solvent activities in polymer solutions.

4.4.3.2.1 Membrane osmometry

Apart from VLE-measurements, membrane osmometry is the next important method that has been used for measuring solvent activities in polymer solutions. This follows from the tables in Refs.[1,2,5,8] according to its occurrence in comparison to the other methods. Most of these measurements were made in the dilute solution regime; only a small number of papers dealt with high-pressure osmometry where one also can measure solvent activities for concentrated solutions with polymer concentrations up to about 50 wt%, e.g. Refs.[139-145]

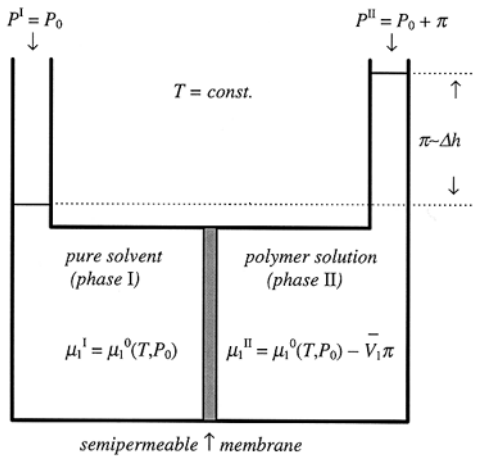

Figure 4.4.16. Principle scheme of a membrane osmometer: 1 - solvent, 2 - polymer, π - osmotic pressure, Δh - hydrostatic height difference, P_0 - ordinary pressure or measuring pressure, $\bar{V}_1$- partial molar volume of the solvent in the polymer solution.

Laboratory designed instruments were developed in the 40's and 50's, e.g. by Zimm[145] or by Flory.[144] Later on, high speed membrane osmometers are commercially available, e.g., from Knauer, Hewlett-Packard or Wescan Instruments. External pressures may be applied to balance the osmotic pressure if necessary, e.g., Vink.[140] The principle scheme of a membrane osmometer together with the corresponding

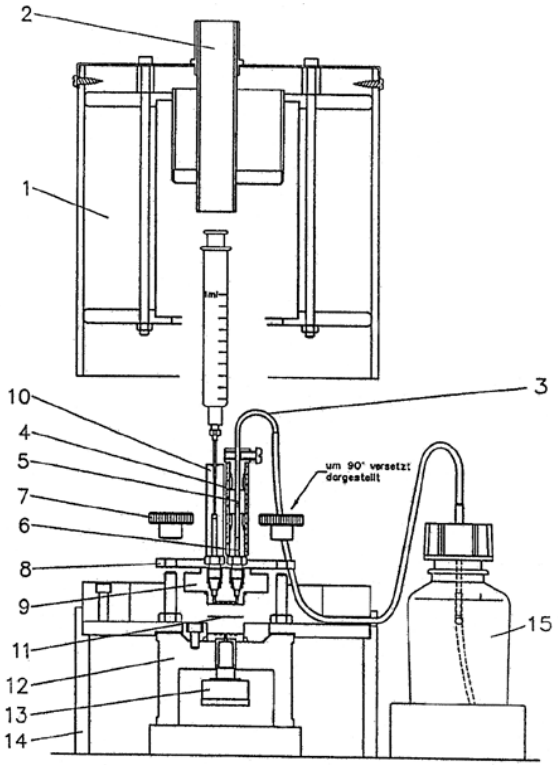

Figure 4.4.17. Description of the principal construction of a Knauer membrane osmometer A 300: 1 - head thermostat, 2 - channel for syringe, 3 - calibration device with suction tube, 4 - calibration glass, 5 - capillary position MEASUREMENT, 6 - capillary position CALIBRATION, 7 - tension screws, 8 - cell retaining disc, 9 - upper half of measuring cell, 10 - sample introduction system, 11 - semipermeable membrane, 12 - lower half of measuring cell, 13 - pressure measuring system, 14 - cell thermostat, 15 - suction of calibration bottle. [Reprinted from the operating manual with permission from Dr. H. Knauer GmbH (Germany)].

thermodynamic situation is illustrated in Figure 4.4.16.

Technical details of the different apparatuses will not be presented here, however, the principle construction of the measuring cell and the heating thermostat of the Knauer membrane osmometer A 300 is shown in Figure 4.4.17 for illustration and as example.

As a general feature of most osmometers, the membrane is clamped into a stainless steel thermostated chamber (the measuring cell and the pressure measuring system of modern osmometers are built into a high-grade electronically stabilized thermostat) and serves as barrier between the pure solvent and the polymer solution sides of the chamber. The solvent side (bottom) is in juxtaposition with a pressure sensor, e.g. the diaphragm of a capacitance strain gauge or a piezo-chip. The solvent transport is measured across the bottom side of the membrane in the direction of the solution which is topside the membrane. The amount of flowing solvent is in the range of 10^{-6} ml and equilibrium is established after some minutes when hydrostatic pressure prevents further solvent flow. This is indicated by the electronics of the equipment as well as any changes in equilibrium such as thermal drift of solute diffusion through the membrane. Other osmometers apply compensation methods where the increase of the hydrostatic height of the solution side is automatically compensated by changing the filling height. Due to this procedure, only very small amounts of solvent have to permeate through the membrane and equilibrium is reached within 10-20 minutes. The classical procedure was only used in older laboratory designed instruments where one started at zero and measured the hydrostatic height difference as a function of time until equilibrium is reached. More details about instrumentation and techniques can be found in the reviews by Adams,[38] Tombs and Peacock,[39] Mays and Hadjichristidis.[40] A very recent presentation can be found in a new book edited by Pethrick and Dawkins.[26]

Some efforts are necessary to keep the osmometer under appropriate working conditions. This relates mainly to the proper preconditioning and installation of the membrane, the attainment of thermal equilibrium, the calibration of the electronic output, the adjustment of solvent zero, and to choosing the desired sensitivity.

For aqueous solutions, cellulose acetate membranes are usually employed, but any dialysis or ultrafiltration or reverse osmosis membrane can be used, too. The membranes should be conditioned in solvent or buffer and degassed before use while still in the solvent. For organic solvents, gel cellulose or cellophane membranes are preferred. They must be conditioned to a new solvent by gradual changes of the corresponding solvent mixture. Details are usually given by the supplier. Membranes in various pore sizes are recommended for solutes of low molar mass. Aging and deswelling of membranes lead to decreasing permeability and increasing measuring times. Adsorption of polymer molecules at the membrane surface, "ballooning" of the membrane due to unfavorable pressure effects, membrane asymmetry and action of surface active substances on the membrane must be avoided.

The relation between osmotic pressure and solvent activity is to be found from the chemical potential equilibrium condition, taking into account the pressure dependence of μ_1. From the rules of phenomenological thermodynamics, one obtains:

$$\left(\frac{\partial \mu_1^0}{\partial P}\right)_T = V_1 \quad and \quad \left(\frac{\partial \ln a_1}{\partial P}\right)_T = \frac{\overline{V}_1 - V_1}{RT} \qquad [4.4.34]$$

where:

$\overline{V}_1$	partial molar volume of the solvent in the polymer solution at temperature T
V_1	molar volume of the pure solvent at temperature T

Integration is performed between P_0, i.e., the ordinary pressure or measuring pressure, and π, the osmotic pressure, and results in Equation [4.4.35].

$$\Delta\mu_1 = RT \ln a_1 = -\overline{V}_1 \pi \qquad [4.4.35]$$

Usually, the experimental data are reduced to virial coefficients and not to solvent activities. Series expansion of Equation [4.4.35] leads to the following relation:

$$\frac{\pi}{c_2} = RT\left[\frac{1}{M_2} + A_2 c_2 + A_3 c_2^2 + \ldots\right] \qquad [4.4\text{-}36]$$

where:

c_2	mass by volume concentration $c_2 = m_2/v$
$A_2, A_3, \ldots$	second, third, ... osmotic virial coefficients

The molar mass of the polymer, M_2, is the number-average, M_n, if polydisperse samples are investigated. Corresponding averages of the virial coefficients can be introduced, too. In the dilute concentration region, the virial equation is usually truncated after the second virial coefficient which leads to a linear relationship. A linearized relation over a wider concentration range can be constructed, Equation [4.4.38], if the Stockmayer-Casassa relation,[146] Equation [4.4.37], between A_2 and A_3 is applied:

$$A_3 M_n = (A_2 M_n / 2)^2 \qquad [4.4.37]$$

$$\left(\frac{\pi}{c_2}\right)^{0.5} = \left(\frac{RT}{M_n}\right)^{0.5} \left[1 + \frac{A_2 M_n}{2} c_2\right] \qquad [4.4.38]$$

Examples for experimentally determined virial coefficients can be found in the above mentioned papers[139-145] and in the tables prepared by Lechner et al.[9] Solvent activities can be calculated via Equations [4.4.35 to 38] from osmotic second virial coefficients with some care regarding the necessary accuracy of all numerical values included. The partial molar volume of the solvent can be approximated in most cases by the molar volume of the pure solvent. Noda et al.[139] published a combined investigation of the thermodynamic behavior of poly(α-methylstyrene)s having sharp molar mass distributions and covering a wide range of molar masses in toluene. They applied osmotic pressure, light scattering and vapor pressure measurements and demonstrated the capabilities of these methods in comprehensive and detailed form. Gaube et al.[126,127] could show that in the case of aqueous dextran solutions, water activity data and virial coefficients measured by VPO and by membrane osmometry are in good agreement.

4.4.3.2.2 Light scattering

Light scattering is one of the most widespread characterization techniques for polymers. Therefore, technical and methodical details will not be explained here - please see Refs.[26-32] for such information. The general set-up of a scattering principle is illustrated by Figure 4.4.18. The scattering vector **q** is the difference between the wave vectors $\mathbf{k}_i$ and $\mathbf{k}_s$ of the incident and the scattered plane waves, the scattering angle θ is the angle between both vectors. Both are related by $|\mathbf{q}| = (4\pi/\lambda_0)\sin(\theta/2)$, where λ_0 is the wavelength of light in vacuum. Laser light is used today for the light source.

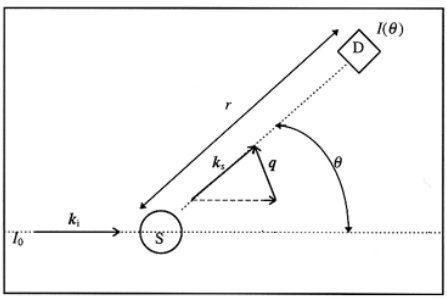

Figure 4.4.18. General set-up of a scattering experiment: $\mathbf{k}_i$, $\mathbf{k}_s$ - wave vectors of the incident and the scattered plane waves, **q** - scattering (or wave) vector, D- detector, S - sample, θ - scattering angle from the transmitted beam, I_0 - incident intensity of unpolarized light, r - the distance between sample and detector.

Light scattering in homogeneous fluids is caused by fluctuations in the dielectric constant. In pure liquids these are due to density fluctuations, in homogeneous solutions mainly to concentration fluctuations which generally lead to much larger fluctuations in dielectric constant than density variations. The difference between solution and pure solvent is called excess scattering. This excess scattering is of interest here, since it is related to the second derivative of Gibbs free energy of mixing with respect to concentration (and via this way to solvent activities):

$$I^{excess} \propto \frac{TP(\theta)}{\left|\frac{\partial^2 \Delta_{mix} G}{\partial \varphi_i \partial \varphi_j}\right|} \qquad [4.4.39]$$

where:

I^{excess}	excess scattering intensity
T	absolute temperature
$\Delta_{mix}G$	Gibbs free energy of mixing.
φ_i	volume fractions of component i (= i^{th} polymer species in the molecular distribution)
P(θ)	properly averaged particle scattering factor
θ	scattering angle from the transmitted beam

The determinant in the denominator is to be calculated at constant temperature and pressure. It reduces to the single second derivative $(\partial^2\Delta_{mix}G/\partial^2\varphi_2)_{P,T} = (\partial\mu_1/\partial\varphi_2)_{P,T}$ for the case of a strictly binary monodisperse polymer solution. The average particle scattering factor is of primary importance in studies of the size and shape of the macromolecules, but it is merely a constant for thermodynamic considerations.

Conventionally, the so-called Rayleigh factor (or ratio) is applied:

$$R(\theta) \equiv \frac{I^{excess} r^2}{I_0 V_0 \left(1+\cos^2\theta\right)} \qquad [4.4.40]$$

where:

R(θ)	Rayleigh factor
I_0	incident intensity of unpolarized light
r^2	square of the distance between sample and detector
V_0	detected scattering volume

and, neglecting P(θ), Equations [4.4.39 and 4.4.40] can be transformed to:

$$R(\theta) \equiv \frac{RTK\varphi_2\overline{V}_1}{\left(\partial\mu_1/\partial\varphi_2\right)_{P,T}} \qquad [4.4.41]$$

where:

$\overline{V}_1$	partial molar volume of the solvent in the polymer solution at temperature T
φ_2	volume fraction of the monodisperse polymer
K	optical constant

The optical constant for unpolarized light summarizes the optical parameters of the experiment:

$$K \equiv 2\pi^2 n_o^2 \left(dn/dc_2\right)^2_{P,T} / \left(N_{Av}\lambda_0^4\right) \qquad [4.4.42]$$

where:

n_o	refractive index of the pure solvent
n	refractive index of the solution
c_2	mass by volume concentration $c_2 = m_2/v$
N_{Av}	Avogadro's number
λ_0	wavelength of light in vacuum

For dilute polymer solutions, the partial derivative in Equation [4.4.41] is a weak function of composition and the scattering intensity increases roughly proportional to the volume fraction of the polymer. While Equation [4.4.41] permits any light scattering data to be

interpreted as partial derivatives of solvent chemical potential or activity, dilute solution measurements are conventionally again presented in terms of the osmotic virial expansion:

$$(Kc_2)/R(\theta=0) = (1/M_2) + 2A_2c_2 + 3A_3c_2^2 + \ldots \qquad [4.4.43]$$

where:

A_2,A_3, ... second, third, ... osmotic virial coefficients
M_2 molar mass of the polymer

According to the scattering theory of polydisperse polymers (please see, for example, the book written by Strobl),[147] the molar mass of the polymer, M_2, is equal to the mass average, M_w, of polydisperse polymers. The exact application of Equation [4.4.43] is at the scattering angle $\theta = 0$. Interpretation of scattering data at larger angles has to take into account the interparticle interference and the angular variation of the excess scattering intensity. Usually, such data have been analyzed with a Zimm plot,[148] where $(Kc_2)/R(\theta)$ is graphed as a function of $\sin^2(\theta/2)$ + const.*c_2 and measurements are extrapolated at constant angle to zero concentration values and at constant concentration to zero angle values. Connecting each of these two sets of points gives the curve specified by Equation [4.4.41]. The intercept gives M_w, the slope of the zero angle data yields the second virial coefficient. In many cases, non-linear Zimm plots were observed.[31]

An illustrative example for the variation of the second virial coefficient with molar mass and temperature from endothermic to exothermic conditions is given in the paper by Wolf and Adam,[149] or in the paper by Lechner and Schulz[150] for the variation of the second virial coefficient on pressure, both obtained by light scattering. A recent example for a light scattering investigation on the molar mass dependence of A_2 and A_3 was published by Nakamura et al.[151]

The virial expansion is inappropriate as the polymer concentration increases. In these cases, scattering data can be analyzed in terms of a thermodynamic ansatz for the Gibbs free energy of mixing. For example, Scholte[152] analyzed light scattering data of concentrated polystyrene solutions by means of the Flory-Huggins approach and determined χ-data. But recently, Hasse, et al.[153] combined laser-light scattering with isopiestic measurements and obtained second and third virial coefficients of aqueous poly(ethylene glycol) solutions with high accuracy. Both virial coefficients could be correlated over a temperature range between 278 and 313K, including a derived theta-temperature of 375.7K in good agreement with results from liquid-liquid equilibrium. Additional measurements using membrane osmometry agreed well with the results of the simultaneous correlation of light scattering and isopiestic data. Corresponding measurements of aqueous dextran solutions by Kany et al.[154] showed again the resources inherent in such a combination of different methods.

Light scattering provides another interesting tool to determine thermodynamic data of polymer solutions. Starting from Equation [4.4.39], Scholte[155,156] developed the idea of measuring spinodal curves, i.e., the border between metastable and unstable liquid-liquid demixing behavior of polymer solutions. At this spinodal curve, the determinant in Equation [4.4.39] vanishes, i.e., it becomes equal to zero. At small enough scattering angles (near 30°) and in a temperature range of about $0.03 < \Delta T < 5$K around the critical temperature, a proportionality of $I^{excess} \propto 1/\Delta T$ can be obtained that leads to a simple linear behavior of $1/I_{30}$ against T for various concentrations around the critical demixing concentration. The extrapolated curves of $1/I_{30}$ vs. T to $1/I_{30} = 0$ lead to spinodal temperatures as function of the corre-

sponding polymer concentrations. If, for example, one combines $\Delta_{mix}G$-ansatz by Koningsveld and Kleintjens,[51] Equation [4.4.15], with the spinodal condition:

$$\left|\frac{\partial^2 \Delta_{mix} G}{\partial \varphi_i \partial \varphi_j}\right| = 0 \qquad [4.4.44]$$

one obtains for a binary polymer solution:

$$\alpha + \frac{\beta(1-\gamma)}{(1-\gamma\varphi_2)^3} - \frac{1}{\varphi_2 r_w} - \frac{1}{1-\varphi_2} = 0 \qquad [4.4.45]$$

where:

α	acts as constant within a certain temperature range
β	describes a temperature function like $\beta = \beta_0 + \beta_1/T$
γ	is also a constant within a certain temperature range.
r_w	mass average segment number, compare r in Equation (4.4.13)
φ_2	total volume fraction of the polymer

The adjustable parameters α, β, γ have to be fitted to spinodal data $\varphi_2^{spinodal}$ vs. $T^{spinodal}$ and solvent activities can be calculated from the following relation:

$$\ln a_1 = \ln(1-\varphi_2) + \left(1 - \frac{1}{r_n}\right)\varphi_2 + \alpha\varphi_2^2 + \frac{\beta(1-\gamma)}{(1-\gamma\varphi_2)^2}\varphi_2^2 \qquad [4.4.46]$$

where:

r_n	number average segment number, compare r in Equation [4.4.13]

Gordon and coworkers[157-159] improved this method and developed the so-called PICS (pulse-induced critical scattering) apparatus - details and history were summarized by Galina et al.[160] PICS enables not only investigations within the metastable range, i.e., nearer to the spinodal, but also of high-viscous solutions and polymer blends for determining spinodal and binodal (cloud-point) curves. How to obtain solvent activities from demixing equilibrium is explained in the text below.

4.4.3.2.3 X-ray scattering

X-ray scattering can be measured by the classical Kratky camera or more modern synchrotron techniques. Technical details can be found in a number of books, e.g., those by Guinier and Fouret,[161] Chen and Yip,[162] or Glatter and Kratky.[163]

Small angle X-ray scattering (SAXS) can be used in analogy to light scattering to measure second virial coefficients of binary polymer solutions. Zimm-diagrams can be constructed following the same ways as in light scattering. This was demonstrated, for example, in papers by Kirste and coworkers.[164-166] In analogy to Equation [4.4.43], one can derive

$$(Kc_2)/I(\theta = 0) = (1/M_2) + 2A_2c_2 + 3A_3c_2^2 + \ldots \qquad [4.4.47]$$

where:

c_2	mass by volume concentration $c_2 = m_2/v$

A_2,A_3, ...	second, third, ... osmotic virial coefficients
M_2	molar mass of the polymer

According to the scattering theory of polydisperse polymers (please see, for example, the book written by Strobl),[147] the molar mass of the polymer, M_2, is equal to the mass average, M_w, of polydisperse polymers. The exact application of Equation [4.4.47] is to be made again at the scattering angle $\theta = 0$. The constant K is now given by:

$$K \equiv e^4 \Delta z^2 \; / \left(m^2 N_{Av} c^4 \right) \qquad [4.4.48]$$

where:

e	electron charge
m	electron mass
Δz	excess number of electrons
c	speed of light in vacuum

In principle, there is agreement between values of second virial coefficients from light scattering or X-ray scattering. Okano et al.[167,168] applied SAXS to semidilute solutions of polystyrene in cyclohexane in the poor solvent regime and obtained virial coefficients in good agreement with liquid-liquid data from a coexistence curve. Takada et al.[169] provided a more recent example for poly(vinyl methyl ether) in cyclohexane, Horkay et al.[170] for poly(vinyl acetate) in toluene and poly(dimethyl siloxane) in octane. In comparison to data from osmotic pressure and neutron scattering, they observed good agreement.

4.4.3.2.4 Neutron scattering

Neutron scattering is an important method for investigating conformation and dynamics of polymer molecules, Higgins,[171] or polymer mixtures, Hammouda.[172] A recent presentation of various techniques can be found in a new book edited by Pethrick and Dawkins.[26] Thermodynamics of polymer solutions is not the first task in neutron scattering experiments. The general set-up of the neutron scattering experiment is equivalent to the one used for light scattering, but applying a neutron source, and elastic neutron scattering at small angles (SANS) can be applied like light scattering or X-ray scattering to obtain second virial coefficients in dilute solutions. Similarly to the scattering of photons, it is the difference in scattering power between solvent molecules and polymer segments which determines the absolute scattering intensity. Formally, the virial equation has the same form as Equations [4.4.43 and 47], again neglecting $P(\theta)$:

$$\left(Kc_2\right) / \Sigma(\theta) = \left(1/M_2\right) + 2A_2 c_2 + 3A_3 c_2^2 + \ldots \qquad [4.4.49]$$

and

$$K = \left(b_2 - b_1 \rho_1 \nu_{2,spez}\right) / N_{Av} \qquad [4.4.50]$$

where:

c_2	mass by volume concentration $c_2 = m_2/v$
A_2,A_3, ...	second, third, ... osmotic virial coefficients
M_2	molar mass of the polymer
$\Sigma(\theta)$	differential scattering cross section per volume unit
K	contrast factor for neutron scattering
b_1,b_2	densities of solvent and polymer scattering length
ρ_1	density of the solvent

$\nu_{2,spez}$ specific volume of the polymer (more exact, $\bar{\nu}^{\infty}_{2,spez}$, the partial specific volume at infinite dilution)

According to the scattering theory of polydisperse polymers, please see, for example, in the book written by Strobl,[147] the molar mass of the polymer, M_2, is equal to the mass average, M_w, of polydisperse polymers. The contrast factor for neutron scattering takes into account for the difference in scattering power of solvent molecules and polymer segments. Again, Zimm plots can be constructed, as was explained above, for light scattering measurements to take into account for angular and concentration dependence - for a demonstration see Vennemann et al.[173]

The transformation of the obtained second virial coefficients into solvent activities is as explained above, Equations [4.4.34 and 4.4.35]. A recent example for the determination of second virial coefficients from SANS is the investigation of aggregation phenomenon in associating polymer solutions by Pedley et al.,[174] where sodium sulfonated polystyrene ionomers in deuterated xylene were considered. Enthalpic and entropic contributions to A_2 were calculated (as in the paper by Wolf and Adams[149] for A_2 from light scattering) and an enthalpy of aggregation was estimated from these data. A high-pressure investigation on aqueous poly(ethylene oxide) solutions was made by Vennemann et al.[173] who measured second virial coefficients by a SANS experiment for pressures up to 200 MPa and combined these data with PVT-measurements to obtain also excess and partial excess volumes and gained information about the pressure dependence of the chemical potential.

4.4.3.2.5 Ultracentrifuge

The analytical ultracentrifuge is a powerful tool for polymer characterization. Technical details of ultracentrifugation will not be considered here - please see Refs.[26,35-37] for more information. In a typical ultracentrifuge experiment, the polymer solution is put in a sample tube and rotated at high speed. Thermodynamic data can be obtained either from the sedimentation velocity (sedimentation coefficient) or from the sedimentation-diffusion equilibrium since the centrifugal forces are balanced by the activity gradient. The concentration gradient is conventionally measured via the refractive index gradient along the axis of the tube using Schlieren photography or various optics.

The sedimentation coefficient is defined as the sedimentation velocity in a unit force field:

$$s = \frac{dh / dt}{\omega^2 h} \qquad [4.4.51]$$

where:

s sedimentation coefficient
h distance from the center of rotation
t time
ω angular velocity

For a given polymer-solvent system, the sedimentation coefficient is dependent on temperature, pressure and polymer concentration. For obtaining thermodynamic data from sedimentation coefficients, one additionally has to measure the diffusion coefficient. This can be made with an ultracentrifuge in special diffusion cells[35] or with dynamic light scattering[32] based on the theory of Pecora.[175] Nearly all diffusion coefficients have been measured by this method since it became available in 1970. The determination of sedimen-

tation and diffusion coefficient yields virial coefficients of a polymer solution. The so-called Svedberg equation reads:

$$\left(\frac{D}{s}\right)\left(1-\bar{\nu}_{2,spez}\rho_1\right)=RT\left[\frac{1}{M_2}+2A_2c_2+3A_3c_2^2+\ldots\right] \qquad [4.4.52]$$

where:

D	diffusion coefficient
$\bar{\nu}_{2,spez}$	partial specific volume of the polymer
ρ_1	density of the solvent
c_2	mass by volume concentration $c_2 = m_2/\nu$
$A_2, A_3, \ldots$	second, third, ... osmotic virial coefficients
M_2	molar mass of the polymer

Equation [4.4.52] is strictly valid for monodisperse polymers, i.e., one single component 2. For polydisperse polymers, different averages were obtained for the sedimentation and the diffusion coefficient, which depends on the applied measuring mode and the subsequent calculations. The averages of M_2 correspond with averages of D and s and are mixed ones that have to be transformed into the desired common averages - for details please see Refs.[35-37]

Sedimentation-diffusion equilibrium in an ultracentrifuge gives also a virial series:[35]

$$\omega^2 h\left(1-\bar{\nu}_{2,spez}\rho_1\right)\left(\frac{\partial \ln c_2}{\partial h}\right)=RT\left[\frac{1}{M_2}+2A_2c_2+3A_3c_2^2+\ldots\right] \qquad [4.4.53]$$

where:

h	distance from the center of rotation
ω	angular velocity

Equation [4.4.53] is again valid for monodisperse polymers only. Polydisperse polymers lead to apparent molar mass averages and to averages of the virial coefficients which have to be transformed into the desired common averages by appropriate calculation methods.[35-37]

A somewhat different way of avoiding the virial expansion in Equation [4.4.53] was developed by Scholte.[176,177] Without going into details, his final relation was:

$$\omega^2 h\left(1-\bar{\nu}_{2,spez}\rho_1\right)\left(\frac{M_1 w_2}{w_2-1}\right)=\left[\frac{\partial \Delta\mu_1}{\partial w_2}+RT\left(\frac{M_1}{M_n}-\frac{M_1}{M_w}\right)\right]\left(\frac{dn}{dh}\right)/\left(\frac{dn}{dw_2}\right) \qquad [4.4.54]$$

where:

w_2	mass fraction of the polymer
M_1	molar mass of the solvent
M_n	number average molar mass of the polymer
M_w	mass average molar mass of the polymer
n	refractive index of the solution

Some assumptions were made for the derivation of Equation [4.4.54], especially the partial specific volume, the refractive index, and the derivative dn/dw_2 must not depend on the molar mass distribution of the polymer. If one further assumes that the Flory-Huggins

χ-function depends only on temperature and concentration, but not on molar mass, the partial derivative of the chemical potential can be calculated by Equation [4.4.13a] to obtain values of the χ-function. Scholte carried out experiments for solutions of polystyrene in cyclohexane or toluene at different temperatures and in a concentration range of 0-80 wt%.

Thus, the sedimentation method is able to cover nearly the total concentration range of a polymer solution; however, values obtained by this method were slightly higher than values determined by other methods. Since the measurement of thermodynamic data by sedimentation equilibrium is not very frequent in the literature this is certainly not a final statement. A combined determination of second osmotic virial coefficients of poly(ethylene glycol)s in methanol, water and N,N-dimethylformamide by Elias and Lys[178] using light scattering, VPO and sedimentation equilibrium showed good agreement between all methods. This was also confirmed in a recent investigation on poly(1-phenyl-1-propene) in toluene by Hirao et al.,[179] where second virial coefficients were determined by light scattering and by sedimentation equilibrium over a wide range of molar mass. Some further A_2 data from sedimentation measurements can be found in the tables by Lechner et al.[9] The transformation of the obtained second virial coefficients into solvent activities is as explained above.

4.4.3.2.6 Cryoscopy (freezing point depression of the solvent)

In the cryoscopic method, the freezing temperature of a solution is compared with that of the pure solvent. The polymer must be solvable in the solvent at the freezing temperature and must not react with the solvent either chemically or physically. Difficulties may arise from limited solubility and from the formation of solid solutions on freezing. Application of cryoscopy to polymer solutions is not widespread in literature despite the simplicity of the required equipment. Cryoscopy was reviewed by Glover,[34] who also discussed technical details and problems in concern with application to polymer solutions. A detailed review on cryometers and cryoscopic measurements for low-molar mass systems was recently made by Doucet.[180] Cryometers are sold commercially, e.g., Knauer. Measurements of thermodynamic data are infrequent. Applications usually determine molar masses. Accurate data require precise temperature measurement and control as well as caution with the initiation of the crystallization process and the subsequent establishment of equilibrium (or steady state) conditions. High purity is required for the solvent and also for the solute.

Data reduction of cryoscopic measurements is made by applying the relation for the freezing point depression of a binary mixture to obtain solvent activities:

$$\frac{1}{{}^{SL}T_1^0} - \frac{1}{{}^{SL}T_1} = \frac{R}{\Delta_{SL}H_1^0} \ln a_1 \qquad [4.4.55]$$

where:

${}^{SL}T_1^0$	solid-liquid equilibrium melting temperature of the pure solvent
${}^{SL}T_1$	solid-liquid equilibrium melting temperature of the solvent in the polymer solution
$\Delta_{SL}H_1^0$	molar enthalpy of fusion of the pure solvent.

Kawai[181] determined some values of the χ-function for benzene solutions of polystyrene or poly(vinyl acetate) and aqueous solutions of poly(vinyl alcohol). In comparison with various data from the tables given by Orwoll,[8] larger deviations with respect to other methods have to be stated. Just recently, Hoei et al.[182] made a more sophisticated analysis of

solid-liquid coexistence data of benzene in natural rubber and found good agreement to other data.

Equation [4.4.55] could in principle also be used for the determination of thermodynamic data from the melting point depression of (semi)crystalline polymers when the subscripts changed from 1 to 2. This enables a second approach to data for the infinite dilution range of the solvent in the polymer. Such investigations have been made in the literature. However, these data are regarded as being less reliable by a number of reasons and no further discussion will be made here.

4.4.3.2.7 Liquid-liquid equilibrium (LLE)

There are two different situations for the liquid-liquid equilibrium in polymer-solvent systems:

(i) the equilibrium between a dilute polymer solution (sol) and a polymer-rich solution (gel) and

(ii) the equilibrium between the pure solvent and a swollen polymer network (gel).

Case (i) is considered now, case (ii) is specially considered below as swelling equilibrium.

LLE-measurements do not provide a direct result with respect to solvent activities. Equation (4.4.8) says that solvent activities at given temperature and pressure must be equal in both coexisting phases. Since the solvent activity of such a coexisting phase is a priori not known, one has to apply thermodynamic models to fit LLE-data as functions of temperature and concentration. Solvent activities can be obtained from the model in a subsequent step only.

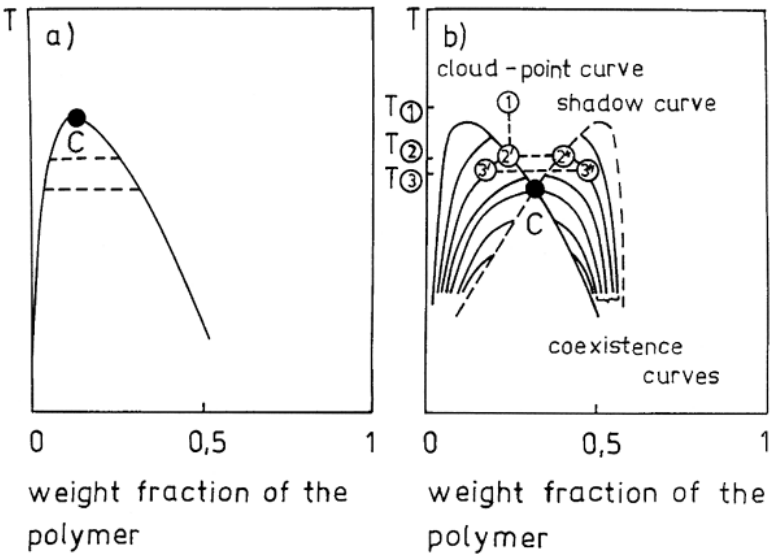

Figure 4.4.19. Principles of liquid-liquid demixing in polymer solutions, a) - strictly binary polymer solution of a monodisperse polymer, b) - quasi-binary polymer solution of a polydisperse polymer which is characterized by a distribution function: C - critical point, dashed lines - tie lines, T(1) - temperature/concentration in the homogeneous region, T(2) - temperature/concentrations of the cloud point (phase´) and the corresponding shadow point (phase´´), T(3) - temperature in the heterogeneous LLE region, coexistence concentrations of phase´ and phase´´ at T(3) are related to the starting concentration = cloud point concentration of (2).

Furthermore, there is another effect which causes serious problems with LLE-data of polymer solutions. This is the strong influence of distribution functions on LLE, because fractionation occurs during demixing - see, for example, Koningsveld.[44,183] Figure 4.4.19 illustrates the differences between the LLE-behavior of a strictly binary polymer solution of a monodisperse polymer and a quasi-binary polymer solution of a polydisperse polymer which is characterized by a distribution function.

One can see the very complicated behavior of quasi-binary solutions where the phase boundary is given by a cloud-point curve and where an infinite number of coexistence curves exists (one pair for each starting concentration, i.e., each cloud-point). The cloud-point is a point in the T-w_2- or the P-w_2-diagram where a homogeneous solution of concentration w_{02} begins to demix (where the "first" droplet of the second phase occurs, T(2) in Figure 4.4.19). If w_{02} is smaller than the critical concentration, the cloud-point belongs to the sol-phase, otherwise to the gel-phase.

As this subchapter is devoted to solvent activities, only the monodisperse case will be taken into account here. However, the user has to be aware of the fact that most LLE-data were measured with polydisperse polymers. How to handle LLE-results of polydisperse polymers is the task of continuous thermodynamics, Refs.[52-54] Nevertheless, also solutions of monodisperse polymers or copolymers show a strong dependence of LLE on molar mass of the polymer,[184] or on chemical composition of a copolymer.[185] The strong dependence on molar mass can be explained in principle within the simple Flory-Huggins χ-function approach, please see Equation [4.4.61].

Experimental methods can be divided into measurements of cloud-point curves, of real coexistence data, of critical points and of spinodal curves:

Due to distinct changes in a number of physical properties at the phase transition border, quite a lot of methods can be used to determine cloud-points. In many cases, the refractive index change is determined because refractive indices depend on concentration (with the seldom exception of isorefractive phases) and the sample becomes cloudy when the highly dispersed droplets of the second phase appear at the beginning of phase separation. Simple experiments observe cloud-points visually. More sophisticated equipment applies laser techniques, e.g., Kuwahara,[186] and light scattering, e.g., Koningsveld and Staverman.[187] The principle scheme of such a scattering experiment is the same as explained with Figure 4.4.18. Changes in scattering pattern or intensity were recorded as a function of decreasing/increasing temperature or pressure. The point, where first deviations from a basic line are detected, is the cloud-point. Since demixing or phase homogenization need some time (especially for highly viscous solutions), special care is to be applied for good data. Around the critical point large fluctuations occur (critical opalescence) and scattering data have to be measured at 90° scattering angle. The determination of the critical point is to be made by independent methods (see below). Various other physical properties have been applied for detecting liquid-liquid phase separation: viscosity, e.g., Wolf and Sezen,[188] ultrasonic absorption, e.g., Alfrey and Schneider,[189] thermal expansion, e.g., Greer and Jacobs,[190] dielectric constant, e.g., Jacobs and Greer,[191] or differential thermal analysis DTA, e.g., Muessig and Wochnowski.[192]

There are only a small number of investigations where real coexistence data were measured. This is mainly due to very long equilibrium times (usually weeks) which are necessary for obtaining thermodynamically correct data. A common method is to cool homogeneous solutions in ampullae very slowly to the desired temperature in the LLE-region and

equilibrium is reached after both phases are sharply separated and clear, Rehage et al.[193] After separating both phases, concentrations and distribution functions were measured. Acceptable results can be obtained for low polymer concentrations (up to 20 wt%). Scholte and Koningsveld[194] developed a method for highly viscous polymer solutions at higher concentrations by constructing a modified ultracentrifuge where the equilibrium is quickly established during cooling by action of gravitational forces. After some hours, concentrations, phase volume ratios and concentration differences can be determined. Rietfeld with his low-speed centrifuge[195] and Gordon with a centrifugal homogenizer[196] improved this technique and expanded its applicability up to polymer melts, e.g., Koningsveld et al.[197]

The methods for obtaining spinodal data have already been discussed above with the light scattering technique, please see Subchapter 4.4.3.2.2.

Special methods are necessary to measure the critical point. For solutions of monodisperse polymers, it is the maximum of the binodal. Binodals of polymer solutions can be rather broad and flat. The exact position of the critical point can be obtained by the method of the rectilinear diameter. Due to universality of critical behavior, a relation like Equation [4.4.56] is valid, deGennes:[198]

$$\left(\varphi_2^{I} - \varphi_2^{II}\right) / 2 - \varphi_2^{crit} \propto \left(1 - T / T^{crit}\right)^{1-\alpha} \qquad [4.4.56]$$

where:

φ_2^{I}	volume fraction of the polymer in coexisting phase I
φ_2^{II}	volume fraction of the polymer in coexisting phase II
φ_2^{crit}	volume fraction of the polymer at the critical point
T^{crit}	critical temperature
α	critical exponent

and critical points can be obtained by using regression methods to fit LLE-data to Equation [4.4.56].

For solutions of polydisperse polymers, such a procedure cannot be used because the critical concentration must be known in advance to measure its corresponding coexistence curve. Additionally, the critical point is not the maximum in this case but a point at the right-hand side shoulder of the cloud-point curve. Two different methods were developed to solve this problem, the phase-volume-ratio method, e.g., Koningsveld,[199] where one uses the fact that this ratio is exactly equal to one only at the critical point, and the coexistence concentration plot, e.g. Wolf,[200] where an isoplethal diagram of values of φ_2^{I} and φ_2^{II} vs. φ_{02} gives the critical point as the intersection point of cloud-point and shadow curves.

Since LLE-measurements do not provide a direct result with respect to solvent activities, Equation [4.4.8] and the stability conditions are the starting points of data reduction. As pointed out above, the following explanations are reduced to the strictly binary solution of a monodisperse polymer. The thermodynamic stability condition with respect to demixing is given for this case by (see Prausnitz et al. [49]):

$$\left(\partial^2 \Delta_{mix} G / \partial^2 \varphi_2\right)_{P,T} > 0 \qquad [4.4.57]$$

If this condition is not fulfilled between some concentrations φ_2^{I} and φ_2^{II}, demixing is obtained and the minimum of the Gibbs free energy of mixing between both concentrations is given by the double tangent at the corresponding curve of $\Delta_{mix}G$ vs. φ_2, Equation [4.4.8].

The resulting curve in the T vs. φ_2 diagram, see Figure 4.4.19a, is the binodal curve. Applying Equations [4.4.3 to 4.4.5 and 4.4.13a], one gets two relations which have to be solved simultaneously to fit an empirical χ(T)-function to experimental binodal (coexistence) data. For the most simple case of χ being only a function of T (or P) and not of φ_2 (the so-called one-parameter approach) these relations read:

$$\ln\frac{\left(1-\varphi_2^{I}\right)}{\left(1-\varphi_2^{II}\right)}+\left(1-\frac{1}{r}\right)\left(\varphi_2^{I}-\varphi_2^{II}\right)+\chi\left(\varphi_2^{I2}-\varphi_2^{II2}\right)=0 \qquad [4.4.58a]$$

and

$$\frac{1}{r}\ln\frac{\varphi_2^{I}}{\varphi_2^{II}}-\left(1-\frac{1}{r}\right)\left(\varphi_2^{I}-\varphi_2^{II}\right)+\chi\left(\varphi_1^{I2}-\varphi_1^{II2}\right)=0 \qquad [4.4.58b]$$

where:

φ_2^{I}	volume fraction of the polymer in coexisting phase I
φ_2^{II}	volume fraction of the polymer in coexisting phase II
r	ratio of molar volumes V_2/V_1 what is the number of segments with $V_{seg} = V_1$
χ	Flory-Huggins interaction function of the solvent

and solvent activities result from Equation [4.4.13a]. However, this simple approach is of limited quality. More sophisticated models have to be applied to improve calculation results.

A special curve is obtained with the border line to the instability region, i.e., the spinodal curve, for which the second derivative in Equation [4.4.57] is equal to zero. If one applies again the one-parameter approach with an empirical χ(T)-function, the following simple result can be derived:

$$2\chi\left(T^{spinodal}\right)-\frac{1}{r\varphi_2^{spinodal}}-\frac{1}{1-\varphi_2^{spinodal}}=0 \qquad [4.4.59]$$

where:

$T^{spinodal}$	spinodal temperature
$\varphi_2^{spinodal}$	volume fraction of the polymer at the spinodal curve

which has to fit an empirical χ(T)-function. An example for the spinodal relation of a polydisperse polymer was given above by Equations [4.4.44 and 4.4.45].

The common point of spinodal and binodal curve is the critical point. The critical point conditions are:

$$\left(\partial^2\Delta_{mix}G/\partial^2\varphi_2\right)_{P,T}=0 \quad \left(\partial^3\Delta_{mix}G/\partial^3\varphi_2\right)_{P,T}=0$$

and [4.4.60]

$$\left(\partial^4\Delta_{mix}G/\partial^4\varphi_2\right)_{P,T}>0$$

If one applies again the one-parameter approach with an empirical χ(T)-function, two simple results can be derived:

$$\varphi_2^{crit} = 1/\left(1+r^{0.5}\right) \quad and \quad \chi^{crit}\left(T^{crit}\right) = 0.5\left(1+1/r^{0.5}\right)^2 \qquad [4.4.61]$$

where:

φ_2^{crit}	volume fraction of the polymer at the critical point
T^{crit}	critical temperature

This means that the critical concentration is shifted to lower values with increasing segment number (molar mass) of the polymer and becomes zero for infinite molar mass. Equation [4.4.61] explains also why the χ(T)-function becomes 0.5 for infinite molar mass. The critical temperature of these conditions is then called theta-temperature. Solvent activities can be calculated from critical χ(T)-function data via Equation [4.4.13]. However, results are in most cases of approximate quality only.

4.4.3.2.8 Swelling equilibrium

Polymers, crosslinked sufficiently to form a three-dimensional network, can absorb solvent up to a large extent. The maximum possible solvent concentration, the degree of swelling, are a function of solvent activity. If solvent is present in excess, this swelling equilibrium is reached when the chemical potential of the pure solvent outside the network is equal to the chemical potential inside the swollen sample. This means, there must be an additional contribution to the Gibbs free energy of mixing (as is the case with the osmotic equilibrium) besides the common terms caused by mixing the (virtually) infinite-molar-mass polymer and the solvent. This additional part follows from the elastic deformation of the network. The different aspects of chemical and physical networks will not be discussed here, for some details please see Refs.[201-205] The following text is restricted to the aspect of solvent activities only.

One method to obtain solvent activities in swollen polymer networks in equilibrium is to apply vapor pressure measurements. This is discussed in detail above in the Subchapter 4.4.3.1.1 and most methods can be used also for network systems, especially all sorption methods, and need no further explanation. The VPO-technique can be applied for this purpose, e.g., Arndt.[206,207] IGC-measurements are possible, too, if one realizes a definitely crosslinked polymer in the column, e.g., Refs.[208-210]

Besides vapor sorption/pressure measurements, definite swelling and/or deswelling experiments lead to information on solvent activities. Swelling experiments work with pure solvents, deswelling experiments use dilute solutions of macromolecules (which must not diffuse into or adsorb at the surface of the network) and allow measurements in dependence on concentration. Deswelling experiments can be made in dialysis cells to prevent diffusion into the network. The determination of the equilibrium swelling/deswelling concentration can be made by weighing, but, in most cases, by measuring the swelling degree. Some methods for measuring the swelling degree are: measuring the buoyancy difference of the sample in two different liquids of known density, e.g. Rijke and Prins,[211] measuring the volume change by cathetometer, e.g., Schwarz et al.,[212] measuring the volume change by electrical (inductive) measurements, e.g., Teitelbaum and Garwin.[213]

The swelling degree can be defined as the ratio of the masses (mass based degree) or of the volumes (volume based degree) of the swollen to the dry polymer network sample:

$$Q_m = 1 + m_1 / m_N \quad or \quad Q_v = 1 + \nu_1 / \nu_n = 1 + \left(Q_m - 1\right)\rho_n / \rho_1 \qquad [4.4.62]$$

where:

Q_m	mass based degree of swelling
Q_v	volume based degree of swelling
m_1	absorbed mass of the solvent
m_N	mass of the dry polymer network
ν_1	absorbed volume of the solvent
ν_N	volume of the dry polymer network
ρ_1	density of the solvent
ρ_N	density of the dry polymer network

Since $Q_v = 1/\varphi_2$, usually volume changes were measured. If the sample swells isotropically, the volume change can be measured by the length change in one dimension. Calculation of solvent activities from measurements of the swelling degree needs a statistical thermodynamic model. According to Flory,[46] a closed thermodynamic cycle can be constructed to calculate the Gibbs free energy of swelling from the differences between the swelling process, the solution process of the linear macromolecules, the elastic deformation and the crosslinking. The resulting equation can be understood in analogy to the Flory-Huggins relation, Equation [4.4.13a] with $r \rightarrow \infty$, and reads:

$$\Delta\mu_1 / RT = \ln(1-\varphi_2) + \varphi_2 + \chi\varphi_2^2 + \nu_c V_1\left(A\eta\varphi_2^{1/3} - B\varphi_2\right) \qquad [4.4.63]$$

where:

ν_c	network density $\nu_c = \rho_N/M_c$
V_1	molar volume of the pure liquid solvent 1 at temperature T
η	memory term
A	microstructure factor
B	volume factor
M_c	molar mass of a network chain between two network knots
φ_2	equilibrium swelling concentration = $1/Q_v$
χ	Flory-Huggins χ-function

A numerical calculation needs knowledge of the solvent activity of the corresponding homopolymer solution at the same equilibrium concentration φ_2 (here characterized by the value of the Flory-Huggins χ-function) and the assumption of a deformation model that provides values of the factors A and B. There is an extensive literature for statistical thermodynamic models which provide, for example, Flory:[46] A = 1 and B = 0.5; Hermans:[214] A = 1 and B = 1; James and Guth[215] or Edwards and Freed:[216] A = 0.5 and B = 0. A detailed explanation was given recently by Heinrich et al.[203]

The swelling equilibrium depends on temperature and pressure. Both are related to the corresponding dependencies of solvent activity via its corresponding derivative of the chemical potential:

$$\left(\frac{\partial T}{\partial \varphi_1}\right)_P = \frac{1}{\Delta S_1}\left(\frac{\partial \mu_1}{\partial \varphi_1}\right)_{P,T} = \frac{T}{\Delta H_1}\left(\frac{\partial \mu_1}{\partial \varphi_1}\right)_{P,T} \qquad [4.4.64]$$

where:

φ_1	equilibrium swelling concentration of the solvent
ΔS_1	differential entropy of dilution at equilibrium swelling
ΔH_1	differential enthalpy of dilution at equilibrium swelling where $\Delta H_1 = T\Delta S_1$

The first derivative in Equation [4.4.64] describes the slope of the swelling curve. Since the derivative of the chemical potential is always positive for stable gels, the positive

or negative slope is determined by the differential enthalpy or entropy of dilution, Rehage.[217]

$$\left(\frac{\partial P}{\partial \varphi_1}\right)_T = \frac{1}{\left(V_1 - \overline{V}_1\right)}\left(\frac{\partial \mu_1}{\partial \varphi_1}\right)_{P,T} \qquad [4.4.65]$$

where:

$\overline{V}_1$ partial molar volume of the solvent in the polymer solution at temperature T
V_1 molar volume of the pure solvent at temperature T

In analogy to membrane osmometry, swelling pressure measurements can be made to obtain solvent activities. Pure solvents as well as dilute polymer solutions can be applied. In the case of solutions, the used macromolecules must not diffuse into or adsorb at the surface of the network. Two types of swelling pressure apparatuses have been developed. The anisochoric swelling pressure device measures swelling degrees in dependence on pressure and swelling volume, e.g., Borchard.[218] The isochoric swelling pressure device applies a compensation technique where the volume is kept constant by an external pressure which is measured, e.g., Borchard.[219] Swelling pressures can also be measured by sedimentation equilibrium using an ultracentrifuge for details, please see Borchard.[220,221]

The swelling pressure π_{swell} is directly related to the solvent activity by:

$$\Delta\mu_1 = RT \ln a_1 = -\overline{V}_1 \pi_{swell} \qquad [4.4.66]$$

and may be in the range of some MPa.

In comparison with all methods of determination of solvent activities from swelling equilibrium of network polymers, the gravimetric vapor sorption/pressure measurement is the easiest applicable procedure, gives the most reliable data, and should be preferred.

4.4.4 THERMODYNAMIC MODELS FOR THE CALCULATION OF SOLVENT ACTIVITIES OF POLYMER SOLUTIONS

Since measurements of solvent activities of polymer solutions are very time-consuming and can hardly be made to cover the whole temperature and pressure ranges, good thermodynamic theories, and models are necessary, which are able to calculate them with sufficient accuracy and which can interpolate between and even extrapolate from some measured basic data over the complete phase and state ranges of interest for a special application.

Many attempts have been made to find theoretical explanations for the non-ideal behavior of polymer solutions. There exist books and reviews on this topic, e.g., Refs.[2,41,42,46-49] Therefore, only a short summary of some of the most important thermodynamic approaches and models will be given here. The following explanations are restricted to concentrated polymer solutions only because one has to describe mainly concentrated polymer solutions when solvent activities have to be calculated. For dilute polymer solutions, with the second virial coefficient region, Yamakawa's book[222] provides a good survey.

There are two different approaches for the calculation of solvent activities of polymer solutions:

(i) the approach which uses activity coefficients, starting from Equation [4.4.11]
(ii) the approach which uses fugacity coefficients, starting from Equations [4.4.5 and 4.4.6].

From the historical point of view and also from the number of applications in the literature, the common method is to use activity coefficients for the liquid phase, i.e., the polymer solution, and a separate equation-of-state for the solvent vapor phase, in many cases the truncated virial equation of state as for the data reduction of experimental measurements explained above. To this group of theories and models also free-volume models and lattice-fluid models will be added in this paper because they are usually applied within this approach. The approach where fugacity coefficients are calculated from one equation of state for both phases was applied to polymer solutions more recently, but it is the more promising method if one has to extrapolate over larger temperature and pressure ranges.

Theories and models are presented below without going into details and without claiming completeness, since this text is not dedicated to theoretical problems but will only provide some help to calculate solvent activities.

4.4.4.1 Models for residual chemical potential and activity coefficient in the liquid phase

Since polymer solutions in principle do not fulfill the rules of the ideal mixture but show strong negative deviations from Raoult's law due to the difference in molecular size, the athermal Flory-Huggins mixture is usually applied as the reference mixture within polymer solution thermodynamics. Starting from Equation [4.4.11] or from

$$RT\ln a_1 = RT\ln x_1\gamma_1 = \Delta\mu_1 = \mu_1 - \mu_1^0 = \left(\frac{\partial n\Delta_{mix}G}{\partial n_1}\right)_{T,P,n_{j\neq1}} \qquad [4.4.67]$$

where:

a_1	activity of the solvent
x_1	mole fraction of the solvent
γ_1	activity coefficient of the solvent in the liquid phase with activity $a_1 = x_1\gamma_1$
μ_1	chemical potential of the solvent
μ_1^0	chemical potential of the solvent at standard state conditions
R	gas constant
T	absolute temperature
n_1	amount of substance (moles) of the solvent
n	total amount of substance (moles) in the polymer solution
$\Delta_{mix}G$	molar Gibbs free energy of mixing,

the classical Flory-Huggins theory[46,47] leads, for a truly athermal binary polymer solution, to:

$$\ln a_1^{athermal} = \Delta\mu_1^{athermal} / RT = \ln(1-\varphi_2) + \left(1-\frac{1}{r}\right)\varphi_2 \qquad [4.4.68a]$$

or

$$\ln\gamma_1^{athermal} = \ln\left[1-\left(1-\frac{1}{r}\right)\varphi_2\right] + \left(1-\frac{1}{r}\right)\varphi_2 \qquad [4.4.68b]$$

where:

φ_2	volume fraction of the polymer

which is also called the combinatorial contribution to solvent activity or chemical potential, arising from the different configurations assumed by polymer and solvent molecules in solution, ignoring energetic interactions between molecules and excess volume effects. The Flory-Huggins derivation of the athermal combinatorial contribution contains the implicit assumption that the r-mer chains placed on a lattice are perfectly flexible and that the flexibility of the chain is independent of the concentration and of the nature of the solvent. Generalized combinatorial arguments for molecules containing different kinds of energetic contact points and shapes were developed by Barker[223] and Tompa,[224] respectively. Lichtenthaler et al.[225] have used the generalized combinatorial arguments of Tompa to analyze VLE of polymer solutions. Other modifications have been presented by Guggenheim[226,227] or Staverman[228] (see below). The various combinatorial models are compared in a review by Sayegh and Vera.[229] Recently, Freed and coworkers[230-232] developed a lattice-field theory, that, in principle, provides an exact mathematical solution of the combinatorial Flory-Huggins problem. Although the simple Flory-Huggins expression does not always give the (presumably) correct, quantitative combinatorial entropy of mixing, it qualitatively describes many features of athermal polymer solutions. Therefore, for simplicity, it is used most in the further presentation of models for polymer solutions as reference state.

The total solvent activity/activity coefficient/chemical potential is simply the sum of the athermal part as given above, plus a residual contribution:

$$\ln a_1 = \ln a_1^{athermal} + \ln a_1^{residual} \qquad [4.4.69a]$$

or

$$\mu_1 = \mu_1^0 + \mu_1^{athermal} + \mu_1^{residual} \qquad [4.4.69b]$$

The residual part has to be explained by an additional model and a number of suitable models is now listed in the following text.

The Flory-Huggins interaction function of the solvent is the residual function used first and is given by Equations [4.4.12 and 4.4.13] with $\mu_1^{\text{residual}} / RT = \chi\varphi_2^2$. It was originally based on van Laar's concept of solutions where excess entropy and excess volume of mixing could be neglected and χ is represented only in terms of an interchange energy $\Delta\varepsilon/kT$. In this case, the interchange energy refers not to the exchange of solvent and solute molecules but rather to the exchange of solvent molecules and polymer segments. For athermal solutions, χ is zero, and for mixtures of components that are chemically similar, χ is small compared to unity. However, χ is not only a function of temperature (and pressure) as was evident from this foundation, but it is also a function of composition and polymer molecular mass, see e.g., Refs.[5,7,8] If we neglect these dependencies, then the Scatchard-Hildebrand theory,[233,234] i.e., their solubility parameter concept, could be applied:

$$\mu_1^{residual} / RT = (V_1 / RT)(\delta_1 - \delta_2)^2 \varphi_2^2 \qquad [4.4.70]$$

with

$$\delta_1 = \left(\Delta_{vap} U_1^0 / V_1\right)^{1/2} \qquad [4.4.71]$$

where:

V_1	molar volume of the pure liquid solvent 1 at temperature T
$\Delta_{vap} U_1^0$	molar energy of vaporization of the pure liquid solvent 1 at temperature T
δ_1	solubility parameter of the pure liquid solvent
δ_2	solubility parameter of the polymer

Solubility parameters of polymers cannot be calculated from energy of vaporization since polymers do not evaporate. Usually they have been measured according to Equation [4.4.70], but details need not be explained here. Equation [4.4.70] is not useful for an accurate quantitative description of polymer solutions but it provides a good guide for a qualitative consideration of polymer solubility. For good solubility, the difference between both solubility parameters should be small (the complete residual chemical potential term cannot be negative, which is one of the disadvantages of the solubility parameter approach). Several approximate generalizations have been suggested by different authors - a summary of all these models and many data can be found in the books by Barton.[11,12] Calculations applying additive group contributions to obtain solubility parameters, especially of polymers, are also explained in the book by Van Krevelen.[235]

Better-founded lattice models have been developed in the literature. The ideas of Koningsveld and Kleintjens, e.g., Ref.,[51] lead to useful and easy to handle expressions, as is given above with Equations [4.4.15, 4.4.17 and 4.4.46] that have been widely used, but mainly for liquid-liquid demixing and not so much for vapor-liquid equilibrium and solvent activity data. Comprehensive examples can be found in the books by Fujita[41] or Kamide.[42]

The simple Flory-Huggins approach and the solubility parameter concept are inadequate when tested against experimental data for polymer solutions. Even for mixtures of n-alkanes, the excess thermodynamic properties cannot be described satisfactorily - Flory et al.[236-239] In particular, changes of volume upon mixing are excluded and observed excess entropies of mixing often deviate from simple combinatorial contributions. To account for these effects, the PVT-behavior has to be included in theoretical considerations by an equation of state. Pure fluids have different free volumes, i.e., different degrees of thermal expansion depending on temperature and pressure. When liquids with different free volumes are mixed, that difference contributes to the excess functions. Differences in free volumes must be taken into account, especially for mixtures of liquids whose molecules differ greatly in size, i.e., the free volume dissimilarity is significant for polymer solutions and has important effects on their properties, such as solvent activities, excess volume, excess enthalpy and excess entropy. Additionally, the free volume effect is the main reason for liquid-liquid demixing with LCST behavior at high temperatures.[240,241]

Today, there are two principal ways to develop an equation of state for polymer solutions: first, to start with an expression for the canonical partition function utilizing concepts similar to those used by van der Waals (e.g., Prigogine,[242] Flory et al.,[236-239] Patterson,[243,244] Simha and Somcynsky,[245] Sanchez and Lacombe,[246-248] Dee and Walsh,[249] Donohue and Prausnitz,[250] Chien et al.[251]), and second, which is more sophisticated, to use statistical thermodynamics perturbation theory for freely-jointed tangent-sphere chain-like fluids (e.g., Hall and coworkers,[252-255] Chapman et al.,[256-258] Song et al.[259,260]). A comprehensive review about equations of state for molten polymers and polymer solutions was given by Lambert et al. [261] Here, only some resulting equations will be summarized under the aspect of calculating solvent activities in polymer solutions.

The theories that are usually applied within activity coefficient models are given now, the other theories are summarized in Subchapter 4.4.4.2.

The first successful theoretical approach of an equation of state model for polymer solutions was the Prigogine-Flory-Patterson theory.[236-242] It became popular in the version by Flory, Orwoll and Vrij[236] and is a van-der-Waals-like theory based on the corresponding-states principle. Details of its derivation can be found in numerous papers and books and need not be repeated here. The equation of state is usually expressed in reduced form and reads:

$$\frac{\tilde{P}\tilde{V}}{\tilde{T}} = \frac{\tilde{V}^{1/3}}{\tilde{V}^{1/3} - 1} - \frac{1}{\tilde{V}\tilde{T}} \qquad [4.4.72]$$

where the reduced PVT-variables are defined by

$$\tilde{P} = P / P^*, \tilde{T} = T / T^*, \tilde{V} = V / T^*, P^* V^* = rcRT^* \qquad [4.4.73]$$

and where a parameter c is used (per segment) such that 3rc is the number of effective external degrees of freedom per (macro)molecule. This effective number follows from Prigogine's approximation that external rotational and vibrational degrees of freedom can be considered as equivalent translational degrees of freedom. The equation of state is valid for liquid-like densities and qualitatively incorrect at low densities because it does not fulfill the ideal gas limit. To use the equation of state, one must know the reducing or characteristic parameters P*, V*, T*. These have to be fitted to experimental PVT-data. Parameter tables can be found in the literature - here we refer to the book by Prausnitz et al.,[49] a review by Rodgers,[262] and the contribution by Cho and Sanchez[263] to the new edition of the Polymer Handbook.

To extend the Flory-Orwoll-Vrij model to mixtures, one has to use two assumptions: (i) the hard-core volumes υ* of the segments of all components are additive and (ii) the intermolecular energy depends in a simple way on the surface areas of contact between solvent molecules and/or polymer segments. Without any derivation, the final result for the residual solvent activity in a binary polymer solution reads:

$$\ln a_1^{residual} = \frac{P_1^* V_1^*}{RT}\left[3\tilde{T}_1 \ln\frac{\tilde{V}_1^{1/3} - 1}{\tilde{V}^{1/3} - 1} + \left(\frac{1}{\tilde{V}_1} - \frac{1}{\tilde{V}}\right)\right] +$$

$$+ \frac{V_1^*}{RT}\left(\frac{X_{12}}{\tilde{V}}\right)\theta_2^2 + \frac{PV_1^*}{RT}(\tilde{V} - \tilde{V}_1) \qquad [4.4.74]$$

where:

X_{12}	interaction parameter
θ_2	surface fraction of the polymer

The last term in Equation [4.4.74] is negligible at normal pressures. The reduced volume of the solvent 1 and the reduced volume of the mixture are to be calculated from the same equation of state, Equation [4.4.72], but for the mixture the following mixing rules have to be used (if random mixing is assumed):

$$P^* = P_1^* \psi_1 + P_2^* \psi_2 - \psi_1 \theta_2 X_{12} \qquad [4.4.75a]$$

$$T^* = P^* / \left[\left(P_1^* \psi_1 / T_1^* \right) + \left(P_2^* \psi_2 / T_2^* \right) \right] \qquad [4.4.75b]$$

where the segment fractions ψ_i and the surface fractions θ_i have to be calculated according to:

$$\psi_i = n_i V_i^* / \sum n_k V_k^* = m_i V_{spez,i}^* / \sum m_k V_{spez,k}^* = x_i r_i / \sum x_k r_k \qquad [4.4.76a]$$

$$\theta_i = \psi_i s_i / \sum \psi_k s_k \qquad [4.4.76b]$$

where:

m_i	mass of component i
x_i	mole fraction of component i
r_i	number of segments of component i, here with $r_i / r_k = V_i^* / V_k^*$ and $r_1 = 1$
s_i	number of contact sites per segment (proportional to the surface area per segment)

Now it becomes clear from Equation [4.4.74] that the classical Flory-Huggins χ-function ($\chi \psi_2^2 = \ln a_1^{residual}$) varies with composition, as found experimentally. However, to calculate solvent activities by applying this model, a number of parameters have to be considered. The characteristic parameters of the pure substances have to be obtained by fitting to experimental PVT-data as explained above. The number of contact sites per segment can be calculated from Bondi's surface-to-volume parameter tables[264] but can also be used as fitting parameter. The X_{12}-interaction parameter has to be fitted to experimental data of the mixture. Fitting to solvent activities, e.g. Refs.,[265,266] does not always give satisfactorily results. Fitting to data for the enthalpies of mixing gives comparable results.[266] Fitting to excess volumes alone does not give acceptable results.[142] Therefore, a modification of Equation [4.4.74] was made by Eichinger and Flory[142] by appending the term $-(V_1^* / R) Q_{12} \theta_2^2$ where the parameter Q_{12} represents the entropy of interaction between unlike segments and is an entropic contribution to the residual chemical potential of the solvent. By adjusting the parameter Q_{12}, a better representation of solvent activities can be obtained.

There are many papers in the literature that applied the Prigogine-Flory-Patterson theory to polymer solutions as well as to low-molecular mixtures. Various modifications and improvements were suggested by many authors. Sugamiya[267] introduced polar terms by adding dipole-dipole interactions. Brandani[268] discussed effects of non-random mixing on the calculation of solvent activities. Kammer et al.[269] added a parameter reflecting differences in segment size. Shiomi et al.[270,271] assumed non-additivity of the number of external degrees of freedom with respect to segment fraction for mixtures and assumed the sizes of hard-core segments in pure liquids and in solution to be different. Also Panayiotou[272] accounted for differences in segment size by an additional parameter. Cheng and Bonner[273] modified the concept to obtain an equation of state which provides the correct zero pressure limit of the ideal gas. An attractive feature of the theory is its straightforward extension to multi-component mixtures,[274] requiring only parameters of pure components and binary ones as explained above. A general limitation is its relatively poor description of the compressibility behavior of polymer melts, as well as its deficiencies regarding the description of the pressure dependence of thermodynamic data of mixtures.

Dee and Walsh[249] developed a modified version of Prigogine's cell model that provides an excellent description of the PVT-behavior of polymer melts:

$$\frac{\tilde{P}\tilde{V}}{\tilde{T}} = \frac{\tilde{V}^{1/3}}{\tilde{V}^{1/3} - 0.8909q} - \frac{2}{\tilde{T}}\left(\frac{1.2045}{\tilde{V}^{2}} - \frac{1.1011}{\tilde{V}^{4}}\right) \qquad [4.4.77]$$

where the reduced variables and characteristic parameters have the same definitions as in the Flory model above. Equation [4.4.77] is formally identical with Prigogine's result, except for the additional constant parameter q, which can also be viewed as a correction to the hard-core cell volume. The value of q = 1.07 corresponds approximately to a 25% increase in the hard-core volume in comparison with the original Prigogine model. Characteristic parameters for this model are given in Refs.[249,262] The final result for the residual solvent activity in a binary polymer solution reads:

$$\ln a_1^{residual} = \frac{P_1^* V_1^*}{RT}\left[3\tilde{T}_1 \ln \frac{\tilde{V}_1^{1/3} - 0.8909q}{\tilde{V}^{1/3} - 0.8909q} + \left(\frac{1.2045}{\tilde{V}_1^{2}} - \frac{1.2045}{\tilde{V}^{2}}\right) - \left(\frac{0.5055}{\tilde{V}_1^{4}} - \frac{0.5055}{\tilde{V}^{4}}\right)\right]$$

$$+ \frac{V_1^* \theta_2^2}{RT}\left(X_{12} - TQ_{12}\tilde{V}\right)\left(\frac{1.2045}{\tilde{V}^{2}} - \frac{0.5055}{\tilde{V}^{4}}\right) + \frac{PV_1^*}{RT}\left(\tilde{V} - \tilde{V}_1\right) \qquad [4.4.78]$$

The last term in Equation [4.4.78] is again negligible at normal pressures, which is the case for the calculation of solvent activities of common polymer solutions. The reduced volume of the mixture is to be calculated from the equation of state where the same mixing rules are valid, as given by Equations [4.4.75, 4.4.76] if random mixing is assumed. Equation [4.4.78] is somewhat more flexible than Equation [4.4.74]. Again, entropic parameter Q_{12} and interaction parameter X_{12} have to be fitted to experimental data of the mixture. There is not much experience with the model regarding thermodynamic data of polymer solutions because it was mainly applied to polymer blends, where it provides much better results than the simple Flory model.

To improve on the cell model, two other classes of models were developed, namely, lattice-fluid and lattice-hole theories. In these theories, vacant cells or holes are introduced into the lattice to describe the extra entropy change in the system as a function of volume and temperature. The lattice size, or cell volume, is fixed so that the changes in volume can only occur by the appearance of new holes, or vacant sites, on the lattice. The most popular theories of such kind were developed by Simha and Somcynsky[245] or Sanchez and Lacombe.[246-248]

The Sanchez-Lacombe lattice-fluid equation of state reads:

$$\frac{\tilde{P}\tilde{V}}{\tilde{T}} = -\frac{1}{r} - 1 - \tilde{V}\ln\frac{\tilde{V}-1}{\tilde{V}} - \frac{1}{\tilde{V}\tilde{T}} \qquad [4.4.79]$$

where the reduced parameters are given in Equation [4.4.73], but no c-parameter is included, and the size parameter, r, and the characteristic parameters are related by

$$P^* V^* = (r/M)RT^* \qquad [4.4.80]$$

where:

r	size parameter (segment number)
M	molar mass

In comparison with Equation [4.4.72], the size parameter remains explicit in the reduced equation of state. Thus, a simple corresponding-states principle is not, in general, satisfied. But, in principle, this equation of state is suitable for describing thermodynamic properties of fluids over an extended range of external conditions from the ordinary liquid to the gaseous state (it gives the correct ideal gas limit) and also to conditions above the critical point where the fluid is supercritical. Equation of state parameters for many liquids and liquid/molten polymers have recently been reported by Sanchez and Panayiotou[275] and for polymers by Rodgers[262] and by Cho and Sanchez.[263] To extend the lattice fluid theory to mixtures, appropriate mixing rules are needed. There is a fundamental difficulty here, because the segment size of any component is not necessarily equal to that of another but the molecular hard-core volume of a component must not change upon mixing. Consequently, the segment number of a component in the mixture, r_i, may differ from that for the pure fluid, r_i^0. But, following the arguments given by Panayiotou,[276] the number of segments may remain constant in the pure state and in the mixture. This assumption leads to a simpler formalism without worsening the quantitative character of the model. Thus, the following mixing rules may be applied:

$$P^* = P_1^* \psi_1 + P_2^* \psi_2 - \psi_1 \psi_2 X_{12} \qquad [4.4.81a]$$

$$V^* = \Sigma\Sigma \psi_i \psi_j V_{ij}^* \qquad [4.4.81b]$$

$$1/r = \Sigma \psi_i / r_i \qquad [4.4.81c]$$

where $V_{ii}^* = V_i^*$ and V_{ij}^* provides an additional binary fitting parameter and Equation [4.4.80] provides the mixing rule for T*. The final result for the residual solvent activity in a binary polymer solution reads:

$$\ln a_1^{residual} = r_1\left(\tilde{V}-1\right)\ln\left(\frac{\tilde{V}-1}{\tilde{V}}\right) - r_1\left(\tilde{V}_1-1\right)\ln\left(\frac{\tilde{V}_1-1}{\tilde{V}_1}\right) - \ln\frac{\tilde{V}}{\tilde{V}_1}$$

$$-\frac{r_1}{\tilde{T}_1}\left(\frac{1}{\tilde{V}}-\frac{1}{\tilde{V}_1}\right) + r_1\left(\frac{X_{12}}{\tilde{V}}\right)\psi_2^2 + \frac{r_1\tilde{P}_1\left(\tilde{V}-\tilde{V}_1\right)}{\tilde{T}_1} \qquad [4.4.82]$$

The last term in Equation (4.4.82) is again negligible at normal pressures. Various other approximations were given in the literature. For example, one can assume random mixing of contact sites rather than random mixing of segments,[277,278] as well as non-random mixing.[277,279] The model is applicable to solutions of small molecules as well as to polymer solutions. Like the Prigogine-Flory-Patterson equation of state, the lattice-fluid model and its variations have been used to correlate the composition dependence of the residual solvent activity.[277,279] These studies show that again entropic parameter Q_{12} and interaction parameter X_{12} have to be fitted to experimental data of the mixture to provide better agreement

with measured solvent activities. The model and its modifications have been successfully used to represent thermodynamic excess properties, VLE and LLE for a variety of mixtures, as summarized by Sanchez and Panayiotou.[275] In addition to mixtures of polymers with normal solvents, the model can also be applied to polymer-gas systems, Sanchez and Rodgers.[280]

In lattice-hole theories, vacant cells or holes are introduced into the lattice, which describe the major part of thermal expansion, but changes in cell volume are also allowed which influence excess thermodynamic properties as well. The hole-theory for polymeric liquids as developed by Simha and Somcynsky[245] provides a very accurate equation of state that works much better than the Prigogine-Flory-Patterson equation of state or the Sanchez-Lacombe lattice-fluid model with respect to the precision how experimental PVT-data can be reproduced. However, the Dee-Walsh equation of state, Equation [4.4.77], with its more simple structure, works equally well. The Simha-Somcynsky equation of state must be solved simultaneously with an expression that minimizes the partition function with respect to the fraction of occupied sites and the final resulting equations for the chemical potential are more complicated. Details of the model will not be provided here. Characteristic parameters for many polymers have recently been given by Rodgers[262] or Cho and Sanchez.[263] The model is applicable to solutions of small molecules as well as to polymer solutions. Binary parameters have to be fitted to experimental data as with the models explained above. Again, one can assume random mixing of contact sites rather than random mixing of segments as well as non-random mixing, as was discussed, for example, by Nies and Stroeks[281] or Xie et al.[282,283]

Whereas the models given above can be used to correlate solvent activities in polymer solutions, attempts also have been made in the literature to develop concepts to predict solvent activities. Based on the success of the UNIFAC concept for low-molecular liquid mixtures,[284] Oishi and Prausnitz[285] developed an analogous concept by combining the UNIFAC-model with the free-volume model of Flory, Orwoll and Vrij.[236] The mass fraction based activity coefficient of a solvent in a polymer solution is given by:

$$\ln\Omega_1 \ln(a_1 / w_1) = \ln\Omega_1^{comb} + \ln\Omega_1^{res} + \ln\Omega_1^{fv} \qquad [4.4.83]$$

where:

Ω_1	mass fraction based activity coefficient of solvent 1 at temperature T
Ω_1^{comb}	combinatorial contribution to the activity coefficient
Ω_1^{res}	residual contribution to the activity coefficient
Ω_1^{fv}	free-volume contribution to the activity coefficient

Instead of the Flory-Huggins combinatorial contribution, Equation [4.4.68], the Staverman relation[228] is used.

$$\ln\Omega_1^{comb} = \ln\frac{\psi_1}{w_1} + \frac{z}{2} q_1 \ln\frac{\theta_1}{\psi_1} + l_1 - \frac{\psi_1 M_1}{w_1} \sum_j \frac{\psi_j M_j}{w_j} \qquad [4.4.84]$$

where the segment fractions ψ_i and the surface area fractions θ_i have to be calculated according to

$$\psi_i = (w_i r_i / M_i) / \Sigma(w_k r_k / M_k) \qquad [4.4.85a]$$

$$\theta_i = (w_i q_i / M_i) / \Sigma(w_k q_k / M_k) \qquad [4.4.85b]$$

and the l_i-parameter is given by

$$l_i = (z/2)(r_i - q_i) - (r_i - 1) \qquad [4.4.85c]$$

where:

i,j	components in the solution
z	lattice coordination number (usually = 10)
q_i	surface area of component i based on Bondi's van-der-Waals surfaces
M_i	molar mass of component i (for polymers the number average is recommended)
w_i	mass fraction of component i
r_i	segment number of component i based on Bondi's van-der-Waals volumes

The molecules must be divided into groups as defined by the UNIFAC method. The segment surface areas and the segment volumes are calculated from Bondi's tables[264] according to

$$r_i = \sum_k \nu_\kappa^{(i)} R_k \quad and \quad q_i = \sum_k \nu_k^{(i)} Q_k \qquad [4.4.86]$$

where:

k	number of groups of type k in the solution
ν_k	number of groups of type k in the molecule i
R_k	Van-der-Waals group volume parameter for group k
Q_k	Van-der-Waals group surface parameter for group k

The residual activity coefficient contribution for each component is given by

$$\ln\Omega_i^{res} = \sum_k \nu_k^{(i)} \left[\ln\Gamma_k - \ln\Gamma_k^{(i)}\right] \qquad [4.4.87]$$

where:

Γ_k	the residual activity coefficient of group k in the defined solution
$\Gamma_k^{(i)}$	the residual activity coefficient of group k in a reference solution containing pure component i only

The residual activity coefficient of group k in the given solution is defined by

$$\ln\Gamma_k = Q_k \left[1 - \ln\left(\sum_m \Lambda_m \exp\left\{-\frac{a_{mk}}{T}\right\} \right) - \sum_m \left(\frac{\Lambda_m \exp\left\{-\frac{a_{km}}{T}\right\}}{\sum_p \Lambda_p \exp\left\{-\frac{a_{pm}}{T}\right\}} \right) \right] \qquad [4.4.88]$$

where:

a_{mn} and a_{nm}	group interaction parameter pair between groups m and n
Λ_m	group surface area fraction for group m

The group surface area fraction Λ_m for group m in the solution is given by

$$\Lambda_m = \frac{Q_m X_m}{\sum_p Q_p X_p} \qquad [4.4.89a]$$

where:

X_m group mole fraction for group m

The group mole fraction X_m for group m in the solution is given by

$$X_m = \frac{\sum_j \nu_m^{(j)} w_j / M_j}{\sum_j \sum_p \nu_p^{(j)} w_j / M_j} \qquad [4.4.89b]$$

The residual activity coefficient of group k in reference solutions containing only component i, $\Gamma_k^{(i)}$ is similarly determined using Equations [4.4.88, 4.4.89], with the exception that the summation indices k, m, p refer only to the groups present in the pure component and the summations over each component j are calculated only for the single component present in the reference solution.

The group interaction parameter pairs a_{mn} and a_{nm} result from the interaction between the groups m and n. These parameter are unsymmetric values that have to be fitted to experimental VLE-data of low-molecular mixtures. They can be taken from UNIFAC tables, e.g., Refs.[2,284,286-289] and, additionally, they may be treated as temperature functions.

The free-volume contribution, which is essential for nonpolar polymer solutions, follows, in principle, from Equation [4.4.74] with parameter $X_{12} = 0$ as applied by Raetzsch and Glindemann,[290] or in a modified form from Equation [4.4.90] as introduced by Oishi and Prausnitz and used also in Danner's Handbook.[2]

$$\ln Q_1^{fv} = 3c_1 \ln\left(\frac{\tilde{V}_1^{1/3} - 1}{\tilde{V}^{1/3} - 1}\right) - c_1 \left(\frac{\tilde{V}_1 - \tilde{V}}{\tilde{V}\left(1 - \tilde{V}_1^{1/3}\right)}\right) \qquad [4.4.90]$$

where:

c_1 external degree of freedom parameter of the solvent 1, usually fixed = 1.1

To get a predictive model, the reduced volumes and the external degree of freedom parameter are not calculated from Flory's equation of state, Equation [4.4.72], but from some simple approximations as given by the following relations:[2]

$$\tilde{V}_i = \frac{\upsilon_{spez,i} M_i}{0.01942 r_i} \qquad [4.4.91a]$$

$$\tilde{V} = \frac{\sum_i \upsilon_{spez,i} w_i}{0.01942 \sum_i r_i w_i / M_i} \qquad [4.4.91b]$$

where:

$\upsilon_{spez,i}$ specific volume of component i in m^3/kg

r_i segment number of component i based on Bondi's van-der-Waals volumes

M_i molar mass of component i (for polymers the number average is recommended)

w_i mass fraction of component i

There has been a broad application of this group-contribution UNIFAC-fv concept to polymer solutions in the literature. Raetzsch and Glindemann[290] recommended the use of the real free-volume relation from the Flory-Orwoll-Vrij model to account for realistic PVT-data. Problems arise for mixtures composed from chemically different components that posses the same groups, e.g., mixtures with different isomers. Kikic et al.[291] discussed the influence of the combinatorial part on results obtained with UNIFAC-fv calculations. Gottlieb and Herskowitz[292,293] gave some polemic about the special use of the c_1-parameter within UNIFAC-fv calculations. Iwai et al.[294,295] demonstrated the possible use of UNIFAC-fv for the calculation of gas solubilities and Henry's constants using a somewhat different free-volume expression. Patwardhan and Belfiore[296] found quantitative discrepancies for some polymer solutions. In a number of cases UNIFAC-fv predicted the occurrence of a demixing region during the calculation of solvent activities where experimentally only a homogeneous solution exists. Price and Ashworth[297] found that the predicted variation of residual solvent activity with polymer molecular mass at high polymer concentrations is opposite to that measured for polydimethylsiloxane solutions. But, qualitative correct predictions were obtained for poly(ethylene glycol) solutions with varying polymer molecular mass.[298-300] However, UNIFAC-fv is not capable of representing thermodynamic data of strongly associating or solvating systems.

Many attempts have been made to improve the UNIFAC-fv model which cannot be listed here. A comprehensive review was given by Fried et al.[301] An innovative method to combine the free-volume contribution within a corrected Flory-Huggins combinatorial entropy and the UNIFAC concept was found by Elbro et al.[302] and improved by Kontogeorgis et al.[303] These authors take into account the free-volume dissimilarity by assuming different van der Waals hard-core volumes (again from Bondi's tables[264]) for the solvent and the polymer segments

$$V_i^{fv} = q_i \left(V_i^{1/3} - V_{i,vdW}^{1/3} \right)^3 \qquad [4.4.92a]$$

$$\varphi_i^{fv} = x_i V_i^{fv} \; / \sum_j x_j V_j^{fv} \qquad [4.4.92b]$$

where:

q_i surface area of component i based on Bondi's van der Waals surfaces
x_i mole fraction of component i
V_i molar volume of component i
$V_{i,vdW}$ van der Waals hard-core molar volume of component i

and introduced these free-volume terms into Equation [4.4.68] to obtain a free-volume corrected Flory-Huggins combinatorial term:

$$\ln \gamma_i^{fv} = \ln\left(\varphi_i^{fv} \; / \; x_i \right) + 1 - \left(\varphi_i^{fv} \; / \; x_i \right) \qquad [4.4.93a]$$

or

$$\ln \Omega_i^{fv} = \ln\left(\varphi_i^{fv} \; / \; w_i \right) + 1 - \left(\varphi_i^{fv} \; / \; x_i \right) \qquad [4.4.93b]$$

To obtain the complete activity coefficient, only the residual term from the UNIFAC model, Equation [4.4.87], has to be added. An attempt to incorporate differences in shape between solvent molecules and polymer segments was made by Kontogeorgis et al.[302] by adding the Staverman correction term to obtain:

$$\ln \gamma_i^{fv} = \ln \frac{\varphi_i^{fv}}{x_i} + 1 - \frac{\varphi_i^{fv}}{x_i} - \frac{z q_i}{2}\left(\ln \frac{\psi_i}{\theta_i} + 1 - \frac{\psi_i}{\theta_i} \right) \qquad [4.4.93c]$$

where the segment fractions ψ_i and the surface area fractions θ_i have to be calculated according to Equations [4.4.85a+b]. Using this correction, they get somewhat better results only when Equation [4.4.93] leads to predictions lower than the experimental data.

Different approaches utilizing group contribution methods to predict solvent activities in polymer solutions have been developed after the success of the UNIFAC-fv model. Misovich et al.[304] have applied the Analytical Solution of Groups (ASOG) model to polymer solutions. Recent improvements of polymer-ASOG have been reported by Tochigi et al.[305-307] Various other group-contribution methods including an equation-of-state were developed by Holten-Anderson et al.,[308,309] Chen et al.,[310] High and Danner,[311-313] Tochigi et al.,[314] Lee and Danner,[315] Bertucco and Mio,[316] or Wang et al.,[317] respectively. Some of them were presented again in Danner's Handbook.[2] Detail are not provided here.

4.4.4.2 Fugacity coefficients from equations of state

Total equation-of-state approaches usually apply equations for the fugacity coefficients instead of relations for chemical potentials to calculate thermodynamic equilibria and start from Equations [4.4.2 to 6]. Since the final relations for the fugacity coefficients are usually much more lengthy and depend, additionally, on the chosen mixing rules, only the equations of state are listed below. Fugacity coefficients have to be derived by solving Equation [4.4.6]. After obtaining the equilibrium fugacities of the liquid mixture at equilibrium temperature and pressure, the solvent activity can be calculated from Equation [4.4.1]. The standard state fugacity of the solvent can also be calculated from the same equation of state by solving the same equations but for the pure liquid. Details of this procedure can be found in textbooks, e.g., Refs.[318,319]

Equations of state for polymer systems that will be applied within such an approach have to be valid for the liquid as well as for the gaseous state like lattice-fluid models based on Sanchez-Lacombe theory, but not the free-volume equations based on Prigogine-Flory-Patterson theory, as stated above. However, most equations of state applied within such an approach have not been developed specially for polymer systems, but, first, for common non-electrolyte mixtures and gases. Today, one can distinguish between cubic and non-cubic equations of state for phase equilibrium calculations in polymer systems. Starting from the free-volume idea in polymeric systems, non-cubic equations of state should be applied to polymers. Thus, the following text presents first some examples of this class of equations of state. Cubic equations of state came later into consideration for polymer systems, mainly due to increasing demands from engineers and engineering software where three-volume-roots equations of state are easier to solve and more stable in computational cycles.

About ten years after Flory's development of an equation of state for polymer systems, one began to apply methods of thermodynamic perturbation theory to calculate the thermo-

dynamic behavior of polymer systems. The main goal was first to overcome the restrictions of Flory's equation of state to the liquid state, to improve the calculation of the compressibility behavior with increasing pressure and to enable calculations of fluid phase equilibria at any densities and pressures from the dilute gas phase to the compressed liquid including molecules differing considerably in size, shape, or strength of intermolecular potential energy. More recently, when more sophisticated methods of statistical mechanics were developed, deeper insights into liquid structure and compressibility behavior of model polymer chains in comparison to Monte Carlo modelling results could be obtained applying thermodynamic perturbation theory. Quite a lot of different equations of state have been developed up to now following this procedure; however, only a limited number was applied to real systems. Therefore, only some summary and a phenomenological presentation of some equations of state which have been applied to real polymer fluids should be given here, following their historical order.

The perturbed-hard-chain (PHC) theory developed by Prausnitz and coworkers in the late 1970s[320-322] was the first successful application of thermodynamic perturbation theory to polymer systems. Since Wertheim's perturbation theory of polymerization[323] was formulated about 10 years later, PHC theory combines results from hard-sphere equations of simple liquids with the concept of density-dependent external degrees of freedom in the Prigogine-Flory-Patterson model for taking into account the chain character of real polymeric fluids. For the hard-sphere reference equation the result derived by Carnahan and Starling[324] was applied, as this expression is a good approximation for low-molecular hard-sphere fluids. For the attractive perturbation term, a modified Alder's[325] fourth-order perturbation result for square-well fluids was chosen. Its constants were refitted to the thermodynamic equilibrium data of pure methane. The final equation of state reads:

$$\frac{PV}{RT} = 1 + c\frac{4y^2 - 2y}{(y-1)^3} + c\sum_n \sum_m \frac{mA_{nm}}{\tilde{V}^m \tilde{T}^n} \qquad [4.4.94]$$

where:

y	packing fraction with $y = V/(V_0\tau)$ and $\tau = (\pi / 6)2^{0.5} = 0.7405$ (please note that in a number of original papers in the literature the definition of y within this kind of equations is made by the reciprocal value, i.e., $\tau V_0/V$)
c	degree of freedom parameter, related to one chain-molecule (not to one segment)
V_0	hard-sphere volume for closest packing
A_{nm}	empirical coefficients from the attractive perturbation term

The reduced volume is again defined by $\tilde{V} = V/V_0$ and the reduced temperature by $\tilde{T} = T / T^*$. The coefficients A_{nm} are given in the original papers by Beret[320,321] and are considered to be universal constants that do not depend on the chemical nature of any special substance. The remaining three characteristic parameters, c, T* and V_0, have to be adjusted to experimental PVT-data of the polymers or to vapor-liquid equilibrium data of the pure solvents. Instead of fitting the c-parameter, one can also introduce a parameter P* by the relation $P^* = cRT^*/V_0$. In comparison with Flory's free-volume equation of state, PHC-equation of state is additionally applicable to gas and vapor phases. It fulfills the ideal gas limit, and it describes the PVT-behavior at higher pressures better and without the need of temperature and/or pressure-dependent characteristic parameters, such as with Flory's model. Values for characteristic parameters of polymers and solvents can be found in the original literature. A review for the PHC-model was given by Donohue and Vimalchand,[326] where a

number of extensions and applications also are summarized. Application to mixtures and solutions needs mixing rules for the characteristic parameters and introduction of binary fitting parameters[322,327,328] (details are not given here). Examples for applying PHC to polymer solutions are given by Liu and Prausnitz[328] or Iwai, Arai and coworkers.[329-331]

The chain-of-rotators (COR) equation of state was developed by Chao and coworkers[332] as an improvement of the PHC theory. It introduces the non-spherical shape of molecules into the hard-body reference term and describes the chain molecule as a chain of rotators with the aim of an improved model for calculating fluid phase equilibria, PVT and derived thermodynamic properties, at first only for low-molecular substances. Instead of hard spheres, the COR-model uses hard dumbbells as reference fluid by combining the result of Boublik and Nezbeda[333] with the Carnahan-Starling equation for a separate consideration of rotational degrees of freedom; however, still in the sense of Prigogine-Flory-Patterson regarding the chain-character of the molecules. It neglects the effect of rotational motions on intermolecular attractions; however, the attractive portion of the final equation of state has an empirical dependence on rotational degrees of freedom given by the prefactor of the double sum. For the attractive perturbation term, a modified Alder's fourth-order perturbation result for square-well fluids was chosen, additionally improved by an empirical temperature-function for the rotational part. The final COR equation reads:

$$\frac{PV}{RT} = 1 + \frac{4y^2 - 2y}{(y-1)^3} + c\left(\frac{\alpha - 1}{2}\right)\frac{3y^2 + 3\alpha y - (\alpha + 1)}{(y-1)^3}$$

$$+\left(1 + \frac{c}{2}\left\{B_0 + B_1 / \tilde{T} + B_2 \tilde{T}\right\}\right)\sum_n \sum_m \frac{mA_{nm}}{\tilde{V}^m \tilde{T}^n} \qquad [4.4.95]$$

where:

y	packing fraction with $y = V/(V_0\tau)$ and $\tau = (\pi / 6)2^{0.5} = 0.7405$ (please note that in a number of original papers in the literature the definition of y within this kind of equations is made by its reciprocal value, i.e., $\tau V_0/V$)
c	degree of freedom parameter, related to one chain-molecule (not to one segment)
V_0	hard-sphere volume for closest packing
A_{nm}	empirical coefficients from the attractive perturbation term
B_0, B_1, B_2	empirical coefficients for the temperature dependence of the rotational part
α	accounts for the deviations of the dumbbell geometry from a sphere

As can be seen from the structure of the COR equation of state, the Carnahan-Starling term becomes very small with increasing chain length, i.e., with increasing c, and the rotational part is the dominant hard-body term for polymers. The value of c is here a measure of rotational degrees of freedom within the chain (and related to one chain-molecule and not to one segment). It is different from the meaning of the c-value in the PHC equation. Its exact value is not known a priori as chain molecules have a flexible structure. The value of α for the various rotational modes is likewise not precisely known. Since α and c occur together in the product $c(\alpha - 1)$, departure of real rotators from a fixed value of α is compensated for by the c-parameter after any fitting procedure. As usual, the value of α is assigned a constant value of 1.078 calculated according to the dumbbell for ethane as representative for the rotating segments of a hydrocarbon chain. The coefficients A_{nm} and the three parameters B_0,

B_1, B_2 were refitted to the thermodynamic equilibrium data of pure methane, ethane, and propane.[332] Both A_{nm} matrices for PHC and COR equation of state contain different numerical values. The remaining three characteristic parameters, c, T* and V_0, have to be adjusted to experimental equilibrium data. Instead of fitting the c-parameter, one can also introduce a parameter P* by the relation $P^* = cRT^*/V_0$. Characteristic parameters for many solvents and gases are given by Chien et al.[332] or Masuoka and Chao.[334] Characteristic parameters of more than 100 polymers and many solvents are given by Wohlfarth and coworkers,[335-348] who introduced segment-molar mixing rules and group-contribution interaction parameters into the model and applied it extensively to polymer solutions at ordinary pressures as well as at high temperatures und pressures, including gas solubility and supercritical solutions. They found that it may be necessary sometimes to refit the pure-component characteristic data of a polymer to some VLE-data of a binary polymer solution to calculate correct solvent activities, because otherwise demixing was calculated. Refitting is even more necessary when high-pressure fluid phase equilibria have to be calculated using this model.

A group-contribution COR equation of state was developed Pults et al.[349,350] and extended into a polymer COR equation of state by Sy-Siong-Kiao et al.[351] This equation of state is somewhat simplified by replacing the attractive perturbation term by the corresponding part of the Redlich-Kwong equation of state.

$$\frac{PV}{RT} = 1 + \frac{4y^2 - 2y}{(y-1)^3} + c\left(\frac{\alpha - 1}{2}\right)\frac{3y^2 + 3\alpha y - (\alpha + 1)}{(y-1)^3} - \frac{a(T)}{RT[V + b(T)]} \quad [4.4.96]$$

where:

a	attractive van der Waals-like parameter
b	excluded volume van der Waals-like parameter
c	degree of freedom parameter, related to one chain-molecule (not to one segment)
y	packing fraction
α	accounts for the deviations of the dumbbell geometry from a sphere

Exponential temperature functions for the excluded volume parameter b and the attractive parameter a were introduced by Novenario et al.[352-354] to apply this equation of state also to polar and associating fluids. Introducing a group-contribution concept leads to segment-molar values of all parameters a, b, c which can easily be fitted to specific volumes of polymers.[351,354]

The statistical associating fluid theory (SAFT) is the first and the most popular approach that uses real hard-chain reference fluids, including chain-bonding contributions. Its basic ideas have been developed by Chapman et al.[256-258] Without going into details, the final SAFT equation of state is constructed from four terms: a segment term that accounts for the non-ideality of the reference term of non-bonded chain segments/monomers as in the equations shown above, a chain term that accounts for covalent bonding, and an association term that accounts for hydrogen bonding. There may be an additional term that accounts for other polarity effects. A dispersion term is also added that accounts for the perturbing potential, as in the equations above. A comprehensive summary is given in Praunsitz's book.[49] Today, there are different working equations based on the SAFT approach. Their main differences stem from the way the segment and chain terms are estimated. The most common version is the one developed by Huang and Radosz,[355] applying the fourth-order perturbation approach as in COR or PHC above, but with new refitted parameters to argon, as given

by Chen and Kreglewski,[356] and a hard-sphere pair-correlation function for the chain term as following the arguments of Wertheim. The Huang-Radosz-form of the SAFT-equation of state without an association term reads:[355]

$$\frac{PV}{RT} = 1 + r\frac{4y^2 - 2y}{(y-1)^3} + (1-r)\frac{5y-2}{(y-1)(2y-1)} + r\sum_n \sum_m \frac{mD_{nm}}{\tilde{V}^m}\left[\frac{u}{kT}\right]^n \quad [4.4.97]$$

where:

D_{nm}	empirical coefficients from the attractive perturbation term
k	Boltzmann's constant
r	chain segment number

In comparison to the PHC equation of state, the new term between the Carnahan-Starling term and the double sum accounts for chain-bonding. The terms are proportional to the segment number, r , of the chain molecule. However, the hard-sphere volume, V_0, is now a slight function of temperature which is calculated according to the result of Chen and Kreglewski:[356]

$$V_0 = V^{00}\left[1 - 0.12\exp(-3u_0 / kT)\right]^3 \quad [4.4.98]$$

where:

V^{00}	hard-sphere volume at T = 0 K
u_0	well-depth of a square-well potential $u/k = u_0/k\ (1 + 10K/T)$ with 10K being an average for all chain molecules.

The ratio u_0/k or u/k is analogous to the characteristic parameter T* in the equations above. There are two additional volume and energy parameters if association is taken into account. In its essence, the SAFT equation of state needs three pure component parameters which have to be fitted to equilibrium data: V^{00}, u_0/k and r. Fitting of the segment number looks somewhat curious to a polymer scientist, but it is simply a model parameter, like the c-parameter in the equations above, which is also proportional to r. One may note additionally that fitting to specific volume PVT-data leads to a characteristic ratio r/M (which is a specific r-value), as in the equations above, with a specific c-parameter. Several modifications and approximations within the SAFT-framework have been developed in the literature. Banaszak et al.[357-359] or Shukla and Chapman[360] extended the concept to copolymers. Adidharma and Radosz[361] provides an engineering form for such a copolymer SAFT approach. SAFT has successfully applied to correlate thermodynamic properties and phase behavior of pure liquid polymers and polymer solutions, including gas solubility and supercritical solutions by Radosz and coworkers[355,357-359,361-368] Sadowski et al.[369] applied SAFT to calculate solvent activities of polycarbonate solutions in various solvents and found that it may be necessary to refit the pure-component characteristic data of the polymer to some VLE-data of one binary polymer solution to calculate correct solvent activities, because otherwise demixing was calculated. Groß and Sadowski[370] developed a "Perturbed-Chain SAFT" equation of state to improve for the chain behavior within the reference term to get better calculation results for the PVT- and VLE-behavior of polymer systems. McHugh and coworkers applied SAFT extensively to calculate the phase behavior of polymers in supercritical fluids, a comprehensive summary is given in the review by Kirby and McHugh.[371] They also state that characteristic SAFT parameters for polymers from PVT-data lead to

wrong phase equilibrium calculations and, therefore, also to wrong solvent activities from such calculations. Some ways to overcome this situation and to obtain reliable parameters for phase equilibrium calculations are provided in Ref.,[371] together with examples from the literature that will not be repeated here.

The perturbed-hard-sphere-chain (PHSC) equation of state is a hard-sphere-chain theory that is somewhat different to SAFT. It is based on a hard-sphere chain reference system and a van der Waals-type perturbation term using a temperature-dependent attractive parameter a(T) and a temperature-dependent co-volume parameter b(T). Song et al.[259,260] applied it to polymer systems and extended the theory also to fluids consisting of heteronuclear hard chain molecules. The final equation for pure liquids or polymers as derived by Song et al. is constructed from three parts: the first term stems (as in PHC, COR or SAFT) from the Carnahan-Starling hard-sphere monomer fluid, the second is the term due to covalent chain-bonding of the hard-sphere reference chain and the third is a van der Waals-like attraction term (more details are given also in Prausnitz's book[49]):

$$\frac{PV}{RT} = 1 + r\frac{4\eta - 2\eta^2}{(1-\eta)^3} + (1-r)\left\{\frac{(1-\eta/2)}{(1-\eta)^3} - 1\right\} - \frac{r^2 a(T)}{RTV} \qquad [4.4.99]$$

where:

η	reduced density or packing fraction
a	attractive van der Waals-like parameter
r	chain segment number

The reduced density or packing fraction η is related to an effective and temperature-dependent co-volume b(T) by $\eta = r\,b(T)\rho/4$, with ρ being the number density, i.e., the number of molecules per volume. However, PHSC-theory does not use an analytical intermolecular potential to estimate the temperature dependence of a(T) and b(T). Instead, empirical temperature functions are fitted to experimental data of argon and methane (see also[49]).

We note that the PHSC equation of state is again an equation where three parameters have to be fitted to thermodynamic properties: σ, ε/k and r. These may be transformed into macroscopic reducing parameters for the equation of state by the common relations $T^*=\varepsilon/k$, $P^* = 3\varepsilon/2\pi\sigma^3$ and $V^* = 2\pi r\sigma^3/3$. Parameter tables are given in Refs.[86,260,372-374] PHSC was successfully applied to calculate solvent activities in polymer solutions, Gupta and Prausnitz.[86] Lambert et al.[374] found that it is necessary to adjust the characteristic parameters of the polymers when liquid-liquid equilibria should correctly be calculated.

Even with simple cubic equations of state, a quantitative representation of solvent activities for real polymer solutions can be achieved, as was shown by Tassios and coworkers.[375,376] Using generalized van der Waals theory, Sako et al.[377] obtained a three-parameter cubic equation of state which was the first applied to polymer solutions:

$$\frac{PV}{RT} = \frac{V - b + bc}{V - b} - \frac{a(T)}{RT(V+b)} \qquad [4.4.100]$$

where:

a	attractive van der Waals-like parameter
b	excluded volume van der Waals-like parameter

c 3c is the total number of external degrees of freedom per molecule

When c = 1, Equation [4.4.100] reduces to the common Soave-Redlich-Kwong (SRK) equation of state.[378] Temperature functions and combining/mixing rules for parameters a,b,c are not discussed here because quite different approximations may be used. Problems, how to fit these parameters to experimental PVT-data for polymers, have been discussed by several authors.[375-380]

Orbey and Sandler[380] applied the Peng-Robinson equation of state as modified by Stryjek and Vera[381] (PRSV):

$$\frac{PV}{RT} = \frac{V}{V-b} - \frac{a(T)}{RT\left(V^2 + 2bV - b^2\right)} \qquad [4.4.101]$$

to calculate solvent activities in polymer solutions using Wong-Sandler mixing rules[382] that combine the equation of state with excess energy models (EOS/GE-mixing rules). They have shown that a two-parameter version can correlate the solvent partial pressure of various polymer solutions with good accuracy over a range of temperatures and pressures with temperature-independent parameters. Harrismiadis et al.[379] worked out some similarities between activity coefficients derived from van der Waals like equations-of-state and Equations (4.4.92 and 93), i.e., the Elbro-fv model. Zhong and Masuoka[383] combined SRK equation of state with EOS/GE-mixing rules and the UNIFAC model to calculate Henry's constants of solvents and gases in polymers. Additionally, they developed new mixing rules for van der Waals-type two-parameter equations of state (PRSV and SRK) which are particularly suitable for highly asymmetric systems, i.e., also polymer solutions, and demonstrated that only one adjustable temperature-independent parameter is necessary for calculations within a wide range of temperatures.[384] In a following paper,[385] some further modifications and improvements could be found. Orbey et al.[386] successfully proposed some empirical relations for PRSV-equation-of-state parameters with polymer molar mass and specific volume to avoid any special parameter fitting for polymers and introduced a NRTL-like local-composition term into the excess energy part of the mixing rules for taking into account of strong interactions, for example, in water + poly(propylene glycol)s. They found infinite-dilution activity coefficient data, i.e., Henry's constants, to be most suitable for fitting the necessary model parameter.[386]

Orbey et al.[387] summarized three basic conclusions for the application of cubic equations of state to polymer solutions:

(i) These models developed for conventional mixtures can be extended to quantitatively describe VLE of polymer solutions if carefully selected parameters are used for the pure polymer. On the other hand, pure-component parameters of many solvents are already available and VLE between them is well represented by these cubic equations of state.

(ii) EOS/GE-mixing rules represent an accurate way of describing phase equilibria. Activity coefficient expressions are more successful when they are used in this format than directly in the conventional gamma-phi approach.

(iii) It is not justifiable to use multi-parameter models, but it is better to limit the number of parameters to the number of physically meaningful boundary conditions and calculate them according to the relations dictated by these boundary conditions.

4.4.4.3 Comparison and conclusions

The simple Flory-Huggins χ-function, combined with the solubility parameter approach may be used for a first rough guess about solvent activities of polymer solutions, if no experimental data are available. Nothing more should be expected. This also holds true for any calculations with the UNIFAC-fv or other group-contribution models. For a quantitative representation of solvent activities of polymer solutions, more sophisticated models have to be applied. The choice of a dedicated model, however, may depend, even today, on the nature of the polymer-solvent system and its physical properties (polar or non-polar, association or donor-acceptor interactions, subcritical or supercritical solvents, etc.), on the ranges of temperature, pressure and concentration one is interested in, on the question whether a special solution, special mixture, special application is to be handled or a more universal application is to be found or a software tool is to be developed, on numerical simplicity or, on the other hand, on numerical stability and physically meaningful roots of the non-linear equation systems to be solved. Finally, it may depend on the experience of the user (and sometimes it still seems to be a matter of taste).

There are deficiencies in all of these theories given above. These theories fail to account for long-range correlations between polymer segments which are important in dilute solutions. They are valid for simple linear chains and do not account for effects like chain branching, rings, dentritic polymers. But, most seriously, all of these theories are of the mean-field type that fail to account for the contributions of fluctuations in density and composition. Therefore, when these theories are used in the critical region, poor results are often obtained. Usually, critical pressures are overestimated within VLE-calculations. Two other conceptually different mean-field approximations are invoked during the development of these theories. To derive the combinatorial entropic part correlations between segments of one chain that are not nearest neighbors are neglected (again, mean-field approximations are therefore not good for a dilute polymer solution) and, second, chain connectivity and correlation between segments are improperly ignored when calculating the potential energy, the attractive term.

Equation-of-state approaches are preferred concepts for a quantitative representation of polymer solution properties. They are able to correlate experimental VLE data over wide ranges of pressure and temperature and allow for physically meaningful extrapolation of experimental data into unmeasured regions of interest for application. Based on the experience of the author about the application of the COR equation-of-state model to many polymer-solvent systems, it is possible, for example, to measure some vapor pressures at temperatures between 50 and 100°C and concentrations between 50 and 80 wt% polymer by isopiestic sorption together with some infinite dilution data (limiting activity coefficients, Henry's constants) at temperatures between 100 and 200°C by IGC and then to calculate the complete vapor-liquid equilibrium region between room temperature and about 350°C, pressures between 0.1 mbar and 10 bar, and solvent concentration between the common polymer solution of about 75-95 wt% solvent and the ppm-region where the final solvent and/or monomer devolatilization process takes place. Equivalent results can be obtained with any other comparable equation of state model like PHC, SAFT, PHSC, etc.

The quality of all model calculations with respect to solvent activities depends essentially on the careful determination and selection of the parameters of the pure solvents, and also of the pure polymers. Pure solvent parameter must allow for the quantitative calculation of pure solvent vapor pressures and molar volumes, especially when equation-of-state

approaches are used. Pure polymer parameters strongly influence the calculation of gas solubilities, Henry's constants, and limiting solvent activities at infinite dilution of the solvent in the liquid/molten polymer. Additionally, the polymer parameters mainly determine the occurrence of a demixing region in such model calculations. Generally, the quantitative representation of liquid-liquid equilibria is a much more stringent test for any model, what was not discussed here. To calculate such equilibria it is often necessary to use some mixture properties to obtain pure-component polymer parameters. This is necessary because, at present, no single theory is able to describe correctly the properties of a polymer in both the pure molten state and in the highly dilute solution state. Therefore, characteristic polymer parameters from PVT-data of the melt are not always meaningful for the dilute polymer solution. Additionally, characteristic polymer parameters from PVT-data also may lead to wrong results for concentrated polymer solutions because phase equilibrium calculations are much more sensitive to variations in pure component parameters than polymer densities.

All models need some binary interaction parameters that have to be adjusted to some thermodynamic equilibrium properties since these parameters are a priori not known (we will not discuss results from Monte Carlo simulations here). Binary parameters obtained from data of dilute polymer solutions as second virial coefficients are often different from those obtained from concentrated solutions. Distinguishing between intramolecular and intermolecular segment-segment interactions is not as important in concentrated solutions as it is in dilute solutions. Attempts to introduce local-composition and non-random-mixing approaches have been made for all the theories given above with more or less success. At least, they introduce additional parameters. More parameters may cause a higher flexibility of the model equations but leads often to physically senseless parameters that cause troubles when extrapolations may be necessary. Group-contribution concepts for binary interaction parameters in equation of state models can help to correlate parameter sets and also data of solutions within homologous series.

4.4.5 REFERENCES

1 Wen Hao, H. S. Elbro, P. Alessi, **Polymer Solution Data Collection, Pt.1**: **Vapor-Liquid Equilibrium, Pt.2: Solvent Activity Coefficients at Infinite Dilution, Pt. 3: Liquid-Liquid Equilibrium**, *DECHEMA Chemistry Data Series*, Vol. XIV, Pts. 1, 2+3, DECHEMA, Frankfurt/M., 1992.

2 R. P. Danner, M. S. High, **Handbook of Polymer Solution Thermodynamics**, DIPPR, *AIChE*, New York, 1993.

3 Ch. Wohlfarth, **Vapour-liquid equilibrium data of binary polymer solutions, Physical Science Data 44**, **Elsevier**, Amsterdam, 1994.

4 J. Brandrup, E. H. Immergut, E. A. Grulke (eds.), **Polymer Handbook**, 4th ed., *J. Wiley & Sons., Inc*., New York, 1999.

5 N. Schuld, B. A. Wolf, in **Polymer Handbook**, J. Brandrup, E. H. Immergut, E. A. Grulke (eds.), 4th ed., *J. Wiley & Sons., Inc*., New York, 1999, pp. VII/247-264.

6 R. A. Orwoll, in **Polymer Handbook**, J. Brandrup, E. H. Immergut, E. A. Grulke (eds.), 4th ed., *J. Wiley & Sons., Inc*., New York, 1999, pp. VII/649-670.

7 R. A. Orwoll, P. A. Arnold, in **Physical Properties of Polymers Handbook**, J. E. Mark (Ed.), *AIP Press*, Woodbury, New York, 1996, pp. 177-198.

8 R. A. Orwoll, *Rubber Chem. Technol*., **50**, 451 (1977).

9 M. D. Lechner, E. Nordmeier, D. G. Steinmeier, in **Polymer Handbook**, J. Brandrup, E. H. Immergut, E. A. Grulke (eds.), 4th ed., *J. Wiley & Sons*., Inc., New York, 1999, pp. VII/85-213.

10 D. C. Bonner, *J. Macromol. Sci. - Revs. Macromol. Chem., C*, **13**, 263 (1975).

11 A. F. M. Barton, **CRC Handbook of Polymer-Liquid Interaction Parameters and Solubility Parameters**, *CRC Press*, Boca Raton, 1990.

12 A. F. M. Barton, **CRC Handbook of Solubility Parameters and Other Cohesion Parameters**, 2nd Ed., *CRC Press*, Boca Raton, 1991.
13 J.-M. Braun, J. E. Guillet, *Adv. Polym. Sci.*, **21**, 108 (1976).
14 A. E. Nesterov, J. S. Lipatov, **Obrashchennaya Gasovaya Khromatografiya v Termodinamike Polimerov**, *Naukova Dumka*, Kiev, 1976.
15 D. C. Locke, *Adv. Chromatogr.*, **14**, 87 (1976).
16 D. G. Gray, *Progr. Polym. Sci.*, **5**, 1 (1977).
17 J. E. G. Lipson, J. E. Guillet, *Developm. Polym. Character*., **3**, 33 (1982).
18 J. S. Aspler, *Chromatogr. Sci.*, **29**, 399 (1985).
19 A. E. Nesterov, **Obrashchennaya Gasovaya Khromatografiya Polimerov**, *Naukova Dumka*, Kiev, 1988.
20 R. Vilcu, M. Leca, **Polymer Thermodynamics by Gas Chromatography**, *Elsevier*, Amsterdam, 1989.
21 G. J. Price, *Adv. Chromatogr.*, **28**, 113 (1989).
22 D. R. Lloyd, T. C. Ward, H. P. Schreiber, C. C. Pizana (eds.), **Inverse Gas Chromatography**, *ACS Symp. Ser., 391*, 1989.
23 P. Munk, in **Modern Methods of Polymer Characterization**, H. G. Barth, J. W. Mays (eds.), *J. Wiley & Sons, Inc.*, New York, 1991, pp.151-200.
24 Bincai Li, *Rubber Chem. Technol*., **69**, 347 (1996).
25 Z. Y. Al-Saigh, *Int. J. Polym. Anal. Charact*. **3**, 249 (1997).
26 R. A. Pethrick, J. V. Dawkins (Eds.), **Modern Techniques for Polymer Characterization**, *J. Wiley & Sons, Inc.*, Chichester, 1999.
27 G. D. Wignall, in **Encyclopedia of Polymer Science and Engineering**, 2nd Ed., J. Kroschwitz (Ed.), *J. Wiley & Sons, Inc.*, New York, 1987, Vol. 10, pp. 112-184.
28 G. C. Berry, in **Encyclopedia of Polymer Science and Engineering**, 2nd Ed., J. Kroschwitz (Ed.), *J. Wiley & Sons, Inc*., New York, 1987, Vol. 8, pp. 721-794.
29 M. B. Huglin (Ed.), **Light Scattering from Polymer Solutions**, *Academic Press*, Inc., New York, 1972.
30 E. F. Casassa, G. C. Berry, in **Polymer Molecular Weights**, Pt. 1, *Marcel Dekker*, Inc., New York, 1975, pp. 161-286.
31 P. Kratochvil, **Classical Light Scattering from Polymer Solutions**, *Elsevier*, Amsterdam, 1987.
32 B. Chu, **Laser Light Scattering**, *Academic Press*, Inc., New York, 1991.
33 A. R. Cooper, in **Encyclopedia of Polymer Science and Engineering**, 2nd Ed., J. Kroschwitz (Ed.), *J. Wiley & Sons, Inc*., New York, 1987, Vol. 10, pp. 1-19.
34 C. A. Glover, in **Polymer Molecular Weights, Pt. 1**, *Marcel Dekker, Inc.*, New York, 1975, pp. 79-159.
35 H. Fujita, **Foundations of Ultracentrifugal Analysis**, *J.Wiley & Sons, Inc.*, New York, 1975.
36 S. E. Harding, A. J. Rowe, J. C. Horton, **Analytical Ultracentrifugation in Biochemistry and Polymer Science**, *Royal Society of Chemistry*, Cambridge, 1992.
37 P. Munk, in **Modern Methods of Polymer Characterization**, H. G. Barth, J. W. Mays (eds.), *J. Wiley & Sons, Inc.*, New York, 1991, pp. 271-312.
38 E.T.Adams, in **Encyclopedia of Polymer Science and Engineering**, 2nd Ed., J. Kroschwitz (Ed.), *J. Wiley & Sons, Inc*., New York, 1987, Vol. 10, pp. 636-652.
39 M. P. Tombs, A. R. Peacock, **The Osmotic Pressure of Macromolecules**, *Oxford University Press*, London, 1974.
40 J. W. Mays, N. Hadjichristidis, in **Modern Methods of Polymer Characterization**, H. G. Barth, J. W. Mays (eds.), *J.Wiley & Sons, Inc.*, New York, 1991, pp. 201-226.
41 H. Fujita, **Polymer Solutions**, *Elsevier*, Amsterdam, 1990.
42 K. Kamide, **Thermodynamics of Polymer Solutions**, *Elsevier*, Amsterdam, 1990
43 Y. Einaga, *Progr. Polym. Sci.*, **19**, 1 (1994).
44 R. Koningsveld, *Adv. Colloid Interfacial Sci*., **2**, 151 (1968).
45 B. A. Wolf, *Adv. Polym. Sci.*, **10**, 109 (1972).
46 P. J. Flory, **Principles of Polymer Chemistry**, *Cornell University Press*, Ithaca, 1953.
47 M. L. Huggins, **Physical Chemistry of High Polymers**, *J.Wiley & Sons., Inc*., New York, 1958.
48 H. Tompa, **Polymer Solutions**, *Butterworth*, London, 1956.
49 J. M. Prausnitz, R. N. Lichtenthaler, E. G. de Azevedo, **Molecular Thermodynamics of Fluid Phase Equilibria**, 3rd Ed., *Prentice Hall*, Upper Saddle River, New Jersey, 1999.
50 R. M. Masegosa, M. G. Prolongo, A. Horta, *Macromolecules*, **19**, 1478 (1986).
51 R. Koningsveld, L. A. Kleintjens, *Macromolecules*, **4**, 637 (1971).
52 M. T. Raetzsch, H. Kehlen, in **Encyclopedia of Polymer Science and Engineering**, 2nd Ed., J. Kroschwitz (Ed.), *J. Wiley & Sons, Inc*., New York, 1989, Vol. 15, pp. 481-491.

53 M. T. Raetzsch, H. Kehlen, *Progr. Polym. Sci.*, **14**, 1 (1989).
54 M. T. Raetzsch, Ch. Wohlfarth, *Adv. Polym. Sci*., **98**, 49 (1990).
55 A. G. Williamson, in **Experimental Thermodynamics, Vol.II, Experimental Thermodynamics of non-reacting Fluids**, B. Le Neindre, B. Vodar (eds.), *Butterworth*, London, pp. 749-786.
56 K. Schmoll, E. Jenckel, *Ber. Bunsenges. Phys. Chem*., **60**, 756 (1956).
57 K. Schotsch, B. A. Wolf, *Makromol. Chem*., **185**, 2161 (1984).
58 E. Killmann, F. Cordt, F. Moeller, *Makromol. Chem.,* **191**, 2929 (1990).
59 J. H. Baxendale, E. V. Enustun, J. Stern, *Phil. Trans. Roy. Soc. London*, *A*, **243**, 169 (1951).
60 M. L. McGlashan, A. G. Williamson, *Trans. Faraday Soc*., **57**, 588 (1961).
61 M. L. McGlashan, K. W. Morcom, A. G. Williamson, *Trans. Faraday Soc*., **57**, 581, (1961).
62 H. Takenaka, *J. Polym. Sci*., **24**, 321 (1957).
63 R. J. Kokes, A. R. Dipietro, F. A. Long, *J. Amer. Chem. Soc.*, **75**, 6319 (1953).
64 P. W. Allen, D. H. Everett, M. F. Penney, *Proc. Roy. Soc. London A*, **212**, 149 (1952).
65 D. H. Everett, M. F. Penney, *Proc. Roy. Soc. London A*, **212**, 164 (1952).
66 C. A. Haynes, R. A. Beynon, R. S. King, H. W. Blanch, J. M. Praunsitz, *J. Phys. Chem.*, **93**, 5612 (1989).
67 W. R. Krigbaum, D. O. Geymer, *J. Amer. Chem. Soc*., **81**, 1859 (1959).
68 M. L. Lakhanpal, B. E. Conway, *J. Polym. Sci.*, **46**, 75 (1960).
69 K. Ueberreiter, W. Bruns, *Ber. Bunsenges. Phys. Chemie*, **68**, 541 (1964).
70 R. S. Jessup, *J. Res. Natl. Bur. Stand.*, **60**, 47 (1958).
71 Van Tam Bui, J. Leonard, *Polym. J.*, **21**, 185 (1989).
72 C. E. H. Bawn, R. F. J. Freeman, A. R. Kamaliddin, *Trans. Faraday Soc.*, **46**, 677 (1950).
73 G. Gee, L. R. J. Treloar, *Trans. Faraday Soc*., **38**, 147 (1942).
74 C. Booth, G. Gee, G. Holden, G. R. Williamson, *Polymer*, **5**, 343 (1964).
75 G. N. Malcolm, C. E. Baird, G. R. Bruce, K. G. Cheyne, R. W. Kershaw, M. C. Pratt, *J. Polym. Sci., Pt. A-2*, **7**, 1495 (1969).
76 L.R. Ochs, M. Kabri-Badr, H. Cabezas, *AIChE-J*., **36**, 1908 (1990).
77 C. Grossmann, R. Tintinger, G. Maurer, *Fluid Phase Equil.*, **106**, 111 (1995).
78 Z. Adamcova, *Sci. Pap. Prag. Inst. Chem. Technol.*, **N2**, 63 (1976).
79 Z. Adamcova, *Adv. Chem.*, **155**, 361 (1976).
80 K. Kubo, K. Ogino, *Polymer*, **16**, 629 (1975).
81 C. G. Panayiotou, J. H. Vera, *Polym. J.*, **16**, 89 (1984).
82 M. T. Raetzsch, G. Illig, Ch. Wohlfarth, *Acta Polymerica,* **33**, 89 (1982).
83 P. J. T. Tait, A. M. Abushihada, *Polymer*, **18**, 810 (1977).
84 J. H. Van der Waals, J. J. Hermans, *Rec. Trav. Chim. Pays-Bas*, **69**, 971 (1950).
85 D. C. Bonner, J. M. Prausnitz, *J. Polym. Sci., Polym. Phys. Ed.*, **12**, 51 (1974).
86 R. B. Gupta, J. M. Prausnitz, *J. Chem. Eng. Data*, **40**, 784 (1995).
87 S. Behme, G. Sadowski, W. Arlt, *Chem.-Ing.-Techn*., **67**, 757 (1995).
88 A. J. Ashworth, D. H. Everett, *Trans. Faraday Soc*., **56**, 1609 (1960)
89 J. S. Vrentas, J. L. Duda, S. T. Hsieh, *Ind. Eng. Chem., Process Des. Dev*., **22**, 326 (1983).
90 Y. Iwai, Y. Arai, *J. Chem. Eng. Japan*, **22**, 155 (1989).
91 J. W. McBain, A. M. Bakr, *J. Amer. Chem. Soc*., **48**, 690 (1926).
92 S. Hwang, J. Kim, K.-P. Yoo, *J. Chem. Eng. Data*, **43**, 614 (1998).
93 J. Kim, K. C. Joung, S. Hwang, W. Huh, C. S. Lee, K.-P. Yoo, *Korean J. Chem. Eng.*, **15**, 199 (1998).
94 Y. C. Bae, J. J. Shim, D. S. Soane, J. M. Prausnitz, *J. Appl. Polym. Sci.,* **47**, 1193 (1993).
95 A. J. Ashworth, *J. Chem. Soc., Faraday Trans. I*, **69**, 459 (1973).
96 A. J. Ashworth, G. J. Price, *Thermochim. Acta*, **82**, 161 (1984).
97 S. Saeki, J. C. Holste, D. C. Bonner, *J. Polym. Sci., Polym. Phys. Ed.,* **20**, 793, 805 (1982).
98 S. Saeki, J. C. Holste, D. C. Bonner, *J. Polym. Sci., Polym. Phys. Ed*., **19**, 307 (1981).
99 S. Saeki, J. Holste, D. C. Bonner, *J. Polym. Sci., Polym. Phys. Ed*., **21**, 2049 (1983)
100 H. C. Wong, S. W. Campbell, V. R. Bhetnanabotla, *Fluid Phase Equil*., **139**, 371 (1997).
101 S. P. V. N. Mikkilineni, D.A. Tree, M. S. High, *J. Chem. Eng. Data*, **40**, 750 (1995).
102 O. Smidsrod, J. E. Guillet, *Macromolecules*, **2**, 272 (1969).
103 Z. Y. Al-Saigh, P. Munk, *Macromolecules*, **17**, 803 (1984).
104 P. Munk, P. Hattam, Q. Du, *J. Appl. Polym. Sci., Appl. Polym. Symp.*, **43**, 373 (1989).
105 D. Glindemann, Dissertation, TH Leuna-Merseburg, 1979.
106 N. F. Brockmeier, R. W. McCoy, J. A. Meyer, *Macromolecules*, **5**, 130, 464 (1972).
107 N. F. Brockmeier, R. E. Carlson, R. W. McCoy, *AIChE-J*., **19**, 1133 (1973).
108 J. R. Conder, J. R. Purnell, *Trans. Faraday Soc*., **64**, 1505, 3100 (1968).

109 J. R. Conder, J. R. Purnell, *Trans. Faraday Soc*., **65**, 824, 839 (1969).
110 G. J. Price, J. E. Guillet, *J. Macromol. Sci.-Chem.*, **A23**, 1487 (1986).
111 D. C. Bonner, N. F. Brockmeier, *Ind. Eng. Chem., Process Des. Developm.*, **16**, 180 (1977).
112 S. Dincer, D. C. Bonner, R. A. Elefritz, *Ind. Eng. Chem., Fundam*., **18**, 54 (1979).
113 W. A. Ruff, C. J. Glover, A. T. Watson, *AIChE-J*., **32**, 1948, 1954 (1986).
114 L. L. Joffrion, C. J. Glover, *Macromolecules*, **19**, 1710 (1986).
115 T. K. Tsotsis, C. Turchi, C. J. Glover, *Macromolecules*, **20**, 2445 (1987).
116 R. P. Danner, F. Tihminlioglu, R. K. Surana, J. L. Duda, *Fluid Phase Equil*., **148**, 171 (1998).
117 J. R. Conder, C. L. Young, **Physicochemical Measurements by Gas Chromatography,** *J.Wiley & Sons, Inc*., New York, 1979.
118 C. Barth, R. Horst, B. A. Wolf, *J. Chem. Thermodyn*., **30**, 641 (1998).
119 H.-M. Petri, N. Schuld, B. A. Wolf, *Macromolecules*, **28**, 4975 (1995).
120 B. Kolb, L. S. Ettre, **Static Headspace Gas Chromatography - Theory and Practice**, *Wiley-VCH*, Weinheim 1997.
121 H. Wang, K. Wang, H. Liu, Y. Hu, *J. East China Univ. Sci. Technol*., **23**, 614 (1997).
122 T. Katayama, K. Matsumura, Y. Urahama, *Kagaku Kogaku*, **35**, 1012 (1971).
123 K. Matsumura, T. Katayama, *Kagaku Kogaku*, **38**, 388 (1974).
124 A. V. Hill, *Proc. Roy. Soc. London, Ser. A*, **127**, 9 (1930).
125 E. Regener, Ch. Wohlfarth, *Wiss. Zeitschr. TH Leuna-Merseburg*, **30**, 211 (1988).
126 J. Gaube, A. Pfennig, M. Stumpf, *J.Chem. Eng. Data,* **38**, 163 (1993).
127 J. Gaube, A. Pfennig, M. Stumpf, *Fluid Phase Equil*., **83**, 365 (1993).
128 A. Eliassi, H. Modarress, G. A. Mansoori, *J. Chem. Eng. Data,* **35**, 52 (1999).
129 V. Majer, V. Svoboda, **Enthalpies of Vaporization of Organic Compounds**, *Blackwell Sci. Publ*., Oxford, 1985.
130 T. E. Daubert, R. P. Danner, **Physical and Thermodynamic Properties of Pure Chemicals. Data Compilation**, *Hemisphere Publ.Corp.*, New York, 1989 and several Supplements up to 1999, data are online available from DIPPR database.
131 B. H. Bersted, *J. Appl. Polym. Sci.*, **17**, 1415 (1973).
132 B. H. Bersted, *J. Appl. Polym. Sci.*, **18**, 2399 (1974).
133 R. V. Figini, *Makromol. Chem.*, **181**, 2049 (1980).
134 R. V. Figini, M. Marx-Figini, *Makromol. Chem.*, **182**, 437 (1980).
135 M. Marx-Figini, R. V. Figini, *Makromol. Chem.*, **181**, 2401 (1980).
136 P. J. T. Tait, A. M. Abushihada, *Polymer*, **18**, 810 (1977).
137 A. J. Ashworth, C.-F. Chien, D. L. Furio, D. M. Hooker, M. M. Kopecni, R. J. Laub, G. J. Price, *Macromolecules*, **17**, 1090 (1984).
138 R. N. Lichtenthaler, D. D. Liu, J. M. Prausnitz, *Macromolecules*, **7**, 565 (1974).
139 I. Noda, N. Kato, T. Kitano, M. Nagasawa, *Macromolecules*, **14**, 668 (1981).
140 H. Vink, Europ. *Polym. J.*, **7**, 1411 (1971) and **10**, 149 (1974).
141 A. Nakajima, F. Hamada, K. Yasue, K. Fujisawa, T. Shiomi, *Makromol. Chem.*, **175**, 197 (1974).
142 B. E. Eichinger, P. J. Flory, *Trans. Faraday Soc*., **64**, 2035, 2053, 2061, 2066 (1968).
143 H. Hoecker, P. J. Flory, *Trans. Faraday Soc.*, **67**, 2270 (1971).
144 P. J. Flory, H. Daoust, *J. Polym. Sci.*, **25**, 429 (1957).
145 B. H. Zimm, I. Myerson, *J. Amer. Chem. Soc.*, **68**, 911 (1946).
146 W. H. Stockmayer, E. F. Casassa, *J. Chem. Phys.*, **20**, 1560 (1952).
147 G. Strobl, **The Physics of Polymers**, *Springer Vlg*., Berlin, 1996.
148 B. H. Zimm, *J. Chem. Phys.*, **16**, 1093 (1948).
149 B. A. Wolf, H.-J. Adams, *J. Chem. Phys*., **75**, 4121 (1981).
150 M. Lechner, G. V. Schulz, Europ. *Polym. J.*, **6**, 945 (1970).
151 Y. Nakamura, T. Norisuye, A. Teramoto, *J. Polym. Sci., Polym. Phys. Ed.*, **29**, 153 (1991).
152 Th. G. Scholte, *Eur. Polym. J.*, **6**, 1063 (1970).
153 H. Hasse, H.-P. Kany, R. Tintinger, G. Maurer, *Macromolecules*, **28**, 3540 (1995).
154 H.-P. Kany, H. Hasse, G. Maurer, *J. Chem. Eng. Data*, **35**, 230 (1999).
155 Th. G. Scholte, *J. Polym. Sci., Pt. A-2*, **9**, 1553 (1971).
156 Th. G. Scholte, *J. Polym. Sci., Pt. C*, **39**, 281 (1972).
157 K. W. Derham, J. Goldsborough, M. Gordon, *Pure Appl. Chem.*, **38**, 97 (1974).
158 M. Gordon, P. Irvine, J. W. Kennedy, *J. Polym. Sci., Pt. C*, **61**, 199 (1977).
159 M. Gordon, *NATO ASI Ser., Ser. E,* **89**, 429 (1985).

160 H. Galina, M. Gordon, B. W. Ready, L. A. Kleintjens, in **Polymer Solutions**, W. C. Forsman (Ed.), *Plenum Press*, New York, 1986, pp. 267-298.
161 A. Guinier, G. Fournet, **Small Angle Scattering of X-rays**, *J.Wiley & Sons, Inc.*, New York, 1955.
162 S. H. Chen, S. Yip (eds.), **Spectroscopy in Biology and Chemistry**, **Neutron, X-ray and Laser**, *Academic Press*, New York, 1974.
163 O. Glatter, O. Kratky (eds.), **Small-Angle X-ray Scattering**, *Academic Press*, London, 1982.
164 R. G. Kirste, W. Wunderlich, *Z. Phys. Chem. N.F.*, **58**, 133 (1968).
165 R. G. Kirste, G. Wild, *Makromol.Chem.*, **121**, 174 (1969).
166 G. Meyerhoff, U. Moritz, R. G. Kirste, W. Heitz, *Europ. Polym. J.*, **7**, 933 (1971).
167 K. Okano, T. Ichimura, K. Kurita, E. Wada, *Polymer*, **28**, 693 (1987).
168 T. Ichimura, K. Okano, K. Kurita, E. Wada, *Polymer*, **28**, 1573 (1987).
169 M. Takada, K. Okano, K. Kurita, *Polym. J.*, **26**, 113 (1994).
170 F. Horkay, A.-M. Hecht, H. B. Stanley, E. Geissler, *Eur. Polym. J.*, **30**, 215 (1994).
171 J. S. Higgins, A. Macconachie, in **Polymer Solutions**, W. C. Forsman (Ed.), *Plenum Press*, New York, 1986, pp. 183-238.
172 B. Hammouda, *Adv. Polym. Sci.*, **106**, 87 (1993).
173 N. Vennemann, M. D. Lechner, R. C. Oberthuer, *Polymer*, **28**, 1738 (1987).
174 A. M. Pedley, J. S. Higgins, D. G. Pfeiffer, A. R. Rennie, *Macromolecules*, **23**, 2492 (1990).
175 B. J. Berne, R. Pecora, **Dynamic Light Scattering**, *J.Wiley & Sons, Inc*., New York, 1976.
176 Th. G. Scholte, *J. Polym. Sci., Pt. A-2*, **8**, 841 (1970).
177 B. J. Rietveld, Th. G. Scholte, J. P. L. Pijpers, *Brit. Polym. J.*, **4**, 109 (1972).
178 H.-G. Elias, H. Lys, *Makromol.Chem*., **92**, 1 (1966).
179 T. Hirao, A. Teramoto, T. Sato, T. Norisuye, T. Masuda, T. Higashimura, *Polym. J.*, **23**, 925 (1991).
180 Y. Doucet, in **Experimental Thermodynamics, Vol.II, Experimental Thermodynamics of non-reacting Fluids,** B. Le Neindre, B. Vodar (eds.), *Butterworth*, London, pp. 835-900.
181 T. Kawai, *J. Polym. Sci.*, **32**, 425 (1958).
182 Y. Hoei, Y. Ikeda, M. Sasaki, *J. Phys. Chem. B*, **103**, 5353 (1999).
183 R. Koningsveld, in **Polymer Science**, E. D. Jenkins (Ed.), *North-Holland Publ.Comp*., Amsterdam, 1972, pp. 1047-1134.
184 A. Imre, W. A. Van Hook, *J. Polym. Sci., Pt. B, Polym. Sci.*, **34**, 751 (1996) and *J. Phys. Chem. Ref. Data*, **25**, 637 (1996).
185 O. Pfohl, T. Hino, J. M. Prausnitz, *Polymer*, **36**, 2065 (1995).
186 N. Kuwahara, D. V. Fenby, M. Tamsuy, B. Chu: *J. Chem. Phys.*, **55**, 1140 (1971).
187 R. Koningsveld, A. J. Staverman, *J. Polym. Sci., Pt. A-2*, **6**, 349 (1968).
188 B. A. Wolf, M. C. Sezen, *Macromolecules*, **10**, 1010 (1977).
189 G. F. Alfrey, W. G. Schneider, *Discuss. Faraday Soc.*, **15**, 218 (1953).
190 S. C. Greer, D. T. Jacobs, *J. Phys. Chem.*, **84**, 2888 (1980).
191 D. T. Jacobs, S. C. Greer, *Phys. Rev. A*, **24**, 2075 (1981).
192 B. Muessig, H. Wochnowski, *Angew. Makromol. Chem.*, **104**, 203 (1982).
193 G. D. Rehage, D. Moeller, D. Ernst, *Makromol. Chem.,* **88**, 232 (1965).
194 Th. G. Scholte, R. Koningsveld, *Kolloid Z. Z. Polym.*, **218**, 58 (1968).
195 B. J. Rietfeld, *Brit. Polym. J*., **6**, 181 (1974).
196 M. Gordon, L. A. Kleintjens, B. W. Ready, J. A. Torkington, *Brit. Polym. J*., **10**, 170 (1978).
197 R. Koningsveld, L. A. Kleintjens, M. H. Onclin, *J. Macromol. Sci. Phys. B*, **18**, 357 (1980).
198 P. G. de Gennes, **Scaling Concepts in Polymer Physics**, *Cornell Univ. Press*, Ithaca, 1979.
199 R. Koningsveld, A. J. Staverman, *J. Polym. Sci., Pt. A-2,* **6**, 325 (1968).
200 B. A. Wolf, *Makromol. Chem.*, **128**, 284 (1969).
201 L. R. G. Treloar, **The Physics of Rubber Elasticity**, 3rd Ed., *Clarendon Press*, Oxford, 1975.
202 K. Dusek, W. Prins, *Adv. Polym. Sci.*, **6**, 1 (1969).
203 G. Heinrich, E. Straube, G. Helmis, *Adv. Polym. Sci.*, **84**, 33 (1988).
204 K. Dusek (Ed.), Responsive Gels I and II, *Adv. Polym. Sci.*, **109** and **110** (1996).
205 G. Rehage, *Ber. Bunsenges. Phys. Chem*., **81**, 969 (1977).
206 K. F. Arndt, J. Schreck, *Acta Polymerica*, **36**, 56 (1985), **37**, 500 (1986).
207 K. F. Arndt, I. Hahn, *Acta Polymerica*, **39**, 560 (1988).
208 R. Sanetra, B. N. Kolarz, A. Wlochowicz, *Polimery*, **34**, 490 (1989).
209 D. G. Gray, J. E. Guillet, *Macromolecules*, **5**, 316 (1972).
210 M. Galin, *Macromolecules*, **10**, 1239 (1977).
211 A. M. Rijke, W. Prins, *J. Polym. Sci.*, **59**, 171 (1962).

212 J. Schwarz, W. Borchard, G. Rehage, *Kolloid-Z. Z. Polym*., **244**, 193 (1971).
213 B. J. Teitelbaum, A. E. Garwin, *Vysokomol. Soedin., Ser. A*, **10**, 1684 (1968).
214 J. J. Hermans, *J. Polym. Sci.*, **59**, 191 (1962).
215 H. M. James, E. Guth, *J. Chem. Phys*., **21**, 1039 (1953).
216 S. F. Edwards, E. K. Freed, *J. Phys. C*, **3**, 739, 750 (1970).
217 G. Rehage, *Kolloid-Z. Z. Polym.*, **199**, 1 (1964).
218 W. Borchard, Dissertation, RWTH Aachen, 1966.
219 W. Borchard, Progr. *Colloid Polym. Sci.*, **57**, 39 (1975).
220 W. Borchard, Progr. *Colloid Polym. Sci.*, **86**, 84 (1991).
221 W. Borchard, H. Coelfen, *Makromol. Chem., Macromol. Symp.*, **61**, 143 (1992).
222 H. Yamakawa, **Modern Theory of Polymer Solutions**, *Harper & Row*, New York, 1971.
223 J. A. Barker, *J. Chem. Phys*., **20**, 1256 (1952).
224 H. Tompa, T*rans. Faraday Soc*., **48**, 363 (1952).
225 R. N. Lichtenthaler, D. S. Abrams, J. M. Prausnitz, *Can. J. Chem*., **53**, 3071 (1973).
226 E. A. Guggenheim, *Proc. Roy. Soc. London, A,* **183**, 203 (1944).
227 E. A. Guggenheim, **Mixtures**, *Clarendon Press*, Oxford, 1952.
228 A. J. Staverman, *Recl. Trav. Chim. Pays-Bas*, **69**, 163 (1950).
229 S. G. Sayegh, J. H. Vera, *Chem. Eng. J.*, **19**, 1 (1980).
230 K. F. Freed, *J. Phys. A, Math. Gen.*, **18**, 871 (1985).
231 M. G. Bawendi, K. F. Freed, *J. Chem. Phys*., **87**, 5534 (1987), **88**, 2741 (1988).
232 W. G. Madden, A. I. Pesci, K. F. Freed, *Macromolecules*, **23**, 1181 (1990).
233 G. Scatchard, *Chem. Rev*., **44**, 7 (1949).
234 J. H. Hildebrand, R. L. Scott, **The Solubility of Nonelectrolytes**, 3rd Ed., *Reinhold Publ. Corp*., New York, 1950.
235 D. W. Van Krevelen, **Properties of Polymers**, 3rd Ed., *Elsevier*, Amsterdam, 1990.
236 P. J. Flory, R. A. Orwoll, A. Vrij, *J. Amer. Chem. Soc*., **86**, 3507, 3515 (1964).
237 P. J. Flory, *J. Amer. Chem. Soc*., **87**, 1833 (1965).
238 P. J. Flory, R. A. Orwoll, *J. Amer. Chem. Soc*., **89**, 6814, 6822 (1964).
239 P. J. Flory, *Discuss. Faraday Soc*., **49**, 7 (1970).
240 P. I. Freeman, J. S. Rowlinson, *Polymer*, **1**, 20 (1960).
241 A. H. Liddell, F. L. Swinton, *Discuss. Faraday Soc*., **49**, 215 (1970).
242 I. Prigogine, **The Molecular Theory of Solutions**, *North-Holland Publ*., Amsterdam, 1957.
243 D. Patterson, *Macromolecules*, **2**, 672 (1969).
244 D. Patterson, G. Delmas, *Discuss. Faraday Soc.*, **49**, 98 (1970).
245 R. Simha, T. Somcynsky, *Macromolecules*, **2**, 342 (1969).
246 I. C. Sanchez, R. H. Lacombe, *J. Phys. Chem.*, **80**, 2352, 2568 (1976).
247 I. C. Sanchez, R. H. Lacombe, *J. Polym. Sci., Polym. Lett. Ed.*, **15**, 71 (1977).
248 I. C. Sanchez, R. H. Lacombe, *Macromolecules*, **11**, 1145 (1978).
249 G. T. Dee, D. J. Walsh, *Macromolecules*, **21**, 811, 815 (1988).
250 M. D. Donohue, J. M. Prausnitz, *AIChE-J*., **24**, 849 (1978).
251 C. H. Chien, R. A. Greenkorn, K. C. Chao, *AIChE-J*. **29**, 560 (1983).
252 K. G. Honnell, C. K. Hall, *J. Chem. Phys*., **90**, 1841 (1989).
253 H. S. Gulati, J. M. Wichert, C. K. Hall, *J. Chem. Phys.*, **104**, 5220 (1996).
254 H. S. Gulati, C. K. Hall, *J. Chem. Phys.*, **108**, 5220 (1998).
255 A. Yethiraj, C. K. Hall, *J. Chem. Phys.*, **95**, 1999 (1991).
256 W. G. Chapman, G. Jackson, K. E. Gubbins, *Mol. Phys.*, **65**, 1057 (1988).
257 W. G. Chapman, K. E. Gubbins, G. Jackson, M. Radosz, *Fluid Phase Equil.*, **52**, 31 (1989).
258 W. G. Chapman, K. E. Gubbins, G. Jackson, M. Radosz, *Ind. Eng. Chem. Res.*, **29**, 1709 (1990).
259 Y. Song, S. M. Lambert, J. M. Prausnitz, *Macromolecules*, **27**, 441 (1994).
260 Y. Song, S. M. Lambert, J. M. Prausnitz, *Ind. Eng. Chem. Res.*, **33**, 1047 (1994).
261 S. M. Lambert, Y. Song, J. M. Prausnitz, in **Equations of State for Fluids and Fluid Mixtures**, J. V. Sengers et al. (eds.), *Elsevier*, Amsterdam, 2000, in press.
262 P. A. Rodgers, *J. Appl. Polym. Sci.*, **48**, 1061 (1993).
263 J. Cho, I. C. Sanchez, in **Polymer Handbook**, J. Brandrup, E. H. Immergut, E. A. Grulke (eds.), 4th ed., *J. Wiley & Sons*., Inc., New York, 1999, pp. VI/591-601.
264 A. Bondi, **Physical Properties of Molecular Crystals, Liquids and Glasses**, *John Wiley & Sons*, New York, 1968.
265 D. C. Bonner, J. M. Prausnitz, *AIChE-J*., **19**, 943 (1973).

266 M. T. Raetzsch, M. Opel, Ch. Wohlfarth, *Acta Polymerica,* **31**, 217 (1980).
267 K. Sugamiya, *Makromol. Chem*., **178**, 565 (1977).
268 U. Brandani, *Macromolecules*, **12**, 883 (1979).
269 H.-W. Kammer, T. Inoue, T. Ougizawa, *Polymer*, **30**, 888 (1989).
270 T. Shiomi, K. Fujisawa, F. Hamada, A. Nakajima, *J. Chem. Soc. Faraday Trans II*, **76**, 895 (1980).
271 F. Hamada, T. Shiomi, K. Fujisawa, A. Nakajima, *Macromolecules*, **13**, 279 (1980).
272 C. G. Panayiotou, *J. Chem. Soc. Faraday Trans. II*, **80**, 1435 (1984).
273 Y. L. Cheng, D. C. Bonner, *J. Polym. Sci., Polym. Phys. Ed.*, **15**, 593 (1977), **16**, 319 (1978).
274 J. Pouchly, D. Patterson, *Macromolecules*, **9**, 574 (1976).
275 I. C. Sanchez, C. G. Panayiotou, in **Models for Thermodynamics and Phase Equilibrium Calculations**, S. I. Sandler (Ed.), *Marcel Dekker*, New York, 1994, pp. 187-285.
276 C. G. Panayiotou, *Makromol. Chem.*, **187**, 2867 (1986).
277 C. G. Panayiotou, J. H. Vera, *Polym. J.*, **14**, 681 (1982).
278 C. G. Panayiotou, J. H. Vera, *Can. J. Chem. Eng*., **59**, 501 (1981).
279 C. G. Panayiotou, *Macromolecules*, **20**, 861 (1987).
280 I. C. Sanchez, P. A. Rodgers, *Pure Appl. Chem.*, **62**, 2107 (1990).
281 E. Nies, A. Stroeks, *Macromolecules*, **23**, 4088, 4092 (1990).
282 H. Xie, E. Nies, *Macromolecules*, **26**, 1689 (1993).
283 H. Xie, R. Simha, *Polym. Int.*, **44**, 348 (1997).
284 A. Fredenslund, J. Gmehling, P. Rasmussen, **Vapor-Liquid Equilibria Using UNIFAC**, *Elsevier Sci. Publ*., New York, 1977.
285 T. Oishi, J. M. Prausnitz, *Ind. Eng. Chem. Process Des. Dev.,* **17**, 333 (1978).
286 S. Skjold-Jorgensen, B. Kolbe, J. Gmehling, P. Rasmussen, *Ind. Eng. Chem. Process Des. Dev.*, **18**, 714 (1979).
287 J. Gmehling, P. Rasmussen, A. Fredenslund, *Ind. Eng. Chem. Process Des. Dev*., **21**, 118 (1982).
288 E. A. Macedo, U. Weidlich, J. Gmehling, P. Rasmussen, *Ind. Eng. Chem. Process Des. Dev*., **22**, 676 (1983).
289 D. Tiegs, J. Gmehling, P. Rasmussen, A. Fredenslund, *Ind. Eng. Chem. Res*., **26**, 159 (1987).
290 M. T. Raetzsch, D. Glindemann, *Acta Polymerica*, **30**, 57 (1979).
291 I. Kikic, P. Alessi, P.Rasmussen, A. Fredenslund, *Can. J. Chem. Eng*., **58**, 253 (1980).
292 M. Gottlieb, M. Herskowitz, *Ind. Eng. Chem. Process Des. Dev*., **21**, 536 (1982).
293 M. Gottlieb, M. Herskowitz, *Macromolecules*, **14**, 1468 (1981).
294 Y. Iwai, M. Ohzono, Y. Arai, *Chem. Eng. Commun*., **34**, 225 (1985).
295 Y. Iwai, Y. Arai, *J. Chem. Eng. Japan*, **22**, 155 (1989).
296 A. A. Patwardhan, L. A. Belfiore, *J. Polym. Sci. Pt. B Polym. Phys*., **24**, 2473 (1986).
297 G. J. Price, A. J. Ashworth, *Polymer*, **28**, 2105 (1987).
298 M. T. Raetzsch, D. Glindemann, E. Hamann, *Acta Polymerica*, **31**, 377 (1980).
299 E. L. Sorensen, W. Hao, P. Alessi, *Fluid Phase Equil*., **56**, 249 (1990).
300 M. Herskowitz, M. Gottlieb, *J. Chem. Eng. Data*, **30**, 233 (1985).
301 J. R. Fried, J. S. Jiang, E. Yeh, *Comput. Polym. Sci.*, **2**, 95 (1992).
302 H. S. Elbro, A. Fredenslund, P. A. Rasmussen, *Macromolecules*, **23**, 4707 (1990).
303 G. M. Kontogeorgis, A. Fredenslund, D. P. Tassios, *Ind. Eng. Chem. Res.*, **32**, 362 (1993).
304 M. J. Misovich, E. A. Grulke, R. F. Blanks, *Ind. Eng. Chem. Process Des. Dev.*, **24**, 1036 (1985).
305 K. Tochigi, S. Kurita, M. Ohashi, K. Kojima, *Kagaku Kogaku Ronbunshu*, **23**, 720 (1997).
306 J. S. Choi, K. Tochigi, K. Kojima, *Fluid Phase Equil.*, **111**, 143 (1995).
307 B. G. Choi, J. S. Choi, K. Tochigi, K. Kojima, *J. Chem. Eng. Japan*, **29**, 217 (1996).
308 J. Holten-Andersen, A. Fredenslund, P. Rasmussen, G. Carvoli, *Fluid Phase Equil.*, **29**, 357 (1986).
309 J. Holten-Andersen, A. Fredenslund, P. Rasmussen, *Ind. Eng. Chem. Res*., **26**, 1382 (1987).
310 F. Chen, A. Fredenslund, P. Rasmussen, *Ind. Eng. Chem. Res.*, **29**, 875 (1990).
311 M. S. High, R. P. Danner, *Fluid Phase Equil*., **53**, 323 (1989).
312 M. S. High, R. P. Danner, *AIChE-J*., **36**, 1625 (1990).
313 M. S. High, R. P. Danner, *Fluid Phase Equil.*, **55**, 1 (1990).
314 K. Tochigi, K. Kojima, T. Sako, *Fluid Phase Equil.*, **117**, 55 (1996).
315 B.-C. Lee, R. P. Danner, *Fluid Phase Equil*., **117**, 33 (1996).
316 A. Bertucco, C. Mio, *Fluid Phase Equil*., **117**, 18 (1996).
317 W. Wang, X. Liu, C. Zhong, C. H. Twu, J. E. Coon, *Fluid Phase Equil*., **144**, 23 (1998).
318 J. M. Smith, H. C. Van Ness, M. M. Abbott, **Introduction to Chemical Engineering Thermodynamics**, 5th Ed., *McGraw-Hill,* Singapore, 1996.
319 S. M. Walas, **Phase equilibria in chemical engineering**, *Butterworth*, Boston, 1985.

320 S. Beret, J. M. Prausnitz, *AIChE-J.*, **21**, 1123 (1975).
321 S. Beret, J. M. Prausnitz, *Macromolecules*, **8**, 878 (1975).
322 M. D. Donohue, J. M. Prausnitz, *AIChE-J.*, **24**, 849 (1978).
323 M. S. Wertheim, *J.Chem.Phys.*, **87**, 7323 (1987).
324 N. F. Carnahan, K. E. Starling, *J.Chem.Phys.,* **51**, 635 (1969).
325 B. J. Alder, D. A. Young, M. A. Mark, *J.Chem.Phys.*, **56**, 3013 (1972).
326 M. D. Donohue, P. Vimalchand, *Fluid Phase Equil.*, **40**, 185 (1988).
327 R. L. Cotterman, B. J. Schwarz, J. M. Prausnitz, *AIChE-J.*, **32**, 1787 (1986).
328 D. D. Liu, J. M. Prausnitz, *Ind. Eng. Chem. Process Des. Dev.*, **19**, 205 (1980).
329 M. Ohzono, Y. Iwai, Y. Arai, *J. Chem. Eng. Japan*, **17**, 550 (1984).
330 S. Itsuno, Y. Iwai, Y. Arai, *Kagaku Kogaku Ronbunshu*, **12**, 349 (1986).
331 Y. Iwai, Y. Arai, *J. Japan Petrol. Inst.*, **34**, 416 (1991).
332 C. H. Chien, R. A. Greenkorn, K. C. Chao, *AIChE-J.*, **29**, 560 (1983).
333 T. Boublik, I. Nezbeda, *Chem. Phys. Lett.*, **46**, 315 (1977).
334 H. Masuoka, K. C. Chao, *Ind. Eng. Chem. Fundam.*, **23**, 24 (1984).
335 M. T. Raetzsch, E. Regener, Ch. Wohlfarth, *Acta Polymerica*, **37**, 441 (1986).
336 E. Regener, Ch. Wohlfarth, M. T. Raetzsch, *Acta Polymerica*, **37**, 499, 618 (1986).
337 E. Regener, Ch. Wohlfarth, M. T. Raetzsch, S. Hoering, *Acta Polymerica*, **39**, 618 (1988).
338 Ch. Wohlfarth, E. Regener, *Plaste & Kautschuk*, **35**, 252 (1988).
339 Ch. Wohlfarth, *Plaste & Kautschuk*, **37**, 186 (1990).
340 Ch. Wohlfarth, B. Zech, *Makromol. Chem.*, **193**, 2433 (1992).
341 U. Finck, T. Heuer, Ch. Wohlfarth, *Ber. Bunsenges. Phys. Chem.*, **96**, 179 (1992).
342 Ch. Wohlfarth, U. Finck, R. Schultz, T. Heuer, *Angew. Makromol. Chem.*, **198**, 91 (1992).
343 Ch. Wohlfarth, *Acta Polymeric*a, **43**, 295 (1992).
344 Ch. Wohlfarth, *Plaste & Kautschuk*, **39**, 367 (1992).
345 Ch. Wohlfarth, *J. Appl. Polym. Sci.*, **48**, 1923 (1993).
346 Ch. Wohlfarth, *Plaste & Kautschuk*, **40**, 272 (1993).
347 Ch. Wohlfarth, *Plaste & Kautschuk*, **41**, 163 (1994).
348 Ch. Wohlfarth, *Macromol. Chem. Phys.*, **198**, 2689 (1997).
349 J. C. Pults, R. A. Greenkorn, K. C. Chao, *Chem. Eng. Sci.*, **44**, 2553 (1989).
350 J. C. Pults, R. A. Greenkorn, K. C. Chao, *Fluid Phase Equil.*, **51**, 147 (1989).
351 R. Sy-Siong-Kiao, J. M. Caruthers, K. C. Chao, *Ind. Eng. Chem. Res.*, **35**, 1446 (1996).
352 C. R. Novenario, J. M. Caruthers, K. C. Chao, *Fluid Phase Equil.*, **142**, 83 (1998).
353 C. R. Novenario, J. M. Caruthers, K. C. Chao, *Ind. Eng. Chem. Res.*, **37**, 3142 (1998).
354 C. R. Novenario, J. M. Caruthers, K. C. Chao, *J. Appl. Polym. Sci.*, **67**, 841 (1998).
355 S. H. Huang, M. Radosz, *Ind. Eng. Chem.*, **29**, 2284 (1990).
356 S. S. Chen, A. Kreglewski, *Ber. Bunsenges. Phys. Chem.*, **81**, 1048 (1977).
357 M. Banaszak, Y. C. Chiew, M. Radosz, *Phys. Rev. E*, **48**, 3760 (1993).
358 M. Banaszak, Y. C. Chiew, R. O'Lenick, M. Radosz, *J. Chem. Phys.*, **100**, 3803 (1994).
359 M. Banaszak, C. K. Chen, M. Radosz, *Macromolecules*, **29**, 6481 (1996).
360 K. P. Shukla, W. G. Shapman, *Mol. Phys.*, **91**, 1075 (1997).
361 H. Adidharma, M. Radosz, *Ind. Eng. Chem. Res.*, **37**, 4453 (1998).
362 S.-J. Chen, M. Radosz, *Macromolecules*, **25**, 3089 (1992).
363 S.-J. Chen, I. G. Economou, M. Radosz, *Macromolecules*, **25**, 4987 (1992).
364 C. J. Gregg, S.-J. Chen, F. P. Stein, M. Radosz, *Fluid Phase Equil.*, **83**, 375 (1993).
365 S.-J. Chen, M. Banaszak, M. Radosz, *Macromolecules,* **28**, 1812 (1995).
366 P. Condo, M. Radosz, *Fluid Phase Equil.*, **117**, 1 (1996).
367 K. L. Albrecht, F. P. Stein, S. J. Han, C. J. Gregg, M. Radosz, *Fluid Phase Equil.*, **117**, 117 (1996).
368 C. Pan, M. Radosz, *Ind. Eng. Chem. Res.*, **37**, 3169 (1998) and **38**, 2842 (1999).
369 G. Sadowski, L. V. Mokrushina, W. Arlt, *Fluid Phase Equil.*, **139**, 391 (1997).
370 J. Groß, G. Sadowski, submitted to *Fluid Phase Equil.*
371 C. F. Kirby, M. A. McHugh, *Chem. Rev.*, **99**, 565 (1999).
372 R. B. Gupta, J. M. Prausnitz, *Ind. Eng. Chem. Res.*, **35**, 1225 (1996).
373 T. Hino, Y. Song, J. M. Prausnitz, *Macromolecules*, **28**, 5709, 5717, 5725 (1995).
374 S. M. Lambert, Song, J. M. Prausnitz, *Macromolecules*, **28**, 4866 (1995).
375 G. M. Kontogeorgis, V. I. Harismiadis, A. Fredenslund, D. P. Tassios, *Fluid Phase Equil.*, **96**, 65 (1994).
376 V. I. Harismiadis, G. M. Kontogeorgis, A. Fredenslund, D. P. Tassios, *Fluid Phase Equil.*, **96**, 93 (1994).
377 T. Sako, A. W. Hu, J. M. Prausnitz, *J. Appl. Polym. Sci.*, **38**, 1839 (1989).

378 G. Soave, *Chem. Eng. Sci.*, **27**, 1197 (1972).
379 V. I. Harismiadis, G. M. Kontogeorgis, A. Saraiva, A. Fredenslund, D. P. Tassios, *Fluid Phase Equil*., **100**, 63 (1994).
380 N. Orbey, S. I. Sandler, *AIChE-J*., **40**, 1203 (1994).
381 R. Stryjek, J. H. Vera, C*an. J. Chem. Eng.*, **64**, 323 (1986).
382 D. S. H. Wong, S. I. Sandler, *AIChE-J.*, **38**, 671 (1992).
383 C. Zhong, H. Masuoka, *Fluid Phase Equil.*, **126**, 1 (1996).
384 C. Zhong, H. Masuoka, *Fluid Phase Equil.*, **126**, 59 (1996).
385 C. Zhong, H. Masuoka, *Fluid Phase Equil.*, **144**, 49 (1998).
386 H. Orbey, C.-C. Chen, C. P. Bokis, *Fluid Phase Equil.*, **145**, 169 (1998).
387 H. Orbey, C. P. Bokis, C.-C. Chen, *Ind. Eng. Chem. Res*., **37**, 1567 (1998).

APPENDIX 4.4A

Table of polymer-solvent systems for which experimental VLE-data have been reported in the literature (the references are given at the end of this table)

Solvent	T, K	Ref.	Solvent	T, K	Ref.
acrylonitrile/butadiene copolymer					
acetonitrile	333.15	121	n-hexane	333.15	121
chloroform	333.15	121	n-octane	333.15	121
cyclohexane	333.15	121	n-pentane	333.15	121
acrylonitrile/styrene copolymer					
benzene	343.15	130, 134	o-xylene	398.15	130, 134
1,2-dichloroethane	343.15	121	m-xylene	398.15	130, 134
1,2-dichloroethane	353.15	121	p-xylene	373.15	130, 134
propylbenzene	398.15	130, 134	p-xylene	398.15	130, 134
toluene	343.15	130, 134	p-xylene	423.15	130, 134
toluene	373.15	130, 134			
p-bromostyrene/p-methylstyrene copolymer					
toluene	293.20	72			
cellulose acetate					
acetone	303.15	81	1,4-dioxane	308.15	81
acetone	308.15	81	methyl acetate	303.15	81
N,N-dimethylformamide	322.85	75	methyl acetate	308.15	81
N,N-dimethylformamide	342.55	75	pyridine	303.15	81
1,4-dioxane	303.15	81	pyridine	308.15	81
cellulose triacetate					
chloroform	303.15	77	dichloromethane	293.15	77
chloroform	308.15	77	dichloromethane	298.15	77

Solvent	T, K	Ref.	Solvent	T, K	Ref.
dextran					
water	293.15	111, 112, 119, 154	water	313.15	111
water	298.15	76	water	333.15	111, 119
di(trimethylsilyl)-poly(propylene oxide)					
toluene	323.15	75	n-decane	342.45	75
toluene	342.65	75			
ethylene/vinyl acetate copolymer					
benzene	303.15	36	n-propyl acetate	343.15	37
benzene	323.15	36	n-propyl acetate	363.15	37
benzene	328.15	36	toluene	303.15	36
benzene	333.15	35	toluene	323.15	36
benzene	343.15	36	toluene	333.15	35
benzene	353.15	35	toluene	343.15	36
benzene	373.15	34, 35	toluene	353.15	35
butyl acetate	323.15	37	toluene	363.15	36
butyl acetate	343.15	37	toluene	373.15	34, 35
butyl acetate	363.15	37	o-xylene	323.15	36
chloroform	333.15	121	o-xylene	343.15	36
cyclohexane	353.15	121	o-xylene	363.15	36
ethyl acetate	303.25	37	p-xylene	323.15	36
ethyl acetate	323.15	37	p-xylene	333.15	35
ethyl acetate	343.15	37	p-xylene	343.15	36
methyl acetate	303.15	37	p-xylene	353.15	35
methyl acetate	323.15	37	p-xylene	363.15	36
n-propyl acetate	303.15	37	p-xylene	373.15	34, 35
n-propyl acetate	323.15	37			
hydroxypropyl cellulose					
acetone	298.15	54	tetrahydrofuran	298.15	54
ethanol	298.15	54	water	298.15	141
hydroxypropyl starch					
water	293.15	117	water	298.15	160

Solvent	T, K	Ref.	Solvent	T, K	Ref.
natural rubber					
acetone	273.15	25	2-butanone	318.15	25
acetone	298.15	25	ethyl acetate	298.15	25
benzene	298.15	6	ethyl acetate	323.15	25
2-butanone	298.15	25	toluene	303.00	82
nitrocellulose					
acetone	293.00	79	ethyl propyl ether	293.00	79
acetone	303.15	81	methyl acetate	303.15	81
acetone	308.15	81	methyl acetate	308.15	81
acetonitrile	293.00	79	3-methyl-2-butanone	293.00	79
ethyl formate	293.15	78	3-methylbutyl acetate	293.15	78
cyclopentanone	293.00	79	nitromethane	293.00	79
3,3-dimethyl-2-butanone	293.00	79	2-pentanone	293.00	79
2,4-dimethyl-3-pentanone	293.00	79	ethyl propionate	293.15	78
1,4-dioxane	293.00	79	propyl acetate	293.15	78
ethyl acetate	293.15	78			
nylon 6,6					
water	296.15	103			
nylon 6,10					
water	296.15	103			
poly(acrylic acid)					
ethanol	303.15	145	water	303.15	145
poly(acrylonitrile)					
1,2-dichloroethane	353.15	121	N,N-dimethylformamide	343.55	75
N,N-dimethylformamide	323.25	75			
polyamidoamine dendrimers					
acetone	308.15	144	methanol	308.15	144
acetonitrile	313.15	144	1-propylamine	308.15	144
chloroform	308.15	144			
poly(benzyl ether) dendrimers					
acetone	323.15	144	tetrahydrofuran	343.15	144
chloroform	323.15	144	toluene	343.15	144
chloroform	343.15	144	n-pentane	313.15	144

Solvent	T, K	Ref.	Solvent	T, K	Ref.
cyclohexane	333.15	144			
poly(γ-benzyl-L-glutamate)					
chloroform	303.15	51			
poly(p-bromostyrene)					
toluene	293.20	72			
polybutadiene					
benzene	296.65	7	ethylbenzene	403.15	106
chloroform	296.65	7	n-hexane	296.65	7
chloroform	298.15	69	n-hexane	333.15	121
chloroform	333.15	121	n-nonane	353.15	106
cyclohexane	296.65	7	n-nonane	373.15	106
cyclohexane	333.15	121	n-nonane	403.15	106
dichloromethane	296.65	7	n-pentane	333.15	121
ethylbenzene	353.15	106	tetrachloromethane	296.65	7
ethylbenzene	373.15	106	toluene	296.65	7
poly(n-butyl acrylate)					
benzene	296.65	61	tetrachloromethane	296.65	61
chloroform	296.65	61	toluene	296.65	61
dichloromethane	296.65	61			
poly(n-butyl methacrylate)					
benzene	323.65	75	mesitylene	373.15	75
benzene	343.45	75	mesitylene	403.15	75
2-butanone	323.65	75	3-pentanone	323.55	75
2-butanone	344.45	75	3-pentanone	343.95	75
chloroform	323.75	75	propylbenzene	344.35	75
chloroform	343.75	121	tetrachloromethane	323.65	75
cumene	373.15	75	tetrachloromethane	344.45	75
cumene	403.15	75	toluene	323.35	75
cyclohexane	308.15	125	toluene	343.75	75
cyclohexane	318.15	125	toluene	373.15	75
cyclohexane	328.15	125	o-xylene	344.45	75
cyclohexane	338.15	125	o-xylene	373.15	75
diethyl ether	298.15	159	o-xylene	403.15	75

Solvent	T, K	Ref.	Solvent	T, K	Ref.
1,2-dichloroethane	323.95	75	m-xylene	343.95	75
1,2-dichloroethane	343.15	75	m-xylene	373.15	75
3,3-dimethyl-2-butanone	323.65	75	m-xylene	403.15	75
3,3-dimethyl-2-butanone	344.45	75	p-xylene	344.45	75
ethylbenzene	343.75	75	p-xylene	373.15	75
ethylbenzene	373.15	75	p-xylene	403.15	75
ethylbenzene	403.15	75			
poly(tert-butyl methacrylate)					
benzene	323.15	75	3-pentanone	342.65	75
benzene	342.65	75	propylbenzene	342.65	75
2-butanone	323.15	75	tetrachloromethane	323.15	75
2-butanone	342.65	75	tetrachloromethane	342.65	75
chloroform	323.15	75	toluene	323.15	75
cumene	373.15	75	toluene	342.75	75
1,2-dichloroethane	323.15	75	toluene	373.15	75
1,2-dichloroethane	342.65	75	o-xylene	342.65	75
3,3-dimethyl-2-butanone	323.15	75	o-xylene	373.15	75
3,3-dimethyl-2-butanone	342.65	75	m-xylene	342.65	75
ethylbenzene	342.65	75	m-xylene	373.15	75
ethylbenzene	373.35	75	p-xylene	342.65	75
mesitylene	373.15	75	p-xylene	373.15	75
3-pentanone	323.15	75			
poly(ε-caprolacton)					
tetrachloromethane	338.15	65			
polycarbonate-bisphenol-A					
chlorobenzene	413.15	123, 139	mesitylene	453.15	139
chlorobenzene	433.15	139	n-pentane	303.15	145
chlorobenzene	453.15	139	toluene	413.15	139
ethanol	303.15	145	water	303.15	145
ethylbenzene	413.15	139	m-xylene	413.15	139
ethylbenzene	433.15	139	m-xylene	453.15	139
mesitylene	413.15	139	p-xylene	413.15	139
mesitylene	433.15	139			

Solvent	T, K	Ref.	Solvent	T, K	Ref.
poly(o-chlorostyrene)					
benzene	298.15	115	2-butanone	313.15	115
benzene	313.15	115			
poly(p-chlorostyrene)					
toluene	293.20	72			
polydecene					
toluene	303.15	3			
poly(dimethyl siloxane)					
benzene	298.15	52, 62	hexamethyl disiloxane	298.15	62
benzene	303.00	63, 66, 101	n-nonane	313.15	157
benzene	313.15	62	octamethyl cyclotetrasiloxane	413.15	85
2-butanone	303.15	53	n-octane	298.15	62
chloroform	303.00	99	n-octane	303.15	157
cyclohexane	293.15	161	n-octane	313.15	62
cyclohexane	303.15	63, 66, 161	n-pentane	303.15	63, 147
dichloromethane	303.00	99	n-pentane	313.15	145
n-heptane	298.15	62	toluene	298.15	62
n-heptane	303.15	63, 157	toluene	308.15	124
n-heptane	313.15	62	toluene	313.15	62
n-hexane	298.09	66	toluene	318.15	124
n-hexane	303.15	63, 66, 100, 147	toluene	328.15	124
n-hexane	308.08	66	2,2,4-trimethylpentane	298.15	62
n-hexane	313.15	145	2,2,4-trimethylpentane	313.15	62
poly(1,3-dioxolane)					
benzene	303.15	105	benzene	313.15	105
polydodecene					
toluene	303.15	3			
poly(ethyl acrylate)					
benzene	296.65	61	tetrachloromethane	296.65	61
chloroform	296.65	61	toluene	296.65	61
dichloromethane	296.65	61			

Solvent	T, K	Ref.	Solvent	T, K	Ref.
polyethylene					
chlorobenzene	393.15	109	propyl acetate	426.15	137
chlorobenzene	403.15	109	propyl acetate	474.15	137
chlorobenzene	413.15	109	2-propylamine	427.15	137
cyclopentane	425.65	137	2-propylamine	475.15	137
cyclopentane	474.15	137	toluene	393.15	109
ethylbenzene	413.15	116	o-xylene	413.15	116
n-heptane	382.05	2	m-xylene	413.15	116
n-pentane	423.65	137	p-xylene	353.15	1
n-pentane	474.15	137	p-xylene	363.15	1, 35
3-pentanol	423.15	137	p-xylene	373.15	35
3-pentanol	473.15	137	p-xylene	383.15	35
3-pentanone	425.15	137	p-xylene	403.15	116
3-pentanone	477.15	137	p-xylene	413.15	116
1-pentene	423.65	137	p-xylene	423.15	116
1-pentene	474.15	137			
poly(ethylene glycol)					
benzene	297.75	43	1-propanol	323.15	45
benzene	307.75	43	1-propanol	333.15	94
benzene	313.15	42	1-propanol	343.15	45
benzene	323.15	42	1-propanol	353.15	94
benzene	343.15	42	1-propanol	373.15	45
1-butanol	323.15	42	tetrachloromethane	303.15	95, 96
1-butanol	343.15	42	toluene	323.15	42, 75
1-butanol	373.15	42	toluene	343.15	42, 75
1-butanol	403.15	42	toluene	373.15	42
chloroform	323.15	146	water	293.15	104, 111, 112, 117, 119
chloroform	333.15	146	water	298.15	39, 40, 41, 76, 128, 129, 158, 160
ethanol	303.15	45, 157	water	303.15	38
ethanol	313.15	45	water	308.15	40, 151
ethanol	323.15	45	water	313.15	104, 111

Solvent	T, K	Ref.	Solvent	T, K	Ref.
ethylbenzene	323.15	42, 44	water	318.15	151
ethylbenzene	343.15	42, 44	water	323.15	38, 108
ethylbenzene	343.75	75	water	328.15	38, 151
ethylbenzene	373.15	42, 44	water	333.15	38, 104, 108, 111, 119, 146
ethylbenzene	403.15	44	water	338.15	38, 151
1-hexanol	323.15	46	water	343.15	108
1-hexanol	373.15	46	p-xylene	323.15	45
1-hexanol	403.15	46	p-xylene	343.15	45
methanol	303.15	157	p-xylene	373.15	45
1-propanol	303.15	45	p-xylene	403.15	45
poly(ethylene glycol) dimethyl ether					
chloroform	278.68	80	tetrachloromethane	303.15	96
tetrachloromethane	278.68	80			
poly(ethylene glycol) monomethyl ether					
tetrachloromethane	303.15	96			
poly(ethylene oxide)					
acetone	323.15	152	benzene	423.55	47
acetone	353.15	136	2-butanone	353.15	136
benzene	318.85	74	chloroform	298.15	48
benzene	323.45	74	chloroform	323.15	152
benzene	328.15	65	chloroform	343.15	152
benzene	343.15	65, 74	chloroform	333.15	121
benzene	348.25	47	cyclohexane	353.15	136
benzene	353.15	136	toluene	353.15	136
benzene	361.25	47	toluene	372.98	68
benzene	375.15	47	p-xylene	353.15	136
benzene	398.85	47			
poly(ethylene oxide)-b-poly(tert-butyl methacrylate) diblock copolymer					
toluene	323.15	75	toluene	343.75	75
poly(ethylene oxide)-b-poly(methyl methacrylate) diblock copolymer					
toluene	323.41	68	toluene	373.27	68

Solvent	T, K	Ref.	Solvent	T, K	Ref.
toluene	343.27	68			
poly(ethylene oxide)-b-poly(methyl methacrylate)-b-poly(ethylene oxide) triblock copolymer					
toluene	323.08	68	toluene	343.17	68
toluene	373.26	68			
poly(ethylene oxide)-b-poly(propylene oxide) diblock copolymer					
tetrachloromethane	303.15	96			
poly(ethylene oxide)-b-poly(propylene oxide)-b-poly(ethylene oxide) triblock copolymer					
tetrachloromethane	303.15	96	toluene	343.75	75
toluene	323.35	75			
poly(ethylene oxide)-b-polystyrene-b-poly(ethylene oxide) triblock copolymer					
toluene	323.35	75	toluene	343.75	75
poly(ethyl methacrylate)					
benzene	296.65	61	tetrachloromethane	296.65	61
chloroform	296.65	61	toluene	296.65	61
dichloromethane	296.65	61			
polyheptene					
toluene	303.15	3			
poly(4-hydroxystyrene)					
acetone	293.15	97	acetone	308.15	97
acetone	298.15	97	acetone	313.15	97
acetone	303.15	97	acetone	318.15	97
polyisobutylene					
benzene	298.15	57, 8, 107	ethylbenzene	338.15	107
benzene	300.05	9	n-heptane	296.65	60
benzene	313.15	8, 57, 70, 107	n-heptane	338.15	156
benzene	333.20	70	n-hexane	298.15	107
benzene	338.15	8, 107	n-hexane	313.15	107
benzene	353.20	70	n-hexane	338.15	107, 156
n-butane	298.15	4	2-methylbutane	298.15	4
n-butane	308.15	4	2-methylbutane	308.15	4
n-butane	319.65	4	2-methylbutane	319.65	4
chloroform	296.65	60	2-methylpropane	308.15	4

Solvent	T, K	Ref.	Solvent	T, K	Ref.
cyclohexane	298.15	8, 58, 60, 107, 147	2-methylpropane	319.65	4
cyclohexane	308.15	125	n-nonane	338.15	156
cyclohexane	313.15	70, 107	n-octane	338.15	156
cyclohexane	315.15	8	n-pentane	298.15	4, 5, 59, 65
cyclohexane	318.15	125	n-pentane	308.15	4, 5
cyclohexane	328.15	125	n-pentane	318.15	5
cyclohexane	333.20	70	n-pentane	319.65	4
cyclohexane	338.15	8, 107, 125	n-pentane	328.15	5
cyclopentane	296.65	60	propane	308.15	4
2,2-dimethylbutane	296.65	60	tetrachloromethane	296.65	60
2,2-dimethylpropane	298.15	4	toluene	298.15	107
2,2-dimethylpropane	308.15	4	toluene	313.15	107
2,2-dimethylpropane	319.65	4	toluene	338.15	107
ethylbenzene	298.15	107	2,2,4-trimethylpentane	296.65	60
ethylbenzene	313.15	107			
1,4-cis-polyisoprene					
benzene	296.65	7	dichloromethane	296.65	7
benzene	353.15	10	tetrachloromethane	296.65	7
chloroform	296.65	7	toluene	296.65	7
cyclohexane	296.65	7			
polyisoprene, hydrogenated					
cyclohexane	323.15	161			
poly(maleic anhydride)					
acetone	323.15	140	methanol	333.15	140
poly(methyl acrylate)					
benzene	296.65	61	tetrachloromethane	296.65	61
chloroform	296.65	61	toluene	296.65	61
dichloromethane	296.65	61			
poly(methyl methacrylate)					
acetone	308.15	131, 150	3,3-dimethyl-2-butanone	343.45	56
acetone	323.15	133	ethyl acetate	308.15	131
benzene	296.65	61	ethylbenzene	398.15	153

Solvent	T, K	Ref.	Solvent	T, K	Ref.
benzene	323.15	56	mesitylene	403.15	67
benzene	343.15	56	methyl acetate	323.15	133
2-butanone	308.15	132, 150	tetrachloromethane	323.15	56
2-butanone	323.15	23, 56	tetrachloromethane	343.75	56
2-butanone	343.55	56	toluene	296.65	61
chloroform	296.65	61	toluene	323.15	23, 56, 75
chloroform	303.15	146	toluene	343.15	56, 75
chloroform	308.15	132	toluene	373.97	68
chloroform	323.15	56, 133, 142, 146	toluene	433.15	19
cyclohexanone	323.15	146	p-xylene	323.15	56
dichloromethane	296.65	61	p-xylene	343.15	56
1,2-dichloroethane	323.15	67	p-xylene	373.15	56
1,2-dichloroethane	343.15	67	p-xylene	403.15	56
3,3-dimethyl-2-butanone	323.35	56	p-xylene	409.35	56
poly(α-methylstyrene)					
cumene	338.15	83	tetrahydrofuran	298.15	92
1,4-dioxane	313.15	89	toluene	298.15	28, 90
α-methylstyrene	303.15	90	toluene	303.15	90
α-methylstyrene	308.15	90	toluene	308.15	90
α-methylstyrene	313.15	90	toluene	313.15	90
α-methylstyrene	338.15	83			
poly(p-methylstyrene)					
toluene	293.20	72			
polyoctadecene					
toluene	303.15	3			
polypropylene					
2,4-dimethyl-3-pentanone	298.15	11	3-pentanone	318.15	11
2,4-dimethyl-3-pentanone	318.15	11	tetrachloromethane	298.15	84
3-pentanone	298.15	11			
poly(propylene glycol)					
n-decane	343.45	75	methanol	298.15	49

Solvent	T, K	Ref.	Solvent	T, K	Ref.
ethylbenzene	342.65	75	tetrachloromethane	303.15	96
n-hexane	298.10	87	toluene	323.15	75
n-hexane	312.65	87	toluene	343.75	75
n-hexane	323.15	87	water	298.15	41, 87
methanol	263.15	49	water	303.15	38
methanol	273.15	49	water	312.65	87
methanol	288.15	49	water	323.15	38
poly(propylene glycol) dimethyl ether					
chloroform	278.68	50	tetrachloromethane	278.68	50
poly(propylene imine) dendrimers					
acetone	323.15	155	n-heptane	348.15	155
acetonitrile	343.15	155	n-hexane	338.15	155
acetonitrile	348.15	155	n-nonane	338.15	155
chloroform	323.15	155	n-octane	338.15	155
chloroform	343.15	155	tetrahydrofuran	323.15	155
n-heptane	338.15	155	toluene	343.15	155
n-heptane	343.15	155	triethylamine	338.15	155
poly(propylene oxide)					
benzene	298.15	147	methanol	298.15	147
benzene	320.35	73	methanol	303.15	157
benzene	333.35	73	methanol	313.15	145
benzene	343.05	73	propanol	303.15	157
benzene	347.85	73	water	303.15	157
ethanol	303.15	157			
poly(propylene oxide)-b-poly(ethylene oxide) diblock copolymer					
ethylbenzene	343.75	75			
poly(propylene oxide)-b-poly(ethylene oxide)-b-poly(propylene oxide) triblock copolymer					
toluene	323.05	75	toluene	342.65	75
polystyrene					
acetone	298.15	27	dichloromethane	296.65	17
acetone	323.15	27, 152	1,4-dioxane	293.15	16
acetone	393.15	122	1,4-dioxane	323.15	23, 26
acetone	423.15	122	dipropyl ether	293.15	16

Solvent	T, K	Ref.	Solvent	T, K	Ref.
acetonitrile	393.15	122	ethyl acetate	313.15	146
acetonitrile	423.15	122	ethyl acetate	333.15	146
anisole	323.15	26	ethylbenzene	303.15	15
benzene	288.15	102	ethylbenzene	323.15	22
benzene	293.15	16	ethylbenzene	343.15	22
benzene	296.65	17	ethylbenzene	398.15	153
benzene	298.15	65	ethylbenzene	403.15	19
benzene	303.15	12, 71, 102, 149	ethylbenzene	413.15	19
benzene	313.15	149	ethylbenzene	433.15	19
benzene	318.15	102	ethylbenzene	443.15	19
benzene	323.15	12, 138	ethylbenzene	451.15	19
benzene	333.15	102, 71	n-hexane	393.15	122
benzene	343.15	12	n-hexane	423.15	122
benzene	353.20	71	methyl acetate	323.15	133
benzene	393.15	122	n-nonane	403.15	106
benzene	403.15	19	n-nonane	423.15	106
benzene	423.15	122	n-nonane	448.15	106
benzene	428.15	19	3-pentanone	293.15	16
2-butanone	298.15	24, 26	propyl acetate	298.15	27
2-butanone	321.65	23	propyl acetate	343.14	27
2-butanone	343.15	24	tetrachloromethane	293.15	16
2-butanone	393.15	122	tetrachloromethane	296.65	17
2-butanone	423.15	122	toluene	293.15	16
butyl acetate	308.15	159	toluene	296.65	17
butyl acetate	323.15	26	toluene	298.15	24, 102, 138
tert-butyl acetate	283.15	64	toluene	303.15	14, 15, 20
tert-butyl acetate	303.15	64	toluene	308.15	127
tert-butyl acetate	323.15	64	toluene	313.15	149
tert-butyl acetate	343.15	64	toluene	321.65	23
tert-butyl acetate	363.15	64	toluene	323.15	14, 20, 71, 138, 149
chloroform	296.65	17	toluene	333.15	24, 71
chloroform	298.15	27, 65, 138	toluene	343.15	20

Solvent	T, K	Ref.	Solvent	T, K	Ref.
chloroform	323.15	27, 138, 152	toluene	353.20	71
cyclohexane	293.15	16	toluene	373.15	20, 21, 123
cyclohexane	296.65	17	toluene	383.15	19
cyclohexane	297.15	13	toluene	393.15	21, 122, 123
cyclohexane	303.15	12, 14, 15, 108, 149	toluene	403.15	19
cyclohexane	308.15	13, 125	toluene	413.15	19
cyclohexane	313.15	71, 108, 149	toluene	423.15	122
cyclohexane	318.15	13, 125	1,2,4-trimethylbenzene	443.15	19
cyclohexane	323.15	12, 14, 108, 152	o-xylene	323.15	26
cyclohexane	328.15	125	o-xylene	373.15	21
cyclohexane	333.15	71, 108	o-xylene	403.15	21
cyclohexane	343.15	12	m-xylene	323.15	146
cyclohexane	353.20	71	m-xylene	373.15	21
cyclohexane	338.15	125	m-xylene	403.15	106
cyclohexane	393.15	122	m-xylene	423.15	106
cyclohexane	423.15	122	m-xylene	448.15	106
cyclohexanone	313.15	146	p-xylene	373.15	21
cyclohexanone	333.15	146	p-xylene	393.15	122
1,2-dichloroethane	343.15	121	p-xylene	403.15	21
1,2-dichloroethane	353.15	121	p-xylene	423.15	122
polystyrene-b-polybutadiene-b-polystyrene triblock copolymer					
cyclohexane	323.15	161	cyclohexane	373.15	161
cyclohexane	348.15	161	cyclohexane	393.15	161
polystyrene-b-poly(ethylene oxide) diblock copolymer					
toluene	322.95	75	toluene	342.65	75
polystyrene-b-polyisoprene-b-polystyrene triblock copolymer					
cyclohexane	323.15	161			
polystyrene-b-poly(methyl methacrylate) diblock copolymer					
benzene	343.15	153	ethylbenzene	398.15	153
1,4-dimethylbenzene	398.15	153	toluene	343.15	153
ethylbenzene	373.15	153	1,3,5-trimethylbenzene	398.15	153

Solvent	T, K	Ref.	Solvent	T, K	Ref.
poly(tetramethylene oxide)					
benzene	318.15	91	1,4-dioxane	303.15	55
tetrahydrofuran	318.15	91	1,4-dioxane	313.15	55
poly(vinyl acetate)					
acetone	298.15	110	1-chloropropane	313.15	30
acetone	303.15	29, 30	1,2-dichloroethane	299.55	86
acetone	308.15	110	ethyl acetate	303.15	29
acetone	313.15	30	methanol	303.15	29
acetone	318.15	110	methanol	353.15	121
acetone	323.15	30	1-propanol	323.15	30
allyl chloride	313.15	30	1-propylamine	313.15	30
benzene	303.15	29, 30, 31	2-propylamine	313.15	30
benzene	313.15	98	toluene	299.55	86
benzene	323.15	30	toluene	308.15	19
benzene	333.15	98	toluene	313.15	19, 98, 120
1-butanol	353.15	121	toluene	333.15	98, 120
chloroform	308.15	19	toluene	353.15	120
chloroform	313.15	19	vinyl acetate	303.15	31
chloroform	333.15	121			
poly(vinyl alcohol)					
water	303.15	32, 145, 147			
poly(vinylcarbazol)					
benzene	279.15	33	benzene	308.15	33
benzene	288.15	33	benzene	318.15	33
benzene	298.15	33	benzene	328.15	33
poly(vinyl chloride)					
2-butanone	333.15	146	tetrachloromethane	338.15	65
cyclohexanone	313.15	146	tetrahydrofuran	315.65	23
cyclohexanone	333.15	146	toluene	316.35	23
dibutyl ether	315.35	23	vinyl chloride	340.15	93
1,4-dioxane	315.65	23			
poly(vinyl methyl ether)					
benzene	298.15	65	ethylbenzene	398.15	118

Solvent	T, K	Ref.	Solvent	T, K	Ref.
benzene	323.15	75	propylbenzene	373.15	75
benzene	343.15	75	toluene	323.15	75
chlorobenzene	343.15	75	toluene	343.15	75
chlorobenzene	373.15	75	o-xylene	363.15	75
chloroform	298.15	65	o-xylene	373.15	118
cyclohexane	308.15	125	o-xylene	398.15	118
cyclohexane	318.15	125	m-xylene	373.15	118
cyclohexane	328.15	125	m-xylene	398.15	118
cyclohexane	338.15	125	p-xylene	373.15	118
ethylbenzene	343.15	75	p-xylene	398.15	118
ethylbenzene	373.15	118			
starch					
water	353.15	143	water	383.15	143
water	363.15	143	water	393.15	143
water	373.15	143	water	403.15	143
styrene/butadiene copolymer					
acetone	323.15	121	ethylbenzene	403.15	113
acetone	333.15	121	n-hexane	343.15	121
benzene	343.15	126, 134	mesitylene	398.15	126, 134
chloroform	323.15	121	n-nonane	373.15	114
cyclohexane	296.65	121	n-nonane	403.15	114
cyclohexane	333.15	121	n-pentane	333.15	121
cyclohexane	343.15	126, 134	toluene	343.15	126, 134
ethylbenzene	373.15	113, 126, 134	toluene	373.15	126, 134
ethylbenzene	398.15	126, 134	p-xylene	398.15	126, 134
styrene/butyl methacrylate copolymer					
acetone	333.15	121	chloroform	343.15	121
styrene/docosyl maleate copolymer					
acetone	323.15	140	cyclohexane	333.15	140
acetone	343.15	140	methanol	333.15	140
styrene/dodecyl maleate copolymer					
acetone	323.15	140	cyclohexane	333.15	140
acetone	343.15	140	methanol	333.15	140

Solvent	T, K	Ref.	Solvent	T, K	Ref.
styrene/maleic anhydride copolymer					
acetone	323.15	140	methanol	333.15	140
styrene/methyl methacrylate copolymer					
acetone	323.15	133	mesitylene	398.15	135
benzene	343.15	135	methyl acetate	323.15	133
chloroform	323.15	133	toluene	343.15	135
ethylbenzene	373.15	135	toluene	373.15	135
ethylbenzene	398.15	135	p-xylene	398.15	135
styrene/pentyl maleate copolymer					
acetone	323.15	140	cyclohexane	333.15	140
acetone	343.15	140	methanol	333.15	140
vinyl acetate/vinyl chloride copolymer					
benzene	398.15	148	ethylbenzene	428.15	148
benzene	418.15	148	n-octane	398.15	148
1-butanol	353.15	121	n-octane	418.15	148
chlorobenzene	398.15	148	p-xylene	398.15	148
ethylbenzene	398.15	148	p-xylene	418.15	148
ethylbenzene	418.15	148			

REFERENCE LIST OF APPENDIX 4.4A

1 G. Krahn, Dissertation, TH Leuna-Merseburg, 1973*).
2 J. H. Van der Waals, J. J. Hermans, *Rec. Trav. Chim. Pays-Bas*, **69**, 971 (1950).
3 P. J. T. Tait, P. J. Livesey, *Polymer*, **11**, 359 (1970).
4 S. Prager, E. Bagley, F. A. Long, *J. Amer. Chem. Soc*., **75**, 2742 (1953).
5 C. H. Baker, W. B. Brown, G. Gee, J. S. Rowlinson, D. Stubley, R. E. Yeadon, *Polymer*, **3**, 215 (1962).
6 P. E. Eichinger, P. J. Flory, *Trans. Faraday Soc*., **64**, 2035 (1968).
7 S. Saeki, J. C. Holste, D. C. Bonner, *J. Polym. Sci., Polym. Phys. Ed*., **20**, 793 (1982).
8 C. E. H. Bawn, R. D. Patel, *Trans. Faraday Soc*., **52**, 1664 (1956).
9 R. S. Jessup, *J. Res. Natl. Bur. Stand*., **60**, 47 (1958).
10 D. C. Bonner, J. M. Prausnitz, *J. Polym. Sci., Polym. Phys. Ed*., **12**, 51 (1974).
11 W. B. Brown, G. Gee, W. D. Taylor, *Polymer*, **5**, 362 (1964).
12 M. T. Raetzsch, M. Opel, Ch. Wohlfarth, *Acta Polymerica*, **31**, 217 (1980).
13 W. R. Krigbaum, D. O. Geymer, *J. Amer. Chem. Soc*., **81**, 1859 (1959).
14 K. Schmoll, E. Jenckel, *Ber. Bunsenges. Phys. Chem*., **60**, 756 (1956).
15 T. Katayama, K. Matsumara, Y. Urahama, *Kagaku Kogaku*, **35**, 1012 (1971).
16 E. C. Baughan, *Trans. Faraday Soc*., **44**, 495 (1948).
17 S. Saeki, J. C. Holste, D. C. Bonner, *J. Polym. Sci., Polym. Phys. Ed.*, **19**, 307 (1981).
18 M. Opel, Dissertation, TH Leuna-Merseburg, 1978*).
19 J. S. Vrentas, J. L. Duda, S. T. Hsieh, *Ind. Eng. Chem., Process Des. Dev.*, **22**, 326 (1983).
20 M. Braeuer, Dissertation, TH Leuna-Merseburg, 1983*).
21 G. Illig, Dissertation, TH Leuna-Merseburg, 1981*).
22 M. T. Raetzsch, G. Illig, Ch. Wohlfarth, *Acta Polymerica*, **33**, 89 (1982).
23 P. J. T. Tait, A. M. Abushihada, *Polymer*, **18**, 810 (1977).

24 C. E. H. Bawn, R. F. J. Freeman, A. R. Kamaliddin, *Trans. Faraday Soc.*, **46**, 677 (1950).
25 C. Booth, G. Gee, G. Holden, G. R. Williamson, *Polymer*, **5**, 343 (1964).
26 G. Illig, Diploma Paper, TH Leuna-Merseburg, 1973*).
27 C. E. H. Bawn, M. A. Wajid, *Trans. Faraday Soc.*, **52**, 1658 (1956).
28 I. Noda, N. Kato, T. Kitano, M. Nagasawa, *Macromolecules*, **14**, 668 (1981).
29 K. Matsumara, T. Katayama, *Kagaku Kogaku,* **38**, 388 (1974).
30 R. J. Kokes, A. R. Dipietro, F. A. Long, *J. Amer. Chem. Soc.*, **75**, 6319 (1953).
31 A. Nakajima, H. Yamakawa, I. Sakurada, *J. Polym. Sci*., **35**, 489 (1959).
32 I. Sakurada, A. Nakajima, H. Fujiwara, *J. Polym. Sci.*, **35**, 497 (1959).
33 K. Ueberreiter, W. Bruns, *Ber. Bunsenges. Phys. Chemie*, **68**, 541 (1964).
34 J. Belorussow, Diploma Paper, TH Leuna-Merseburg, 1973*).
35 K. Peinze, Diploma Paper, TH Leuna-Merseburg, 1972*).
36 M. Boblenz, D. Glindemann, Diplom Paper, TH Leuna-Merseburg, 1975*).
37 D. Kiessling, Diploma Paper, TH Leuna-Merseburg, 1976*).
38 G. N. Malcolm, J. S. Rowlinson, *Trans. Faraday Soc*., **53**, 921 (1957).
39 Z. Adamcova, *Sci. Pap. Prag. Inst. Chem. Technol.*, **N2**, 63 (1976).
40 M. L. Lakhanpal, K. S. Chhina, S. C. Sharma, *Indian J. Chem.*, **6**, 505 (1968).
41 Z. N. Medved, P. P. Petrova, O. G. Tarakanov, *Vysokomol. Soedin., Ser. B*, **24**, 674 (1982).
42 Ch. Wohlfarth, M. T. Raetzsch, *Acta Polymeric*a, **37**, 86 (1986).
43 M. L. Lakhanpal, H. G. Singh, S. C. Sharma, *Indian J. Chem.*, **6**, 436 (1968).
44 Ch. Wohlfarth, W. Zschoch, M. T. Raetzsch, *Acta Polymerica*, **32**, 616 (1981).
45 Ch. Wohlfarth, H. Hahmann, M. T. Raetzsch, *Acta Polymerica*, **32**, 674 (1982).
46 E. Regener, Diploma Paper, TH Leuna-Merseburg, 1983*).
47 S. H. Chang, D. C. Bonner, *J. Appl. Polym. Sci*., **19**, 2457 (1975).
48 G. Allen, C. Booth, G. Gee, M. N. Jones, *Polymer*, **5**, 367 (1964).
49 M. L. Lakhanpal, B. E. Conway, *J. Polym. Sci.,* **46**, 75 (1960).
50 R. W. Kershaw, G. N. Malcolm, *Trans. Faraday Soc*., **64**, 323 (1968).
51 K. Kubo, K. Ogino, *Polymer*, **16**, 629 (1975).
52 M. J. Newing, *Trans. Faraday Soc*., **46**, 613 (1950).
53 A. Muramoto, *Polymer*, **23**, 1311 (1982).
54 J. S. Aspler, D. G. Gray, *Polymer*, **23**, 43 (1982).
55 S. C. Sharma, M. L. Lakhanpal, *J. Polym. Sci., Polym. Phys. Ed.*, **21**, 353 (1983).
56 E. Regener, Ch. Wohlfarth, M. T. Raetzsch, S. Hoering, *Acta Polymerica*, **39**, 618 (1988).
57 P. E. Eichinger, P. J. Flory, *Trans. Faraday Soc*., **64**, 2053 (1968).
58 P. E. Eichinger, P. J. Flory, *Trans. Faraday Soc.*, **64**, 2061 (1968).
59 P. E. Eichinger, P. J. Flory, *Trans. Faraday Soc.*, **64**, 2066 (1968).
60 S. Saeki, J. C. Holste, D. C. Bonner, *J. Polym. Sci., Polym. Phys. Ed.*, **20**, 805 (1982).
61 S. Saeki, J. Holste, D. C. Bonner, *J. Polym. Sci., Polym. Phys. Ed.*, **21**, 2049 (1983).
62 E. Dolch, M. Glaser, A. Heintz, H. Wagner, R. N. Lichtenthaler, *Ber. Bunsenges. Phys. Chem*., **88**, 479 (1984).
63 A. J. Ashworth, C.-F. Chien, D. L. Furio, D. M. Hooker, M. M. Kopecni, R. J. Laub, G. J. Price, *Macromolecules*, **17**, 1090 (1984).
64 K. Schotsch, B. A. Wolf, *Makromol. Chem*., **185**, 2161 (1984).
65 C. Panayiotou, J. H. Vera, *Polym. J.*, **16**, 89 (1984).
66 A. J. Ashworth, G. J. Price, *Thermochim. Acta*, **82**, 161 (1984).
67 D. Hailemariam, Diploma Paper, TH Leuna-Merseburg, 1985*).
68 M. Krcek, Diploma Paper, TH Leuna-Merseburg , 1986*).
69 C. Booth, G. Gee, M. N. Jones, W. D. Taylor, *Polymer*, **5**, 353 (1964).
70 N.-H. Wang, S. Takashima, H. Masuoka, *Kagaku Kogaku Ronbunshu*, **15**, 313 (1989).
71 N.-H. Wang, S. Takashima, H. Masuoka, *Kagaku Kogaku Ronbunshu*, **15**, 795 (1989).
72 R. Corneliussen, S. A. Rice, H. Yamakawa, *J. Chem. Phys.*, **38**, 1768 (1963).
73 C. Booth, C. J. Devoy, *Polymer*, **12**, 320 (1971).
74 C. Booth, C. J. Devoy, *Polymer*, **12**, 309 (1971).
75 Ch. Wohlfarth, unpublished data, TH Leuna-Merseburg, Institute of physical chemistry 1979 - 1993, Martin-Luther-University, Institute of physical chemistry 1993 - 1999*).
76 C. A. Haynes, R. A. Beynon, R. S. King, H. W. Blanch, J. M. Praunsitz, *J. Phys. Chem.*, **93**, 5612 (1989).
77 W. R. Moore, R. Shuttleworth, *J. Polym. Sci., Pt. A*, **1**, 1985 (1963).

78 A. L. Jones, *Trans. Faraday Soc*., **52**, 1408 (1956).
79 E. C. Baughan, A. L. Jones, K. Stewart, *Proc. Roy. Soc., London, Ser. A*, **225**, 478 (1954).
80 G. N. Malcolm, C. E. Baird, G. R. Bruce, K. G. Cheyne, R. W. Kershaw, M. C. Pratt, *J. Polym. Sci., Pt. A-2*, **7**, 1495 (1969).
81 W. R. Moore, R. Shuttleworth, *J. Polym. Sci., Pt. A*, **1**, 733 (1963).
82 K. H. Meyer, E. Wolff, Ch. G. Boissonnas, *Helv. Chim. Acta*, **23**, 430 (1940).
83 S. G. Canagratna, D. Margerison, J. P. Newport, *Trans. Faraday Soc*., **62**, 3058 (1966).
84 H. Ochiai, K. Gekko, H. Yamamura, *J. Polym. Sci., Pt. A-2*, **9**, 1629 (1971).
85 R. C. Osthoff, W. T. Grubb, *J. Amer. Chem. Soc*., **76**, 399 (1954).
86 A. A. Tager, A. I. Suvorova, Yu.S. Bessonov, A. I. Podlesnyak, I.A. Koroleva, L. V. Adamova, *Vysokomol. Soedin., Ser. A*, **13**, 2454 (1971).
87 A. A. Tager, L. V. Adamova, Yu.S. Bessonov, V. N. Kuznetsov, T. A. Plyusnina, V. V. Soldatov, *Vysokomol. Soedin., Ser. A*, **14**, 1991 (1972).
88 T. V. Gatovskaya, V. A. Kargin, A. A. Tager, *Zh. Fiz. Khim*., **29**, 883 (1955).
89 J. Leonard, Van Tam Bui, *Polymer*, **28**, 1041 (1987).
90 A. Hamdouni, J. Leonard, Van Tam Bui, *Polymer Commun*., **31**, 258 (1990).
91 Van Tam Bui, J. Leonard, *J. Chem. Soc., Faraday Trans. I*, **82**, 899 (1986).
92 Van Tam Bui, J. Leonard, *J. Chem. Soc., Faraday Trans. I*, **81**, 1745 (1985).
93 A. H. Abdel-Alim, *J. Appl. Polym. Sci.*, **22**, 3597 (1978).
94 U. Messow, Inst. Phys. Chem., Univ. Leipzig, personal communication.
95 F. Cordt, Dissertation, TU Muenchen, 1985.
96 F. Moeller, Dissertation, TU Muenchen, 1989.
97 G. Luengo, G. Rojo, R. G. Rubio, M. G. Prolongo, R. M. Masegosa, *Macromolecules*, **24**, 1315 (1991).
98 N. H. Wang, K. Hattori, S. Takashima, H. Masuoka, *Kagaku Kogaku Ronbunshu*, **17**, 1138 (1991).
99 A. J. Ashworth, G. J. Price, *Macromolecules*, **19**, 362 (1986).
100 A. J. Ashworth, G. J. Price, *J. Chem. Soc., Faraday Trans. I*, **81**, 473 (1985).
101 A. J. Ashworth, G. J. Price, *Macromolecules*, **19**, 358 (1986).
102 I. Noda, Y. Higo, N. Ueno, T. Fujimoto, *Macromolecules*, **17**, 1055 (1984).
103 H. W. Starkweather, Jr., *J. Appl. Polym. Sci*., **2**, 129 (1959).
104 M. Herskowitz, M. Gottlieb, *J. Chem. Eng. Data*, **30**, 233 (1985).
105 Van Tam Bui, J. Leonard, *Polym. J.*, **21**, 185 (1989).
106 Y. Iwai, Y. Arai, *J. Chem. Eng. Japan*, **22**, 155 (1989).
107 H. Masuoka, N. Murashige, M. Yorizane, *Fluid Phase Equil*., **18**, 155 (1984).
108 Y. C. Bae, J. J. Shim, D. S. Soane, J. M. Prausnitz, *J. Appl. Polym. Sci.*, **47**, 1193 (1993).
109 Ch. Wohlfarth, *Plaste & Kautschuk*, **40**, 272 (1993).
110 G. Luengo, R. G. Rubio, I. C. Sanchez, C. G. Panayiotou, *Macromol. Chem. Phys.*, **195**, 1043 (1994).
111 J. Gaube, A. Pfennig, M. Stumpf, *J. Chem. Eng. Data*, **38**, 163 (1993).
112 J. Zhu, Dissertation, Univ. Kaiserslautern, 1991.
113 Y. Iwai, S. Miyamoto, K. Nakano, Y. Arai, *J. Chem. Eng. Japan*, **23**, 508 (1990).
114 Y. Iwai, T. Ishidao, S. Miyamoto, H. Ikeda, Y. Arai, *Fluid Phase Equil*., **68**, 197 (1991).
115 K. Gekko, K. Matsumara, *Bull. Chem. Soc. Japan*, **46**, 1554 (1973).
116 Ch. Wohlfarth, *Plaste & Kautschuk*, **41**, 163 (1994).
117 M. Koester, Diploma Paper, TH Darmstadt, 1994.
118 Ch. Wohlfarth, ELDATA: *Int. Electron. J. Phys.-Chem. Data*, **1**, 113 (1995).
119 C. Grossmann, R. Tintinger, G. Maurer, *Fluid Phase Equil.*, **106**, 111 (1995).
120 S. P. V. N. Mikkilineni, D.A. Tree, M. S. High, *J. Chem. Eng. Data*, **40**, 750 (1995).
121 R. B. Gupta, J. M. Prausnitz, *J. Chem. Eng. Data*, **40**, 784 (1995).
122 J. S. Choi, K. Tochigi, K. Kojima, *Fluid Phase Equil.*, **111**, 143 (1995).
123 S. Behme, G. Sadowski, W. Arlt, *Chem.-Ing.-Techn.*, **67**, 757 (1995).
124 H.-M. Petri, N. Schuld, B. A. Wolf, *Macromolecules*, **28**, 4975 (1995).
125 H.-M. Petri, Dissertation, Univ. Mainz, 1994.
126 Ch. Wohlfarth, ELDATA: *Int. Electron. J. Phys.-Chem. Data*, **2**, 13 (1996).
127 K. Wang, Y. Chen, J. Fu, Y. Hu, Chin. *J. Chem. Eng.*, **1**, 65 (1993).
128 D.-Q. Lin, L.-H. Mei, Z.-Q. Zhu, Z.-X. Han, *Fluid Phase Equil*., **118**, 241 (1996).
129 L.R. Ochs, M. Kabri-Badr, H. Cabezas, *AIChE-J*., **36**, 1908 (1990).
130 Ch. Wohlfarth, *ELDATA: Int. Electron. J. Phys.-Chem. Data*, **2**, 163 (1996).
131 K. Wang, Q. Xue, J. Fu, Y. Hu, *Huadong Ligong Daxue Xuebao*, **22**, 330 (1996).

132 K. Wang, Q. Xue, Y. Hu, *Huadong Ligong Daxue Xuebao*, **23**, 109 (1997).
133 J. O. Tanbonliong, J. M. Prausnitz, *Polymer*, **38**, 5775 (1997).
134 Ch. Wohlfarth, *Macromol. Chem. Phys*., **198**, 2689 (1997).
135 Ch. Wohlfarth, ELDATA: *Int. Electron. J. Phys.-Chem. Data*, **3**, 47 (1997).
136 K. Tochigi, S. Kurita, M. Ohashi, K. Kojima, *Kagaku Kogaku Ronbunshu*, **23**, 720 (1997).
137 R. K. Surana, R. P. Danner, A. B. De Haan, N. Beckers, *Fluid Phase Equil*., **139**, 361 (1997).
138 H. C. Wong, S. W. Campbell, V. R. Bhetnanabotla, *Fluid Phase Equil*., **139**, 371 (1997).
139 G. Sadowski, L. V. Mokrushina, W. Arlt, *Fluid Phase Equil*., **139**, 391 (1997).
140 C. Mio, K. N. Jayachandran, J. M. Prausnitz, *Fluid Phase Equil*., **141**, 165 (1997).
141 J. S. Aspler, D. G. Gray, *Macromolecules*, **12**, 562 (1979).
142 K. N. Jayachandran, P. R. Chatterji, J. M. Prausnitz, *Macromolecules*, **31**, 2375 (1998).
143 Benczedi, D., Tomka, I., Escher, F., *Macromolecules*, **31**, 3062 (1998).
144 C. Mio, S. Kiritsov, Y. Thio, R. Brafman, J. M. Prausnitz, C. Hawker, E. E. Malmstroem, *J. Chem. Eng. Data*, **43**, 541 (1998).
145 S. Hwang, J. Kim, K.-P. Yoo, *J. Chem. Eng. Data*, **43**, 614 (1998).
146 F. Wie, W. Wenchuan, F. Zhihao, *J. Chem. Ind. Eng. China*, **49**, 217 (1998).
147 J. Kim, K. C. Joung, S. Hwang, W. Huh, C. S. Lee, K.-P. Yoo, *Korean J. Chem. Eng.*, **15**, 199 (1998).
148 N. H. Kim, S. J. Kim, Y. S. Won, J. S. Choi, *Korean J. Chem. Eng.*, **15**, 141 (1998).
149 Y. Dahong, S. Jibin, L. Xiaohui, H. Ying, *J. East China Univ. Sci. Technol*., **23**, 608 (1997).
150 W. Hiyan, W. Kun, L. Honglai, H. Ying, *J. East China Univ. Sci. Technol*., **23**, 614 (1997).
151 A. Eliassi, H. Modarress, G. A. Mansoori, *J. Chem. Eng. Data*, **44**, 52 (1999).
152 C. Mio, J. M. Prausnitz, *Polymer*, **39**, 6401 (1998).
153 Ch. Wohlfarth, *ELDATA: Int. Electron. J. Phys.-Chem. Data*, **4**, 83 (1998).
154 H.-P. Kany, H. Hasse, G. Maurer, *J. Chem. Eng. Data*, **44**, 230 (1999).
155 J. G. Lieu, M. Liu, J. M. J. Frechet, J. M. Prausnitz, *J. Chem. Eng. Data*, **44**, 613 (1999).
156 J. G. Lieu, J. M. Prausnitz, *Polymer*, **40**, 5865 (1999).
157 J. Kim, E. Choi, K.-P. Yoo, C. S. Lee, *Fluid Phase Equil*., **161**, 283 (1999).
158 L. Ninni, M. S. Camargo, A. J. A. Meirelles, *Thermochim. Acta*, **328**, 169 (1999).
159 K. Wang, Y. Hu, D. T. Wu, *J. Chem. Eng. Data*, **39**, 916 (1994).
160 D.-Q. Lin, Y.-T. Wu, Z.-Q. Zhu, L.-H. Mei, S.-J. Yao, *Fluid Phase Equil*., **162**, 159 (1999).
161 R. N. French, G. J. Koplos, *Fluid Phase Equil*., **158-160**, 879 (1999).

*) all data from the Merseburg group before 1994 have been published in Ref. Ch. Wohlfarth, Vapor-liquid equilibrium data of binary polymer solutions, Physical Science Data 44, Elsevier, Amsterdam, 1994